Coastal and Shelf Sediment Transport

Edited by
P. S. Balson and M. B. Collins

Geological Society
Special Publication 274

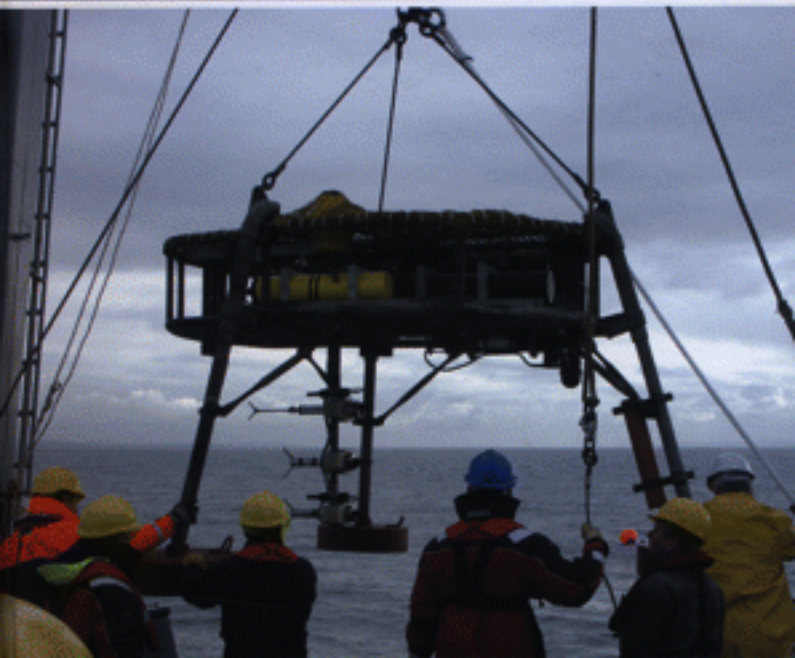

Coastal and Shelf Sediment Transport

Geological Society books refereeing procedures

The Society makes every effort to ensure that the scientific and production quality of its books matches that of its journals. Since 1997, all book proposals have been refereed by specialist reviewers as well as by the Society's Books Editorial Committee. If the referees identify weaknesses in the proposal, these must be addressed before the proposal is accepted.

Once the book is accepted, the Society Book Editors ensure that the volume editors follow strict guidelines on refereeing and quality control. We insist that individual papers can only be accepted after satisfactory review by two independent referees. The questions on the review forms are similar to those for *Journal of the Geological Society*. The referees' forms and comments must be available to the Society's Book Editors on request.

Although many of the books result from meetings, the editors are expected to commission papers that were not presented at the meeting to ensure that the book provides a balanced coverage of the subject. Being accepted for presentation at the meeting does not guarantee inclusion in the book.

More information about submitting a proposal and producing a book for the Society can be found on its web site: www.geolsoc.org.uk.

It is recommended that reference to all or part of this book should be made in one of the following ways:

BALSON, P. S. & COLLINS, M. B. 2007. *Coastal and Shelf Sediment Transport*. Geological Society of London, Special Publications, **274**.

SOUZA, A. J., HOLT, J. T. & PROCTOR, R. 2007. Modelling SPM on the Northwest European shelf seas. *In*: BALSON, P. S. & COLLINS, M. B. *Coastal and Shelf Sediment Transport*. Geological Society of London, Special Publications, **274**, 000–000.

GEOLOGICAL SOCIETY SPECIAL PUBLICATION NO. 274

Coastal and Shelf Sediment Transport

EDITED BY

P. S. BALSON
British Geological Survey, UK

and

M. B. COLLINS
University of Southampton, UK
and AZTI Tecnalia, Spain

2007
Published by
The Geological Society
London

THE GEOLOGICAL SOCIETY

The Geological Society of London (GSL) was founded in 1807. It is the oldest national geological society in the world and the largest in Europe. It was incorporated under Royal Charter in 1825 and is Registered Charity 210161.

The Society is the UK national learned and professional society for geology with a worldwide Fellowship (FGS) of over 9000. The Society has the power to confer Chartered status on suitably qualified Fellows, and about 2000 of the Fellowship carry the title (CGeol). Chartered Geologists may also obtain the equivalent European title, European Geologist (EurGeol). One fifth of the Society's fellowship resides outside the UK. To find out more about the Society, log on to www.geolsoc.org.uk.

The Geological Society Publishing House (Bath, UK) produces the Society's international journals and books, and acts as European distributor for selected publications of the American Association of Petroleum Geologists (AAPG), the Indonesian Petroleum Association (IPA), the Geological Society of America (GSA), the Society for Sedimentary Geology (SEPM) and the Geologists' Association (GA). Joint marketing agreements ensure that GSL Fellows may purchase these societies' publications at a discount. The Society's online bookshop (accessible from www.geolsoc.org.uk) offers secure book purchasing with your credit or debit card.

To find out about joining the Society and benefiting from substantial discounts on publications of GSL and other societies worldwide, consult www.geolsoc.org.uk, or contact the Fellowship Department at: The Geological Society, Burlington House, Piccadilly, London W1J 0BG: Tel. +44 (0)20 7434 9944; Fax +44 (0)20 7439 8975; E-mail: enquiries@geolsoc.org.uk.

For information about the Society's meetings, consult *Events* on www.geolsoc.org.uk. To find out more about the Society's Corporate Affiliates Scheme, write to enquiries@geolsoc.org.uk

Published by The Geological Society from:
The Geological Society Publishing House, Unit 7, Brassmill Enterprise Centre, Brassmill Lane, Bath BA1 3JN, UK

(*Orders*: Tel. +44 (0)1225 445046, Fax +44 (0)1225 442836)
Online bookshop: www.geolsoc.org.uk/bookshop

British Library Cataloguing in Publication Data

A catalogue record for this book is available from the British Library.
ISBN 1-86239-217-X
ISBN 13 978-1-86239-217-5
Typeset by The Charlesworth Group
Printed by The Cromwell Press, Wiltshire, UK.

Distributors

North America
For trade and institutional orders:
The Geological Society, c/o AIDC, 82 Winter Sport Lane, Williston, VT 05495, USA
Orders: Tel +1 800-972-9892
Fax +1 802-864-7626
Email gsl.orders@aidcvt.com

For individual and corporate orders:
AAPG Bookstore, PO Box 979, Tulsa, OK 74101-0979, USA
Orders: Tel +1 918-584-2555
Fax +1 918-560-2652
Email bookstore@aapg.org
Website http://bookstore.aapg.org

India
Affiliated East-West Press Private Ltd, Marketing Division, G-1/16 Ansari Road, Darya Ganj, New Delhi 110 002, India
Orders: Tel. +91 11 2327-9113/2326-4180
Fax +91 11 2326-0538
E-mail affiliat@vsnl.com

CONTENTS

CONTENTS

Coastal and shelf sediment transport: an introduction

MICHAEL B. COLLINS[1,3] & PETER S. BALSON[2]

[1]*School of Ocean & Earth Science, University of Southampton, Southampton Oceanography Centre, European Way, Southampton SO14 3ZH, UK (e-mail: mbc@noc.soton.ac.uk)*

[2]*Marine Research Division, AZTI Tecnalia, Herrera Kaia, Portu aldea z/g, Pasaia 20110, Gipuzkoa, Spain*

[3]*British Geological Survey, Kingsley Dunham Centre, Keyworth, Nottingham NG12 5GG, UK.*

Interest in sediment dynamics is generated by the need to understand and predict: (i) morphodynamic and morphological changes, e.g. beach erosion, shifts in navigation channels, changes associated with resource development; (ii) the fate of contaminants in estuarine, coastal and shelf environment (sediments may act as *sources* and *sinks* for toxic contaminants, depending upon the surrounding physico-chemical conditions); (iii) interactions with biota; and (iv) of particular relevance to the present Volume, interpretations of the stratigraphic record. Within this context of the latter interest, coastal and shelf sediment may be regarded as a *non-renewable* resource; as such, their dynamics are of extreme importance. Over the years, various approaches and techniques have been applied to the determination of sediment transport pathways and the derivation of erosion, transport, and deposition rates. Such wide-ranging approaches include the refinement and application of numerical modelling; and the development of new and more efficient field equipment, e.g. video systems (coastal/inshore) and multibeam.

In general, sediment transport can be defined on the basis of direct observations, indirect observations and by modelling. Direct observation methods include: acoustic backscatter; optical backscatter; sediment traps; artificial tracers, for sand and pebbles; natural tracers or labelled sediments, for silts and clays; and the determination of water movements, using drifters, SPM (suspended particulate matter) and remote sensing. Indirect observational methods include: sediment characteristics, including GSTA (grain size trend analysis) and mineralogy; geomorphology, including coastal landforms, estuarine volumes and asymmetric bedforms (ripples, sandwaves and sandbanks); and, finally, the internal structure of the sediment bodies (cross-bedding and accretionary sequences). On the basis of these various approaches and techniques, it may be concluded that:

(a) no single method for the determination of sediment transport pathways provides the complete picture;
(b) observational evidence needs to be gathered in a particular study area, in which contemporary and historical data, supported by broad-based measurements, is interpreted by an experienced practitioner (Soulsby 1997);
(c) the form and internal structure of sedimentary sinks can reveal long-term trends in transport directions, rates and magnitude;
(d) complementary short-term measurements and modelling are required, to (b) (above) — any model of regional sediment transport must account for the size, location and composition of sedimentary sinks.

On the basis of the above summary, it is evident that it is timely to review a representative selection of the different approaches, by reference to recently undertaken coastal and shelf investigations. A number of such studies (13) are included within this Special Publication, operating at a variety of temporal and spatial scales, within different regions of the UK/European continental shelf, and elsewhere.

The concept of different scales, in relation to sediment dynamics has been proposed (Horikawa 1970) for classifying coastal phenomena into three (temporal and spatial) categories: *macroscale* (year/kilometre); *mesoscale* (day-hour/metre); and *microscale* (second/millimetre). Subsequently, the following observations have been made (Horikawa 1981):

(a) to treat the *macroscale* phenomena, the approach of the geologist and geomorphologist is helpful for understanding the general tendencies of the coastal processes;
(b) changes in shoreline and sea-bottom topography, bar and cusp formation, together with nearshore currents, all fall into the category of *mesoscale* phenomena;

From: BALSON, P. S. & COLLINS, M. B. 2007. *Coastal and Shelf Sediment Transport*. Geological Society of London, Special Publications, **274**, 1–5. 0305-8719/07/$15.00

(c) within the context of a *microscale* approach, extensive research needs were identified such as, in particular, various aspects of wave-current interaction.

Interestingly, the observation is made that, theoretically, the complete superposition of *microscale* phenomena should compose the *mesoscale* phenomena and that of *mesoscale* phenomena, the *macroscale* phenomena. At the time of the publication (Horikawa 1981), such connections could not be made.

The above concept has been developed further by Larson & Kraus (1995), in relation to spatial and temporal scales for investigating sediment transport and morphological processes. In Figure 1, *microscale* is seen to refer to changes from sub-wave period to several periods, over

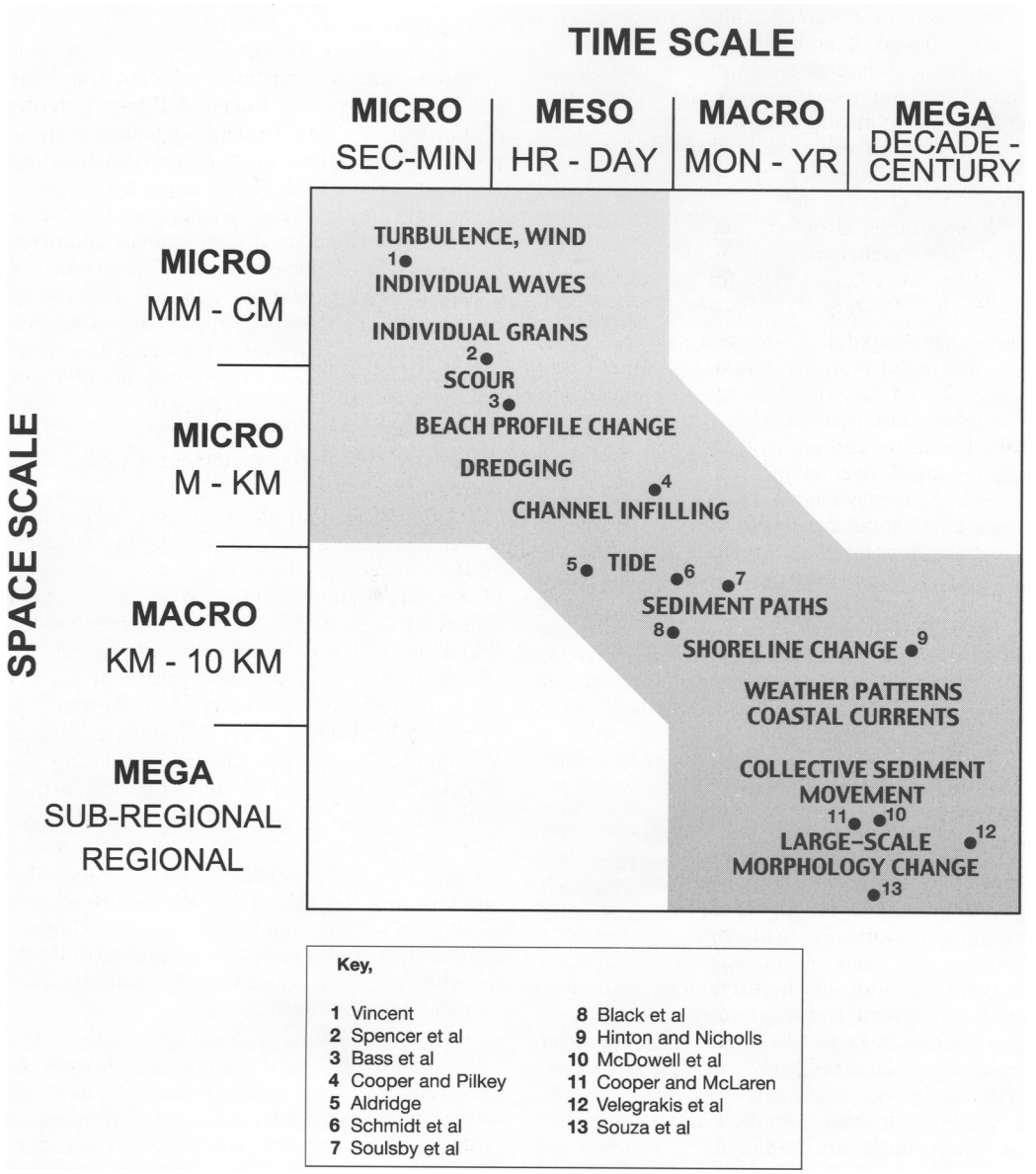

Fig. 1. Relationships of contributions to the Special Publication, in terms of their spatial and temporal scales (based upon Larson & Kraus 1995).

lengths of millimetres to centimetres. At *mesoscale*, net transport rates over many wave periods are evaluated for distances of metres to a kilometre. *Macroscale* involves seasonal changes and a space scale of kilometres, whilst *megascale* describes decade to century changes over coastal sub-reaches and reaches, e.g. over a littoral cell. The concepts applied here are applicable, equally, to the inner continental shelf (<60 m water depth) – at the very least. The main conclusions reached (Larsen & Kraus 1995) are that calculations at different scales can be related and reconciled, if limitations in the predictions of initial and boundary conditions and in the fluid flow, are recognised. Against this background the contribution of the present publication are superimposed; these range from *micro-* to *mega*-scales, on the basis of the generalized classification.

Interestingly, Dronkers (2005) has adopted a similar approach, based upon the original synthesis of Holman (2001). The former investigator makes the following pertinent observations:

(a) at small spatial scales, seabed morphology and water motion adapt to each other, with a short delay, but at a large spatial scale, the adaptation period can be very long;
(b) if erosion and sedimentation are balanced, averaged over large temporal and spatial scales, it may happen that these is an imbalance at smaller scales or vice versa – in fact, the phenomena of erosion, sedimentation and sediment transport always have to be defined with respect to particular spatial and temporal scales;
(c) the physics of sedimentary coastal environments is related to temporal and spatial scales – the physical processes that determine coastal morphology span a range of temporal scales, covering more than ten orders of magnitude.

For large temporal, but small spatial scale processes, time-series are restricted; sometimes, they are not of sufficient high quality to overcome any uncertainties, i.e. separating processes from background noise. From an engineering perspective, on the basis of the scientific limitations in understanding, the best available method to predict sediment transport *rates* in the marine environment may not be able to achieve much better than a factor of 5; cf. 2, in the case of rivers (Soulsby 1997).

Initially, in this Special Publication errors and uncertainties are examined, in relation to the measurement of SSC (suspended sand concentration) using Acoustic Backscatter (**Vincent**). A major uncertainty is identified, in terms of the suspended sediment component close to the bed, together with the bedload itself. The labelling of pure clays and estuarine sediments, with lanthanide (La) is described by **Spencer *et al.*** Here, it is concluded that further investigation is required, of the use of alternative lanthanide group elements, for such studies. Optical and acoustic backscatter sensors are described then (**Bass *et al.***), within the context of the measurements of the mud and sand component in transit, at a site located to seawards of the Wash embayment, southern North Sea.

The problems of field measurements and quantification of longshore sediment transport (LST) is considered by **Cooper & Pilkey**, in terms of mechanisms and present approaches. It is pointed out, by these authors, that the inability to measure the total LST has important implications for coastal zone management; this is because so many coastal management initiatives rely upon quantified volumes of LST. In terms of coastal and shelf seas, in general, a relatively simple analytic (algebraic) approach is described (**Aldridge**), to complement full-scale numerical calculations and assist in the interpretation of the numerical results. However, the results obtained rely upon the implicit assumption that the supply of material available for transport is not exhausted, over the tidal cycle.

The repeated survey of banner tidal sandbanks, using multibeam, is described by **Schmidt *et al.*** Interestingly, dunes connect over the crest of the bank despite opposing sediment transport directions on the flanks. A new numerical model, that identifies the paths taken by a large number of identified ('tagged') sand grains in coastal areas in response to waves and currents, is described by **Soulsby *et al.*** Within this context, a validation exercise is applied simulating the dispersal of radioactive sand tracers. Particle tracking is considered, in terms of a somewhat different approach, by **Black *et al.*** Used in conjunction with a range of more traditional methods, particle tracking (particle or sediment tracing, including the deliberate marking of natural or synthetic sediment with an identifiable signature) is an additional tool, which provides further lines of evidence.

Changes in shoreline morphology along the Dutch coast are investigated by **Hinton & Nicholls**; this is a wave-dominated uniform coastline, uninterrupted by tidal inlets. The analysis undertaken has shown that the upper, middle and lower shoreface are coupled; this has widespread significance in the understanding of long-term coastal-evolution. Surficial nearshore

sediments are described then, in terms of their distribution and spatial patterns (**McDowell *et al.***). Temporal changes in substrate and bedforms suggest bedform development and facies boundary migration, between winter and summer seasons.

The application of grain size trend analysis to Carmathen Bay, Bristol Channel, is described by **Cooper & McLaren**. Complex patterns of movement are interpreted, incorporating a number of tidally-induced gyres. This approach is included, within the context of seabed sediment transport investigations, by **Velegrakis *et al.*** An integrated approach is outlined, in relation to case studies from the southern UK inner (< 60 m water depth) continental shelf. Conceptual sediment transport models are presented, associated with different levels of confidence in their interpretation. Finally, at the scale of the NW European continental shelf, SPM is modelled (**Souza *et al.***). Tidal signals and seasonal variations are identified within the spatial patterns.

The various investigations incorporated within this Volume, as outlined above, represent a wide range of temporal and spatial scales; these are, in turn, associated with appropriate instrumentation and analyses. Consequently, it is appropriate to incorporate each of the studies here into an 'overview'.

In parallel with this approach/concept lies the importance of extreme (storm) events which, interestingly, appears to vary according to the location of a particular environment, within the overall sediment dynamics system. For example, the 'episodicity' of the transport of sediment, within the coastal zone, has been described (Seymour & Castel 1985). On the basis of 1 to 3 years of nearshore directional wave measurements from seven US west coast beaches, time-series of daily net longshore transport rates were derived. Transport was found to be very episodic, with approximately only 10% of the time required to move half of the sediment transported during a year. Elsewhere, measurements of large-scale coastal response to multiple storms on three coastal beaches have revealed a heterogeneous response, with isolated hotspots of erosion (List *et al.* 2006). Within a few days, these hotspots of erosion are reversed rapidly by post-storm accretion. Such observations provide a new view on the coastal response to storms, at scales much larger than site-specific experiments (List *et al.* 2006).

In contrast to the importance of storms in controlling the morphology of the coastline, the effect of wave/current interaction on sediment transport from the inner continental shelf (< 60 m water depth) area – the southern North Sea – reveals a different pattern. Using a high quality data set of waves and currents, from a particular site, the contribution of different combinations to long-term transport, has been assessed (Soulsby 1987). Under such conditions, waves act as a stirring agent to move sediment, whilst it is transported by the current. The conditions analysed ranged from calm seas and neap tides, to major storms coupled with spring tides. Interestingly, the following conclusions were reached:

(a) waves enhance transport, by up to a factor of 10, compared with transport in the absence of waves: and
(b) in terms of long-term (sediment) transport, the largest contributions were provided by 'fairly large', but not infrequent waves, superimposed upon currents lying approximately between the peak speeds of mean neap and mean spring tides.

Nonetheless, because the sediment transport rate depends non-linearly on the current speed, also because the effect of wave-stirring is important, the direction of the long-term transport may be very different from the residual current direction (Soulsby 1997). The very strong currents and very large waves were found not to make significant contributions to long-term transport. As such, the transition between storm-induced processes at the coastline, compared with the influence of various non-linear wave/current interactions offshore, is an important area of sediment dynamics research.

Overall, the presentations made at the meeting (transposed, mainly on the basis of a peer-review process, into the contributions in this Issue), incorporate the concept and approaches reviewed above: direct/indirect observations and/or modelling; different temporal and spatial scales, in relation to sediment dynamics; the importance of wave/current interactions; and the impact of episodic events. As such, it is hoped that 'state-of-the-art' science and instrumentation is incorporated into this unique publication. However, it should be remembered that sediment transport is still an inexact science on the basis of: biological effects; the presence of (mixed) sediments, containing a wide range of grain size components; time-history effects; and wave-current interactions. Finally, it is speculated that strong non-linear processes, such as sediment morphodynamics, may exhibit chaotic behaviour (in a mathematical sense), in the same way as the weather (Soulsby 1997)

The Editors acknowledge the contribution of the reviewers and the patience of the authors, during the production of this volume.

The authors are grateful for discussion of some of the concepts here, with Adonis Velegrakis (University of the Aegean, Greece). Likewise, Dr Haris Plomaritis and Kate Davis are acknowledged for their assistance in preparing/commenting upon the manuscript and preparing the figures, respectively.

References

DRONKERS, J. 2005. *Dynamics of coastal systems.* Advanced Series on Ocean Engineering, **25**, World Scientific Publishing Co. Pte. Ltd., London.

HOLMAN, R. A. 2001. Pattern formation in the nearshore. *In*: SEMINARA, G. & BLONDEAUX, P. (eds) *River, Coastal and Estuarine Morphodynamics.* Springer–Verlag, Berlin, 141–162.

HORIKAWA, K. 1970. Advanced treatise on coastal sedimentation. *In: Summer Seminar on Hydraulic Engineering*, Japanese Society of Civil Engennrs., 501–534 [in Jananese].

HORIKAWA, K. 1981. Coastal Sediment Processes. *Annual Review of Fluid Mechanics*, **13**, 9–32.

LARSON, M. & KRAUS, N. C. 1995. Prediction of Cross-Shore Sediment Transport at Different Spatial and Temporal Scales. *Marine Geology*, **126**, 111–127.

LIST, J. H., FARRIS, A. S. & SULLIVAN, C. 2006. Reversing Storm Hotspots on Sandy Beaches: Spatial and Temporal Characteristics. *Marine Geology*, **226**, 261–279.

SEYMOUR, R. J. & CASTEL, D. 1985. Episodicity in Longshore Sediment Transport. *Journal of Waterway Port Coastal and Ocean Engineering*, **111**, 542–551.

SOULSBY, R. L. 1987. *The relative contributions of waves and tidal currents to marine sediment transport.* Hydraulic Research Ltd., *Report SR* **125**.

SOULSBY, R. L. 1997. *Dynamics of Marine Sands: A Manual for Practical Applications.* Thomas Telford, London.

Measuring suspended sand concentration using acoustic backscatter: a critical look at the errors and uncertainties

CHRIS E. VINCENT

School of Environmental Sciences, University of East Anglia, Norwich NR4 7TJ, UK (e-mail: c.vincent@uea.ac.uk)

Abstract: Suspended sand concentrations in the near-bed layer of the sea can be estimated using acoustic backscatter systems (ABS) and hence, when combined with velocity, sand transport. ABS measurements are now relatively routine and widely regarded as one of the best tools to help to measure sand transport in coastal seas and estuaries. Potentially the ABS can be used to give estimates of both concentration and sediment size with a vertical resolution of 5–10 mm and a temporal resolution of fractions of a second, but in practice there are many practical limitations to what can be achieved in the field. Often these uncertainties are overlooked or ignored because of the difficulty in estimating their magnitude or of making measurements that are any better. The major limitations and sources of errors in the ABS are discussed, including the influence of sediment size and shape. In moderately to well-sorted sandy environments with appropriate calibration, acoustic estimates of mass concentration should be within $\pm 30\%$ of the true value.

The uncertainties inherent in estimating suspended sediment concentration using ABS in field situations are illustrated using samples from a timed settling tube (TST) in an environment where the bed sediments had a wide range of sizes (mud, silt, fine sand and medium sand). The ABS signal is dominated by backscatter from the sand fractions so the uncertainties can be reduced by calibrating against bed material or sediment from a settling tube sample from which the mud and silt have been removed (hence treating the ABS as a sand-measuring instrument). However changes in the size of the sediment in suspension can result in significant errors (typically $\pm 50\%$ for the field example used here) which, combined with other uncertainties, leads to the conclusion that a factor of 2 is a conservative estimate of the uncertainties associated with the suspended sand concentration. However a major uncertainty in the total sand transport remains the suspended sediment component very close to the bed (below 0.01m) and the bedload itself, which may be an order of magnitude larger than the suspended component.

Acoustic instruments are increasingly the instrument of choice for coastal and deep oceanographic applications. This is exemplified by the use of acoustic doppler current profilers (ADCP) for current profiling both from static moorings and ships and acoustic doppler velocimeters (ADV) for point measurements of turbulence. Acoustic current meters are generally less prone to fouling and are less intrusive (their measurement volume is generally remote from the sensors themselves), as well as having the ability to profile through the water column (e.g. ADCPs). In coastal seas acoustic backscatter (ABS) instruments have been used for many years to measure suspended concentration profiles close (generally within 1 m of the sea bed) and now engineers and oceanographers are beginning to take advantage of the backscattered signal strength recorded by ADCP and ADV instruments to make estimates of the concentration of suspended particulate matter (SPM) in the water column (Heywood *et al.* 1991; Thevenot & Kraus 1993; Hamilton *et al.* 1998; Land & Jones 2001). This expansion of the use of backscatter signals makes the assessment of the likely accuracy of such systems an immediate priority.

In this paper the ABS (an instrument designed to measure concentration) is examined and the affects of various factors on the likely accuracy of the concentration measurements are considered; there will be similar limitations on concentration estimates from ADCPs and ADVs. This paper is designed to be a practical guide to the major sources of errors when using an ABS (or, by extension, an ADCP or ADV). Thorne & Hanes (2002) provide a thorough review of the different applications of the ABS, including the complete equations and their derivations.

Figure 1 shows an example of the suspension patterns seen by the ABS resulting from a wave group over a bed of fine sand. Note the detail shown by the system and the rapid changes in the concentration profile due to resuspension from

From: BALSON, P. S. & COLLINS, M. B. 2007. *Coastal and Shelf Sediment Transport*. Geological Society of London, Special Publications, **274**, 7–15. 0305-8719/07/$15.00

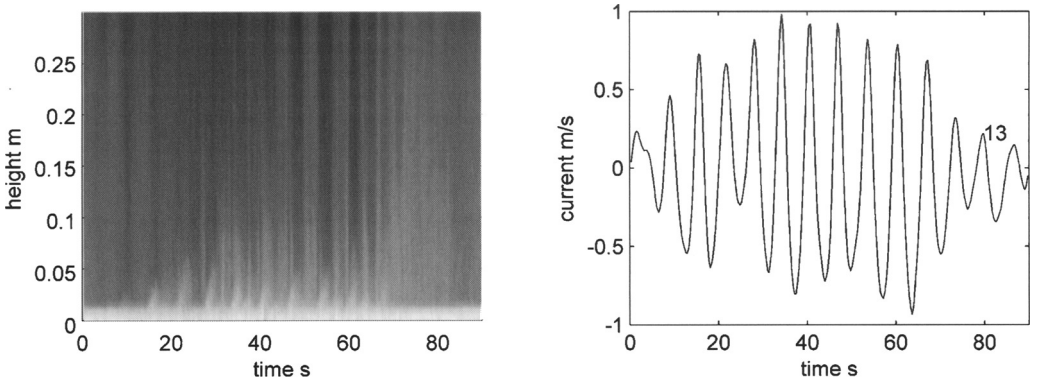

Fig. 1. Gray-scale plot (left panel) of $\log_{10}$(concentration) of fine sand resulting from the passage of a wave group whose oscillatory currents just above the bed are shown in the right panel (white are concentrations >1 g l^{-1}, black < 0.002 g l^{-1}).

the bed, sediment settling and from advection of sand through the ABS beam by the oscillatory motion due to the waves (Vincent & Hanes 2002). The measured concentration varies over a three orders of magnitude, from <0.002 g l^{-1} (black) to >1 g l^{-1} (white) with a very strong echo from the sand bed. But how accurate can we expect these measurements to be? Are they accurate to $\pm 1\%$ or $\pm 10\%$, or should we be even more cautious and suggest they might be correct to only an order of magnitude?

What does the backscattered intensity depend on?

The problem is to invert the backscattered signals from the ABS (or ADCP) into profiles of mass concentration of sediment. In theory this should be a simple process as the physics behind the ABS is well understood (Thorne & Hanes 2002). In addition to the mass concentration of suspended sediment the strength of the acoustic signal depends on system-specific factors such as the acoustic power emitted, the pulse-length and the gain of the receiver amplifiers etc. If all these are kept the same they can be rolled into a single constant that can be determined by calibration. Theoretically, this constant only needs to be determined once at a single range, and the physics should account for range variation and changes in sediment size. Included in this will be the attenuation of sound by water (the absorption of sound increases as frequency increases making it difficult to work in profiling mode at frequencies greater this *c.* >6 MHz) and by the sediment itself; backscatter reduces the intensity of the sound continuing on through the profile so must also be accounted for. The sediment attenuation, usually based on attenuation of spherical particles (see Sheng and Hay 1988), becomes important at higher concentrations (of order of 1 g l^{-1}).

The changes in sediment size are included through the use of a backscatter 'form-function'. The shape of this form-function is complex but basically the sound is backscattered most efficiently by particles that have a similar size to the wavelength of the sound. Figure 2 shows the 'sensitivity' of the sound (form-function^2 / sediment radius) to sediment size, expressed as the ratio of the sediment radius a to the wavenumber k of the sound, where $k=2\pi/\lambda$ and λ is the wavelength), based on the form-function defined by Sheng & Hay (1988) for spherical particles. Unfortunately, real sand is often far from spherical, and shape and density also influence the backscatter (Fig. 3). The practical way of dealing with real sediments is to calibrate the ABS in the laboratory using sand from the field location where the ABS is to be used. The differences can be quite considerable as shown in Figure 3 where an ABS was calibrated initially using sieved (nearly spherical) glass beads (ballotini) and a system constant derived which best fitted the form-function to the ballotini backscatter. When real sand was used (again sieved) the 'apparent' form-function differs significantly for sand whose size is comparable to the acoustic wavelength (for sand significantly smaller that the wavelength of sound shape does not appear to matter).

Quantifying the uncertainties in the ABS system

For the ABS system itself we can be rather confident of the uncertainties. Using sediment

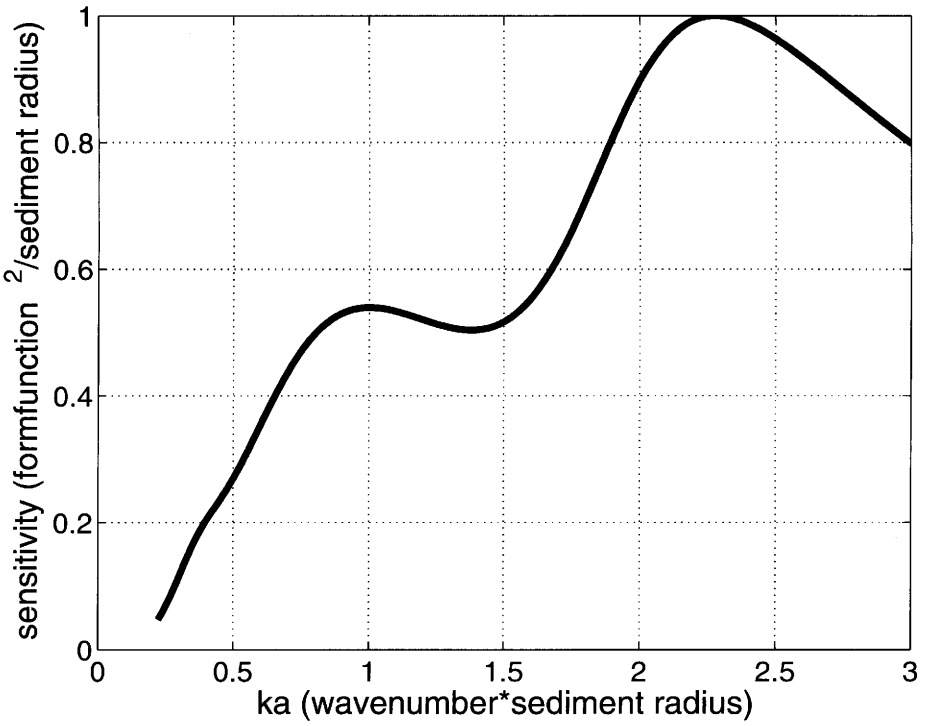

Fig. 2. The sensitivity (form-function^2/sediment radius)of the ABS to sediment size, expressed in terms of the (non-dimensional) product of sediment size a and wavenumber k of the sound.

from the measurement location and a site-specific tank calibration, the uncertainties are about $\pm 20\%$. This value is based on multiple estimates of the calibration constant (A_0) for each individual sand shown in Figure 3; each point typically has an uncertainty of $\pm 10\%$ and the mass concentration depends on A_0^2. Additionally, there is uncertainty associated with the 'configurational noise'. The amplitude of the backscatter from any particular range is due to the sum (both amplitude and *phase*) of the backscatter from many particles (the ABS emits a pulse of sound typically of the order of 10 mm length and the beam is usually several centimetres in diameter). Due to the random phases, the measured amplitude can vary between zero and some maximum value (which would occur when all the backscattered signals were in-phase); hence the 'confidence' in the backscatter of a single pulse (ping) is zero. If the particles in the water are moving around independently then backscattered signals will be Rayleigh-distributed. It is therefore necessary to average many pings to reduce the uncertainty, while still maintaining sufficient time-resolution to see features such as those in Figure 1; the configurational noise is typically $\pm 10\%$ (see Thorne *et al.* 1991; Thorne & Hanes 2002; for further details). Combining these uncertainties gives a value of $\pm 25\%$ as the best accuracy that might be achieved by an ABS.

Practical affects of sediment size on the ABS signal

Of course, in the real world we rarely encounter locations where the sand is unimodal or very well sorted. Usually the sediment will have a wide range of sizes and the sand in suspension will vary in size with height above the bed. Crawford & Hay (1993) discussed the use of multi-frequency ABS to determine size as well as mass concentration but the inversion is fraught with problems (due to the speed at which the size and concentration changes in both turbulent and wave-dominated environments and the limitations imposed by the averaging needed to reduce the configurational noise). Green *et al.* (2004) have had success in using the multi-frequency ABS in an environment with two widely-separated and distinct sand populations: they assumed the presence of the two sizes and used

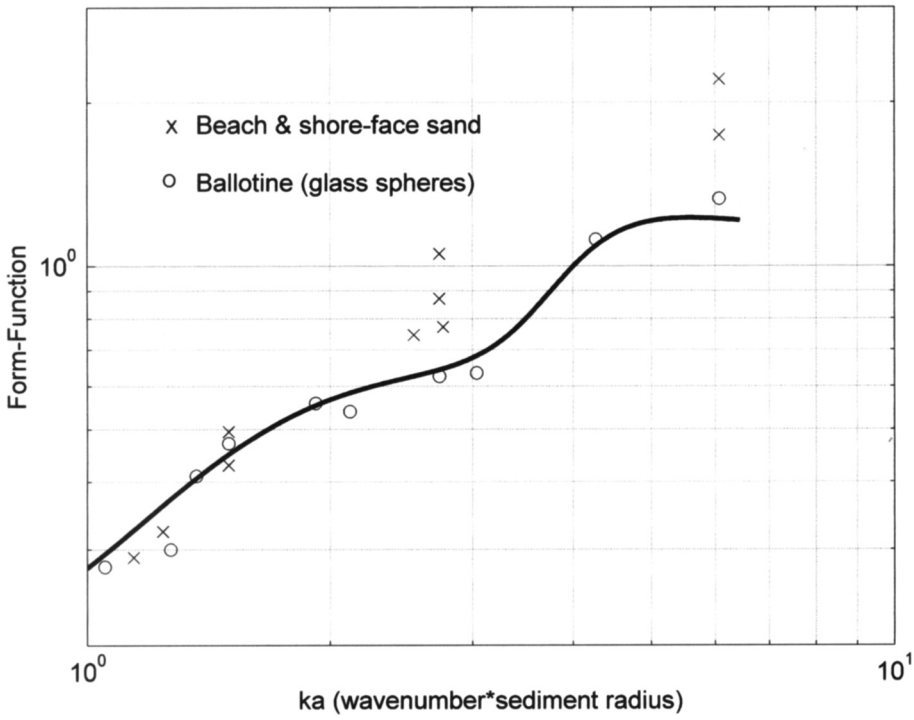

Fig. 3. Laboratory calibrations of the form-function show that glass beads (o) fall close to the theoretical form-function. Beach/shoreface sand (x) (grains are angular and irregular) deviates from this curve when their size is comparable to, or larger than, the wavelength of the sound. The uncertainty of individual values shown here $\pm 10\%$.

the backscatter at two acoustic frequencies to partition the signal between the two sizes. In most cases, however, the ABS (and ADCP or ADV) data are inverted using a single size equal to the modal size of the sample used for calibration.

How much error does such a 'single-size' assumption introduce into the measurement of mass concentration? Figure 4 shows an example of the potential effect of a (steady) combined concentration and size gradient on the ABS calculation of concentration when a constant size is assumed. Figure 4a shows two exponentially decreasing concentration profiles typical of those measured in field experiments (Vincent *et al.* 1991; Lee *et al.* 2002).

$$C(z) = C_0 \exp(-z/h)$$

with reference concentrations $C_0 = 1$ and 5 g l^{-1}, with mixing heights h of 0.075 and 0.10 m, respectively. Both profiles have a size gradient dropping from 350 μm close to the bed to 200 μm at 0.6 m (Fig. 4b). ABS instruments usually operate in the frequency range of 1 to 5 MHz and Figure 4c shows the acoustic signal (nominal units of pressure) seen by 1 MHz and 5 MHz ABS transducers mounted at 0.7 m above the bed. Note how, at high concentrations and longer ranges, the signal strength at 5 MHz drops away rapidly, due to attenuation of sound by the sediment and the water.

Figure 4 (d and e) shows the concentration profiles that are calculated from the four ABS signal-profiles in Figure 4c when the size gradient is neglected. When the 'best-estimate' of size is used (defined as the concentration-weighted size over the whole profile) the errors resulting from neglecting size are small ($< 10\%$). However, it is rare that we will know what the best-size is so the errors have been calculated for an uncertainly of $\pm 20\%$ of this best-size. For 1 MHz the errors range from -28% to $+17\%$, while for 5 Mz the errors range from -21% to $+140\%$. The largest errors occur when (i) the concentration is high (> 1 g l^{-1}) and (ii) the attenuation of the sound due to the sediment is large; under these conditions errors in the estimation of concentration propagate exponentially with range (see Fig. 4e) and may result in physically unreasonable

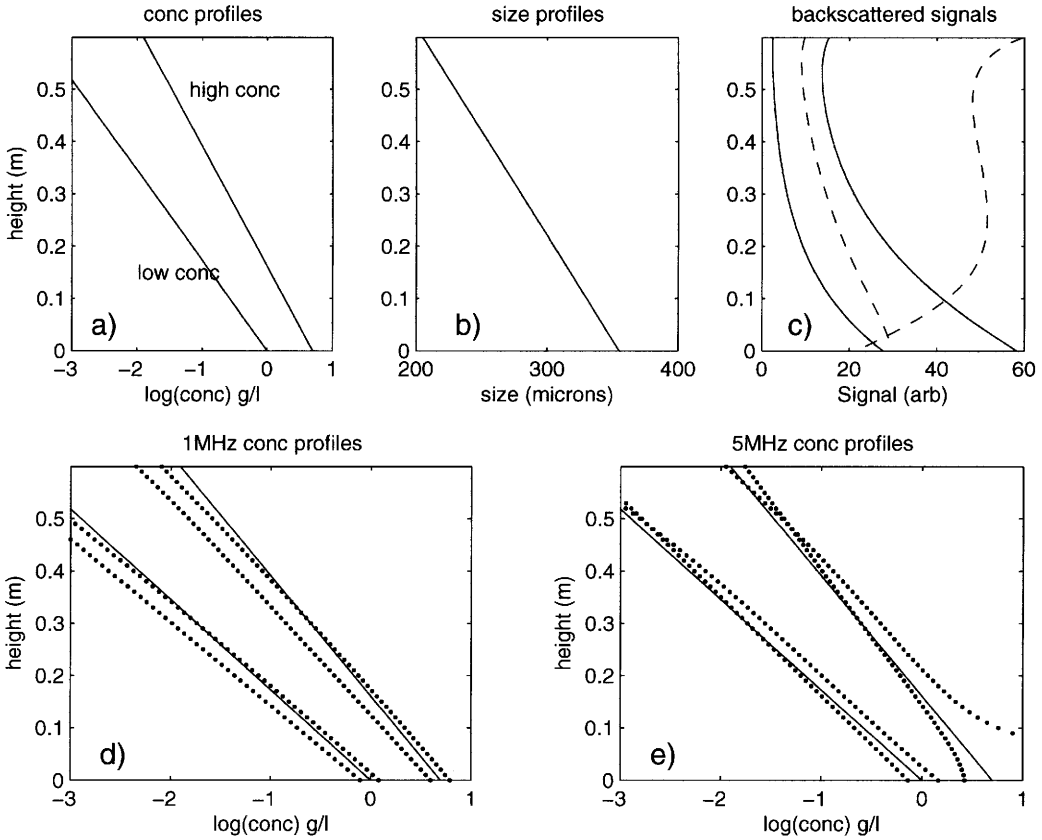

Fig. 4. Two typical concentration profiles (**a**), size profile (**b**) and ABS signal strength (**c**) seen by 1 MHz (solid line) and 5 MHz (dashed) transducers for these concentrations. Profiles calculated (dotted lines) using constant-with-height sizes of 20% greater, and 20% less than the 'best' size estimate for 1 MHz (**d**) and 5 MHz (**e**); (actual profiles are also shown as solid lines).

results. If ABS operating frequencies are kept below 3 MHz sediment attenuation is not so much of a problem for sediment concentration profiles encountered in most coastal environments (e.g. Vincent *et al.* 1991; Lee *et al.* 2002) and errors are typically $\pm 20\%$.

Assuming independence between the uncertainties due to configurational noise, $\pm 10\%$, that due to the calibration, $\pm 20\%$, and errors in our knowledge of the size of the sediment, $\pm 20\%$, the total error is likely to be $\pm 30\%$.

In the field, of course, sediments are rarely well-sorted and rarely just sand. The effects of actual field variations in suspended size have therefore been examined using data from a site where the sediments were know to have a wide range of sizes. The 'actual' suspended sediment was sampled using a 'timed sediment tube' (TST). The TST is a simple passive sedimentation trap that incorporates a timer unit that drops a plastic disk into the tube at defined intervals (Figure 5 and Vincent *et al.* 2003 for a more detailed description). The TST used here was mounted, with its aperture at 0.38 m, on the leg of a benthic lander (Fig. 5) deployed in the southern North Sea by the UK Centre for Environment, Fisheries and Aquaculture Science (CEFAS) at 20 m depth in the southern North Sea. The timing disks were dropped at 24 hour intervals. Bottom sediments in this region were sandy with some silt and mud. Details of the deployment, the analyses of the sediment from the TST and the effects of sediment size on the accuracy of the miniature OBS measurements are given in Vincent *et al.* (2003)

Sediment size analysis (Fig. 6) showed that the suspended sediments consisted of three modes corresponding to mud, fine sand and coarse sand, with a broad silt component between 10 and 40 mm. Rather than consider every size

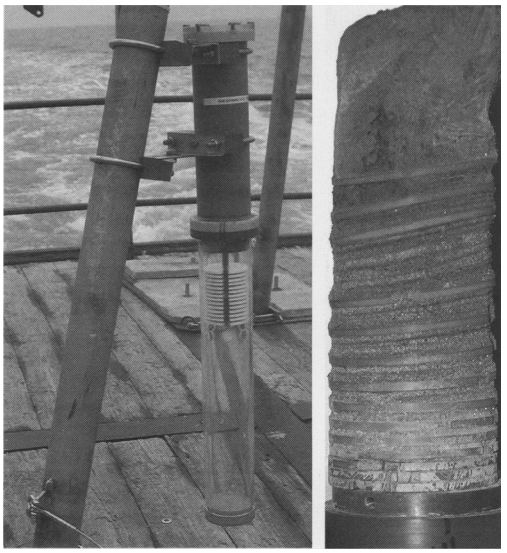

Fig. 5. (Left) The timed settling tube (TST) mounted on the leg of a CEFAS sea bed lander. The apertures can be seen just below the white timing disks. (Right) The sediment core after recovery and removal from the TST. Note the timing disks and the sediment banding.

component in the distribution separately the effects on the uncertainty in the ABS mass concentration of just four components (mud, silt, fine sand and coarse sand) are considered.

The sensitivity of the ABS frequencies used in this deployment (1 and 4 MHz) to sediment size determines the relative contribution of each component to the total backscatter. Applying the Sheng & Hay (1988) form-function to the mass distribution shows that the silt and mud have a negligible influence (Fig. 6) and could be ignored (and the laboratory calibration should use *only* the sand component of the sediment). This is similar to the conclusions for the optical backscatter sensor (OBS) by Vincent *et al.* (2003) which were that the OBS should be calibrated against the mud and slit only, and that, in mixed sedimentary environments, the OBS should be treated as a silt/mud meter. In mixed sedimentary environments the ABS should be treated as a sand-only sensor.

The TST sediment core showed a banded structure (different sediment size distributions, Fig. 5) during some 24 hour periods, corresponding to spring tides and/or wave events. However, even with a clearly-defined time marker, it was often difficult to associate the bands with particular events during a day with high confidence (Fig. 7). The greatest daily sediment accumulation (about 4 cm in thickness) showed 12 bands (Figs 5 and 7). Figure 8 shows the size distribution of the five bands during another day; two sand-rich bands sit between three mud-silt dominated accumulations. The hourly ABS measurements were associated (with a degree of subjectivity) with bands within the TST core (Fig. 7) and two calculations performed. The first used the calibration of the ABS with bulk-sediment from the TST; the second used the two sand fractions, in the proportions found in the appropriate TST band. The difference in the two estimates is a measure of the likely uncertainty or error associated with the temporal variations in the size of sand in suspension on the ABS concentration estimates. Table 1 shows the standard

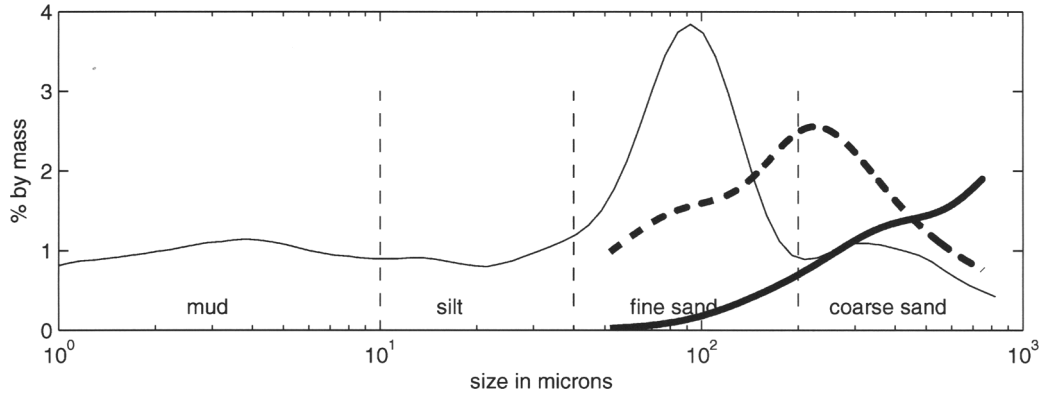

Fig. 6. The size distribution by mass for the bulk sample in the timed sediment tube, also showing the relative sensitivities (defined as form-function^2/sediment radius) of the ABS at 1 MHz (heavy line) and 5 MHz (heavy dashed line) to the sediment in suspension.

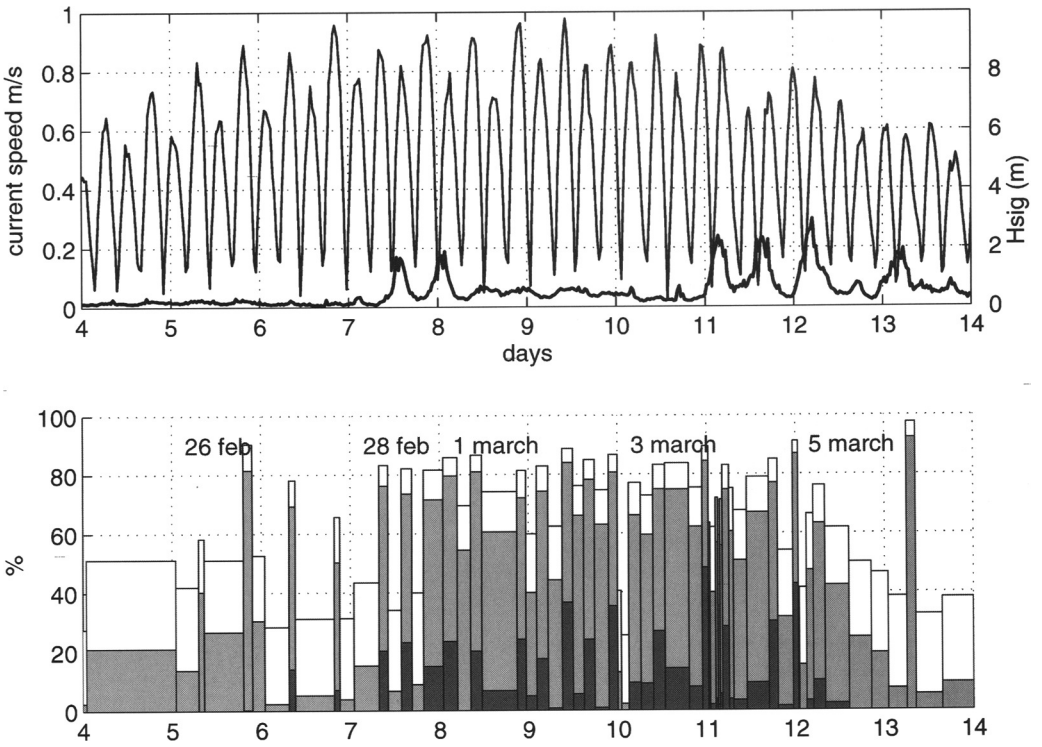

Fig. 7. Top panel burst-average tidal currents speeds and significant wave heights for the period 25 Feb to 6 March. Lower panel: proportion of coarse sand (dark grey), fine sand (light grey), silt (white) and mud (the remainder) for the bands within the TST core.

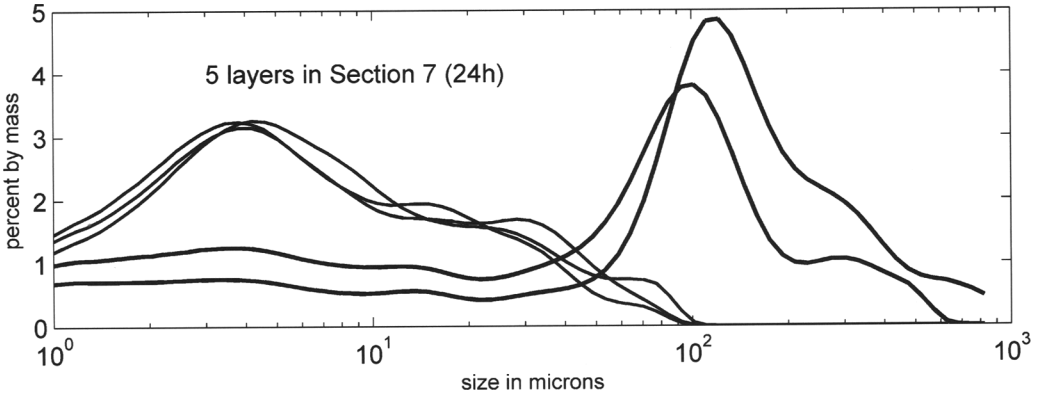

Fig. 8. The size distributions from the TST sediment of the five bands (interleaved fine/coarse) in one 24 hour period.

deviation of the differences between the two estimates for all 625 ABS runs, firstly using the full sample (including mud and silt), secondly with sand only.

Discussion and conclusions

The overall uncertainty of ABS measurements of suspended sand results both from inherent

Table 1. *The normalised range (max/min) and standard deviation (%) of the concentration estimates obtained using the TST core samples compared to values using the core-average size distribution*

[652 Observations]	Whole Sample (silt-mud-sand)		Sand component only	
	Range	St Dev (%)	Range	St Dev (%)
ABS (1MHz)	2000	110	35	**87**
ABS (4MHz)	45	65	2.5	**18**

The last two columns show the comparative values when the ABS is used to estimate the sand (fine + medium) fractions only.

factors associated with acoustic backscatter and from natural variability in the scatterers found in marine environments. The ABS system uncertainties of $\pm 25\%$ are somewhat smaller than the errors that are likely to result from the variations in sediment size for field applications; marine measurements from the TST suggest uncertainties, based on ± 1 standard deviation, of the order of $\pm 50\%$. Combining these uncertainties suggests that backscattered estimates of suspended sand are likely to be correct to better than a factor of 2.

There are a number of other sources of errors that can also be important. Both bubbles and fish are very effective at scattering sound so the surf zone should be avoided. Fish can also be a problem; experience shows that fish can seek out the shelter provided by downward-looking ABS transducers particularly during calm conditions. Video pictures of an ABS underwater on the shoreface at Duck, N. Carolina show fish maintaining their position directly below the transducers (D. M. Hanes, pers. comm.).

The ABS and the ADCP are profiling instruments and can, in theory, measure over the whole suspended sediment profile. In practice, neither the ADCP nor the ABS is good at measuring very close to the seabed where the sediment concentrations are highest. The ADCP has relatively large measurement volumes and the angled beams, essential for the measurement of current speed that result in an angled intersection with the seabed and unwanted echoes from the side lobes. Even the ABS, with its single narrow, vertical beam has difficulty with the exact location of the seabed (rather the problem is distinguishing between backscatter from the high concentration very close to the bed and from the bed itself). Green *et al.* (1999) suggested that looking at the 'break-in-slope' provided a useful mechanism for identifying the backscattered signal closest to the bed that was uncontaminated by the bed echo. This method has an uncertainty of at least ± 1 bin (usually ± 10 mm) associated with it but may be much greater. A very informative study by Dohmen-Janssen & Hanes (2002) compared the transport (the product of the concentration and the grain velocity) in the sheet-flow layer (-4 mm to $+11$ mm) over a flat bed with the transport in the suspension layer and found that the sheet flow layer contributed 90% of the total flux. If this conclusion is valid for general marine conditions where the bed is rarely flat and bed forms abound, the uncertainties in the ABS measurements of suspended sand concentrations are relatively insignificant.

References

CRAWFORD, A. M. & HAY, A. E. 1993. Determining suspended sand size and concentration from multifrequency acoustic backscatter. *Journal of the Acoustical Society of America*, **94**, 3312–3324.

DOHMEN-JANSSEN, C. M. & HANES, D. M. 2002. Sheet flow dynamics under monochromatic nonbreaking waves. *Journal of Geophysical Research*, 10.1029/2001JC001045.

GREEN, M. O., DOLPHIN, A., SWALES, A. & VINCENT, C. E. 1999. Transport of mixed-size sediments in a tidal channel, *In*: KRAUS, N. C. & MCDOUGAL, W. G. (eds) *Coastal Sediments '99*. ASCE, Long Island, New York, 644–658.

GREEN, M. O., VINCENT, C. E. & TREMBANIS, A. C. 2004. Suspension of coarse and fine sand on a wave-dominated shoreface, with implications for the development of rippled scour depressions, *Continental Shelf Research*, **24**, 317–335, 2004.

HAMILTON, L. J., SHI, Z. & ZHANG, S. Y. 1998. Acoustic backscatter measurements of estuarine suspended cohesive sediment concentration profiles. *Journal of Coastal Research*, **14**, 1213–1224.

HEYWOOD, K. J., SCOPE-HOWE, S. & BARTON, E. D. 1991. Estimation of zooplankton abundance from shipborne ADCP backscatter. *Deep-Sea Research*, **38**, 677–691.

LAND, J. M. & JONES, P. D. 2001. Acoustic measurement of sediment flux in rivers and near-shore waters. *In*: *7th Federal Interagency Sedimentation Conference*, Reno, Nevada, 127–134.

LEE, G.-H., FRIEDRICHS, C. T. & VINCENT, C. E. 2002. Examination of diffusion versus advection dominated sediment suspension on the shoreface under storm and swell conditions. *Journal of Geophysical Research*, **107** (C7), doi:10.1029/2001JC000918.

SHENG, J. & Hay, A. E. 1998. An examination of the spherical scatter approximation in aqueous suspensions of sand. *Journal of the Acoustical Society of America*, **83**(2), 598–610.

THEVENOT, M. M. & KRAUS, N. C. 1993. Comparison of acoustical and optical measurements of suspended material in the Chesapeake Estuary. *Journal of Marine Environment Engineering*, **1**, 65–79.

THORNE, P. D. & HANES, D. M. 2002. A review of acoustic methods for the study of small scale sediment transport processes. *Continental Shelf Research*, **22**, 603–632.

THORNE, P. D., VINCENT, C. E., HARDCASTLE, P. J., REHMAN, S. & PEARSON, N. 1991. Measuring suspended sediment concentrations using acoustic backscatter devices. *Marine Geology*, **98**, 7–16.

VINCENT, C. E. & HANES, D. M. 2002. The accumulation and decay of nearbed suspended sand concentration due to waves and wave groups. *Continental Shelf Research*, **22**, 1987–2000.

VINCENT, C. E., HANES, D. M. & BOWEN, A. J. 1991. Acoustic measurements of suspended sand on the shoreface and the control of concentration by bed roughness. *Marine Geology*, **96**, 1–18.

VINCENT, C. E., BASS, S. J. & REES, J. M. 2003. Uncertainties in suspended sediment concentration and transport due to variations in sediment size. In: *Proceedings of the International Conference on Coastal Sediments 2003*. World Scientific Publishing Corp. and East Meets West Productions, Corpus Christi, Texas, USA.

Sorption of lanthanum onto clay minerals: a potential tracer for fine sediment transport in the coastal marine environment?

K. L. SPENCER[1], S. L. JAMES[2], J. A. TAYLOR[1] & T. KEARTON-GEE[3].

[1]*Geography Department, Queen Mary, University of London, Mile End Road, Londen E1 4NS, UK (e-mail: k.spencer@qmul.ac.uk.)*

[2]*Department of Mineralogy, The Natural History Museum, Cromwell Road, London SW7 5BD, UK*

[3]*School of Geography, Earth and Environmental Sciences, University of Birmingham, Edgbaston, Birmingham B15 2TT, UK*

Abstract: In order to improve predictions of coastal morphological response to sea-level rise and sustainably manage dredged sediment there is an urgent need to develop a field methodology that can measure accurately transport pathways of the <63 μm sediment fraction in coastal and estuarine environments. Techniques such as sediment trend analysis and sediment tracing using fluorescent sands are well established for the silt and sand fraction but are unsuitable for clay sediments due to their cohesive nature. Geochemically labelled clays have been used as fine sediment tracers in freshwater environments with some success, although little is known about their chemical or physical behaviour once released in saline environments.

A number of pure clays and natural estuarine sediments were labelled with La following agitation in a 0.01M solution of La Cl_3. In order to examine the retention of La on the clay mineral surface the labelled sediment was washed sequentially four times using both de-ionised water and artificial seawater. A labelled bentonite retained 43000 μg g^{-1} La and this was only reduced to 36000 μg g^{-1} La after washing in seawater. This suggests that retention of La is good even in saline conditions and concentrations of La are high enough to enable detection after considerable signal dilution. Sorption of La is dependent predominantly upon the cation exchange capacity of the sediment.

Understanding dispersion patterns for the fine sediment fraction (<63 μm) and its associated contaminants is of fundamental importance to the sustainable management of coastal and marine resources. Information on sediment transport pathways can be used to improve predictions of coastal morphological response to extreme events such as storm surges and sea level rise, as well as coastal engineering schemes. Recent trends towards the beneficial re-use of dredged sediment for inter-tidal habitat re-creation and the adoption of new dredging techniques such as water injection dredging, mean that understanding fine sediment transport is more pertinent than ever. Consequently, understanding and managing fine sediment transport in estuarine and coastal waters is of increasing importance to local authorities, port and harbour authorities and central government.

The prediction of sediment dispersion in the coastal zone relies on accurate and reliable techniques for the measurement of sediment transport pathways. Historically, this role has been fulfilled by the use of sediment tracing techniques using fluorescent sands (Voulgaris *et al.* 1998) and sediment trend analysis (McLaren & Bowles 1985; Gao & Collins 1992, 1994). These techniques are relatively well established, but due to the cohesive nature of clays are unsuitable and inaccurate for measuring transport pathways of fine grained sediments. The release of short-lived radionuclides into the natural environment has previously been used for tracing the dispersion and transport of the fine sediment fraction (Courtois & Monaco 1969; Heathershaw & Carr 1978). However, there is increasing reticence to use such environmentally sensitive techniques and it is unlikely that a discharge licence would be granted by the Environment Agency of England and Wales. Therefore, there is a need to develop and trial a methodology suitable for studying the dispersion and transport of the <63 μm fraction and in particular the clay component. It is important that the tracer developed should: (1) be easily detectable using routinely available analytical

From: BALSON, P. S. & COLLINS, M. B. 2007. *Coastal and Shelf Sediment Transport*. Geological Society of London, Special Publications, **274**, 17–24. 0305-8719/07/$15.00

techniques; (2) be environmentally benign; and (3) have physical properties similar to the sediment it is intended to mimic.

Labelling clay minerals for use as environmental sediment tracers has received some interest in the past. Iridium-labelled sediments have been used to investigate the redistribution of marine sediments (Yin *et al.* 1993) and lanthanide-labelled clay particles have been used successfully to determine sediment transport pathways in karst systems (Mahler *et al.* 1998) and in lake sediments (Krezoski 1989). The lanthanide group of elements (also known as the rare earth elements, REEs) all have similar properties and can be incorporated easily into the clay-mineral lattice as they are trivalent and have similar ionic radii to Ca^{2+}. Previous research has shown that lanthanides are accepted readily into the montmorillonite lattice and up to 100% of the cation exchange capacity (CEC) can be achieved (Bruque *et al.* 1980). Mahler *et al.* (1998) also found that the retention of lanthanides in saline conditions was good and that they may be suitable for use in coastal marine environments. Additionally, lanthanides have been used as geochemical tracers for groundwater mixing (Johanesson *et al.* 1997), to investigate the dynamics of soils (Braun *et al.* 1998; Matisoff *et al.* 2001; Zhang *et al.* 2003; Xue *et al.* 2004) and as chemical analogues to study the uptake of trivalent actinides in the field of storage/disposal of nuclear waste (Chapman & Smellie 1986). Consequently, there has been considerable work looking at sorption mechanisms including the irreversibility of sorption (Miller *et al.* 1983), migration into the clay structure (Miller *et al.* 1982) and the effect of pH (Bruque *et al.* 1980). However, there is still uncertainty concerning whether sorption leads to fractionation of the lanthanide group and little is known about the nature of the chemical bonds between metal cations and the clay structure (Coles & Yong 2002; Coppin *et al.* 2002). There are a limited number of studies reporting partitioning coefficients of REEs between clay minerals and aqueous solutions (Sinitsyn *et al.* 2000) and applications in the saline environment have not been studied in any detail.

Here, we have investigated whether the use of La-labelled clays and natural sediments may be suitable for use as a tracer of fine sediment in the estuarine environment. Dispersion in the estuarine environment means that once the tracer sediment is released, the tracer element signal will be diluted considerably. Hence, one of the key aims of this project is to determine whether sufficiently high concentrations of sorbed La are achievable in labelled sediments to enable their use as sediment tracers. As the tracer element may be exchanged with competing cations in saline environments, a second aim is to ascertain the extent of La desorbtion when exposed to both freshwater and saline conditions.

Methodology

Two samples of natural estuarine sediment were collected from an area of mud flat and vegetated salt marsh the Medway Estuary, Kent, representing sediments with both low and high organic content respectively. These sediments have been previously studied in detail (Spencer 2002) and the $<2\,\mu m$ fraction has the approximate composition: smectite (49%), kaolinite (22%), illite (27%) and chlorite (2%). Samples of bentonite, smectite, kaolinite, phlogopite and illite were also used in order to determine the effect of clay mineral type and cation exchange capacity (CEC) on La sorption. A 1% sediment suspension was prepared by adding 2.5 g of oven-dried, crushed sediment to 250 ml of 0.01M $LaCl_3$ solution. The pH of the suspension was recorded and the sediments were then left to equilibrate before being shaken for 30 minutes using a mechanical wrist shaker. The suspension was then centrifuged at 3000 rpm for 15 minutes. The pH of the supernatant was recorded and retained for analysis by inductively coupled plasma optical emission spectrometry (ICP OES) using a Perkin Elmer Optima 3300RL. In order to determine whether La was desorbed from the labelled sediment when exposed to a freshwater environment, the labelled sediment samples were washed sequentially four times with de-ionised water. After each wash, the suspension was shaken for 30 minutes and then centrifuged at 3000 rpm for 15 minutes. The pH of the supernatant wash was recorded and the wash retained for analysis by ICP-OES. Initially, the labelled sediments were washed eight times, however La concentrations were consistently below 1 mg L^{-1} after four washes and therefore this was considered sufficient. In order to mimic the re-suspension of the labelled sediment in saline waters, the sediments were also washed in artificial seawater made up to the manufacturer's recommendations (Tropic-Marin™). The CEC of both the pure and natural sediments was calculated following the US EPA 9081 method (US Environmental Protection Agency 2005). Total La concentrations were determined in the sediments before labelling and after washing in de-ionized and in saline water using a total HF–$HClO_4$–HCl dissolution technique (Thompson & Walsh 1989). Resultant digestates were analysed by ICP-OES.

Precision was determined by carrying out all labelling experiments in triplicate and was generally < 5% relative standard deviation (RSD) for La concentrations in sediment analyses, < 2% RSD in the supernatant, but very variable in the sample washes. Accuracy was assessed by analysing in-house reference materials and was between 12 and 16% bias. The in-house reference materials used were prepared from four igneous rock samples representing a range of major and trace metal concentrations.

Results and discussion

Equilibration times for the sorption of REEs onto clay minerals used in the literature vary considerably from 10 minutes (Bonnot-Courtois & Jaffrezic-Renaut 1982) to 72 hours (Coppin *et al.* 2002). In this study a preliminary experiment was completed where bentonite was equilibrated with 0.01 M $LaCl_3$ for 30 minutes, 1 hour, 24 hours and 1 week. The amount of La sorbed onto the clay mineral surface was calculated from the decrease in aqueous La concentration at the end of the experiment. This calculation assumes that any La removed from solution is removed due to sorption on the clay mineral surface and/or migration to the mineral lattice and not due to loss from precipitation or sorption onto the container walls. It is possible that La hydroxide may be precipitated during sorption experiments and this is discussed in detail later in this paper. The sorption coefficient, K_d, values (in ml g^{-1}) have been normalised to the solution volume/solid mass ratio as used by Coppin *et al.* (2002) and shown in Equation 1.

$$K_d = \frac{(C_{initial} - C_{final})}{C_{final}} \frac{V}{M} \quad (1)$$

where,

K_d = solid/solution partitioning coefficient (ml g^{-1})
$C_{initial}$ = aqueous concentration of La at the beginning of the experiment (mg L^{-1})
C_{final} = aqueous concentration of La in the supernatant (mg L^{-1})
V = solution volume (ml)
M = mass of the solid (g)

Figure 1 shows the K_d values for La for the timed equilibration experiments. The results indicate that equilibrium between the La aqueous solution and the clay fraction was not achieved after 168 hours, although the K_d values increase rapidly after 1 hour. This would suggest that equilibration times in excess of 1 week are required. If we consider the La sediment concentrations rather than K_d values, a final La sediment concentration of 44 000 μg gDW^{-1} (dry weight) was achieved after the sediment had been equilibrated for 30 minutes and this only increased to 46 000 μg gDW^{-1} after 1 week. This demonstrates that La uptake may increase with equilibration times in excess of 168 hours and this is in disagreement with other workers who have shown the REE uptake by clay minerals is complete after as little as 5 minutes (Aja 1998). However, the increase in the final La sediment concentration is minimal after 24 hours. Consequently, we equilibrated the La solution and all the sample clays for 24 hours before shaking and centrifuging the samples the following day. It should be noted that it may be inappropriate to apply K_d values calculated for bentonite to the other clay minerals used in this experiment, however this does give an approximate guideline as to equilibration times needed.

Coppin *et al.* (2002) have also suggested that some clays may undergo dissolution during

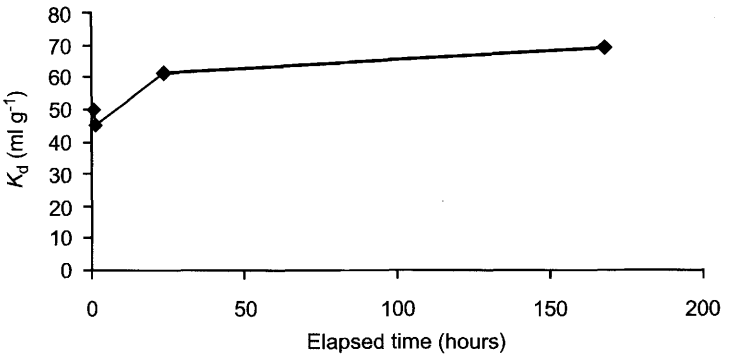

Fig. 1. Calculated K_d values for La and bentonite as a function of elapsed time.

sorption experiments. This would release elements present in the aluminosilicate clay mineral lattice to aqueous solution including Al and any La naturally present in the clay minerals. Therefore K_d values may be decreased due to this additional input of La to aqueous solution. Here, Al is present in both the supernatant and consequent washes at low concentrations (<1 mg l^{-1}) for the freshwater washes and below detection limits for the majority of the saline washes. Dissolution of clays is largely pH dependent and loss of Al due to the dissolution of montmorillonites occurs only at pH values <2 (Bruque *et al.* 1980). In the present study pH values of the initial sediment suspension were >4. This suggests that dissolution of the clay minerals is likely to be minimal and has not been considered further.

Total La concentrations for each of the sediments studied are given in Table 1 and demonstrate considerable variation in the natural concentrations of La in the sample materials. Concentrations of La in the sediments collected from the Medway Estuary are similar to those analysed in other estuarine sediments (e.g. Weltje *et al.* 2002). In order to determine whether La would be desorbed from the sediments when exposed to either freshwater or saline environments the total La concentration in sediments before and after labelling have also been compared (Table 1). All sediments show significant increases in the amount of La present after labelling and this is retained to varying extents after subsequent washing in both fresh and saline waters. The highest La concentrations are present in bentonite, with a concentration of 43 200 μg gDW^{-1} after washing in de-ionized water only decreasing to 36 000 μg gDW^{-1} after repeated washing in saline water. The lowest concentrations of La are present in kaolinite with concentrations of 1900 μg gDW^{-1} after washing in de-ionized water. Concentrations of La in all the samples, with the exception of kaolinite, decrease in the sediments that have been washed in saline water with respect to washing in de-ionized water. This suggests that for most of the sediments La is desorbed to some extent under saline conditions and in the presence of a high concentration of competing cations. The loss of La due to desorption varies from 17% for bentonite to 49% for phlogopite. This again suggests that bentonite may be the most effective clay for retaining La in both fresh and saline conditions. The different behaviour of kaolinite may be due to the nature of the mineral lattice. The CEC of kaolinite is controlled primarily by pH dependent charges arising from broken bonds along mineral edges (Coles & Yong 2002). Consequently the concentration of metal cations sorbed to the mineral surface is strongly dependent upon changes in ambient pH. In the present study the differences in the amount of La sorbed after washing in saline and fresh water environments may have been due to variations in the pH. Most authors who have studied partitioning coefficients between clay minerals and REEs in aqueous solutions have also noted a dependency on the ionic strength of the REE solution. Beall *et al.* (1979) studied the uptake of La in NaCl solutions buffered to pH 5 and they found that metal uptake decreased with increasing ionic strength. However, they did not consider the effects of competing metal complexation in the saline environment.

If chemical parameters during sorption are optimised, it is possible that 100% of the CEC can be achieved. Table 1 shows the percentage of CEC occupied by La after desorption in both fresh and saline environments assuming that all

Table 1. *Total sediment La concentration after shaking in de-ionized water (FW) and saline water (SW) and % of CEC (in milliequivalents) occupied by La after desorption in de-ionized water (FW) and saline water (SW)*

	La in mg $kgDW^{-1}$*	La in mg $kgDW^{-1}$ (FW)	La in mg $kgDW^{-1}$ (SW)	CEC in meq $100g^{-1}$	La as % of total CEC (FW)	La as % of total CEC (SW)
Bentonite	57	43200	36000	121	75	64
Illite	49	NA	9600	30	NA†	70
Kaolinite	7	1900	5100	22	19	51
Smectite	28	20600	16000	58	76	59
Phlogopite	4	8500	4300	27	68	34
Natural sediment 1 (low organic content)	36	16900	13200	44	77	60
Natural sediment 2 (high organic content)	39	19200	13600	65	64	46

*Natural La concentration in sediments, NA, data not available.

the La present is sorbed to cation exchange sites. This indicates that higher La concentrations in the final labelled sediments could be achieved if the chemical parameters for partitioning and equilibrium are examined for each of the clay sediments in detail. Metal uptake onto clay mineral surfaces may be a function of pH, ionic strength of the solution and the initial concentration of the sorbant in aqueous solution (Sinitsyn *et al.* 2000). Additionally, these factors are influenced by both the type of clay and the lanthanide element used. However, there are a limited number of studies reporting optimum chemical parameters for the partitioning of REEs between clays and aqueous solution. Bruque *et al.* (1980) examined the sorption of La onto montmorillonite and found that maximum sorption was achieved between pH values of 4–5, while at values >5, precipitation of La hydroxide may occur. Whilst Sinitsyn *et al.* (2000) found that maximum uptake of Eu and Nd onto illite occurred at pH values >5. In the present study, pH values of the initial sediment suspension were between 4 and 5 and pH values of the washes increased as the solutions were not buffered. Thus, a decrease in La concentrations in sediment washes (Fig. 2) may be an indication of La hydroxide precipitation and increases in total La concentrations in the final labelled sediments may be due to the presence of precipitated La hydroxide. Lanthanum concentrations in wash solutions show a strong relationship with pH and the sorption edges as a function of wash pH (fresh water washes) are given in Figure 3. This shows that La concentrations in the wash solution decrease significantly at a pH value of between 5.5 and 6. This is in agreement with the sorption edge data for saline washes, although the data are incomplete and are therefore not presented.

In order to determine whether La hydroxide was being precipitated out during washing, labelled sediments were investigated using semi-quantitative scanning electron microscopy (SEM) with Link Isis energy dispersive x-ray analysis (Hitachi S-3000-N SEM). Discreet particles with a micro-crystalline structure were observed adhered to the surfaces of clay particles in both fresh and saline washed sediments. Figure 4 shows a SEM image for bentonite and the accompanying element distribution map clearly shows that the crystalline structures are La rich. The sediments were also analysed using x-ray diffraction (XRD), however diffraction traces were not observed for La hydroxide or any other commonly occurring La salts. This suggests that although some of the total La concentrations in labelled sediments may be attributed to the presence of La hydroxide, concentrations are low and can not be detected by XRD analysis. One of the primary mechanisms for the sorption of metal cations to clay mineral surfaces is due to cation exchange. Scatterplots of CEC against total La concentration in labelled sediments from both fresh water and salt water washes are shown in Figure 5. These indicate that

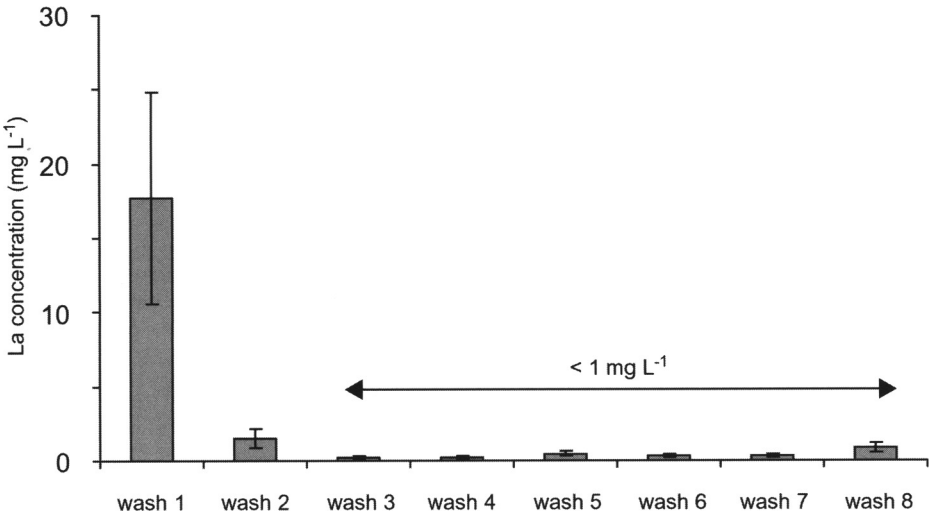

Fig. 2. Lanthanum concentrations in sequential fresh water sediment washes.

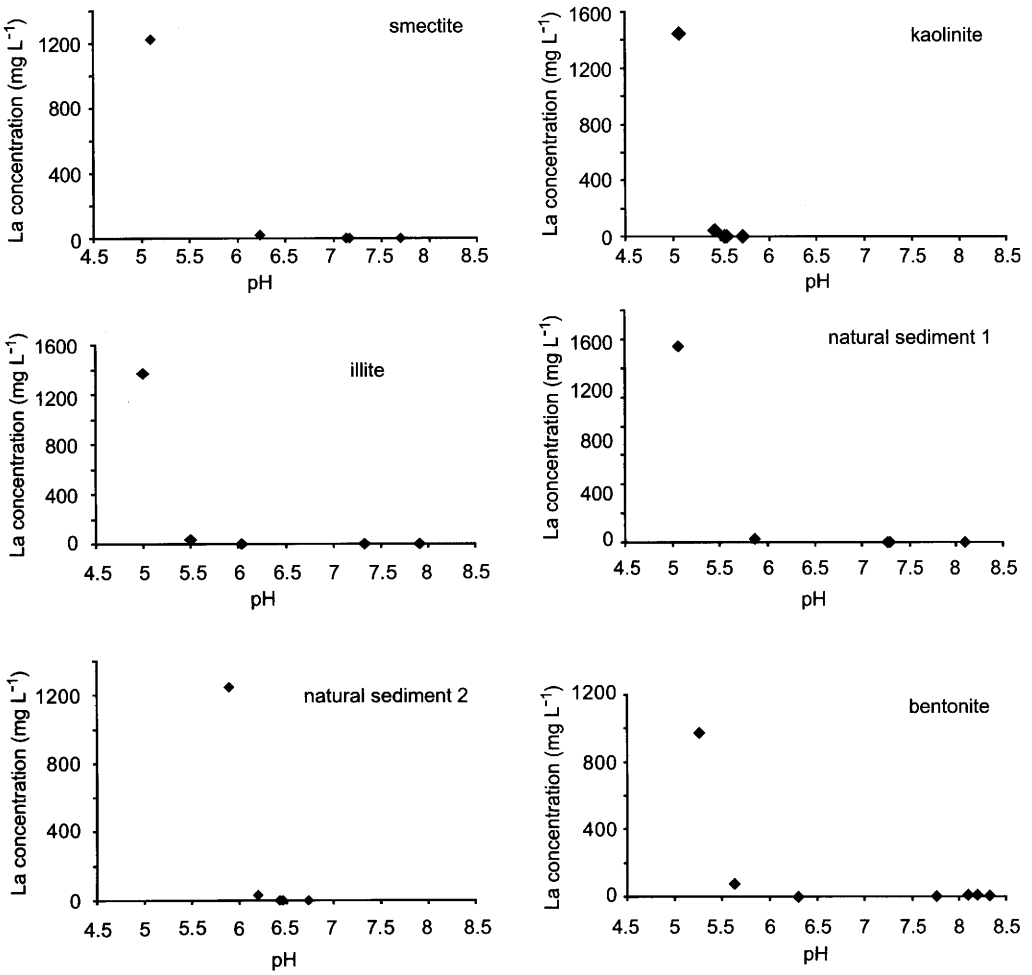

Fig. 3. Relationship between La concentrations in sequential saline sediment washes and pH.

total sediment La concentration is controlled strongly by the CEC of the sediment with correlation coefficients of $r=0.99$ for freshwater washes and $r=0.98$ for salt water washes. This indicates that although La hydroxide is present in the labelled sediments, it probably does not contribute significantly to the final total La concentrations. Consequently, the K_d values calculated earlier in this paper are also valid. These scatterplots also demonstrate that CEC and hence sediment type is probably the most important controlling factor for La sorption. Hence, the clay mineral used as a potential sediment tracer must be selected carefully.

Summary and conclusions

The concentration of La in labelled sediments indicates that metal uptake is strongly dependent upon CEC and hence sediment type. In these experiments the highest concentrations of La were sorbed to bentonite. Concentrations in excess of 40 000 μg gDW^{-1} can be achieved easily and may be improved by carefully controlling the chemical parameters of the sorption process. The precipitation of La hydroxide may occur during the labelling process but is unlikely to contribute significantly to the total La concentrations recorded in the labelled sediments. Under saline conditions La is desorbed to a small extent

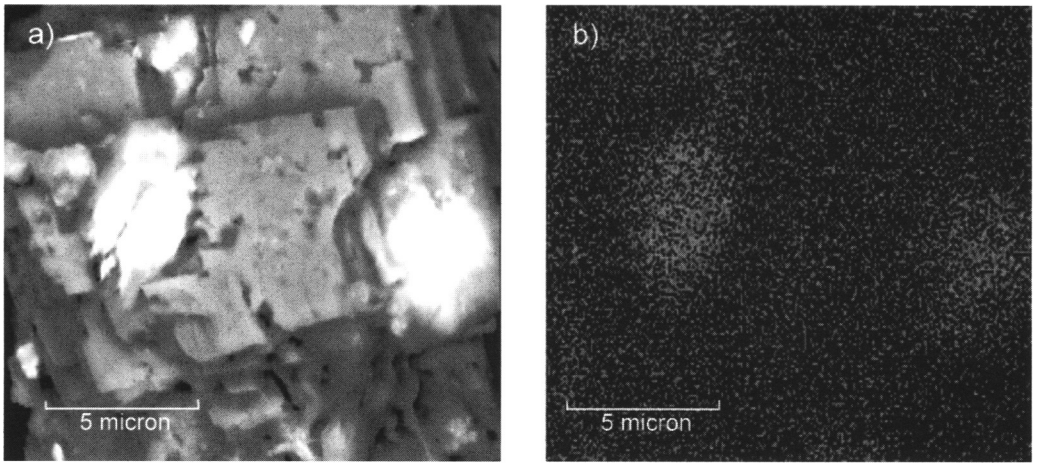

Fig. 4. (**a**) SEM image of bentonite and (**b**) element distribution map for La.

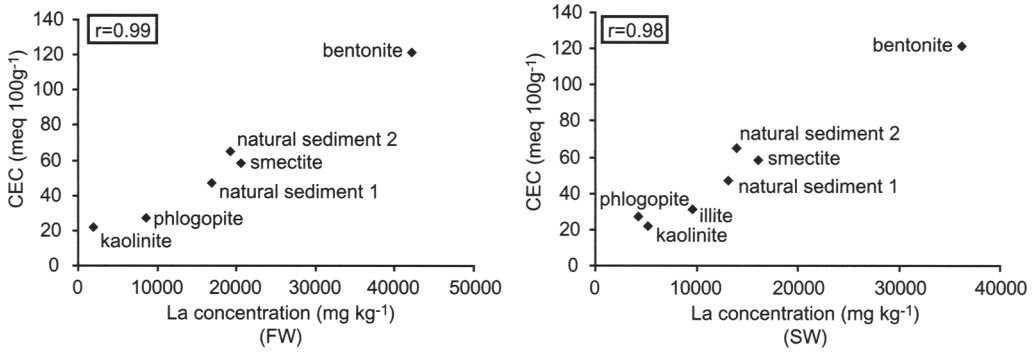

Fig. 5. Scatterplots of CEC against total sediment La concentration for fresh water (FW) and salt water (SW) washed sediments.

in the presence of competing cations, but total La concentrations in the labelled sediment are still in excess of 35 000 μg gDW^{-1}.

In order to use successfully geochemically labelled sediment as a tracer of the fine-grained sediment fraction, concentrations of the geochemical label must be high enough to allow routine detection even after the sediment has dispersed. We have estimated that the tracer signal must be detectable after dilution by a factor of 10^6 to 10^9 in the estuarine system. Using pre-concentration, detection limits of 1 ng g^{-1} are achievable for most lanthanide group elements using inductively coupled plasma mass spectrometry (Jarvis 1988, 1989). Consequently we should be able to detect our tracer after dispersion, although La concentrations will be near the instrumental detection limit. It may, however, be difficult to distinguish the tracer signal from natural background concentrations within estuarine and coastal sediments. Further investigation is required as to the use of alternative lanthanide group elements that have lower natural background concentrations and the use of REE ratios that are more diagnostic than single element signatures alone.

This project was funded by a NERC Connect A grant (NER/E/S/2002/00022).

References

AJA, S. U. 1998. The sorption of the rare earth element, Nd, onto kaolinite at 25 °C. *Clays and Clay Mineralogy*, **46**, 103–109.

BEALL, G. W., KETELLE, B. H., HAIRE, R. G. & O'KELLY, D. G. 1979. Sorption behaviour of trivalent actinides and rare earths on clay minerals. In: FRIED, S. (ed.) *Radioactive Waste in Geological Storage.* ACS Symposium Series, **100**, 201–213.

BONNOT-COUTOIS, C. & JAFFREZIC-RENAUT, N. 1982. Etude des échanges entre terres rares et cations interfoliaires de deux argiles. *Clay Mineralogy*, **17**, 409–420.

BRAUN, J. J., VIERS, J., DUPRE, B., POLVE, M., NDAM, J. & MULLER, J. P. 1998. Solid/liquid REE fractionation in the lateric system of the Goyoum, East Cameroon: the implication for the present dynamics of the soil covers of the humid tropical regions. *Geochimica et Cosmochimica Acta*, **62**, 273–299.

BRUQUE, S., MOZAZ, T. & RODRIGUEZ, A. 1980. Factors influencing retention of lanthanide ions by montmorillonite. *Clay Minerals*, **15**, 413–420.

CHAPMAN, N. A. & SMELLIE, J. A. T. 1986. Introduction and summary of the workshop: natuaral analogues to the conditions around a final repository for high-level radioactive waste. *Chemical Geology*, **55**, 167–173.

COLES, C. A. & YONG, R. N. 2002. Aspects of kaolinite characterisation and retention of Pb and Cd. *Applied Clay Science*, **22**, 39–45.

COPPIN, F., BERGER, G., BAUER, A., CASTET, S. & LOUBET, M. 2002. Sorption of lanthanides on smectite and kaolinite. *Chemical Geology*, **182**, 57–68.

COURTOIS, G. & MONACO, A. 1969. Radioactive methods for the quantitative determination of coastal drift rate. *Marine Geology*, **7**, 183–206.

GAO, S. & COLLINS, M. B. 1992. Net sediment transport patterns inferred from grain-size trends, based upon definition of "transport vectors". *Sedimentary Geology*, **81**, 47–60.

GAO, S. & COLLINS, M. B. 1994. Analysis of grain-size trends, for defining sediment transport pathways in marine environments. *Journal of Coastal Research*, **10**, 70–78.

HEATHERSHAW, A. D. & CARR, A. P. 1978. Measurement of sediment transport rates using radioactive tracers. *In: Coastal Sediments '77.* American Society of Civil Engineers, New York, 399–416.

JARVIS, K. E. 1988. Inductively Coupled Plasma Mass Spectrometry: A new technique for the rapid or ultra-trace level determination of the rare-earth elements in geological materials. *Chemical Geology*, **68**, 31–39.

JARVIS K. E. 1989. Determination of rare earth elements in geological samples by Inductively Coupled Plasma Mass Spectrometry. *Journal of Analytical Atomic Spectroscopy*, **4**, 563–570.

JOHANNESSON, K. H., STETZENBACH, K. J. & HODGE, V. F. 1997. Rare earth elements as geochemical tracers of regional groundwater mixing. *Geochimica et Cosmochemica Acta*, **61**, 3605–3618.

KREZOSKI, J. R. 1989. Sediment reworking and transport in eastern Lake Superior – in situ rare earth element tracer studies. *Journal of Great Lakes Research*, **15**, 26–33.

MAHLER, B. J., BENNETT, P. C. & ZIMMERMAN, M. 1998. Lanthanide-labeled clay: A new method for tracing sediment transport in Karst. *Ground Water*, **36**, 835–843.

MATISOFF, G., KETTERER, M. E., WILSON, C. G., LAYMAN, R. & WHITING, P. J. 2001. Transport of Rare Earth element-tagged soil particles in the response to thunderstorm runoff. *Environmental Science and Technology*, **35**, 3356–3362.

MCLAREN, P. & BOWLES, D. 1985. The effects of sediment transport on grain-size distributions. *Journal of Sedimentary Petrology*, **55**, 457–470.

MILLER, S. E., HEATH, G. R. & GONZALEZ, R. D. 1982. Effects of temperature on the sorption of lanthanides by monmorillonite. *Clays and Clay Mineralogy*, **30**, 111–122.

MILLER, S. E., HEATH, G. R. & GONZALEZ, R. D. 1983. Effects of pressure on the sorption of Yb by montmorillonite, *Clays and Clay Mineralogy*, **31**, 17–21.

SINITSYN, V. A., AJA, U., KULIK, D. A. & WOOD, S. A. 2000. Acid-base surface chemistry and sorption of some lanthanides on K^+-saturated Marblehead Illite: I. Results of an experimental investigation. *Geochimica et Cosmochimica Acta*, **64**, 185–194.

SPENCER, K. L. 2002. Spatial variability of metals in the inter-tidal sediments of the Medway Estuary, Kent, UK. *Marine Pollution Bulletin*, **44**, 933–944.

THOMPSON, M. & WALSH, J. N. 1989. *Handbook of Inductively Coupled Plasma Spectrometry, 2nd Edition*, Blackie, Glasgow.

US ENVIRONMENTAL PROTECTION AGENCY 2005. Test Methods. http://www.epa.gov/epaoswer/hazwaste/test/main.htm#table.

VOULGARIS, G., SIMMONDS, D., MICHEL, D., HOWA, H., COLLINS, M. B. & HUNTLEY, D. A. 1998. Measuring and modelling sediment transport on a macrotidal ridge and runnel beach: An intercomparison. *Journal of Coastal Research*, **14**, 315–330.

WELTJE, L., HEIDENREICH, H., ZHU, W., WOLTERBEEK, H., KORHAMMER, S., DE GOEIJ, J. J. M. & MARKERT, B. 2002. Lanthanide concentrations in freshwater plants and molluscs, related to those in surface water, pore water and sediment. A case study in The Netherlands. *Science of the Total Environment*, **286**, 191–214.

XUE, Y. Z., LIU, P. L., YANG, M. Y. & JU, T. J. 2004. Study of spatial and temporal processes of soil erosion on sloping land using rare earth elements as tracers. *Journal of Rare Earths*, **22**, 707–713.

YIN, Y., CHANG, N., ZHONG, W., SUN, S., ZHANG, Y., CUI, H., CHEN, S., FENG, Y. & SUN, L. 1993. A study of neutron activation tracer sediment technique. *Science in China, Series A*, **36**, 243–248.

ZHANG, X. C., NEARING, M. A., POLYAKOV, V. O. & FRIEDRICH, J. M. 2003. Using rare-earth oxide tracers for studying soil erosion dynamics. *Soil Science Society of America*, **67**, 279–288.

Sand and mud flux estimates using acoustic and optical backscatter sensors: measurements seaward of the Wash, southern North Sea

SARAH J. BASS[1], I. N. MCCAVE[2], J. M. REES[3] & C. E. VINCENT[4]

[1]*School of Earth, Ocean and Environmental Sciences, University of Plymouth, Drake Circus, Plymouth PL4 8AA UK (e-mail: sbass@plymouth.ac.uk)*

[2]*Department of Earth Sciences, University of Cambridge, Downing St., Cambridge CB2 3EQ, UK.*

[3]*CEFAS Laboratories, Pakefield Road, Lowestoft, NR33 0HT, UK*

[4]*School of Environmental Sciences, University of East Anglia, Norwich, NR4 7TJ, UK*

Abstract: Optical and acoustic backscatter sensors, more sensitive to fine and sandy sediment respectively, were used to measure the mud and sand components of a mixed suspension at a site seaward of the Wash embayment, in the southern North Sea. Data were acquired from a free-standing instrument frame during a five-week deployment in 12 m water depth about 6 km offshore. Suspended mud at this site was characterized by tidal advection of fine sediment along the coast resulting in semi-diurnal peaks in concentration near slack water. Suspended sand concentrations correlated well with tidal current speeds indicating local resuspension behaviour. Predicted sand flux direction followed the residual current while mud fluxes at the site were different in direction to both the residual current and sand flux. Residual fluxes may be biased by cumulative errors resulting from instrument calibration and inferred vertical concentration profiles. These factors are assessed in relation to both predicted flux magnitudes and directions.

Measurement and prediction of sediment fluxes are important goals in environmental and engineering coastal studies. Errors in sediment transport estimates may be a result of a number of things including uncertainties in current measurements, vertical distributions of current velocity, sediment concentrations and instrument calibrations. Net sediment transport predictions will be particularly sensitive to any offsets or bias in the current or concentration estimates. The potential for error is compounded in a mixed sediment environment by the varying responses of different sediment size to the flow which implies required monitoring of both end members of the size spectrum.

Field measurements of suspended sediment flux frequently do not take into account the wide variation of sediment size with time. The difficulty of measuring the full varying size spectrum of suspended sediment often leads to the measurement of only a portion of that spectrum and/or the assumption of a time-invariant sediment size distribution. In a mixed sediment environment such an assumption can lead to large errors in predictions of the magnitudes of concentrations and even flux directions (e.g. Ludwig & Hanes 1990; Bass 2000; Green *et al.* 2000; Jago & Bull 2000). Unlike coarser sandy material the behaviour of fine sediments is influenced by their cohesive nature, which allows particles to flocculate and affects their erodibility and settling velocity. In addition their relatively slower settling velocity allows muddy sediments to remain in suspension much longer than sand and they may be easily advected into or away from a region of study.

Optical and acoustic backscatter sensors (OBS and ABS), more sensitive to fine and sandy sediment respectively, offer the possibility of monitoring suspensions over a wide range of particle sizes. Multi-frequency ABS have been shown to provide information on the varying size distribution of sandy sediments (Crawford & Hay 1993), but their application to muddy sediments has been limited by the lack of understanding of the acoustic response to mud and by attenuation of sound at the higher frequencies required to sense fine particles. However, while ABS and OBS instruments are routinely used in sediment transport research (e.g. Vincent *et al.* 1998; Lee *et al.* 2002), few studies have taken advantage of these two sensors together to obtain information about the behaviour of fine and coarse sediment in mixed sediment environments (Lynch *et al.* 1994; Bass 2000; Green *et al.* 2000). Acoustic and optical backscatter measurements

From: BALSON, P. S. & COLLINS, M. B. 2007. *Coastal and Shelf Sediment Transport*. Geological Society of London, Special Publications, **274**, 25–35. 0305-8719/07/$15.00

representing mud and sand components of a mixed suspension from a 38-day deployment seaward of the Wash embayment, southern North Sea, are presented. Predicted sand and mud flux magnitudes and directions are discussed in relation to vertical concentration profiles and calibration uncertainties.

Experiment background and methods

The deployment took place during April and May 1997 for 38 days as part of an experiment by the UK Centre for Environment, Fisheries and Aquaculture Science (CEFAS) to study the effect of fine sediment plumes created by dredging activity in the North Sea. The results presented here are from one deployment about 6 km offshore, outside the entrance of the Wash embayment (NW corner), eastern England, in the southern North Sea (Fig. 1). Residual currents in this region are generally to the SE (Eisma 1981). Along the Lincolnshire coast the net water flux is southwards with local circulation cells among the complex tidal channels and banks (Eisma 1981) and into the Wash at the NW corner (Ke *et al.* 1996).

The most likely sources of suspended sediment supplying this region of the North Sea are the eroding coastlines of Lincolnshire and Yorkshire, and the fine sediment plume discharged by the Humber (McCave 1987). The Wash as a whole is a region of net sediment accumulation. A net sediment influx occurs along the Lincolnshire coast into the NW corner of the Wash and a net outward flux at the SE corner along the north Norfolk coastline (Ke *et al.* 1996) with an overall excess of input over output. Bed and suspended sediment samples collected at the deployment site were predominantly bimodal with a fine mode at about 7 μm and coarser mode between 120 and 300 μm.

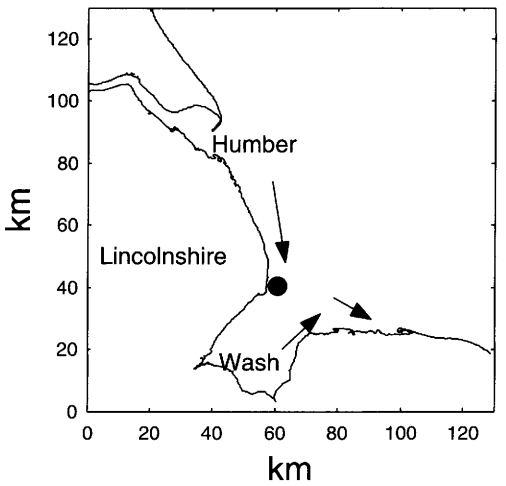

Fig. 1. The location of the experiment area on the east coast of England showing the deployment site (filled circle). General net sediment transport patterns in the region are indicated by the arrows.

Instruments were housed on a benthic lander, or Minipod, designed to measure boundary layer processes in shelf seas. The Minipod carries an independent data logger controlling a number of sensors under a variety of possible sampling schemes (the logger and instrumentation are described in detail in Green *et al.* 1992). The data presented here were acquired with: one two-axis Marsh–McBirney electro-magnetic current meter (0.44 m above bed, axes horizontal); a Paroscientific Digiquartz pressure sensor; two miniature OBS (0.57 and 0.77 mab); and a two-frequency ABS developed at CEFAS. The OBS were developed at the University of Cambridge. The ABS was mounted at a nominal height of 0.85 mab and directed vertically downwards. Only data from the 4.5 MHz ABS are considered here because of a problem with the gain on the lower frequency ABS. Three automated syringe water-samplers were used to obtain accurately timed suspension samples at the height of the lowest OBS. The syringe samplers are operated using a motor-driven piston to withdraw a 1.8 l sample over three minutes at a preset intake height. The syringes were triggered when backscatter levels from the lower OBS exceeded a set threshold. A passive sediment trap collected material in suspension from a height of about 0.3 m throughout the deployment. The trap was an enclosed, 30 cm long cylindrical tube with holes around the circumference near the top mounted vertically on one of the Minipod legs. Some of the suspended sediment in the water flowing through the holes is trapped and later used for instrument calibration.

The ABS, sampling at 2.5 Hz, recorded backscatter profiles at 0.01 m intervals. The two OBS and the pressure sensor sampled at a rate of 1 Hz. Current velocities were sampled at 5 Hz. Data were collected in sets or bursts every hour, each burst lasting 512 s. Data presented here represent burst-averages, i.e. hourly 512 s averages.

Sediment concentrations

Suspended sediment concentrations were determined from the backscatter data through

calibration with sub-sampled layers of muddy and sandy sediment in the sediment traps. The response of the OBS and ABS to particle size is shown in Fig. 2. Sediment at the site was bimodal and suspension concentrations estimated from the OBS and ABS are taken as a crude representation of mud and sand suspensions respectively. OBS calibrations with sub-samples from the traps were verified with suspended load estimates from the syringe samples. It is assumed that the high acoustic backscatter signals were from suspended sand with a size distribution similar to the sand layers in the sediment traps, and thus calibrations with the sandier sub-samples from the sediment trap were applied to the ABS.

Burst-averaged concentration estimates for the full deployment are presented in Fig. 3 with corresponding current speeds and near-bed significant wave-orbital speeds (U_{sig}) in Fig. 4. U_{sig} was calculated from the pressure data using linear wave theory (e.g. Thornton & Guza 1983). A 36 hour time interval from the series (Fig. 5) shows typical phase relationships between suspended sediment concentrations and current speeds. Peak sand suspension concentrations were coincident with peaks in current speeds (Fig. 5c) indicating local resuspension of sandy material from the bed. During spring tides, sand suspensions due to tidal currents reached up to 0.15 kg m^{-3} at 0.1 m height. The influence of waves is also apparent with increased background concentrations during storms.

Mud concentrations (Fig. 3b) exhibited strong semi-diurnal peaks throughout most of the deployment in contrast to the quarter-diurnal signal in the current speed (produced by the semi-diurnal M2 tide). Similar temporal patterns in fine sediment suspension concentrations have been observed elsewhere (e.g. Jago *et al.* 1993; Blewett & Huntley 1998; Williams *et al.* 1998) and modelled as a combination of advection and resuspension by e.g. Weeks *et al.* (1993), Jones *et al.* (1996), Aldridge (1996) and Bass *et al.* (2002). Throughout the deployment, peaks in mud concentrations were centred about high-water slack tide (as in Fig. 5b) suggesting they may have been dominated by advection of muddy material on the flood tide. The effect of waves on suspended sediment concentrations is apparent by the increase in peak concentrations during storm events (e.g. for storms with peak wave orbital velocities at bursts 1, 180, 270, 370, 510 and 760; Fig. 4). Previous work (Bass 2000; Bass *et al.* 2002) has shown through modelling that the mud in suspension was primarily supplied by advection of fine sediment on the flood (predominantly southerly) tide settling toward the bed at slack water and being resuspended on the accelerating ebb. The modelling studies suggest a horizontal concentration gradient in suspended mud increasing to the NW. This result is supported by observations of the East Anglian plume and cliff erosion in Lincolnshire and Holderness which are important sources of suspended sediment to the southern North Sea (e.g. McCave 1987; Dyer & Moffat 1998).

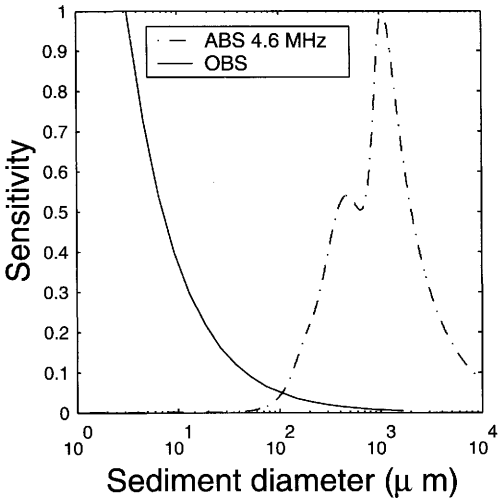

Fig. 2. Optical and acoustic backscatter response to particle size.

Sediment fluxes

Suspended sediment flux, Q, is calculated for a steady uniform current as the depth integral of the product of the concentration of suspended sediment, C, and the sediment velocity, where it is assumed that the sediment velocity is equal to the water velocity, U. Q represents the depth-integrated mass of sediment moving across a unit width of sea bed per unit time.

The sand suspension flux, Q_s, was estimated using the acoustic backscatter estimates of concentration and predicted current profiles, assuming a logarithmic profile and drag coefficient of 0.0025 (Bass 2000). Estimates of Q_s are obtained by summing, over the bottom 41 cm range bins, the product of concentration for each bin and the corresponding predicted velocity. The mass flux of muddy suspensions, Q_m, is calculated as the product of the OBS point estimate of concentration at 0.77 m above the bed, the depth-averaged velocity and water depth. This calculation of Q_m assumed that the mud concentrations were constant with depth. Possible vertical gradients in mud concentration are considered later.

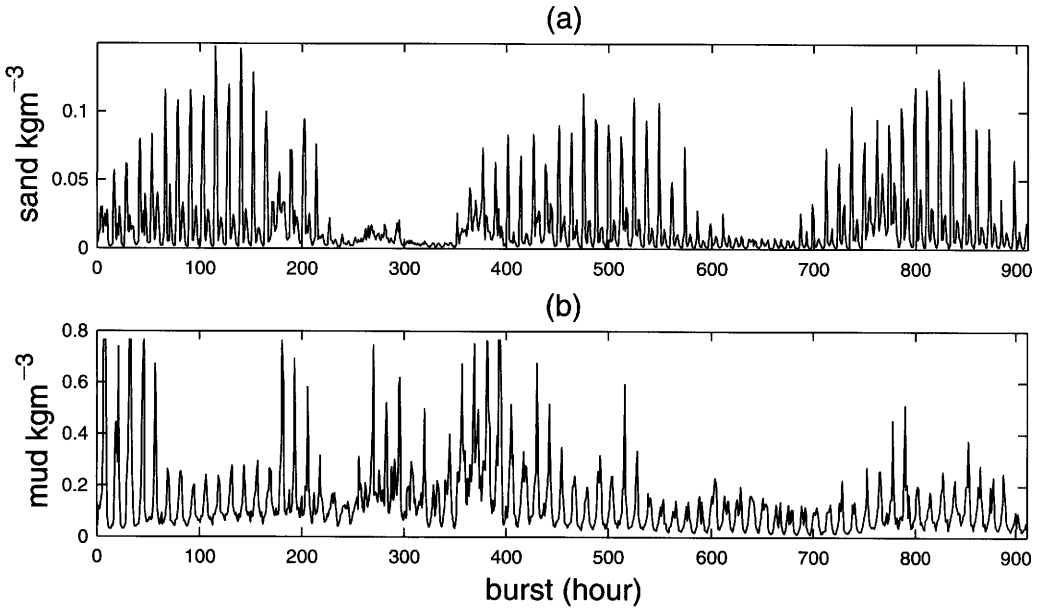

Fig. 3. Time series of **(a)** ABS estimates of suspended sand concentrations at 0.1 m above bed and **(b)** OBS estimates of suspended mud concentrations at 0.57 m above bed.

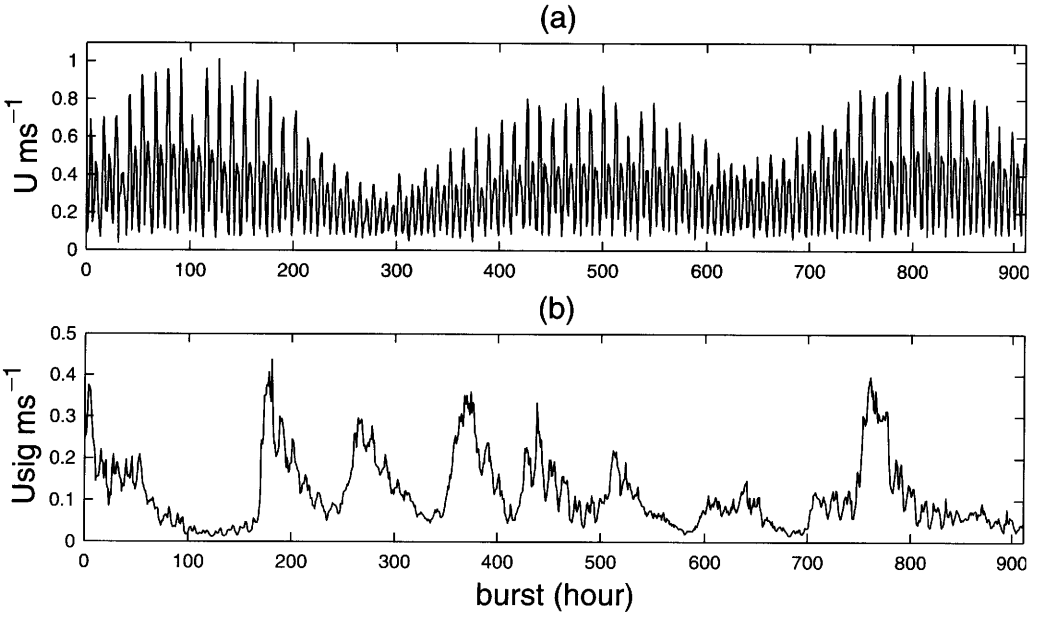

Fig. 4. Time series of **(a)** current speeds at 0.44 m above bed and **(b)** near-bed significant wave-orbital speed.

Fluxes at time scales of wave periods were not considered.

Suspended mud and sand flux time series for the full deployment are presented in Fig. 6. Mud and sand transport events appear to be tidally driven rather than storm driven and tend to have higher magnitudes during spring tides when current speeds and tidal displacements were

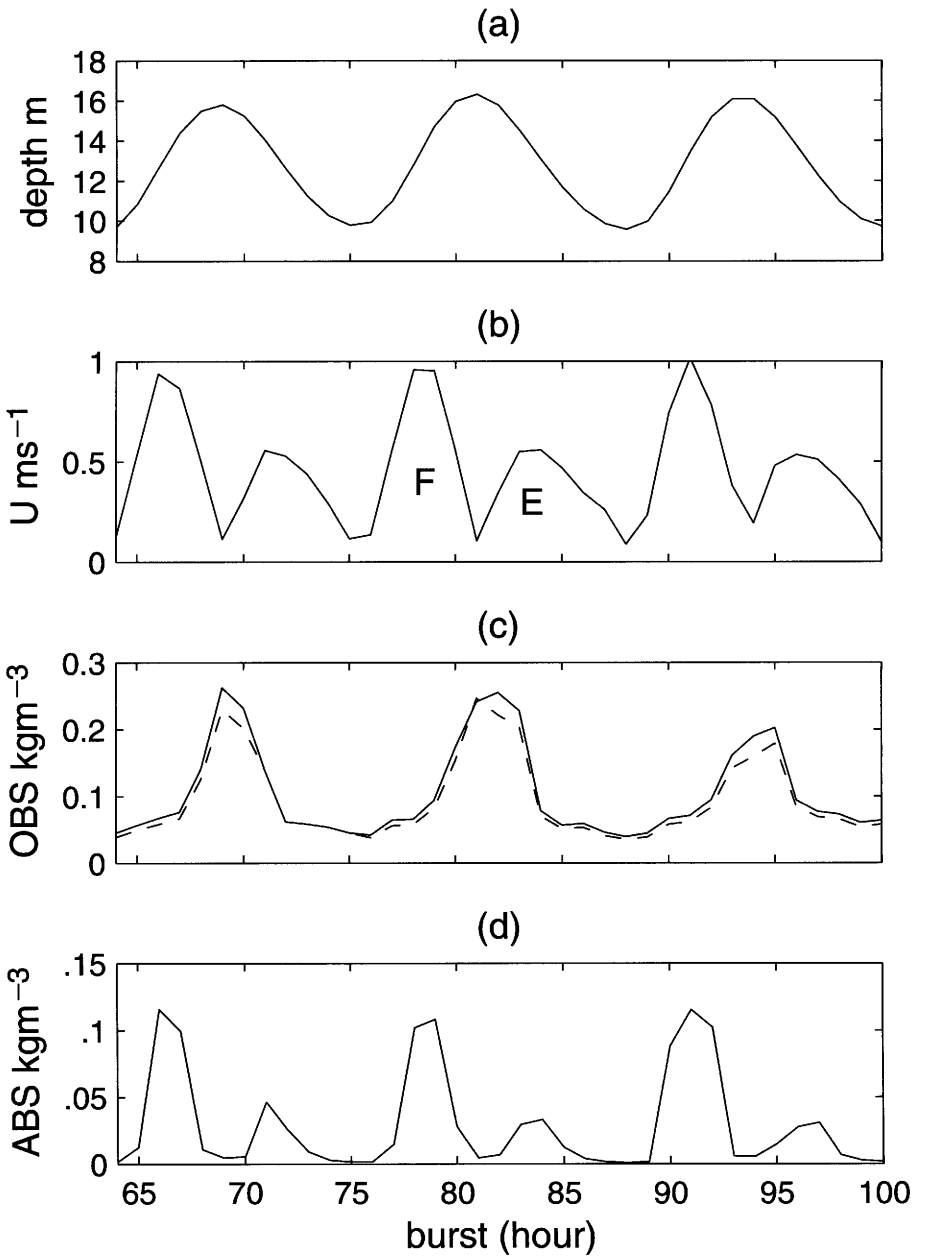

Fig. 5. Water depth **(a)**, current speed **(b)**, suspended mud concentrations **(c)** and sand concentrations **(d)** for a 36 hour time interval during spring tides when wave orbital velocities were low (bursts 64–100).

greatest. The influence of storms is seen more readily through the smoothed flux–time series presented as 36 hour running averages. In both cases the smoothed time series indicates some increase in sediment transport during storms. The magnitudes of mud flux are greater than for sand by an order of magnitude and are possibly overestimations due to the assumption that the concentration at 0.77 m above bed was constant throughout the depth.

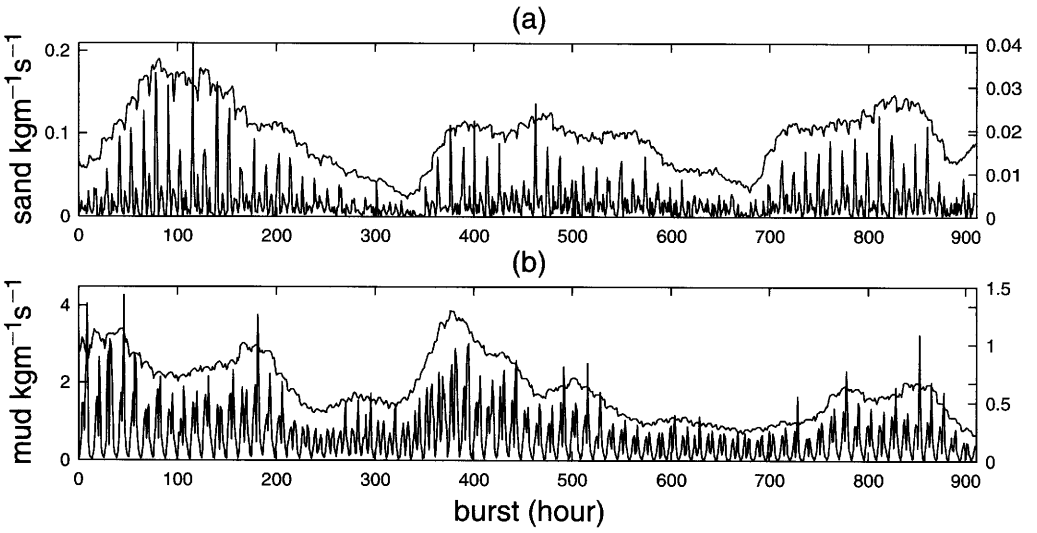

Fig. 6. Time series of **(a)** suspended sand flux magnitudes and **(b)** suspended mud flux magnitudes. Tidal variations are filtered out by smoothing the time series using a 36 hour running point average (superimposed envelope). Corresponding waves and currents are presented in Fig. 4.

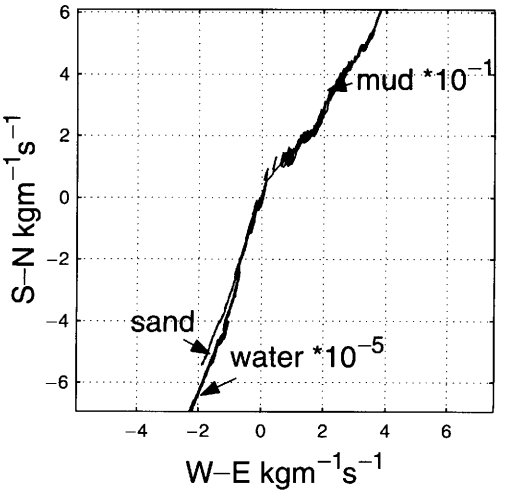

Fig. 7. Progressive vector diagrams of water, mud and sand flux for the full 38-day deployment. Water and mud flux magnitudes have been scaled so that they are comparable to net sand flux. Note that sand and water cumulative fluxes are in the same direction.

Cumulative mass fluxes of sand, mud and water are compared in a progressive vector diagram (Fig. 7). The mass flux of water was computed as the product of the water density, the estimated depth–mean current and the water depth. The predicted residual current and sand flux direction at the site agree with the predominantly southerly flow along the Lincolnshire coast and observations of net sediment transport into the Wash at the NW corner (Fig. 1). However, the estimated residual mud flux was in the opposite direction (north and offshore) to the sand and water flux (south and onshore). This result is surprising because fine sediment suspensions are very often assumed to move with the water because of the relatively low settling velocity associated with mud. Considering that the above net flux estimates are cumulative and thus sensitive to cumulative errors associated with any bias in the concentration time series, the following section explores potential biases in concentration estimates associated with the time-varying sediment–size distribution, calibration errors and varying vertical gradients of muddy sediments.

The effect of concentration errors on flux estimates

Calibration uncertainties

It is recognized that there is some degree of overlap in the mud and sand concentration estimates because both optical and acoustic sensors will detect both mud and sand but with different degrees of sensitivity. Uncertainties may result from the time variation of the size distribution

at a given height, and from the varying states of aggregation depending on the turbulent intensity, mud concentration and biological activity in the water. The time variation of size distributions during the deployment was not known well enough to incorporate into the calibration procedure. It is, however, clear that mud and sand suspensions from this deployment dominated at different stages during the tidal cycle: mud concentrations were highest around slack tide at high-water and peaks in sand concentrations were coincident with peaks in local current speed. Acoustic and optical backscatter instruments are typically calibrated with either a bed or suspension sample from the deployment location and the single calibration is then applied to the full time series despite inevitable temporal changes in suspended sediment size distribution. For the data in question, when different calibrations were applied the predicted mud and sand flux magnitudes were altered but not the directions. Of more concern is that calibration with one sediment sample for all times is not representative of the suspension where the size distribution varies periodically. The question explored below is whether high concentrations of mud or sand contaminate or bias the acoustic or optical backscatter respectively at particular times during a tidal cycle.

The acoustic response to flocculating fine sediment is not understood well. It is not clear whether the backscatter intensity is reduced due to increased attenuation in flocculating suspensions or whether fine particle aggregates result in increased backscatter intensity because of an increase in particle size. Consequently, the acoustic backscatter data presented here may be an overestimate or an underestimate of sand concentrations during periods of concentrated mud suspensions. Fig. 8 presents the acoustic backscatter intensity at 0.1 m above bed as a function of the current speed. Sand resuspension due to local current shear occurs around 0.4 m s^{-1} in agreement with theoretical predictions based on the modal sand grain size from the suspended sediment samples. Concentrations for times when the ratio of significant wave-orbital speed (U_{sig}) to current speed (U) was greater than 0.5 are marked by circles in Fig. 8. These particular times suggest that the enhanced acoustic estimates of sand concentration at low current shear may be related to storms. Marked

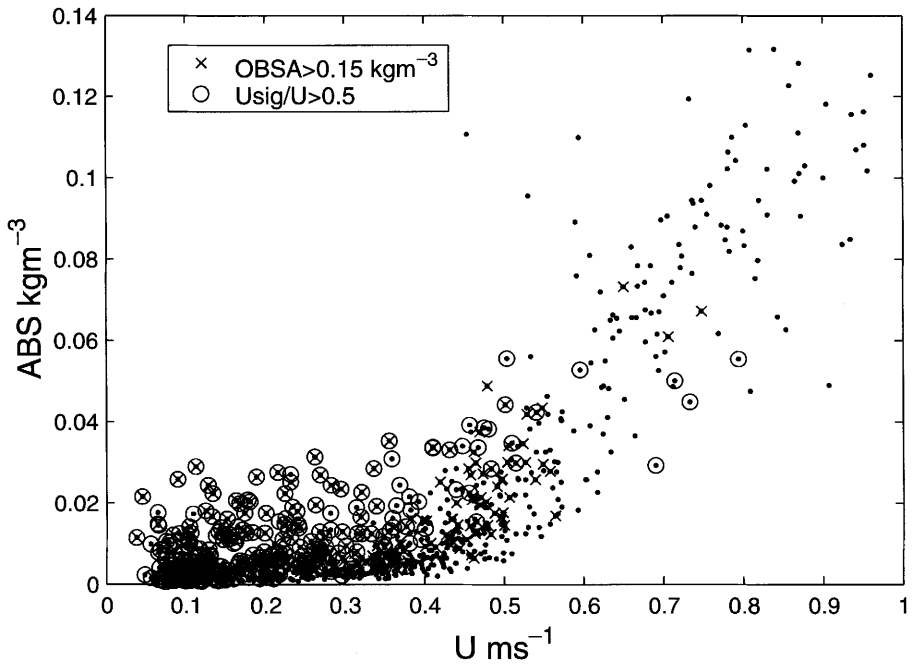

Fig. 8. Acoustic backscatter intensity at 0.1 m above bed as a function of the current speed. Sand resuspension due to local current shear occured around 0.4 ms^{-1}. Concentrations for times when the ratio of significant wave-orbital (U_{sig}) to current speed (U) was greater than 0.5 are marked as circles) as are the times for which mud concentrations are high (crosses).

by crosses in Fig. 8 are the times for which mud concentrations are high (>0.15 kg m^{-3}), for when there is no indication of reduced backscatter intensity. Some of the concentrated mud suspensions correspond to increased backscatter for lower current velocities but it may be argued that the increase in backscatter at these times was due to wave-current resuspension during storms. The potential effect of an overestimate in sand concentration during periods of high mud concentrations and low current shear was tested by ignoring all contributions to the net flux when the current speed was less than 0.4 m s^{-1}, effectively assuming a tidally controlled flux of sand only, and also by ignoring those contributions when mud concentrations were high. The resulting progressive vector fluxes of sand are compared with the previous estimate (Fig. 9). While the net flux magnitudes are 10–20% larger there is little change in predicted sand flux direction (about 1°). The net sand flux estimated for lower mud suspensions (when concentrations were less than 0.15 kg m^{-3}) is less realistic as it was biased by the dominance of mud on one tide, in particular high mud concentrations on the accelerating ebb tide.

Optical backscatter sensor calibrations were verified by suspended load estimates obtained from syringe suction samples at the lower OBS height. These suction samples were triggered by high optical backscatter events and thus the concentration estimates are considered reliable when the mud concentration was high. Low mud concentrations, which have no second estimate to be compared with, generally coincided with higher current speeds and may be more problematic in cumulative flux estimates. During these periods of higher current shear it is more likely that mud concentrations are overestimated due to the presence of more sand in suspension and the break-down of flocs into smaller particles. In the extreme case of removing the influence of sand on the optical backscatter, cumulative mud flux was estimated by ignoring contributions during periods of high sand concentrations and also when current speeds were high (Fig. 10). Comparing these extreme cases with the previous estimate of cumulative flux, the net flux is larger by up to 65% and the direction approximately 5° closer to north, but the net flux remains approximately opposite that of the water.

Effect of vertical concentration profile estimates on mud fluxes

Mud flux estimates presented in Figs. 6 and 7 were calculated assuming a depth-constant mud concentration because only two closely-spaced data points were available (from the two OBS at 0.57 and 0.77 m above the bed). However,

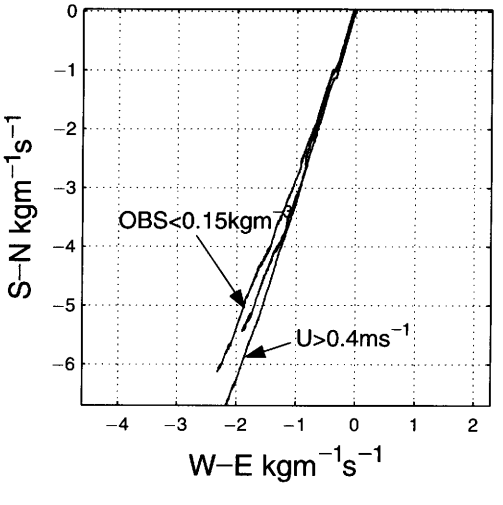

Fig. 9. Progressive vector diagram of sand flux calculated by only including concentrations for which current speeds were high enough to resuspend sand ($U>0.4$ ms^{-1}) and for which OBS estimated mud concentrations were low (<0.15 kg m^{-3} at 0.57 cm elevation). The cumulative sand flux estimate from Fig. 7 is also included (unlabelled) for comparison.

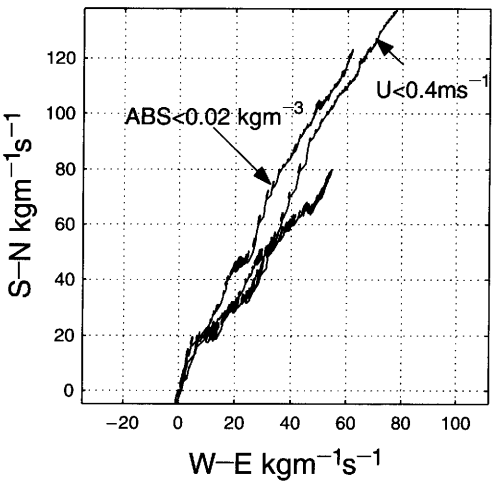

Fig. 10. Progressive vector diagram of mud flux calculated by only including concentrations for which current speeds were low ($U<0.4$ ms^{-1}), and therefore less sand in suspension, and for which ABS estimates of sand concentrations were relatively low (<0.02 kg m^{-3} at 0.10 cm elevation).

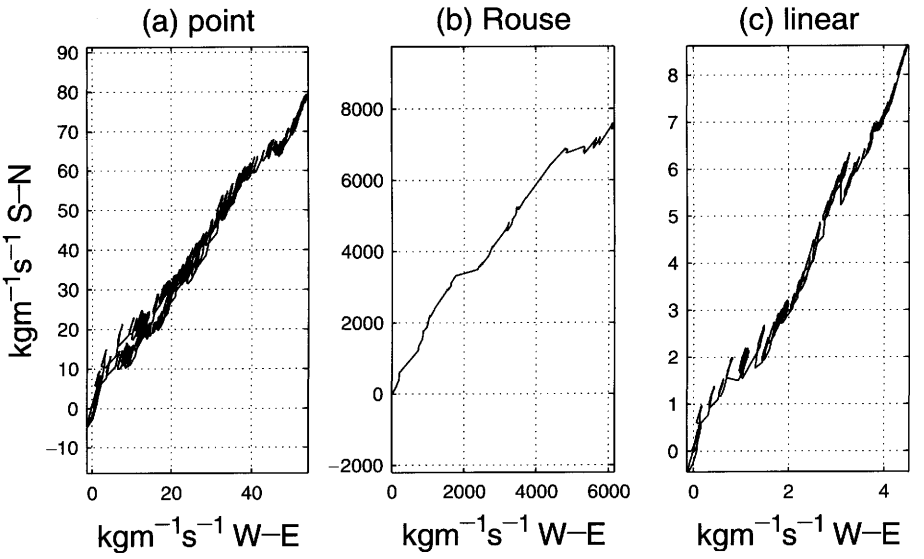

Fig. 11. Cumulative mud fluxes estimated assuming depth-constant **(a)**, Rouse-type exponential **(b)** and linear **(c)** vertical concentration profiles.

assuming there is little uncertainty in the OBS estimates of concentration, a larger vertical gradient was exhibited during peak suspension concentrations at high-water slack tide. It is possible to imagine, with a time varying vertical gradient in concentration, that the integrated mass of sediment in the water column may be lower for a high-gradient, high near-bed concentration than for a low-gradient, low near-bed concentration.

Based on the two OBS measurements a potentially varying vertical gradient in mud concentration is considered by comparing the previous depth-constant flux estimate with estimates using a linear and an exponential Rouse-type profile:

$$c_{lin}(z) = mz + b \tag{1}$$

$$c_{rous}(z) = Az^{-B} \tag{2}$$

Equations 1 and 2 are multiplied by a logarithmic velocity profile and integrated over the depth z to obtain linear and Rouse flux estimates, Q_{lin} and Q_{rouse}:

$$Q_{lin} = \frac{m\sqrt{C_D}U}{2\kappa}\left[h^2(\ln h - \ln z_o) + 1/2(z_o^2 - h^2)\right] - \frac{b\sqrt{C_D}U}{\kappa}\left[h(\ln h - \ln z_o) + (z_o - h)\right] \tag{3}$$

$$Q_{rouse} = \frac{c(z_o)\sqrt{C_D}U}{\kappa(1-b^2)}\left[\left(\frac{h}{z_o}\right)^{1-b}\left[\ln(h/z_o) - b\ln(h/z_o) - 1\right] + 1\right]. \tag{4}$$

where h is the water depth and z_o is the roughness length determined from the drag coefficient, C_D, and k is van Karman's constant.

Net fluxes for the linear, Rouse and point estimates have been compared in progressive vector diagrams (Fig. 11). The flux direction was about the same for all flux estimates, but the net magnitudes differed widely. The linear estimate is an order of magnitude smaller than the point estimate and the Rouse estimate is two orders of magnitude larger. The Rouse profile estimates were dominated by very high transport events that are a result of very high near-bed concentrations when the gradient between the two OBS concentrations was high which dominated the net transport estimates. No further judgement can be made on the residual flux magnitudes without further information on the vertical concentration profiles of the mud suspensions. Despite the different profiles, the flux direction was consistent, which suggests that suspended mud at this location was moving NE at least for the duration of this deployment.

Discussion and conclusions

OBS and ABS used in conjunction have been shown to provide useful information on the behaviour of muddy and sandy components of a mixed sediment suspension. The influence of uncertainties in sediment concentration estimates from OBS and ABS as a result of varying sediment size distributions and vertical concentration profiles have been considered.

Potential 'contamination' of the OBS and ABS signals with sand and mud respectively did not appear to affect significantly predicted flux magnitudes or directions, indicating that division of the suspension into broad size classes is a reasonable and better approach than ignoring the wide fluctuation in particle size. Large uncertainty in the net mud flux magnitude was a result of uncertainty in the vertical concentration profile. Various profile estimates produced residual fluxes which varied by orders of magnitude, but with little change in direction. It is noted that stratification of the flow and non-logarithmic velocity profiles were not taken into account, and only two point measurements were available to make assumptions about the vertical structure of sediment. The direction of mud flux, which differs from both the current residual and net sand transport, appears to be a result of timing of the availability of mud for transport rather than a result of a complicated vertical structure. Peaks in suspended mud concentrations were consistently centred around high-water slack tide but often biased towards the northeasterly ebb current. Overall, results indicate that OBS and ABS calibrated with fine and sandy sediments respectively provide adequate estimates of near-bed mud and sand flux directions and temporal variations though further information on the vertical distribution of fine sediments is required to reduce uncertainty in the mud flux magnitude.

Mud and sand transport in this region of the North Sea is tidally periodic. Storms influence net sand transport when current speeds are high. The influence of storms or tides on locally observed mud transport is dependent on the availability of mud from a non-local source and is therefore difficult to explain in terms of local conditions. At this particular site the sediment transport direction is strongly dependent on particle size; the striking result is the prediction of mud and sand flux in opposite directions. Such results underline the importance of monitoring both sediment size components separately and for mud flux it is clear that measurements above the bottom boundary layer are imperative.

Many thanks go to the UK Centre for Environmental, Fisheries and Aquaculture Science (CEFAS). Helpful discussions with Brian Dade at the University of Cambridge are gratefully acknowledged. Thanks also to Jon Williams, whose considered comments have improved the clarity of the text. This work formed part of the Cohesive Sediment Dynamics study jointly funded by the Ministry of Agriculture, Fisheries and Food and the Department of the Environment, UK. SJB was supported by a Commonwealth Scholarship as a PhD student at the University of Cambridge.

References

ALDRIDGE, J. N. 1996. Optimal fitting of a model to observations of sediment concentrations in the Irish Sea. *In*: SPALDING, M. L. & CHENG, R. T. (eds) *Estuarine and Coastal Modelling, Proceedings of the 4th International Conference, San Diego, USA*, 417–428.

BASS, S. J. 2000. *Sand and mud dynamics in shelf seas.* PhD Thesis, University of Cambridge, United Kingdom.

BASS, S. J., ALDRIDGE, J. N., MCCAVE, I. N. & VINCENT, C. E. 2002. Phase relationships between fine sediment suspensions and tidal currents in coastal seas. *Journal of Geophysical Research*, **107(C10)**, 3146–3160.

BLEWETT, J., HUNTLEY, D. 1998. Measurement of suspended sediment transport processes in shallow water off the Holderness Coast, UK. *Marine Pollution Bulletin*, **37**, 134–143.

CRAWFORD, A. M. & HAY, A. E. 1993. Determining suspended sand size and concentration from multi-frequency acoustic backscatter. *Journal of the Acoustical Society of America*, **94**, 3312–3324.

DYER, K. R. & MOFFAT, T. J. 1998. Fluxes of suspended matter in the East Anglian plume Southern North Sea. *Continental Shelf Research*, **18**, 1311–1331.

EISMA, D. 1981. Supply and deposition of suspended matter in the North Sea. *In*: NIO, S. D., SCHUTTENHELM, R. T. E. & VAN WEERING, T. C. E. (eds) *Holocene Marine Sedimentation in the North Sea Basin*, International Association Sedimentologists Special Publications, **5**, 415–428.

GREEN, M. O., PEARSON, N. D., THOMAS, M. R., REES, C. D., REES, J. M. & OWEN, T. R. E. 1992. Design of a data logger and instrument mounting platform for seabed sediment-transport research. *Continental Shelf Research*, **12**, 543–562.

GREEN, M. O., BELL, R. G., DOLPHIN, T. J. & SWALES, A. 2000. Silt and sand transport in a deep tidal channel of a large estuary (Manukau Harbour, New Zealand). *Marine Geology*, **163**, 217–240.

JAGO, C. F. & BULL, C. F. J. 2000. Quantification of errors in transmissometer-derived concentration of suspended particulate matter in the coastal zone: implications for flux determinations. *Marine Geology*, **169**, 273–286.

JAGO, C. F., BALE, A. J. *et al.* 1993. Resuspension processes and seston dynamics, southern North Sea. *Philosophical Transactions of the Royal Society of London*, **A 343**, 475–491.

JONES, S. E., JAGO, C. F. & SIMPSON, J. H. 1996. Modelling suspended sediment dynamics in tidally stirred and periodically stratified waters: Progress and pitfalls. *In*: PATTIARATCHI, C. (ed.) *Mixing in Estuaries and Coastal Seas*. Coastal and Estuarine Studies. AGU, Washington DC, **50**, 302–324.

KE, X., EVANS, G. & COLLINS, M. B. 1996. Hydrodynamics and sediment dynamics of the Wash embayment, eastern England. *Sedimentology*, **43**, 157–174.

LEE, G.-H., FRIEDRICHS, C. T. & VINCENT, C. E. 2002. Examination of the diffusion versus advection dominated sediment suspension on the shoreface under storm and swell conditions. *Journal of Geophysical Research*, **107(C10)**, 1505–1524.

LUDWIG, K. A. & HANES, D. M. 1990. A laboratory evaluation of optical backscatterance suspended solids sensors exposed to sand-mud mixtures. *Marine Geology*, **94**, 173–179.

LYNCH, J. F., IRISH, J. D., SHERWOOD, C. R. & AGRAWAL, Y. C. 1994. Determining suspended sediment particle-size information from acoustical and optical backscatter measurements. *Continental Shelf Research*, **14**, 1139–1165.

MCCAVE, I. N. 1987. Fine sediment sources and sinks around the East Anglian coast, UK. *Journal of the Geological Society*, **144**, 149–152.

THORNTON, E. B. & GUZA, R. T. 1983. Transformation of wave height distribution. *Journal of Geophysical Research*, **C88**, 5925–5938.

VINCENT, C. E., STOLK, A. & PORTER, C. F. 1998. Sand suspension and transport on the Middlekerke Bank (southern North Sea) by storms and tidal currents. *Marine Geology*, **150**, 113–129.

WEEKS, A. R., SIMPSON, J. H. & BOWERS, D. 1993. The relationship between concentrations of suspended particulate material and tidal processes in the Irish Sea. *Continental Shelf Research*, **13**, 1325–1334.

WILLIAMS, J. J., HUMPHERY, J. D., HARDCASTLE, P. J. & WILSON, D. H. 1998. Field observations of hydrodynamic conditions and suspended particulate matter in the southern North Sea. *Continental Shelf Research*, **18**, 1215–1233.

Field measurement and quantification of longshore sediment transport: an unattainable goal?

J. A. G. COOPER[1] & O. H. PILKEY[2]

[1]*Centre for Coastal and Marine Research, School of Environmental Studies, University of Ulster, Coleraine BT52 1SA, Northern Ireland, UK (e-mail: jag.cooper@ulster.ac.uk)*

[2]*Nicholas School of the Environment and Earth Sciences, Division of Earth and Ocean Sciences, Duke University, Durham, North Carolina 27708, USA*

Abstract: Longshore sediment transport (LST) is an important component of many coastal systems. This common term is frequently expressed as an annual volume, either net or gross, passing a particular point. In spite of its importance as a factor in coastal morphodynamics it has received relatively little attention as a process. We review the mechanisms of longshore sediment transport and current approaches to its assessment using field measurement and geoindicators. We conclude that approaches to date have never succeeded in quantifying longshore sediment drift rates in an adequate way. This shortcoming is attributed to the spatial and temporal variability of contributing processes coupled with a technical inability to quantify simultaneously longshore sediment transport in all its modes.We also conclude that research involving the measurement of longshore transport can enhance our understanding of the processes of transport and rates of transport under certain conditions. However, the accurate quantification of drift rates as annual volumes is an unattainable goal. We propose that such quantifications be replaced by qualitative values (small, medium, large) or measures of the relative importance of longshore transport in effecting morphological change (e.g. drift-dominated, cross-shore dominated, mixed processes).

Longshore sediment transport (LST) is an important element in coastal morphodynamics, particularly in sand- and gravel-dominated systems (Komar 1977, 1988), but also in muddy areas (Rodriguez & Mehta 1998). Frequently LST is cited as an annual volume, especially for engineering and mathematical modelling purposes. Volumes are typically cited as net or gross sediment transport volumes. Gross measurements seek to quantify the total flux of sediment in both directions alongshore whereas net volumes refer to the difference between volumes moving in opposing directions. Both measures are important for practical purposes. Channel infilling for example may take place from both directions and hence the gross volume potentially affects it. Net sediment volumes are utilized in sediment budget calculations and in assessing the impact of structures that interrupt the net drift. In addition, LST is a critical element in the design of nourished beaches and in evaluation of the environmental impact of coastal stabilization structures. There are, however, inherent problems in the field measurement of LST. Madsen *et al.* (2003) note the loss of environmental control associated with field measurement of LST.

Once cited, LST volumes have a long lifespan and persist long after initial measurements have been made (Greer & Madsen 1978; Schoonees & Theron 1993). Adoption of such figures without critical appraisal of how they were calculated and whether they are correct is widespread practice both in coastal geomorphology and coastal engineering (Madsen *et al.* 2003). The longevity of such figures is increased when they are used to 'calibrate' models of LST. A prime example is the measurements used by Komar & Inman (1970) to develop a longshore sediment transport formula that has led to the CERC equation (USACE 2002) for longshore transport. Greer & Madsen (1978) on a review of the Komar (1969) data concluded that it was not reliable. Schoonees & Theron, (1993, p. 18) subsequently concluded that despite the deficiencies reported by Greer & Madsen (1978), the Komar (1969) dataset is still 'among the best data sets available'. That a 30 year old data set is still regarded as among the best available is symptomatic of the difficulties in field measurement of LST. Further, most citations of annual LST volumes assume that one year is like every other year and take no account of interannual variability or the occurrence of extreme events.

The aim in this paper is to outline briefly the processes by which longshore sediment transport occurs and to assess contemporary approaches to its measurement and quantification. On the

From: BALSON, P. S. & COLLINS, M. B. 2007. *Coastal and Shelf Sediment Transport*. Geological Society of London, Special Publications, **274**, 37–43. 0305-8719/07/$15.00

basis of this review we make some recommendations on (a) future practical approaches to longshore sediment transport assessment and reporting and (b) the application of field techniques to advance our understanding of longshore sediment transport.

Processes of longshore transport

Longshore transport has been defined in many different ways. Most definitions, however, refer to the movement alongshore of a volume of sediment under the combined action of waves and currents (Komar 1977, 1988). An array of potential factors contributes to the strength of longshore sediment transport (Pilkey & Cooper 2002). These may be categorized into dynamic factors and sediment/topographic factors, but commonly only a few of these factors are considered when longshore transport is quantified.

Surf zone

The dominant mechanism envisaged in longshore transport is movement of sediment by longshore-directed currents generated by oblique waves (USACE 2002, part II, Chapter 4). Since most wave energy dissipation takes place in the surf zone, this is a zone of high sediment transport potential. Both suspended load and bedload longshore transport takes place in the surf zone (USACE 2002) and recent results have suggested that the relative proportions vary during storm and non-storm conditions (Madsen *et al.* 2003).

Longshore transport volumes have been shown to vary according to breaking wave type (Wang *et al.* 2002) with plunging breakers producing higher LST rates than spilling breakers under laboratory conditions.

Diffraction currents produced by gradients in breaking wave height are also cited as contributing to longshore transport (USACE 2002). Aagaard & Greenwood (1995) also drew attention to the contribution of far infragravity waves to LST in the surf zone and concluded that up to 30% of longshore transport was accomplished by such oscillations.

Additional complexity in the process of longshore drift in the surf zone is present in the growth of large-scale topographic features (oblique bars) that develop due to flow instabilities in the longshore current (Falques *et al.* 1996) or very large-scale features that grow allometrically through self-organization (Ashton *et al.* 2001).

Swash zone

Landward of the surf zone, sediment movement in the swash zone is widely acknowledged as contributing to longshore drift if swash and backwash operate with different azimuths. Kamphuis (1991) noted peaks in longshore sediment transport in laboratory experiments in both the surf and swash zones. Elfink & Baldock (2002) reviewed sediment transport in the swash zone and noted a wide variety of fluid motions including short waves (sea and swell), long waves, edge waves, shear waves, cross-shore and longshore currents, turbulence and vortices. Both bedload and suspended load transport occur in the swash zone (Elfink & Baldock 2002). Those authors also note that little attention has been paid to longshore sediment transport in the swash zone.

Whether the swash zone is saturated or not is a key determinant of the processes that occur within it. The relative strength of swash and backwash for example, is mediated by sediment porosity and thus sediment grain size is commonly cited as an important constraint on longshore sediment transport. Laboratory experiments (Kamphuis 1991; van Wellen *et al.* 2000) suggest that swash zone transport may contribute up to 50% of the longshore transport volume.

Nearshore zone

Sediment transport on the inner continental shelf, seaward of the surf zone, has been little studied and is seldom considered in studies of longshore drift. A number of studies, however, confirm that substantial volumes of sediment move alongshore on the continental shelf immediately seaward of the surf zone. Anthony & Leth (2002), for example, reported widespread development of large-scale bedforms in depths between 12 and 18 m off the western Danish coast that produced a net northward (alongshore) sediment transport. Transport in the nearshore zone is highly dependent on sediment availability, topography and geology (Thieler *et al.* 1995). Additionally, tidal currents have been identified as responsible for significant longshore transport of sediments, particularly in areas of high tidal range such as the English Channel (Anthony and Orford 2002).

Temporal variability and spatial variability

The spatial distribution of longshore transport has been noted above. However, it is important

to note that the spatial extent of these zones (swash, surf zone and nearshore) are subject to change in response to the magnitude of the processes operating. Surf zones for example expand dramatically during storms to cover extensive areas of the inner shelf (Malvarez & Cooper 2000). Similarly, during storms, additional processes may be operative, such as infragravity waves. Regnauld & Louboutin (2002) showed that coastal sediment transport under storms was linked to antecedent conditions. Storms occurring after prolonged calm conditions act upon a sediment-rich zone-while storms occurring shortly after an earlier storm act on a sediment-starved shoreface and produce relatively little transport.

The annual LST rate which is frequently cited is a value that is related to the dynamics, sedimentary conditions and topography during that year. Schoonees (2000) calculated and compared LST rates for sites in South Africa over several years and showed interannual variability in calculated rates that spanned three orders of magnitude.

Measurement of longshore transport

The spatial distribution of longshore sediment transport across the coastal zone, the temporal variability in process intensity and type, and the feedback relationship between dynamics and coastal topography render quantification of longshore transport difficult. This has been conceded by other authors. Wang *et al.* (2002, p. 118) note that 'the non-controllable nature of field conditions increases the difficulties of isolating and examining the contributions of, and interactions among, individual parameters'. Wang & Kraus (1999) noted that the surf zone is dynamic and 'non-repeatable' such that considerable uncertainty is introduced into field measurement.

A comprehensive review of measurement techniques for coastal sediment transport is provided by White (1998). Below we outline those utilized in longshore transport assessment and comment on their limitations in the context of quantifying total alongshore sediment transport.

Quantification methods

Sediment budget

The sediment budget approach assesses evidence of morphological/volumetric change in coastal systems using historical data on topography and bathymetry. These may include accumulations against groynes and in inlets, which are addressed separately below. Such an approach enables measurements of losses and gains to be matched with knowledge of contemporary processes in order to build up a picture of annual or decadal rates of change (e.g. Kana 1995). In many sediment-budget approaches, flux of sediment from one location to another is related to longshore drift. An estimate is then made of the annual LST rate.

There are several constraints on this approach. Firstly, because the sediment budget approach relies on measurements of morphological change it measures accumulation/erosion and not transportation. In such an approach a million cubic metres of sediment flux through a system might produce no morphological change. Secondly the quantification of losses onshore and offshore is difficult due to data constraints. Morton *et al.* (1995) showed, for example, on a Texas beach that contribution from dunes was a significant component of beach recovery after a storm. Thirdly, the limits to the extent of longshore transport vary over time and the lateral extent of data may not encompass the active transport zone at the timescale under consideration.

Navigation channel filling

The infilling of navigation channels has been a persistent problem for maritime transport for several centuries. Because of this, a large body of information has been amassed on channel infilling rates and dredging volumes. This large volume of information potentially provides much data on longshore sediment transport volumes. The disadvantages of such an approach is in knowing what portion of the total drift is being measured. How much has escaped by inlet bypassing or via flood or ebb-current dispersal is generally unknown. This is especially true during storms. Morton *et al.* (1995) noted that storm-related transport across an inlet in Texas was the most important factor controlling local geomorphology.

Groyne and jetty accumulation

The advantage of accumulation rates on groynes is that there is much data. The abundance of shore-normal structures and measures of updrift accumulation have provided a large database of accumulation rates (Schoonees & Theron 1993). Groynes provide a good impression of the net direction of longshore drift. Limitations of accumulation against groynes include the need

also to take account of transport around the groyne and sediment losses offshore and onshore. Sediment accumulation and dispersal around jetties that stabilize tidal inlets may also involve remobilization and dispersal of ebb-delta sediments that may give a false impression of the volume of sediment in longshore transport. Groyne accumulation also relates to a finite length of time during which a variety of dynamic conditions may have occurred. The role of storms in promoting accumulation or enhancing losses cannot typically be quantified.

Sediment traps

A variety of sediment traps have been deployed to measure longshore drift (e.g. Allen 1985; Kraus 1987). These are of varying design and may be used to trap suspended load and/or bedload. Determining the relative contribution of each transport mode may require simultaneous deployment of various types of trap.

Traps of all types assess gross sediment transport at specific points. They do not measure net transport. The representativeness of these measures in space and time is of major concern in calculating total longshore drift. Because they are deployed for short periods of time, they do not provide reliable estimates of long-term transport rates. As with all short-term measurements, there is a frequent temptation to extrapolate the results for longer periods of time and/or to accept them as generalized measurements of transport conditions. Can it be said with any certainty whether a sediment trap experiment tells us anything more than transport volumes under the precise sedimentary, topographic and dynamic conditions (and immediate antecedent conditions) at the time of measurement?

From a technical perspective sediment traps too are typically incapable of deployment during storms. Similarly they cannot take account of evolving bedforms (moving bedforms change the loci of sediment transport). Trap technology also suffers from problems of turbulence, fouling, filling, etc.

Tracers

Tracers have been used in determining the direction of longshore sediment transport. These have a range of forms from tagged natural sediments (radioactive, dyes, geochemical and biological tags have been used) to artificial sediments made to specific density and grain-size criteria. Natural tracers such as heavy minerals have also been employed to detect direction of longshore transport. Tracer experiments have typically been conducted in the intertidal zone because of ease of recovery but White (1998) reports some deployments in and seaward of the surf zone.

Most tracer experiments have been attempts to measure the total longshore transport in the surf zone. Tracer experiments suffer from practical problems of sampling, injection, detection and determining concentration. They are regarded as difficult and laborious techniques (White 1998). An experiment on the Gold Coast of Australia involving two truckloads of dyed sand resulted in the total loss of all dyed sand within two days (Sam Smith, pers. comm.).

Tracer experiments measure net transport in a short timeframe. As with all such methods, the long-term relevance is questionable.

Optical and acoustic methods

Optical and acoustic methods are used to measure suspended sediment concentrations (devices are laboratory calibrated against known concentrations), which are then combined with current meters to calculate sediment flux. Optical backscatter (OBS) has become a popular technique for short term studies of nearshore sediment transport. An array of OBS equipment was deployed by Miller (1999) to measure LST during storms at Duck pier, North Carolina.

Acoustic backscatter is an alternative technique to the estimation of suspended sediment concentrations. A major problem of using acoustic backscatter in the surf zone relates to bubbles, which are efficient sound-scattering agents (Webb & Vincent 1999).

In both acoustic and optical methods, the sediment size has to be known for concentrations to be calculated accurately. Measurements are made at points or on vertical and/or horizontal profiles in order to assess spatial distribution of material in suspension.

Trench backfilling

In rare circumstances, trenches excavated across the nearshore provide an opportunity to assess LST. In Denmark for example, Diegaard *et al.* (1986) reported the accumulation of sediment in a trench that spanned the nearshore zone. Such a measure is of gross sediment accumulation that is temporally integrated over a range of dynamic and sedimentary conditions.

Discussion

The information above shows that longshore transport is a complex phenomenon that takes place through a variety of processes, several of which are poorly understood (e.g. infragravity

waves, diffraction). The process is temporally variable with marked differences not only in the *magnitude* of processes (e.g. nearshore currents are more vigorous during storms than in fair-weather), but also the *nature* of processes (e.g. suspended transport is relatively more important than bedload during storms; LST is greater under plunging waves than spilling waves; infragravity waves are themselves associated with storms). This temporal variability is also associated with changes in the spatial extent of the surf and swash zones. Coupled with these highly variable processes is heterogeneity in the volume and texture of sediment available for transport, and the geomorphological character of the nearshore zone in which underlying geology and seabed topography are important local constraints on LST.

In this context, quantification of LST is not a straightforward task at any timescale. A variety of instrumental techniques have been employed to measure different components of the longshore transport at various timescales and locations within the active transport zone. Each of these has its own strengths and weaknesses. The individual and collective constraints on all of these techniques, however, mean that while it may be technically possible to measure longshore transport across the entire active zone under certain conditions, it is impossible to do so under all conditions. This makes generalizations regarding the LST volume very difficult.

Studies that have attempted to measure LST have typically used only one technique which invariably means that some element of LST will have been omitted. An impressive field experiment conducted by Kumar *et al.* (2003) utilized an array of mesh traps for suspended load and streamer traps for bedload transport deployed across the surf zone for four months. Swash zone transport, however, was not measured and the equipment could not be deployed when wave heights exceeded 1 m.

Measurement of LST during storms remains a problem. Schoonees & Theron (1993) note that almost all of the data they reviewed was of transport rates less than 2×10^6 m^3 per year, which they ascribed to the fact that they were collected under lower waves with concomitant ease of measurement. Miller (1999) reports measurements from a specially constructed pier of suspended sediment concentrations, current velocities and wave characteristics during several storms that enhance our understanding of the role of storms in LST. Even under these ideal conditions, however, the contribution of bedload is not known, nor can it be certain that the entire longshore transport was measured.

At present it appears that we have no reliable measure of *total* longshore sediment transport at any timescale at any location worldwide.

Longshore drift mathematical models are all based on the assumption that field data exist against which the model can be 'verified' or 'calibrated'. Given the constraints on measuring longshore transport, it is clear that these conditions do not exist. Models, in addition, simplify nearshore dynamics, sedimentology and geomorphology and are incapable of accommodating the complexity of longshore transport outlined above (Thieler *et al.* 2000). There is also no means of testing them. This in part explains the fact that 'numerical models that have not been calibrated to a site with field data differ from each other and from prototype measures by orders of magnitude (Schoonees & Theron 1995; White 1996, 1998). Implicit in our conclusion that LST cannot be determined in the field is the corollary conclusion that mathematical models that use LST are basically invalid or at the least, inaccurate.

This raises the question of whether total longshore sediment transport will ever be measured except under exceptional circumstances (e.g. perched beaches that lack a shoreface). We believe it unlikely that field measurement will ever proceed to a generic level of conclusion regarding longshore sediment transport volumes. Field approaches do, however, yield important insights into the *mechanisms* of longshore transport and enhance our understanding of nearshore morphodynamics. This is significantly different from providing a quantification of transport rates.

The random occurrence of storms on a heterogeneous set of antecedent dynamic, sedimentary and morphological conditions precludes the prediction or measurement of longshore transport volumes in a quantitative way. We thus cannot calculate annual longshore sediment transport volumes. The only conclusion that can be drawn therefore, is that longshore sediment transport cannot be quantified at meaningful timescales. Accepting this conclusion, coupled with the ongoing need to take account of the process in coastal management, we believe that a reappraisal of expectations is necessary on the part of managers and policy makers. We may, however, be in a position to identify the relative importance of longshore transport on certain stretches of the coast.

Future research directions

The quantification of LST is an unattainable goal and none of the methods outlined above

has the potential to measure total longshore sediment transport with accuracy and at a meaningful timescale. The methods, however, can be usefully employed to ascertain the contributions of various processes and the role of various sedimentary/topographic factors in LST. Several cited examples illustrate this potential to determine the contribution of wave type, of winds, of infragravity waves and the constraints imposed by bottom topography, sediment characteristics to LST. These findings through field and model studies will contribute greatly to our understanding of nearshore processes and highlight the fact that our knowledge of the contributory factors is still in its infancy. Therefore, additional field measurements of longshore sediment transport under a range of environmental conditions to enhance our understanding of the relative contributions of different processes, is an important research goal.

We believe that much attention could be devoted to understanding the role of storms via field measurement. This might involve pre- and post-storm geomorphological changes to understand patterns of change over a broad area (immediately pre- and post-storm profiling). This may have to be undertaken over several kilometers rather than locally in order to understand fully the processes at work.

Long-term morphological studies to determine how beach and nearshore volumes change from year to year provide a means of understanding the relative contribution of longshore sediment transport to beach morphology (Norcross *et al.* 2002).

Implications for coastal management

The inability to measure the total LST has important implications for coastal zone management because so many coastal management initiatives rely on quantified volumes of LST. These are frequently used in engineering design and cost-benefit analyses to determine whether various approaches are viable. A change in expectation is required to acknowledge that LST cannot be quantified. Two potential options exist for coastal managers. The first is the work on a qualitative basis and express LST in 'small, medium or large' terms. This acknowledges that order of magnitude estimates are probably the best that can be expected and even these may be wrong when unusual events occur (e.g. prolonged calm, extreme storms or unexpected variations in wind climate). The second option is to consider the *relative* contributions of longshore and cross-shore sediment transport and to designate stretches of coast in terms of dominance. Thus coasts might be categorized in terms of the dominant direction of sediment transport relative to the shoreline, i.e. longshore-dominant, cross-shore-dominant or mixed coasts. Understanding the nature of sediment transport at the coast would provide managers with an understanding of the likely patterns of change to be expected, but not the absolute rates.

References

AAGAARD, T. & GREENWOOD, B. 1995. Longshore and cross-shore suspended sediment transport at far infragravity frequencies in a barred environment. *Continental Shelf Research*, **10**, 1235–1249.

ALLEN, J. R. 1985. Field measurement of longshore sediment transport: Sandy Hook, New Jersey, USA. *Journal of Coastal Research*, **1**, 231–240.

ANTHONY, D. & LETH, J. O. 2002. Large scale bedforms, sediment distribution and sand mobility in the eastern North Sea off the Danish west coast. *Marine Geology*, **182**, 247–263.

ANTHONY, E. J. & ORFORD, J. D. 2002. Between wave- and tide-dominated coasts: the middle ground revisited. *Journal of Coastal Research*, Special Issue **36**, 8–15.

ASHTON, A., MURRAY, B. & ARNAULY, O. 2001. Formation of coastline features by large scale instabilities induced by high angle waves. *Nature*, **414**, 296–299.

DIEGAARD, R., FREDSOE, J. & HEDEGAARD, I. B. 1986. Mathematical model for littoral drift. *Journal of Waterway, Port, Coastal and Ocean Engineering*, **112**, 351–369.

ELFINK, B. & BALDOCK, T. 2002. Hydrodynamics and sediment transport in the swash zone: a review and perspectives. *Coastal Engineering*, **45**, 149–167.

FALQUES, A., MONTOTO, A. & IRANZO, V. 1996. Bed-flow instability of the longshore current. *Continental Shelf Research*, **16**, 1927–1964.

GREER, M. N. & MADSEN, O. S. 1978. Longshore sediment transport data: a review. *In: Proceedings of the 16th Coastal Engineering Conference*, ASCE, 1563–1576.

KAMPHUIS, J. W. 1991. Alongshore sediment transport rate distribution. *In: Coastal Sediments '91*. ASCE, 170–183.

KANA, T. W. 1995. A mesoscale sediment budget for Long Island, New York. *Marine Geology*, **126**, 87–110.

KOMAR, P. D. 1969. *The longshore transport of sand on beaches*. PhD Dissertation, University of California at San Diego.

KOMAR, P. D. 1977. Selective longshore transport rates of different grainsize fractions within a beach. *Journal of Sedimentary Petrology*, **47**, 1444–1453.

KOMAR, P. D. 1988. *Beach processes and sedimentation*. Second Edition. Prentice Hall, New Jersey.

KOMAR, P. & INMAN, D. 1970. Longshore sand transport on beaches. *Journal of Geophysical Research*, **75**, 5914–5927.

KRAUS, N. C. 1987. Application of portable traps for obtaining point measurements of sediment transport rates in the surf zone. *Journal of Coastal Research*, **3**, 139–152.

KUMAR, V. S., ANAND, N. M., CHANDRAMOHAN, P. & NAIK, G. N. 2003. Longshore sediment transport rate – measurement and estimation, central west coast of India. *Coastal Engineering*, **48**, 95–109.

MADSEN, O. S., TAJIMA, Y. & EBERSOLE, B. A. 2003. Longshore sediment transport: a realistic order-of-magnitude estimate. *In: Coastal Sediments '03*. ASCE, 1–14.

MALVAREZ, G. C. & COOPER, J. A. G. 2000. A whole-surf zone approach to modelling nearshore circulations. *Journal of Coastal Research*, **16**, 800–815

MILLER, H. C. 1999. Field measurement of longshore sediment transport during storms. *Coastal Engineering*, **36**, 301–321.

MORTON, R. A., GIBEAUT, J. C. & PAINE, J. C. 1995. Meso-scale transfer of sand during and after storms: implications for prediction of shoreline movement. *Marine Geology*, **126**, 161–179.

NORCROSS, Z. M., FLETCHER, C. H. & MERRIFIELD, M. 2002. Annual and interannual changes on a reef-fringed pocket beach: Kailua Bay, Hawaii. *Marine Geology*, **203**, 1–28.

PILKEY, O. H. & COOPER, J. A. G. 2002. Longshore transport volumes: a critical view. *Journal of Coastal Research*, Special Issue **36**, 572–580.

REGNAULD, H. & LOUBOUTIN, R. 2002. Variability of sediment transport in beach and dune environments, Brittany, France. *Sedimentary Geology*, **150**, 17–29.

RODRIGUEZ, H. N. & MEHTA, A. J. 1998. Considerations on wave-influenced fluid mud streaming at open coasts. *In*: BLACK, K. S., PATERSON, D. M. & CRAMP, A. (eds) *Sedimentary Processes in the Intertidal Zone*. Geological Society of London, Special Publications, **139**, 177–186.

SCHOONEES, J. S. 2000. Annual variation in the net longshore sediment transport rate. *Coastal Engineering*, **40**, 141–160.

SCHOONEES, J. S. & THERON, A. K. 1993. Review of the field-data base for longshore sediment transport. *Coastal Engineering*, **19**, 1–25.

SCHOONEES, J. S. & THERON, A. K. 1995. Evaluation of 10 cross-shore sediment transport/morphological models. *Coastal Engineering*, **25**, 1–41.

THIELER, E. R., BRILL, A. L., CLEARY, W. J., HOBBS, C. H. & GAMMISCH, R. A. 1995. Geology of the Wrightsville Beach, North Carolina shoreface: implications for the concept of the shoreface profile of equilibrium. *Marine Geology*, **126**, 271–287.

THIELER, E. R., PILKEY, O. H., YOUNG, R. S., BUSH, D. M. & CHEI, F. 2000. The use of mathematical models to predict beach behavior for US coastal engineering. *Journal of Coastal Research*, **16**, 48–70.

USACE 2002. *Coastal Engineering Manual 1110-2-1100*. US Army Corps of Engineers, Washington, D.C.

VAN WELLEN, E., BALDOCK, T. E., CHADWICK, A. J. & SIMMONDS, D. 2000. Longshore sediment transport in the swash zone. *In: Proceedings of the 27th Internation. Conference on Coastal, Engineering*, ASCE, New York, 3139–3150.

WANG, P. & KRAUS, N. C. 1999. Longshore transport rate measured by short-term impoundment. *Journal of Waterway, Port, Coastal and Ocean Engineering*, **125**, 118–126.

WANG, P., SMITH, E. R. & EBERSOLE, B. A. 2002. Large-scale laboratory measurements of longshore sediment transport under spilling and plunging breakers. *Journal of Coastal Research*, **18**, 118–135.

WEBB, M. P. & VINCENT, C. E. 1999. Comparison of time-averaged acoustic backscatter concentration profile measurements with existing predictive models. *Marine Geology*, **162**, 71–90.

WHITE, T. E. 1996. Field tests of five suspended-load transport theories used in numerical models. *In: Proceedings of the 25th ICCE, Orlando*. ASCE, New York, 2799–2812.

WHITE, T. E. 1998. Status of measurement techniques for coastal sediment transport. *Coastal Engineering*, **35**, 17–45.

Simple analytical results for bedload transport due to tides

JOHN N. ALDRIDGE

Centre for Environment, Fisheries, and Aquaculture Science, Pakefield Rd, Lowestoft, Suffolk NR33 OHT, UK (e-mail: j.n.aldridge@cefas.co.uk)

Abstract: Patterns of sediment erosion and deposition arising from tide induced bedload transport are explored using standard bedload formulae and a simple analytic approach. Decomposing the current into a principal M_2 tidal constituent, an M_4 first harmonic and a tidal residual, it is straightforward to derive an expression for the contribution each makes to the integrated tidal flux. The resulting expressions are applied to calculate the net change in bed level induced by bedload transport due to a superposition of a Kelvin tidal wave, a harmonic overtide and a residual tide.

Understanding and predicting the movement of sediment in coastal and shelf seas remains a difficult problem. Recently, calculations have been undertaken to predict large-scale net transport rates and identify regions of erosion and deposition using numerical approaches (e.g. Van der Molen & De Swart 2001; Gerritsen & Berentsen 1998; Van der Molen 2002, and contributions to this volume). Nevertheless, we believe that considerable insight can be gained using a relatively simple analytic (algebraic) approach to complement full-scale numerical calculations and aid in interpretation of numerical results. Using a reasonably general bedload formulation, it is relatively easy to derive an expression giving the tidally integrated sediment transport flux and hence the net change in bed level over a tidal cycle. Indeed, similar results have been derived in Hunter (1979) and Van der Molon & De Swart (2001). The main contribution of this paper is to apply the resulting expressions to determine the patterns of erosion and deposition for the case of Kelvin solutions representative of shelf seas. In particular, the result for the supersition of a principal M_2 wave system and the harmonic overtide M_4 are calculated. As demonstrated by the numerical calculations of Pingree & Griffiths (1979), directions of sand transport observed around the British coast (Stride 1963) can be reproduced by considering the average stress vectors associated with these tidal constituents. The actual mechanism is the well-known one (Postma 1961; Dronkers 1986) involving tidal asymmetry, where the average tidal stress is higher for one direction of the tidal flow than the other leading to a net transport in the direction associated with the greatest average stress. In addition we consider the result for the superposition of the principal M_2 tide, and a residual flow. All the results rely on the implicit assumption that the supply of bed material available for transport is not exhausted over the tidal cycle.

Bedload formulae

Soulsby (1997) presents a number of the more recently derived bedload formulae. Although the exact forms vary, most indicate a dependence of the magnitude of the volumetric transport flux vector $q_b(\mathrm{m^2\,s^{-1}})$ that is approximately cubic in terms of the applied velocity. In particular, the Bagnold (1963), Yalin (1963) and Nielsen (1992) formulae can all be written

$$q_b^* = \begin{cases} a_1\theta^{1/2}(\theta-\theta_{cr}) & \theta \geq \theta_{cr}, \\ 0 & \theta < \theta_{cr} \end{cases} \qquad (1)$$

where $q_b^* = |q_b|/\sqrt{g(s-1)d^3}$ is the non-dimensional transport rate, and a_1 is a non-dimensional constant which varies with the particular form of bedload formulae chosen. A key quantity is the Shields parameter $\theta = \tau/(g\rho(s-1)d)$, where τ is the instantaneous bed stress, d is the particle diameter, and $s = \rho_p/\rho$ is the ratio of sediment to water density. For θ less than a fixed critical value θ_{cr}, no transport occurs. It is assumed that the applied hydrodynamic bed stress can be related to the depth mean velocity $\bar{u}$ by an empirical drag law

$$\tau_c = \rho C_D|\bar{u}|^2, \qquad (2)$$

with drag coefficient C_D. The value of C_D can be calculated by a number of methods and may include a dependence on bottom roughness, water depth and possibly other parameters. Substituting for $\theta^{1/2}$ using (Equation 2) and making the assumption that bedload transport occurs in the direction of the applied bed stress,

From: BALSON, P. S. & COLLINS, M. B. 2007. *Coastal and Shelf Sediment Transport*. Geological Society of London, Special Publications, **274**, 45–51. 0305-8719/07/$15.00

gives a vector relation for the dimensional bedload flux as $q_b = a_1\sqrt{C_D}\,\bar{u}d(\theta-\theta_{cr})$ when $\theta \geq \theta_{cr}$. Substituting again for θ, leads finally to

$$q_b = \begin{cases} k\bar{u}(|\bar{u}|^2 - u_{cr}^2) & |\bar{u}| \geq u_{cr} \\ 0 & |\bar{u}| < u_{cr}, \end{cases} \quad (3)$$

with $k_1 = a_1 C_D^{3/2}/(g(s-1))$ and $u_{cr}^2 = \tau_{cr}/(\rho C_D)$. Note, neglecting the critical erosion velocity yields a form, that looks very similar to the bedload component of the Bailard (1981) total load formula as presented by Soulsby (1997).

Derivation of expressions for the net tidal bedload flux

For the rest of the paper, consideration is given to the net tidal flux generated by Equation 3 for tidal forcing at the principal (M_2) tidal frequency, a zero frequency residual (Z_0) constituent and a first harmonic (M_4) constituent at double the frequency. The depth-mean tidal velocity vector is thus decomposed as

$$u = \bar{v}_2 + \bar{v}_0 + \bar{v}_4, \quad (4)$$

where $\bar{v}_2$, $\bar{v}_0$ and $\bar{v}_4$ are the M_2, Z_0 and M_4 velocity components respectively. In the non-linear tidal equations, the Z_0 and M_4 constituents can be regarded as deriving from the astronomically generated M_2 tide via non-linear interactions. It is assumed $\bar{v}_0, \bar{v}_4 \ll \bar{v}_2$, and in the following, products of two or more of $\bar{v}_0$, $\bar{v}_4$ are neglected (this can be made rigorous in a full non-dimensional analysis which, for brevity, is not undertaken here). Consideration will be given to the net flux over an M_2 tide and integration over the M_2 period T_{M2} is denoted by $\langle f \rangle = \int_0^{T_2} f(t)\,dt$.

Introducing the Heaviside step function $H(\zeta)$ (with $H(\zeta)=0$ for $\zeta<0$, and $H(\zeta)=1$ for $\zeta \geq 0$), Equation 3 can be written equivalently as

$$q_b = k_1\,\bar{u}\,(\bar{u}.\bar{u} - u_{cr}^2)\,\Theta \quad (5)$$

with $\Theta = H(|\bar{u}|^2 - u_{cr}^2)$. Then, substituting Equation 4 into Equation 5 and integrating over the tidal period yields

$$\langle q_b \rangle = k_1(\Phi_2 + \Phi_0 + \Phi_4), \quad (6)$$

where, after neglecting triple products containing two or more occurrences of $\bar{v}_0$ and $\bar{v}_4$,

$$\Phi_2 = \langle \bar{v}_2\,(\bar{v}_2.\bar{v}_2 - u_{cr}^2)\Theta \rangle, \quad (7)$$

$$\Phi_0 = \langle \bar{v}_0\,(\bar{v}_2.\bar{v}_2 - u_{cr}^2)\Theta \rangle + 2\langle \bar{v}_2(\bar{v}_2.\bar{v}_0)\Theta \rangle, \quad (8)$$

$$\Phi_4 = \langle \bar{v}_4\,(\bar{v}_2.\bar{v}_2 - u_{cr}^2)\Theta \rangle + 2\langle \bar{v}_2(\bar{v}_2.\bar{v}_4)\Theta \rangle. \quad (9)$$

For a given constituent, the velocity at time t and position x can be written, quite generally, as

$$\bar{v}_{2n}(t, x) = (U_n \cos[\pi\omega t - \varphi_n],\, V_n \cos[\pi\omega t - \psi_n]), \quad (10)$$

where $n = 0, 1, 2$ for Z_0, M_2 and M_4 respectively. The functions U_n, V_n and φ_n, ψ_n give the spatial distribution of the tidal amplitude and phase for each velocity component.

For flow fields given by Equation 10 the pure M_2 contribution Φ_2 is identically zero. Does this mean that a single oscillatory tide can give rise to no net movement of sediment? Clearly the above arguments neglect the influence of waves, and (more subtly) assumes that there is an unlimited supply for sediment to erode throughout a tidal cycle. If either of these conditions is relaxed, a non-zero net flux due to the M_2 tide alone seems possible. However, even maintaining these assumptions, we believe a non-zero net flux from the M_2 tide alone can arise. This mechanism must be equivalent to the Lagrangian transport of particles due to spatial gradients in the driving flow, even if these have a zero Eulerian mean. Physical reasoning suggests that for bedload, this effect will be small since the distance traveled over a tidal cycle by bedload particles will generally be very small compared to the lengthscale of changes in mean flow. Nevertheless, the fact that the conventional bedload flux relations, when averaged over a tidal cycle, do not appear to yield such an effect suggests that the standard bedload flux formulation may be incomplete.

Nevertheless, in this paper, the patterns of erosion and deposition generated by the remaining terms in Equation 6 are explored. At this stage, the dependence on a critical threshold is dropped. It is possible to maintain this concept by introducing the Fourier expansion of the Heaviside step function. However this complicates the treatment considerably and to maintain simplicity and brevity is not pursued here. In addition, the study of erosion and deposition in the North Sea of Van der Molen & De Swart (2001) used a formulation without a threshold and obtained patterns that showed some agreement with observation sediment distributions. Thus the net bedload flux is now assumed to be given by

$$\langle q_b \rangle = k_1(\Phi_0 + \Phi_4),$$

with

$$\Phi_0 = <\bar{v}_0\,(\bar{v}_2.\bar{v}_2)> + 2<\bar{v}_2(\bar{v}_2.\bar{v}_0)>,$$

$$\Phi_4 = <\bar{v}_4\,(\bar{v}_2.\bar{v}_2)> + 2<\bar{v}_2(\bar{v}_2.\bar{v}_4)>.$$

If Equation 10 is substituted into the above, and the tidal averaging carried out, an explicit expression for the transport flux in terms of the phase and amplitudes of the tidal constituents is obtained

$$\Phi_0 = \frac{\pi}{\omega}\,(\cos[\varphi_2-\psi_2]U_2V_0V_2 + U_0[2U_2^2+V_2^2],$$
$$(\cos[\varphi_2-\psi_2]U_0U_2V_2 + V_0[U_2^2+2V_2^2]),$$

$$\Phi_4 = \frac{\pi}{2\omega}\,(2\cos[2\varphi_2-\varphi_4]U_2^2U_4 + \cos[\varphi_4-2\psi_2]$$
$$U_4V_2^2 + \cos[\varphi_2+\psi_2-\psi_4]U_2V_4V_2,$$
$$\cos[\varphi_2-\varphi_4+\psi_2]U_2U_4V_2 + \cos[2\varphi_2-\psi_4]U_2^2V_4$$
$$+2\cos[2\psi_2-\psi_4]V_2^2V_4).$$

We note that a similar set of expressions was presented in Van der Molen & De Swart 2001. For uni-directional flow, the results become particularly simple. Assuming that only the u-component is non-zero then

$$\Phi_0 = \frac{2\pi}{\omega}\,(U_0U_2^2,\,0), \tag{11}$$

$$\Phi_4 = \frac{\pi}{\omega}\,(\cos[2\varphi_2-\varphi_4]U_2^2U_4,\,0) \tag{12}$$

The standard form of bed elevation change (e.g. Soulsby 1997) averaged over a tidal cycle and assuming only gradients in the x direction flux becomes

$$\Delta\eta = -\frac{1}{1-\varepsilon}\frac{\partial}{\partial x}<q_b>, \tag{13}$$

where ω is the bed porosity.

Results

Predicted patterns of changes in bed level for the case of counter propagating tidal Kelvin waves in water of constant depth are calculated using the results derived in the previous section. However, because the flow associated with such waves is uni-directional, it is possible to use the simplified expressions, Equations 12 and 13. We note that real tidal systems (e.g. the North Sea) include regions where the tide is not rectilinear. Nevertheless, Kelvin wave solutions are realistic enough to provide a useful model of many of the observed features of tides on continental shelves, including the occurrence of amphidromic systems.

For superimposed leftward and rightward propagating M_2 and M_4 Kelvin waves (without friction in an infinitely long channel), together with a uniform residual flow, the quantities required in Equations 12 and 13 have the explicit representation

$$U_0 = constant, \tag{14}$$

$$U_2 = \sqrt{\sinh^2 my\cos^2 kx + \cosh^2 my\sin^2 kx}, \tag{15}$$

$$\varphi_2 = \arctan[-\tan k\,x\coth m\,y], \tag{16}$$

$$U_4 = [\sinh^2 m(y-y_0)\cos^2 2k(x-x_0) + \cosh^2 m(y-y_0)\sin^2 2k(x-x_0)]^{1/2}, \tag{17}$$

$$\varphi_4 = \arctan[-\tan 2k(x-x_0)\coth m(y-y_0)] - \Upsilon, \tag{18}$$

where $k=\omega/\sqrt{gh}$ and $m=\Omega/\sqrt{gh}$ are the wave numbers in the x and y directions. Here ω is the M_2 frequency, $\Omega \approx 1.4\times10^{-4}\cos(\phi)$ is the coriolis parameter at latitude ϕ, g is the acceleration due to gravity, and h is the water depth. A uniform residual constituent has been included, and the M_4 constituent is spatially offset with respect to M_2 by $x_0=(x_0, y_0)$ and offset in phase from M_2 by an arbitrary global phase difference Υ. The solution for M_2 leads to a classical system of elevation and velocity amphidromes. Since the Kelvin wave solution has velocity and elevation amphidromes in anti-phase along the x-axis, the elevation amphidromic points correspond to *maxima* in tidal velocity.

The expression for Φ_4 (Equation 13), indicates that the quantity $2\varphi_2-\varphi_4$ will play a key role in determining the net transport flux produced by the M_2 and M_4 interaction. This quantity will have a non-trivial spatial dependence as φ_2 and φ_4 vary with position. However, it will also depend on the values of the spatial offset x_0 and the global phase difference Υ. In reality, the phase relation between the two constituents would be fully determined by the non-linear generation of the M_4 constituent from M_2. However, since the M_2 and M_4 constituents are here being treated independently, there is nothing to fix Υ or x_0 and in order to reflect the full generality of the possible phase difference between M_2 and M_4 tides, the values of x_0 and Υ are introduced as free parameters.

Results are shown for a domain with extent 700 km by 200 km in the x-direction and y-direction respectively (Fig. 1). The uniform water depth is taken to be 30 m. Given that there is zero velocity in the y-direction, conceptually it might be imagined that the top and bottom y limits

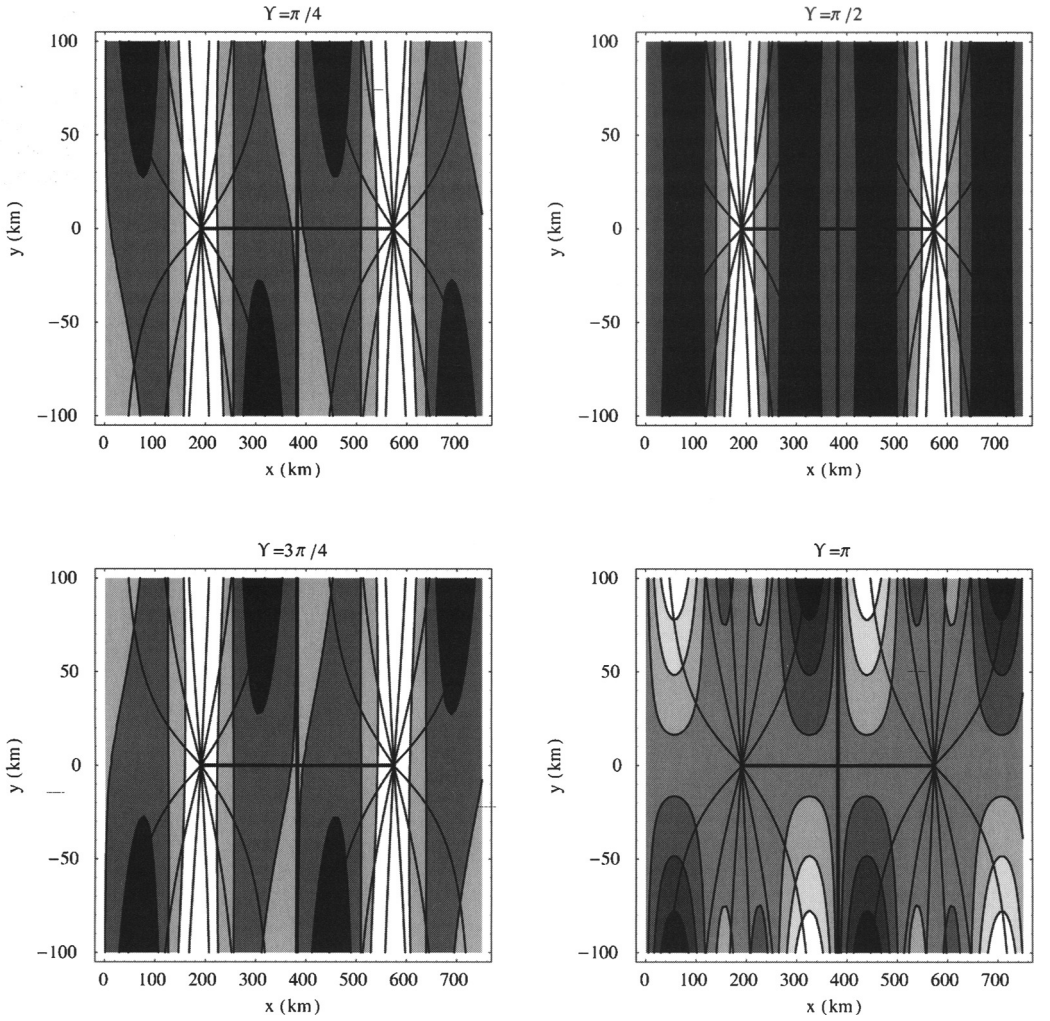

Fig. 1. $M_2 \times M_4$ generated net erosion and deposition patterns. The value of Υ is indicated on each figure. Lighter shades represent erosion, darker shades represent deposition. To aid interpretation, co-tidal lines of surface elevation for M_2 are superimposed.

represent a coast. All patterns are generated by redistribution of sediment parallel to these 'coasts'. The solution in the alongshore direction is periodic, reflecting the periodic tidal forcing.

M_4 and M_2 interaction

Results are shown for four representative values of the global phase difference $0 < \Upsilon \leq \pi$. These are sufficient to illustrate the broad features of the complete range of possible patterns.The results for $\Upsilon > \pi$ are identical, but with regions of erosion and deposition reversed. The effect of changing the M_2 M_4 spatial offset is mainly to translate the patterns in space without essentially changing the form, and in the results shown here, x_0 is taken to be zero. Changing the strength of one of the two counter-propagating waves also has a relatively trivial effect, simply reducing the magnitude of the pattern on one side without changing the overall form. However, apparently quite different patterns emerge for different values of Υ (Fig. 1). Nevertheless, the results share a common feature in the prediction of alternate bands of net erosion and deposition. This is illustrated more clearly in Figure 2 where the annual change in bed level is plotted for two values of Υ along the section $y = 50$ km. In this

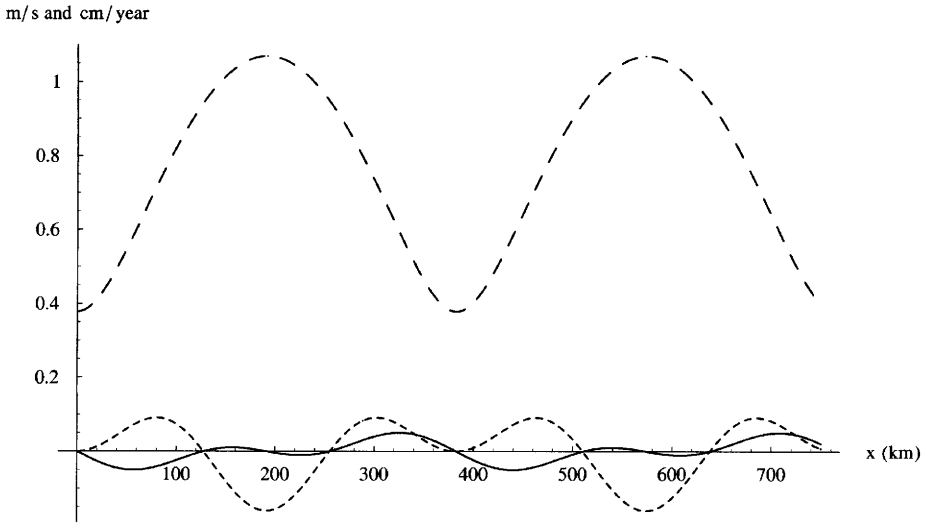

Fig. 2. M_4 generated annual net bed level change along the domain for $y = 50$ km. Solid line is $\Upsilon = 0$; fine dotted line is $\Upsilon = \pi/2$; dashed line is M_2 velocity amplitude.

figure, annual change is calculated from Equation 11 by multiplying by the number of M_2 tidal cycles per year. The M_4 tidal amplitude is assumed to be 0.1 of the M_2 amplitude, C_D is taken as 0.0013, and a porosity of 0.4 is used. The Nielsen (1992) bedload formulae is used for which the constant in Equation 1 is just $a_1 = 12$. Also shown on the plot is the M_2 velocity amplitude. Note erosion and deposition patterns are not directly related to maxima and minima of the M_2 tidal velocity. It is the phase relation between M_2 and M_4 that is essential in determining the regions of net accumulation or erosion. The actual mechanism is the well known one (Postma 1961; Pingree & Griffiths 1979) involving tidal asymmetry where the average tidal stress is higher for one direction of the tidal flow than the other leading to a net transport in the direction where the average stress is highest. Although sediment type is often well correlated with total tidal stress, with areas of gravel in high energy regions, there are notable cases where sand is found in regions of large velocities. The occurrence of significant systems of sand banks at the velocity maximum off Great Yarmouth and Lowestoft, and at the degenerate amphidromic point off county Wicklow in SE Ireland, being examples. The tidal asymmetry mechanism may be involved with this phenomenon. Interestingly, a banded structure with alternating zones of net erosion and deposition (although showing a much less regular pattern that the analytic results) can be discerned in the calculations presented in Van der Molen & De Swart (2001) and Gerritsen & Berentsen (1998), using realistic tidal forcing in the North Sea. Moreover, the predicted order of magnitude of the annual change in bed level 1 mm is very close to the range of values found in Van der Molen (2002). We note, although the bed level change appears relatively small, the changes occur over a large area and the volume of material being redistributed is quite substantial. In addition, such changes operating over centuries would lead to significant changes in bed levels.

Z_0 and M_2 interaction

The spatially uniform residual tide used here is not particularly representative of the results produced by numerical models of the continental shelf which often show eddy like features, particularly near the coast (Aldridge & Davies 1993). Nevertheless, it is of interest to illustrate patterns of net erosion and deposition from the interaction with M_2 for this simple form of the residual tide. Again a banded structure emerges (Fig. 3). The plot of bed level change along a section through the domain (Fig. 4) indicates the essential nature of the resulting pattern. Erosion occurs in regions where the M_2 velocity amplitude increases in the direction of the residual velocity vector (in this case in the positive x direction), with deposition occurring as the M_2 velocity amplitude decreases.

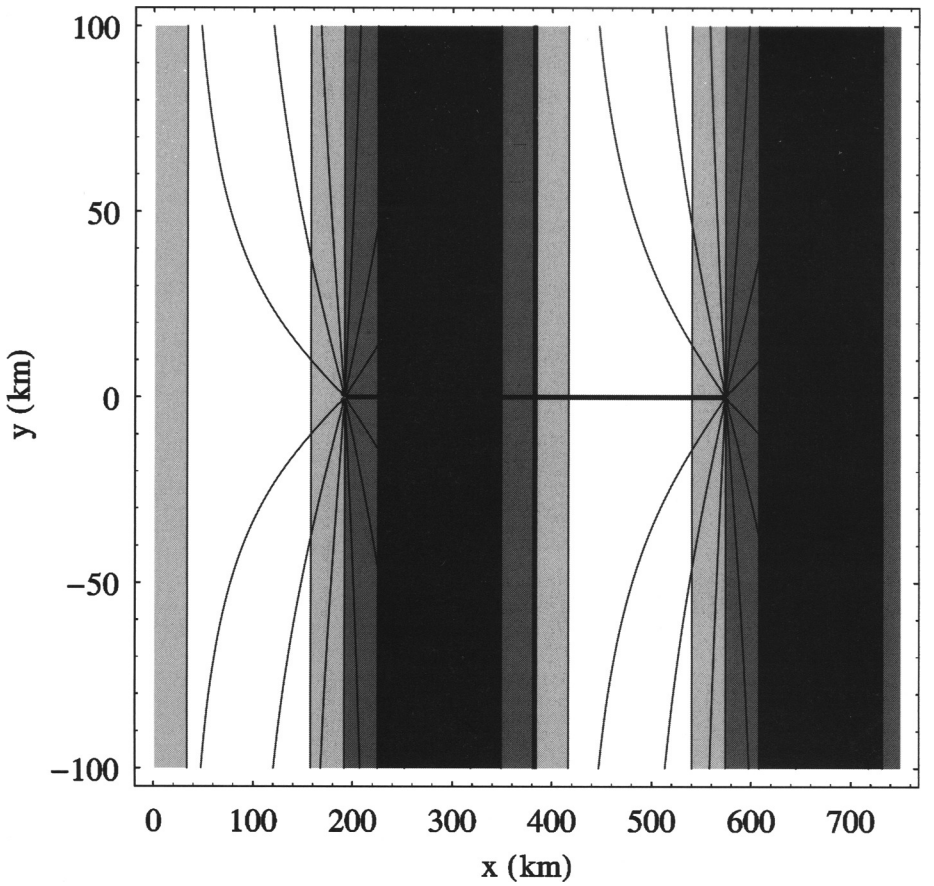

Fig. 3. Z_0 generated net erosion and deposition patterns for a uniform residual tide. Lighter shades represent erosion, darker shades represent deposition. Axis units are kilometres. To aid interpretation, co-tidal lines of surface elevation for M_2 are superimposed.

Summary and conclusions

A standard formulation of bedload transport in terms of the Shields parameter was rewritten, assuming a quadratic drag law, in terms of an applied depth mean current. Taking the current to be tidal, the velocity field was decomposed into a principal M_2 constituent together with the M_4 overtide and a residual Z_0 tidal flow. When substituted into the bedload formulation and averaged over an M_2 tidal cycle, an expression for the net sediment transport flux is obtained. We note that an implicit assumption of an unlimited supply of available sediment is required in order to obtain this result.

In the approach adopted here, the pure M_2 tidal contribution averages to zero, and non-zero contributions to the flux occur only as a result of interactions between M_2 and the other constituents. We conjecture that a non-zero contribution arising from a pure M_2 interaction should occur, which is not captured in standard formulations of bedload transport. Nevertheless, the results for the net tidal flux due the presence of M_4 and Z_0 are calculated and expressed in terms of the phase and amplitude of the tidal constituents. Results are illustrated for the case of an idealised tidal Kelvin wave solution.

In the case of unidirectional flow, patterns of erosion and deposition are essentially determined by the spatial gradient of the quantity $\cos(2\varphi_2 - \varphi_4)$ where φ_2 and φ_4 are the M_2 and M_4 tidal phase. Typically, this leads to a banded pattern of erosion and deposition. This is independent of the magnitude of the M_2 tidal energy in the sense that accumulation can occur in areas

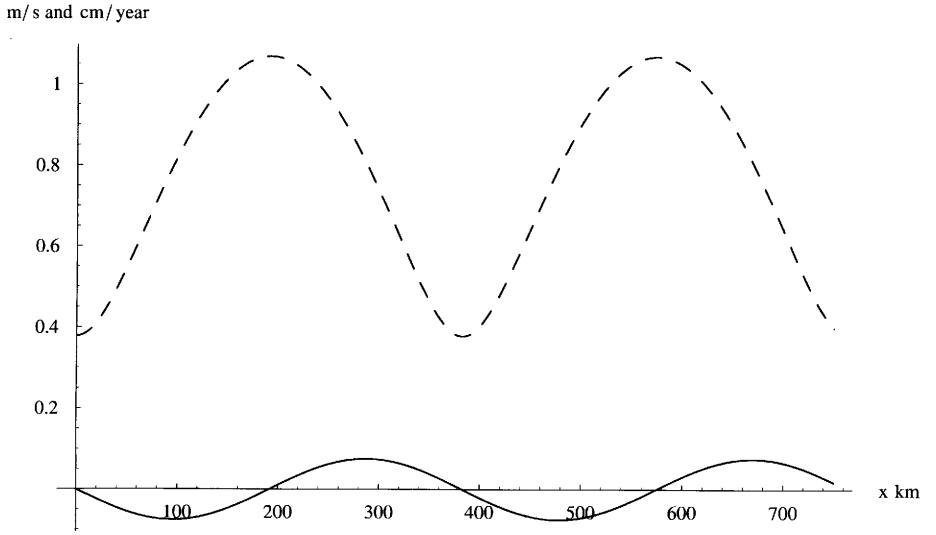

Fig. 4. Z_0 generated annual net bed level change along the domain at $y = 50$ km (solid line); M_2 velocity amplitude (dashed line). See caption for Figure 2 for information on the calculation of the magnitude of the this plot. The Z0residual velocity is assumed to be 0.1 of the M_2 amplitude and directed in the positive x direction.

of high M_2 velocity amplitude. For the case of the M_2 interaction with the Z_0 tidal residual, a link with the M_2 tidal velocity amplitude is apparent, with erosion occurring in regions where the spatial gradient of the M_2 velocity amplitude increases in the direction of the residual velocity vector, and deposition where it decreases.

References

ALDRIDGE, J. N. & DAVIES, A. M. 1993. A high-resolution three dimensional hydrodynamic tidal model of the Eastern Irish Sea. *Journal of Physical Oceanography*, **23**, 207.

BAGNOLD, R. A. 1963. Mechanics of marine sedimentation. *In*: HILL, M. N. (ed.) *The Sea: Ideas and Observations*, **3**. Wiley Interscince, New York, 507–528.

BAILARD, J. A. 1981. An energetics total load sediment transport model for a plane sloping beach. *Journal Geophyical Research*, **86(C11)**, 10938–10954.

DRONKERS, J. 1986*b*. Tidal asymmetry and estuarine morphology. *Netherlands Journal of Sea Research*, **20**, 117–131.

GERRITSEN, H. & BERENTSEN, W. S. 1998. A modelling study of the tidally induced equilibrium sand balances in the North Sea during the Holocene, *Journal of Continental Shelf Research*, **18**, 151–200.

HUNTER, J. 1979. On the interaction of M_2 and M_4 tidal harmonics in relation to quadratic and higher power laws, *Deutsche Hydrographische Zeitschrift*, **32**, 146–153.

NIELSEN, P. 1992. *Coastal Bottom Boundary Layers and Sediment Transport.* Advanced Series on Oceanography. World Scientific Publishing, Singapore, **4**.

PINGREE, R. D. & GRIFFITHS, D. K. 1979. Sand transport paths around the British Isles resulting from M_2 and M_4 tidal interactions. *Journal of the Marial Biological Association UK*, **59**, 497–513.

POSTMA, H. 1961. Transport and accumulation of suspended matter in the Dutch Wadden Sea. *Netherlands Journal of Sea Research*, **1**, 148–190.

SOULSBY, R. L. 1997. *Dynamics of Marine sands.* Thomas Telford Publications, London.

STRIDE, A. H. 1963. Current-swept sea floors near the southern half of Great Britian. *Quarterly Journal of the Geological Society London*, **119**, 175–199.

VAN DER MOLEN, J. 2002. The influence of tides, wind and waves on the net sand transport in the North Sea. *Continental Shelf Researth*, **22**, 2739–2762.

VAN DER MOLEN, J. & DE SWART, H. E. 2001. Holocene tidal conditions and tide-induced sand transport in the southern North Sea. *Journal of Geophysical Research*, **106(C5)**, 9339–9362.

YALIN, M. S. 1963. An expression for bedload transportation. *Proceeding of the American Association, of Civil Englineers*, **89(HY3)**, 105–119.

Use of swath bathymetry in the investigation of sand dune geometry and migration around a near shore 'banner' tidal sandbank

THIERRY SCHMITT*, NEIL C. MITCHELL & TONY S. RAMSAY

School of Earth, Ocean and Planetary Sciences, Cardiff University, Main Building, Park Place, Cardiff CF10 3YE, UK

**Present address: Centre Interdisciplinaire de Développement en Cartographie des Océans, 310 Allée des Ursulines, GSL 3A1 Rimouski (Quebec), Canada (e-mail: Thierry.Schmitt@cidco.ca)*

Abstract: Banner tidal sandbanks in the Bristol Channel have been repeatedly surveyed with a multibeam sonar to study the geometry and migration patterns of superimposed dunes. The data presented in this paper constitute one of the first studies concerned with sediment transport around a banner sandbank (Helwick Sands in the Bristol Channel) using repeated swath- bathymetry. The data reveal that the dunes maintain their shapes over a period of 11 months, and that they migrate in opposite directions on the alternate sides of the bank. Curiously, dunes connect over the crest of the bank despite opposing sediment transport directions on the flanks. Dune height increases with water depth as found in similar environments. We suggest how the morphology of the dunes results from the complex interaction between surface waves and tidal currents that occurs within the proximity of the headland.

Banner sandbanks occur where sediment is abundant, currents are able to induce bedload transport and spatial gradients in the sediment transport flux cause deposition (Dyer & Huntley 1999). Such conditions can be found in some estuarine environments, such as the Bristol Channel (Fig. 1). Popular theories concerning the formation and maintenance of banner banks involve convergence of sediment transport flux induced by residual (averaged over a tidal cycle) current eddies in the pattern of currents eddies originating from coastal irregularities (Pingree 1978; Ferentinos & Collins 1980; Dyer & Huntley 1999). Associated bedforms such as sand dunes are usually well developed on the flanks of active sandbanks. Their orientations in plan view, their asymmetry and geometry in cross-section have been widely used as indicators of the local net sediment transport and hydrodynamic conditions (Harris 1982; Lees 1983; Twichell 1983; Collins *et al.* 1995; Reynaud *et al.* 1999; Hennings *et al.* 2000). Most of the previous studies have focused on the morphology of the dunes rather than on their temporal evolution, and surveys were carried out either with single-beam echosounders or sidescan sonars, with a positioning accuracy of a few tens to hundreds of metres. Recent improvements in positioning at sea and computing methods for processing large amounts of data, however, have facilitated the collection of decimetric accuracy high-resolution bathymetric data with swath sonar (Hare *et al.* 1995). Furthermore, repeated full bathymetric coverage of sub-tidal sedimentary structures using swath-sonar technology will provide information of their dynamics and three-dimensional characteristics, which are of interest for the understanding of coastal and shelf sedimentary transport.

This paper describes the morphology and dynamical characteristics of sand dunes at the eastern end of the Helwick Sandbank, lying near a headland in the Bristol Channel (Fig. 1). The analysis is based on two sets of swath-bathymetry data collected on 26 September 2001 and 20 August 2002.

The main objective of this paper is to demonstrate the potential for tracking dune migration and dune geometry changes from repeated bathymetric multibeam surveys. This paper is therefore intended to (a) describe the morphological characteristics of the dunes and their spatiotemporal evolution, (b) estimate dune migration rate and from that infer sediment transport flux and (c) relate these data to the work elsewhere of sediment transport around sandbanks and their maintenance. In describing the sand dunes in this paper, we follow the terminology developed by Ashley (1990).

Study area

Helwick Bank is a linear sandbank located off the western end of the Gower Peninsula (Fig. 1).

From: BALSON, P. S. & COLLINS, M. B. 2007. *Coastal and Shelf Sediment Transport*. Geological Society of London, Special Publications, **274**, 53–64. 0305-8719/07/$15.00

The bank extends for 13.5 km westward with a bearing of 265°N. It has a maximum width of 2.7 km and a maximum height of 40 m above the surrounding seabed. The area of interest (Fig. 1) encompasses the eastern end of the bank, Port Eynon Bay and the Carboniferous limestone bedrock of Port Eynon Point close to the bank. Its cross-section is asymmetric, with a steep south flank (3.5°) facing south and a gentle north flank (0.6°) facing the coast. Britton (1978) suggested from seismic data acquired over the bank and boreholes in its vicinity that the Helwick Sands reached its present day morphology sometime during the Flandrian transgression (5000 BP). His seismic data show maximum thickness of 40 m of sand overlying a flat surface of Lias bedrock (Neville 1970). Gravel and till deposits, lying between the bedrock and the sand are observed sparsely in the seismic records and have a maximum thickness of 2 m. Britton (1978) suggests that this layer is a relic of piedmont glaciers that extended as far south as the Gower Peninsula during the Devensian glacial period (70 000 BP to 10 000 BP). However, due to the quality of the seismic records, the residual current eddy origin of the development of the bank is still questioned, though considered here being the most probable (HR Wallingford 1997). Hydrodynamic and granulometry data were not collected simultaneously with the bathymetric surveys, but such data have been reported by Postford Duvivier & ABP Mer (2000). That report shows that fine to medium sand composes the surface of the bank ($D_{50}=0.4$ mm). One acoustic Doppler current profiler (ADCP) moored just north of the bank within the Helwick Passage (Fig. 1) recorded maximum ebb (N124°E) and flood (N241°E) which reached 0.84 m s^{-1} and 0.82 m s^{-1}, respectively. A second ADCP moored closer to the crest recorded weaker currents with a maximum flood (N295°E) flow reaching 0.35 m s^{-1} and a maximum ebb (N90°E) reaching 0.21 m s^{-1}. Prevailing waves approach from the SW (N230°E), according to the ADCP records. The data show a 4.25 m maximum significant height (one third of the highest waves) and 9.63 s period.

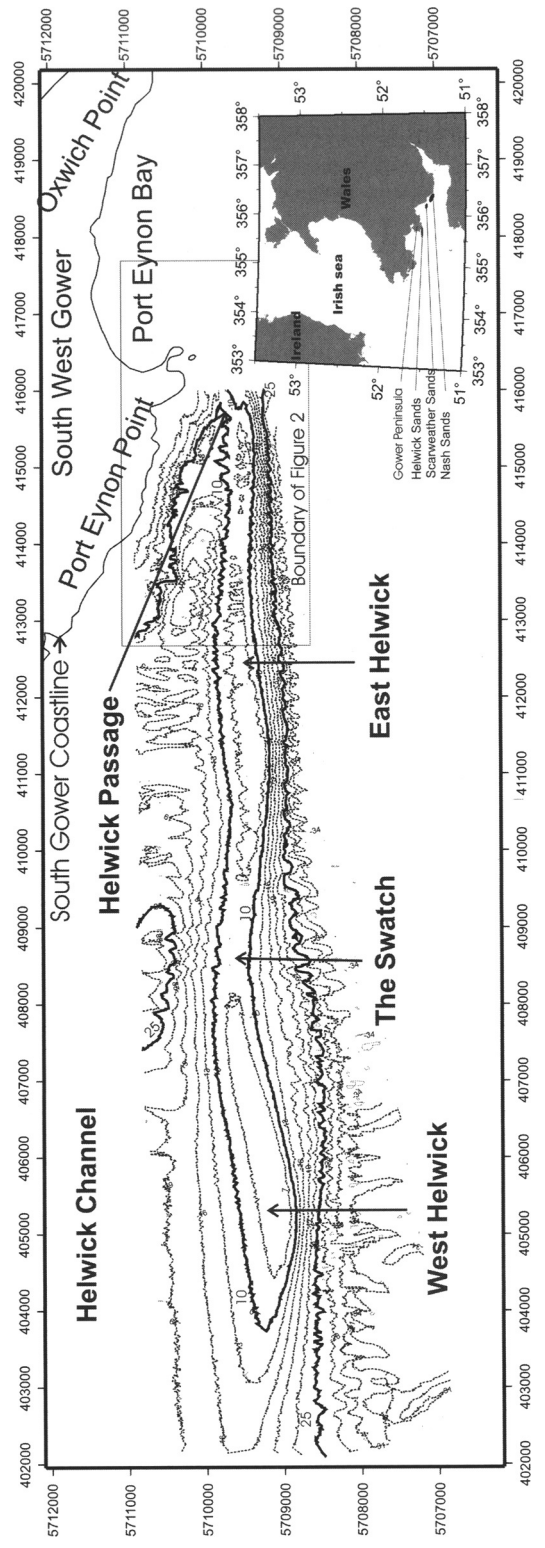

Fig. 1. Physiographic map of the Helwick Sandbank and Port Eynon Bay. Depth contours are displayed every 3 m, with 10 and 25 m in bold (depths are relative to Chart Datum). The coordinates are converted to the Universal Transverse Mercator system zone 30 (projected using the WSGS84 ellipsoid), so that distances be measured in metres directly from the maps. Inset: The Bristol Channel and location of Helwick Sands. Location of two other banner sandbanks (Scarweather and Nash) is displayed.

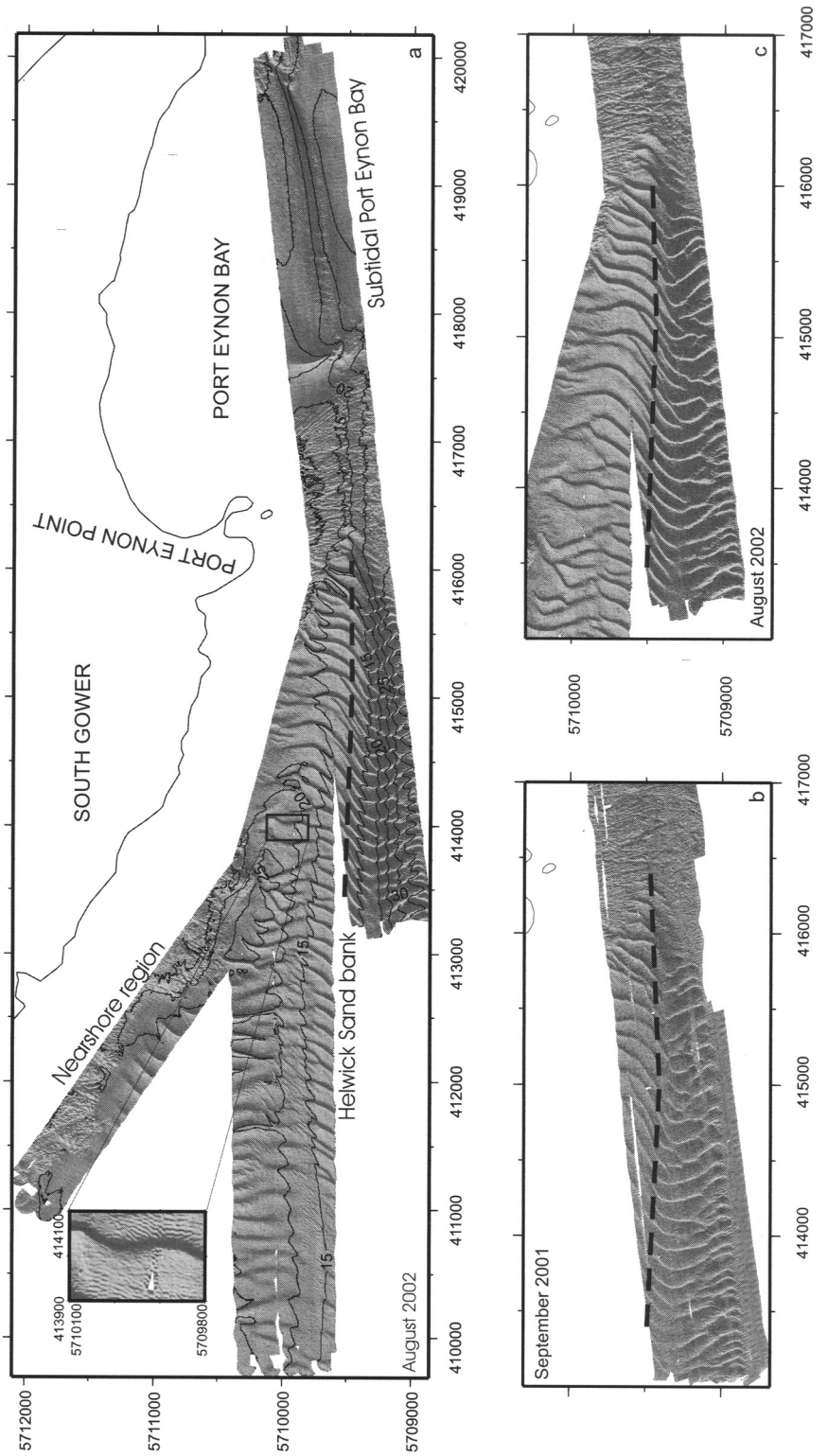

Fig. 2. Grey-shaded maps of bathymetric data collected with a Reson Seabat 8101 multibeam sonar along the southwest coast of the Gower Peninsula. The gridded data have 1 m spatial resolution. The data are illuminated from the NW. Dashed lines represent the crest of the bank. (**a**) Overview of the data encompassing the eastern Helwick Sands, its connection with the bedrock near Port Eynon Point, the subtidal Port Eynon Bay and a nearshore region west of Port Eynon Point. Continuous lines represent water depths contoured every 5 m. Inset: example of small dunes superimposed on the stoss side of medium ones. (**b**) and (**c**) The area of repeated coverage (26 September 2001 and 20 August 2002 respectively). The 2001 dataset is noisier due to an erroneous setting of the heave filter, but positions still have decimetrical precision. Note the similarity in plan-form shapes of the dunes between the two surveys.

The present-day morphology of the bank is likely a result of the action of both the tidal currents and surface waves, as has been inferred for numerous other shallow banks (Huthnance 1982*a*; Pattiarchi & Collins 1987; Houthuys *et al.* 1994; Collins *et al.* 1995; Reynaud *et al.* 1999; Mallet *et al.* 2000).

Repeated multibeam sonar surveys

The data presented in this paper are based on two bathymetric surveys over the same area carried out with a Reson Seabat 8101 multibeam sonar. The system consists of 101 echo-sounding beams, each with an aperture of 1.5° by 1.5°, which ensonify the seabed across a 150° fan. The location and water depth of each footprint within the swathe are geo-referenced using the position and motion data of the boat That are collected simultaneously with an Applanix POS/MV220 motion sensor. Processing of the data involves the manual editing of erroneous depth measurements, merging the data from the different sensors with corrections related to the tidal height and the celerity of the acoustic pulse in the water column.

The 2001 survey covered mainly the southern flank, but also a small part of the northern flank (Fig. 2b). The 2002 survey covered the eastern end of Helwick bank, on both flanks and adjacent coastal areas (Fig. 2a and c).

During both surveys, data were acquired in relatively calm seas. In 2001, tidal heights were collected at the Mumbles UK national tide gauge, whereas in 2002, they were also collected simultaneously on an adjacent beach located less than 5 km from the surveyed area. The comparison of the two tidal signals allowed the determination of a tidal range multiplier and a phase offset, which have been applied to the 2001 Mumbles tide gauge data to correct the 2001 bathymetric dataset.

All depths in this paper are given relative to Chart Datum. The surveys extend from 4 m at the crest of the bank to 40 m at the base of the southern flank. The crest of the bank connects to the bedrock sub-tidal extension of Port Eynon Point through a depression where the water depth ranges from 8 m to 10 m (Fig. 2).

Mapping of dunes

Small and medium dunes are superimposed on both flanks and the crest of the bank. Small dunes have been described as transient or highly dynamic morphological features, which can be obliterated by meteorological events such as storms (Houthuys *et al.* 1994). They are present on the stoss sides of several bigger dunes, mostly located on the base of each flank of the bank (see inset to Fig. 2a). The direction of their crests, on the northern flank, is sub-parallel to the crests of the medium dunes that they cover. At the base of the southern flank they are orientated *c.* 30° oblique to the dune crest. Bennett & Best (1995) suggest that flow separation occurring at the crest of large dunes induce a zone of detachment, in which turbulences affect the mode of sediment transport and may lead to the formation of smaller scale dunes.

Although, medium and large dunes can occasionally reverse within a tidal cycle (Hawkins & Sebbage 1972; Berné 1993; Lanckneus & De Moor 1995) or more especially because of atmospheric events (Le Bot & Trentesaux 2004), they are generally recognized as persistent features over many tidal cycles (Lanckneus & De Moor 1991; McCave 1971). Therefore, their morphology has been widely used as an indicator of the time-averaged direction of sediment transport (Perillo & Ludwick 1984; Smith 1988; Lobo *et al.* 2000; Berné *et al.* 1994; Van Lanker & Jacobs 2000).

The artificial illumination on Figure 2 (from the NW) highlights the dune crests and their western slopes facing the illumination. The strike of the dune crest lines is roughly transverse to the axis of the sandbank except towards the crest of the bank (dashed line on Fig. 2) where they curve at an oblique direction of N50°E. They are generally laterally continuous from one flank of the bank to the other. This configuration leads to a high degree of sinuosity, with a maximum inflexion coinciding with the crest of the bank. Bifurcation of dune crests was observed occasionally, such as along the southern base of the bank, below 35 m depth and, to a lesser extent, over the crest of the bank (in the area of maximum inflexion of the dune crestlines). A similar dune plan-form geometry was observed in the 2001 and 2002 surveys (Fig. 2b and c respectively), confirming that dune geometries are stable over a period of 11 months.

Fig. 3. Geometrical characteristics of dunes in the area of repeated surveys. Dune height, spacing and asymmetry have been measured from profiles run roughly parallel to the sandbank crest. (**a**) 2002 survey dune height measured from crests to the average of the adjacent troughs (m). (**b**) Dune spacing measured from two consecutive troughs (m). (**c**) Sense and magnitude of the asymmetry of the medium sized dunes (ratio of the horizontal length of the lee side to the length of the stoss side).

a) Dune height (m)

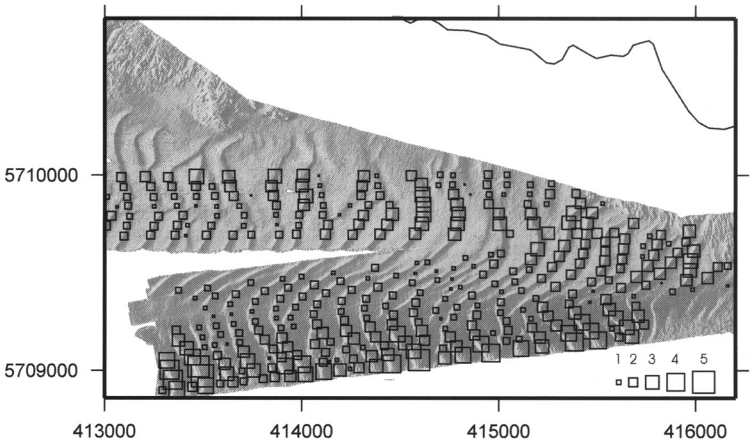

b) Dune spacing (m)

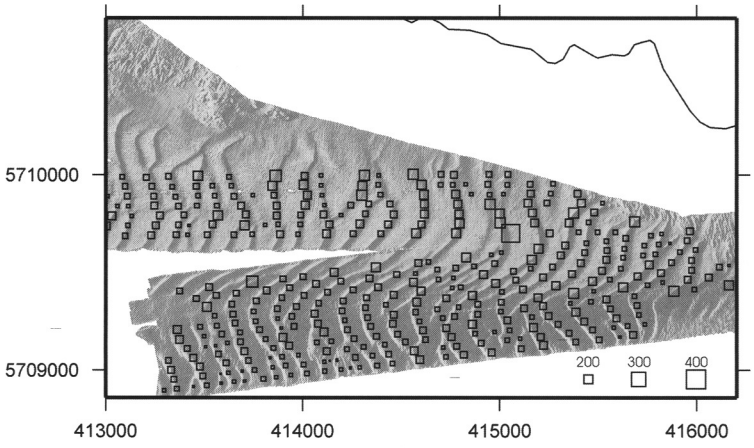

c) Symmetry index (dimensionless)

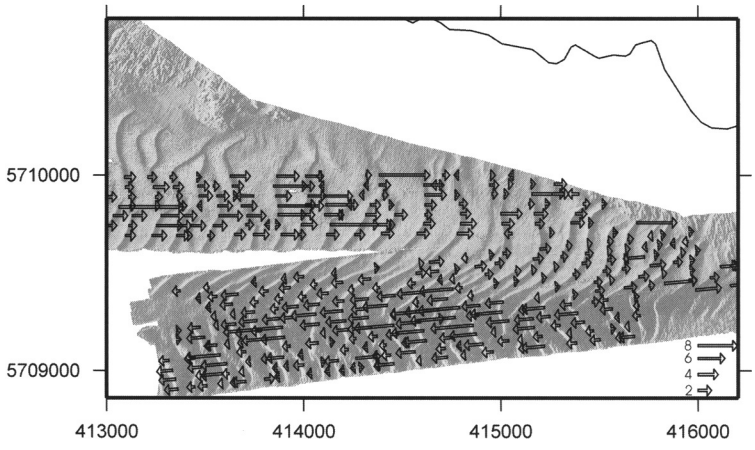

Morphometric characteristics of the dunes

Sand-dune morphology has generally been summarized using their height, spacing and asymmetry. Bathymetric cross-sections were taken parallel to the crest of the bank to measure these parameters from. Figure 3a shows a map of the heights (H), derived from the vertical distance between the dune crest and the average of the depths of the adjacent troughs. Dunes taller than 2 m are found on the southern flank, with maximum values around 4 m at the base of the bank. Slightly smaller dunes within the 2–3 m range are located on the northern flank of the bank, near the headland. At the crest of the bank, the dune heights tend to reduce to 1 m, especially where the plan-view sinuosity inflexion occurs. The smallest dunes in the studied area can be seen north of the 15 m contour (northern limit of the data in Fig. 3a), where they reach heights of 0.6 m to 1 m and at the far southeastern corner of the studied area where their heights are around 1 m.

Dune Spacing or horizontal length (L) was measured as the horizontal distance between two consecutive troughs and is shown in Figure 3b. Smaller dune spacing (*c.* 60 m) than the 110 m average occurs at the base of the southern flank, where most of the bifurcation occurs. The dune spacing increases (190–200 m) towards the crest of the bank. Finally, on the northern side of the bank, as it approaches the headland, dune crests are spaced by 40–80 m.

As mentioned earlier, the asymmetry of the dunes is a good indicator of the direction of the sediment transport. Various definition of the symmetry index can be found in the literature. Allen (1980) defines it as the ratio of the horizontal lengths of the lee and stoss slopes. These were measured as the distance between the crest of the dune and the corresponding trough along the profiles and results are shown in Figure 3c. Symmetric dunes are present in three areas: (1) at the crest of the bank, (2) where the bank lies closest to the headland and (3) at the westerly side of the southern flank of the bank (Fig. 3c), where the dune crests are linear and perpendicular to water depth contours. Dunes with easterly facing lee sides dominate the northern flank of the bank. Their lee and stoss slopes are typically *c.* 2.2° and *c.* 0.7°, respectively. The dunes are symmetric over the crest of the bank, with slopes of *c.* 1°. Further south, the dunes are asymmetric with lee slopes of 1.5° to 2° facing west and stoss slopes of 0.5° to 1°. At the southern base of the flank, the lee sides of the dunes dip at angles of between 4° and 7° compared to angles of 2° to 3° for the stoss side. From the above, the sediment transport is towards the east on the north side of the bank and towards the west on the south side, while there is no resolvable transport direction over the crest.

Geometrical features of dunes reflect the current strength, the wave regime and characteristics of the sediment (Flemming 2000). A detailed study of the dune heights (H), dune crest water depth (z) and dune spacing (L) was therefore carried out to relate the characteristics of the sand dunes to the conditions of sediment transport as found in other studies.

The size (height and spacing) of the dunes show some variation along crestlines (Fig. 3a and b). To suppress this dispersion of the data, we only use the maximum height of the dune (H_{max}) and its corresponding spacing and water depth to plot Figure 4. The properties of the dunes were measured in three depths region based on the above observations: below 25 m, corresponding to the foot of the bank, between 25 m and 15 m, corresponding to the flanks of the bank and from 15 m to the crest of the bank. Correlation between the shape of the dune and the water depth can be expected as water depth can affect the size of the turbulent boundary layer and limit the development of wakes and turbulences on the lee side of the dunes (McLean 1989). Figure 4a clearly shows that sand dune height increases with increasing water depth. A linear trend fitted to the data by least-squares indicates that the relation H/z is 0.11, which is comparable with the widely accepted relation of Yalin (1992): $H/z = 0.167$ for dunes submitted to a unidirectional flow. Figure 4b, displaying the relation between the dune spacing and the water depth, shows no correlation, as spacing varies weakly. Flemming (2000) defines steepness as the ratio of dune height over its spacing. Figure 4c shows the steepness of the dunes for each of the depths groups. Flemming found a relation $H_{max} = 0.0667L^{0.8}$ by power regression on 1491 data, with a coefficient of correlation, $R = 0.98$, which holds for dunes that have reached their equilibrium. For each of the dune groups, power regressions were fitted through the data. At the foot of the bank (below 25 m), dunes are steeper than those analysed by Flemming, while above 25 m the dunes tend to flatten (Fig. 4c). The tendency to flatten could arise from one or more effects: (1) increasing resuspension and bedload movements by surface waves that are likely to

Fig. 4. Relationships between dune geometrical parameters. Data used to plot these graphs correspond to the maximum height of each dune in the corresponding water-depth range. Dune height (a) and hence dune flatness (c) are depth dependant. Wave-induced flattening of dune crests are speculated to be important at the crest of the bank.

a)

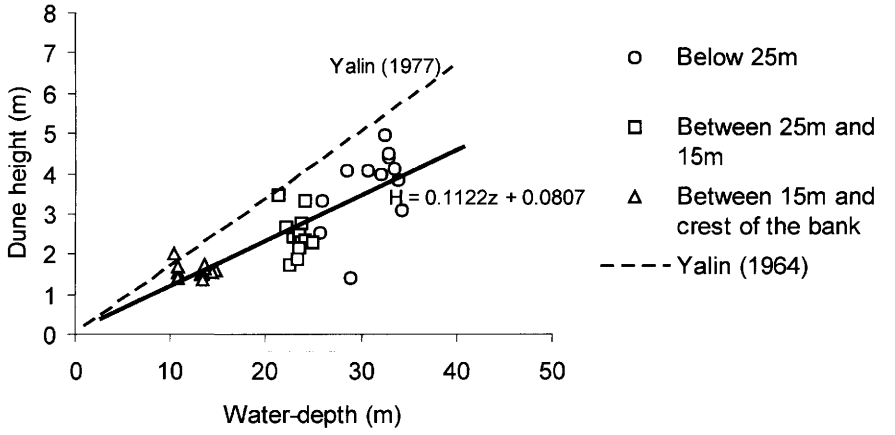
Dune height (m)
Water-depth (m)
Yalin (1977)
H = 0.1122z + 0.0807
Below 25m
Between 25m and 15m
Between 15m and crest of the bank
Yalin (1964)

b)

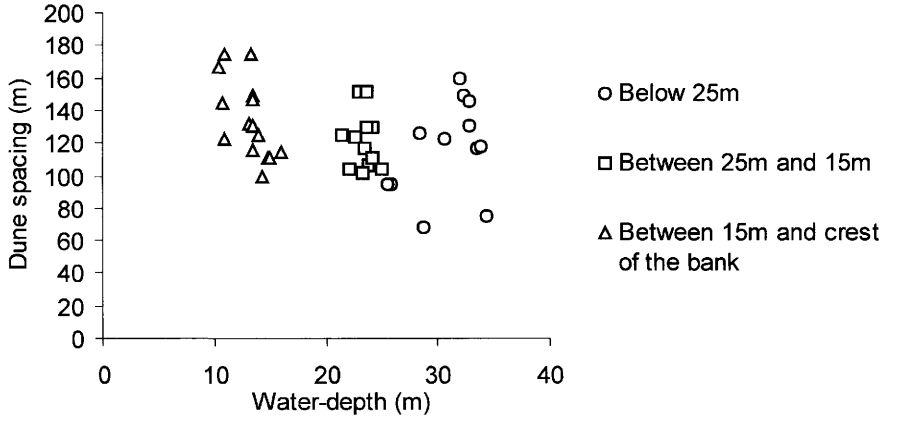
Dune spacing (m)
Water-depth (m)
Below 25m
Between 25m and 15m
Between 15m and crest of the bank

c)

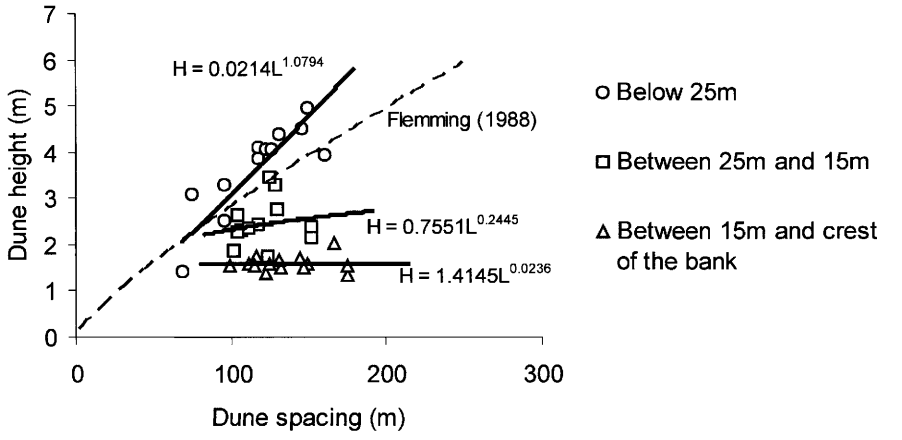
Dune height (m)
Dune spacing (m)
H = 0.0214L^1.0794
Flemming (1988)
H = 0.7551L^0.2445
H = 1.4145L^0.0236
Below 25m
Between 25m and 15m
Between 15m and crest of the bank

intensify towards shallow water and with proximity of the surface; (2) the tidal current intensifying as it is concentrated through a narrower depth extent as proposed for flattening of sand banks at larger scale (Huthnance 1982*b*); and (3) the effect of shallow water in reducing the vigour of lee-side eddies (Kostaschuk 2000).

Dune migration

Langhorne (1982) noticed that the shapes of dune crests can be strongly influenced by reversing tidal currents. Berné (1993) showed that rounded crests, or 'cat-back' profiles, can form in response to varied tidal asymmetry over neap–spring cycles and strong currents. Cat-back profiles are common on the southern flank indicating the predominance of such strong and directionally varying tidal asymmetry. Therefore, difficulties arise in mapping the transient crests of such cat-back dunes, and hence changes in the location of the dune crests can not be considered to be the best measurement for resolving their long-term migration. We therefore developed an alternative method based on isolating and displaying the 'mobile dune layer' along with cross-sections in order to identify and quantify dune migration. A drawing defining the mobile sand layer (h(x,t)) is presented in the inset to Figure 5. This layer represents the thickness of sand continually redistributed by dune migration. To resolve this layer, dune troughs were digitized from cross-sections and a surface was fitted to them using a continuous curvature gridding algorithm with maximum tension (Smith & Wessel 1990). This surface was then subtracted from the bathymetry, leaving only the dune layer h(x,t). This process was repeated for both surveys to facilitate comparisons. As varied deposition can occur in the low-stress areas of dune troughs (Bennett & Best 1995) and as small digitizing or interpolation errors can make h(x,t) somewhat irregular in the troughs, the $h = 0.5$ m contour of the mobile sand layer is shown on Figure 5. As also illustrated in the inset to Figure 5, this contour level and the shaded relief of the mobile bedform layer above it encompass the two evolving slopes of the dunes and was found to highlight their plan-view shapes quite well.

Comparison of vertical profiles, such as those in Figure 6, along with Figure 5 enabled us to track dunes from one survey to the other. Confidently tracked dunes are referred as A to M on the 2001 survey along the southern flank and 1 to 15 along the northern flank. Apostrophes are applied to the 2002 data. Changes in cross-sectional area and migration rates for tracked dunes are displayed in Table 1. Most of the dunes show a simple migration during the 11 month-period separating both surveys, with a mean of 22 m (10 m standard deviation) along the southern profile, compared with 34 m (13 m standard deviation) on the northern profile. The respective annual migration rate 24 m a^{-1} and 37 m a^{-1} are relatively slow migrations compared with the values reported by in Forschungsanstalt der Bundeswehr fur Wasserschall und Geophysik (2003) review, which range from 7 to 220 m a^{-1}. Among 11 dunes, 8 show a volume change of less than 25%. The geometrical similarity between the dunes in plan-form and cross-section between the two surveys (Figs 5 and 6) is interpreted as the product of predominantly bedload transport leading to simple dune migration (Van den Berg 1987).

The tracked dunes reveal migrations with the same directions expected from the dune asymmetry (Figs 3c and 5). Along the southern side of Figure 5 dunes are migrating westward, whereas along the northern side dunes are moving eastward. The boundary between the zones of opposite migration coincides with the crestline of the bank (Fig. 2, and dotted line on Fig. 5).

Splitting can be observed. For example, dune D, on the southern side of the bank, was connected in 2001 with dune 7 on the northern side. In 2002, dune D' has migrated eastward (Fig. 4a and b). As defined by the $h = 0.5$ m contour, it is clearly disconnected from dunes in the north. Dune 7 has been migrating eastward, and has connected with dune C' temporarily in the period between the two surveys, but was disconnected from dune C' by the time of the 2002 survey. Dune 8' was then laterally connected with dune C'.

Merging can also be observed. For example, dune H was split in two parts and barely connected with dune 10 on the 2001 survey (Fig. 5a). In the time between the surveys, the southern part of dune H migrated faster than the northern part. In 2002, the northern part of dune H' has

Fig. 5. Grey image of the 'Mobile dune layer' h(x,t) defined as the height relative to the trough level for the 2001 (**a**) and the 2002 (**b**) surveys. The inset illustrates how this layer was constructed by referencing the topography to a surface interpolated between the dune troughs. Dunes are assigned a number from 1 to 15 on the north side and a letter A to M on the south side. Apostrophes are applied for the 2002 dunes. Note similarities in plan-form shapes of dunes defined by the $h = 0.5$ m level (contours in the map) suggesting that dunes have migrated by relatively simple translation without changing shape. The solid arrows plotted on the 2001 survey mark the two profiles of Figure 6 (orientation of the profile is indicated by the arrow)

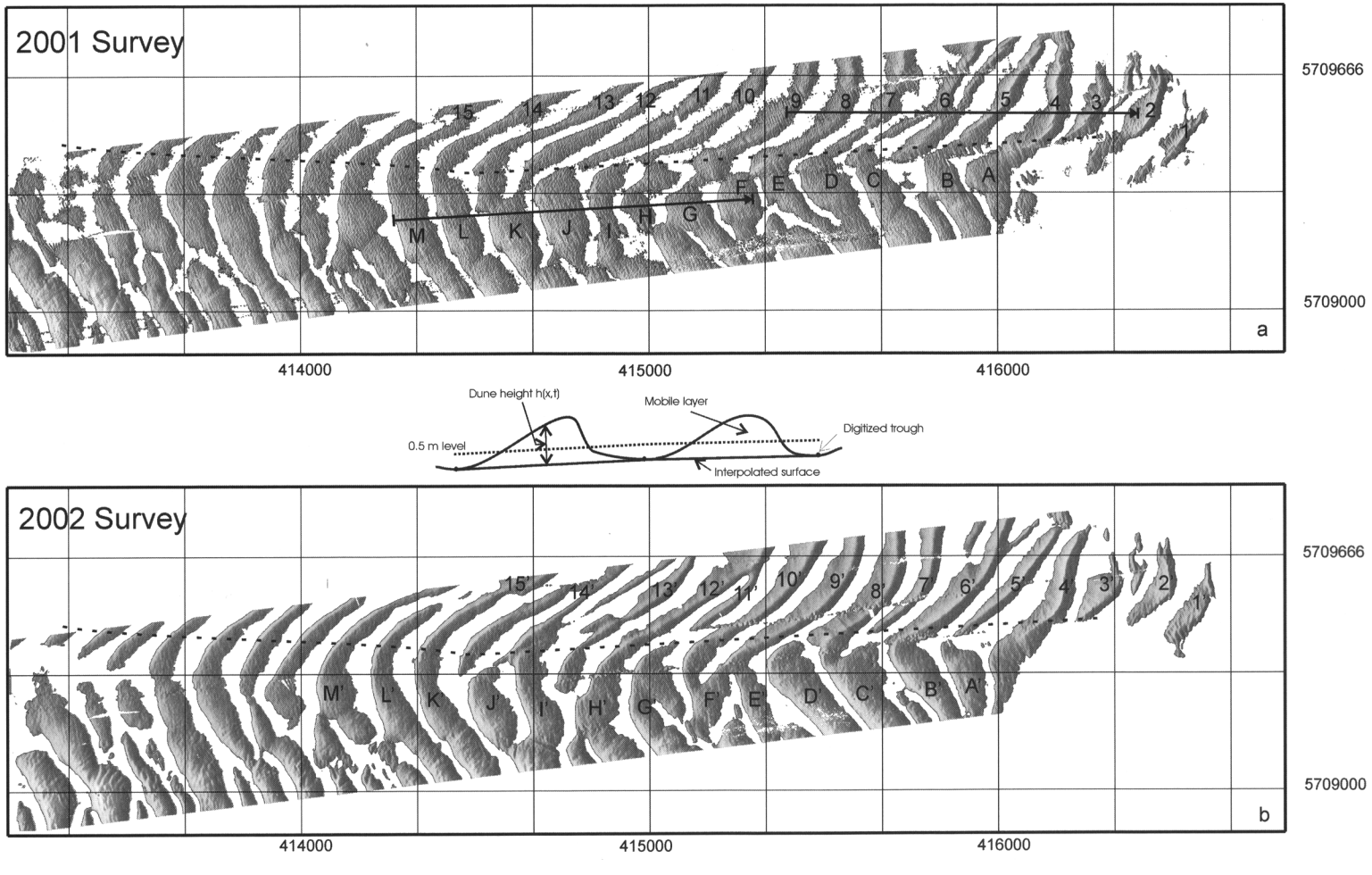
2001 Survey
15
14
13
12
11
10
9
8
7
6
5
4
3
2
1
M
L
K
J
I
H
G
F
E
D
C
B
A
5709666
5709000
a
414000
415000
416000
Dune height h(x,t)
Mobile layer
Digitized trough
0.5 m level
Interpolated surface
2002 Survey
15'
14'
13'
12'
11'
10'
9'
8'
7'
6'
5'
4'
3'
2'
1'
M'
L'
K'
J'
I'
H'
G'
F'
E'
D'
C'
B'
A'
5709666
5709000
b
414000
415000
416000

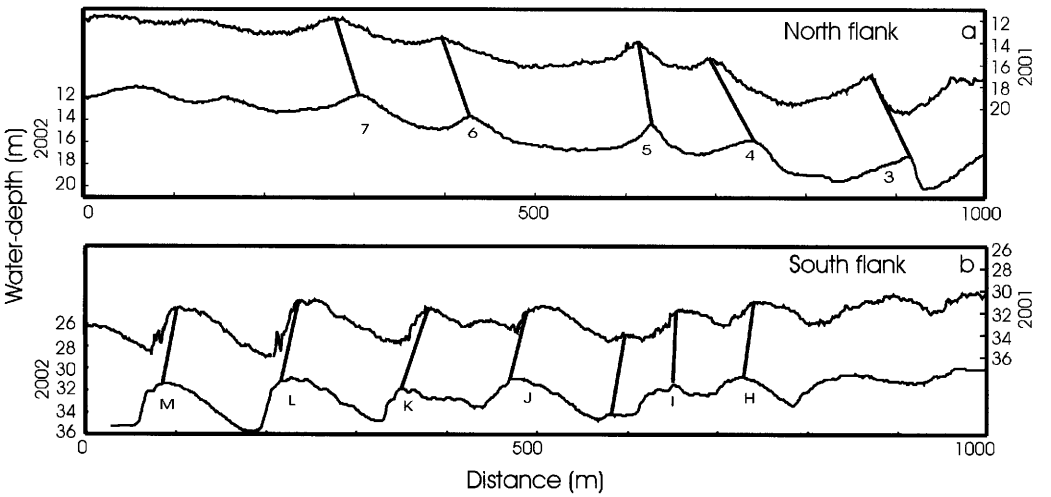

Fig. 6. Segments of collocated profiles (**a**) on the northern flank and (**b**) along the southern flank. In each figure, the data from 2001 are shown above the 2002. Interpreted similar dunes both in plan-form and cross-section are connected by lines between crests.

Table 1. *Morphologic evolution and migration of the dunes reported in Figure 5*

Dune (as referenced on Fig. 5)	Cross-sectional area (m^2)		Cross-sectional area changes (%)	Migration (m)
	26/09/2001	20/08/2002		
7	151	202	+33.77	34
6	97	88	−9.278351	29
5	159	146	−8.176101	14
4	118	169	+43.2203	44
3	190	149	−21.57895	50
M	279	267	−4.301075	32
L	281	295	+4.98221	28
K	109	90	−17.43119	30
J	135	196	+45.1852	25
I	112	57	−49.10714	8
H	122	115	−5.737705	10

merged with dune 12' to form a single laterally continuous dune from one side of the bank to the other. In some cases, dunes have also amalgamated. For example, dune 6 presents a 'X' plan-form on the 2001 survey. In 2002, both southern legs of the 'X' shape are amalgamated and form dune 6' which is laterally connected to dune B'.

An unusual feature of the dunes in Figure 5 is that many show an across-bank continuity (over the crest of the bank) despite migrating in opposite directions along the flanks. Opposite migration on the flanks of sand banks has been widely reported (Caston 1981; Reynaud *et al.* 1999; Mallet *et al.* 2000; Bastos *et al.* 2002) but the continuity of the dunes over the crest of a bank has been rarely described and not as far as we are aware ever properly explained. The observations suggest that a three-step mechanism is involved. First, dune crests deform or bend, due to the gradient of the clockwise circular net residual current along the sandbank inferred by numerical modelling (HR Wallingford 1997). Second, they split or break laterally, and third rejoin with another crest. We speculate that the latter may be encouraged by along-dune crest sediment transport driven by surface waves

because the predominant wave direction is from the SW here (Postford Duvivier & ABP Mer 2000), parallel to the crestal dunes. This last mechanism was suggested by McCave & Langhorne (1982) for bank-crossing small dunes, at the end of the Haisborough Sand in the southern North Sea. Our ongoing research is attempting to resolve whether sand fluxes due to surface waves recorded here are sufficient to cause this evolution.

The sand dune asymmetry and migration therefore indicate a circular (clockwise) sediment transport around the bank, as described in the literature for other types of sandbanks. As predicted by Pingree & Maddock (1979), gradients in the residual tidal currents arise from the interaction of the currents with the headland and the topography of the bank itself. Huthnance (1982*b*) also predicted a deflection of the flow over the crest of sand banks caused by the effect of friction. These mechanisms are partly responsible for the oblique dune orientation over the crest of the bank. The determination of tidally- or wave-driven flux of sediments at the crest of the bank is still under investigation.

Conclusion

Two multibeam surveys over the eastern end of Helwick Bank, as it approaches Port Eynon Point headland, have been used to assess the characteristics of sediment transport. The sense of sand dune asymmetries indicates the directions of the sediment transport. The dunes are also correlated by geometrical similarity both in plan-form and in cross-section between the two surveys. The tracked dunes suggest that they migrate relatively simply without major change in shape, which is characteristic of bedload transport.

Both asymmetry and migration of dunes indicate opposing transport directions on the two sides of the bank, suggesting a clockwise sand circulation. Some dune crests connect continuously over the crest of the bank. This phenomenon remains unexplained, but we speculate that wave-induced sediment transport could play an important role. It has also been shown that dune height increases with increasing water depth, whereas dune spacing does not, a result of flattening of the dunes over the crest of the bank. Dune flattening would also be consistent with stronger wave-driven transport at the crest of the bank.

This study illustrates how multiple swath-bathymetric surveys provide quantitative information of both the morphology and the evolution of sand dunes. Frequent usage of this technique will provide more *in-situ* information, which will be highly valuable in the development of our understanding of sedimentary processes affecting coastal and shelf areas.

This study has been partly financed by the Natural Environment Research Council (NERC), the Royal Society and Countryside Council for Wales.

The Reson Seabat 8101 multibeam sonar forms part of an equipment pool primarily funded by the Higher Education Funding Council for Wales (HEFCW) and the Higher Education Funding Council for England (HEFCE).

Tidal data were collected with the help of Longdin and Browning (Surveys) Ltd. Current and wave data was provided by ABPmer and by agreement with the National Assembly for Wales from the Bristol Channel Marine Aggregate (BCMA) project.

Finally the first author wishes to thank the School of Earth, Ocean and Planetary Sciences of Cardiff University from which he received a PhD studentship.

References

ALLEN, J. R. L. 1980. Sand Wave: A model of origin and internal structure. *Sedimentary Geology*, **26**, 281–328.

ASHLEY, G. M. 1990. Classification of large-scale subaqueous bedforms: a new look at an old problem. *Journal of Sedimentary Petrology*, **60**, 160–172.

BASTOS, A., KENYON, N. & COLLINS, M. B. 2002. Sedimentary processes, bedforms and facies, associated with a coastal headland: Portland Bill, Southern UK. *Marine Geology*, **187**, 235–258.

BENNETT, J. P. & BEST, J. L. 1995. Mean flow and turbulence structure over fixed, two-dimensional dunes: implications for sediment transport and bedform stability. *Sedimentology*, **42**, 491–513.

BERNÉ, S. 1993. Morphology, internal structure and reversal of asymmetry of large subtidal dunes in the Gironde Estuary (France). *Journal of Sedimentary Petrology*, **63**, 780–793.

BERNÉ, S., TRENTESAUX, A., STOLK, A., MISSIAEN, T. & DE BATIST, M. 1994. Architecture and long term evolution of a tidal sandbank: The Middelkerke Bank. *Marine Geology*, **121**, 57–72.

BRITTON, R. 1978. *Structure of some marine sedimentary bodies and their dynamic environments*. PhD Thesis, University of Wales, Swansea.

CASTON, V. N. 1981. Potential gain and loss of sand banks in the Southern Bight of the North Sea. *Marine Geology*, **41**, 239–250.

COLLINS, M. B., SHIMWELL, S. J., GAO, S., POWELL, H., HEWITSON, C. & TAYLOR, J. A. 1995. Water and sediment movement in the vicinity of linear sandbanks: the Norfolk Banks, southern North Sea. *Marine Geology*, **123**, 125–142.

DYER, K. R. & HUNTLEY, D. A. 1999. The origin, classification and modelling of sand banks and ridges. *Continental Shelf Research*, **19**, 1285–1330.

FERENTINOS, G. & COLLINS, M. B. 1980. Effects of shoreline irregularities on a rectilinear tidal current and their significance in sedimentation. *Journal of Sedimentary Petrology*, **50**, 1081–1094.

FLEMMING, B. W. 2000. The role of grain size, water depth and flow velocity as scalling factors controlling the size of subaqueous dunes. *In*: GARLAN, T. & TRENTESAUX, A. (eds) *Marine Sandwave Dynamics, Proceedings of an International Workshop, 23–24 March 2000*. University of Lille 1, France, 55–60.

FORSCHUNGSANSTALT DER BUNDESWEHR FUR WASSERSCHALL UND GEOPHYSIK 2003. *Speed of migrating bedforms on tye seafloor – a review*. FWG-Report **50**.

HARE, R., GODIN, A. & MAYER, L. A. 1995. Depth and position error budgets for multibeam echosounding. *International Hydrographic Review*, **72**, 37–69.

HARRIS, P. T. 1982. *The distribution and dynamics of sedimentary bedforms in the central and inner Bristol Channel*. MSc Thesis, University of Wales, Swansea.

HAWKINS, A. B. & SEBBAGE, M. J. 1972. The reversal of sand waves in the Bristol Channel. *Marine Geology*, **12**, M7–M9.

HENNINGS, I., LURIN, B., VERNEMMEN, C. & VANHESSCHE, U. 2000. On the behaviour of tidal current directions due to the presence of submarine sand waves. *Marine Geology*, **169**, 57–68.

HOUTHUYS, R., TRENTESAUX, A. & DE WOLF, P. 1994. Storm influences on a tidal sandbank's surface (Middelkerke Bank, southern North Sea). *Marine Geology*, **121**, 23–41.

HR WALLINGFORD 1997. *Morphodynamic simulation of Helwick Bank*. HR Report **TR31**.

HUTHNANCE, J. M. 1982*a*. On one mechanism forming linear sand banks. *Estuarine, Coastal and Shelf Science*, **14**, 74–99.

HUTHNANCE, J. M. 1982*b*. On the formation of Sand Banks of finite extent. *Estuarine, Coastal and Shelf Science*, **15**, 277–299.

KOSTASCHUK, R. A. 2000. A field study of turbulence and sediment dynamics over subaqueous dunes with flow separation. *Sedimentology*, **47**, 519–531.

LANCKNEUS, J. & DE MOOR, G. 1991. Present-day evolution of sand waves on a sandy shelf bank. *Oceanologica acta*, **Special issue 11**, 123–127.

LANCKNEUS, J. & DE MOOR, G. 1995. Bedforms on the Middelkerke Bank, southern North Sea. *In*: FLEMMING, B. W. & BARTOLOMA, A. (eds) *Tidal Signatures in Modern and Ancient Sediments*. International Association of Sedimentologists Special Publication, **24**, 33–51.

LANGHORNE, D. N. 1982. A study of the dynamics of a marine sandwave. *Sedimentology*, **29**, 571–594.

LE BOT, S. & TRENTESAUX, A. 2004. Types of internal structure and external morphology of submarine dunes under the influence of tide- and wind-driven processes (Dover Strait, northern France). *Marine Geology*, **211**, 143–168.

LEES, B. J. 1983. The relationship of sediment transport rates and paths to sandbanks in a tidally dominated area off the coast of East Anglia, UK. *Sedimentology*, **30**, 461–483.

LOBO, F. J., HERNANDEZ-MOLINA, F. J., SOMOZA, L., RODERO, J., MALDONADO, A. & BARNOLAS, A. 2000. Patterns of bottom current flow deduced from dune asymmetries over the Gulf of Cadiz shelf (southwet Spain). *Marine Geology*, **164**, 91–117.

MALLET, C., HOWA, H. L., GARLAN, T., SOTTOLICHIO, A. & LE HIR, P. 2000. Residual transport model in correlation with sedimentary dynamics over an elongate tidal sandbar in the Gironde estuary (Southern France). *Journal of Sedimentary Research*, **70**, 1005–1016.

MCCAVE, I. N. 1971. Sand waves in the North ea off the coast of Holland. *Marine Geology*, **10**, 199–225.

MCCAVE, I. N. & LANGHORNE, D. N. 1982. Sand waves and sediment transport around the end of a tidal sand bank. *Sedimentology*, **29**, 95–110.

MCLEAN, S. R. 1989. The stability of ripples and dunes. *Earth science Reviews*, **29**, 131–144.

NEVILLE, G. T. 1970. *British Regional Geology. South Wales*. Her Majesty's Stationery Office, London.

PATTIARCHI, C. B. & COLLINS, M. B. 1987. Mechanisms for linear sandbank formation and maintenance in relation to dynamical oceanographic observations. *Progress in Oceanography*, **19**, 117–176.

PERILLO, G. M. E. & LUDWICK, J. C. 1984. Geomorphology of a sand wave in Lower Chesapeake Bay, Virginia, USA. *Geo-Marine Letters*, **4**, 105–112.

PINGREE, R. D. 1978. The formation of the shambles and other banks by tidal stirring of the seas. *Journal of the Marine biological Association of U.K.*, **58**, 211–226.

PINGREE, R. D. & MADDOCK, L. 1979. The tidal physics of headland flows and offshore tidal bank formation. *Marine Geology*, **32**, 269–289.

POSTFORD DUVIVIER & ABP MER 2000. *Bristol Channel marine aggregates: Resources and constraints research project*. Postford Duvivier & ABP Mer, Peterborough.

REYNAUD, J.-Y., TESSIER, B., BERNE, S., CHAMLEY, H. & DEBATIST, M. 1999. Tide and wave dynamics on a sand bank from the deep shelf of the Western Channel approaches. *Marine Geology*, **161**, 351–359.

SMITH, D. B. 1988. Morphological development of the sandettie – south falls gap: a degeneration ebb dominated tidal-passage in the southern North Sea. *In*: DE BOER, P. L. *et al.* (eds) *Tide influenced sedimentary environments and facies*. D. Reidel Publishing Company, 51–64.

SMITH, W. H. F. & WESSEL, P. 1990. Gridding with continuous curvature splines in tension. *Geophysics*, **55**, 293–305.

TWICHELL, D. C. 1983. Bedform distribution and inferred sand transport on Georges Bank, United States, Atlantic Continental Shelf. *Sedimentology*, **30**, 695–710.

VAN DEN BERG, J. H. 1987. Bedform migration and bedload transport in some rivers and tidal environments. *Sedimentology*, **34**, 681–698.

VAN LANKER, V. R. M. & JACOBS, P. 2000. The dynamical behaviour of shallow-marine dunes. *In*: GARLAN, T. & TRENTESAUX, A. (eds) *Marine Sandwave Dynamics, Proceedings of an International Workshop, 23–24 March 2000*. University of Lille 1, France, 213–220.

YALIN, M. S. 1992. *River Mechanics*. Pergamon Press, Oxford.

A model for simulating the dispersal tracks of sand grains in coastal areas: 'SandTrack'

R. L. SOULSBY, C. T. MEAD & B. R. WILD

HR Wallingford, Howbery Park, Wallingford, Oxon OX10 8BA, UK

(email: rls@hrwallingford.co.uk)

Abstract: A new model is described that simulates the paths taken by a large number of identified ('tagged') sand grains in coastal areas in response to waves and currents. A number of practical applications require such a Lagrangian approach, as distinct from the more traditional Eulerian calculations of the transport rates of bulk quantities of identical, non-tagged, grains. Such applications might include studies on the dispersal of dredged spoil, or on the release of contaminated particulate material.

The particle-tracking algorithm determining the movement of tagged grains takes account of the following processes:

- burial and re-emergence
- initiation of motion and entrainment by combined waves and currents
- bedload transport
- suspended transport
- turbulent diffusion.

A novel method of simulating these processes has been devised, by formulating functions to parameterize each of them, and then specifying a grain speed as the product of the functions. The particle-tracking algorithm is implemented within HR Wallingford's SEDPLUME-RW model, originally devised to track the dispersal of muddy sediments. This in turn is driven by currents and waves computed by the hydrodynamic model TELEMAC. A validation exercise simulating dispersal of radioactive sand tracer measured in the 1960s in Morecambe Bay is described.

Conventional Eulerian sand transport models predict the bulk flux of sand grains, ignoring the identity of the grains. However, for certain problems a Lagrangian approach is required, and the identity of the grains is important (i.e. we need to simulate the paths taken by 'tagged' grains). Applications of such an approach include dispersal of dredged spoil and fate of contaminated particles. Existing particle-tracking models for very fine sediments, such as HR Wallingford's model SEDPLUME-RW (Mead & Rodger 1991), do not cope with burial, bedload or incipient motion. The objective of the development of the SandTrack model was to devise an algorithm to simulate sand-grain movements, to use within SEDPLUME-RW.

The processes that must be simulated are:

- burial and re-emergence of grains
- threshold & mobility of surface grains
- speed of mobile grains (bedload & suspended).

This paper presents the concepts underlying the SandTrack algorithm that determines the grain motion in response to wave and current action. It does not give the full mathematical formulation, which will be the subject of a separate publication.

Formulation

The aim of the model is to track the movements of a large number (typically hundreds or thousands) of tagged particles at each time-step throughout the duration of the required simulation, and over the study area of the problem. To achieve this, each grain is moved a 2D-vector horizontal distance $\Delta x = \Delta t.\ U_{gr}$ at each time-step Δt. Here the velocity of grain movement, U_{gr}, (different for every grain) is represented by:

$$U_{gr} = F.P.R.U_c + \text{diffusion}$$

where:

F is a 'Freedom function' (buried = 0, free = 1)
P is a 'Probability of movement' function ($0 < P < 1$)
R is a 'Relative speed' function ($0 < R < 1$)
U_c is the (2D-vector) current velocity averaged over the bottom 1 m of the flow turbulent diffusion is represented by the well-known random walk process

In coastal waters, the grain motion is driven by combined waves and currents, so the formulation

From: BALSON, P. S. & COLLINS, M. B. 2007. *Coastal and Shelf Sediment Transport*. Geological Society of London, Special Publications, **274**, 65–72. 0305-8719/07/$15.00

must include both. In some cases, the wave motion may be necessary to mobilize the grains, which are then moved by a current that is too weak to mobilize the grains on its own. The model in its present form is designed for deepish water; it does not model the detailed processes within the surf-zone.

Although gridded hydrodynamic models are needed to generate distributions of currents and waves, the SandTrack model does not itself have a grid, because the position coordinates of each particle are stored exactly. The hydrodynamics at the location of the particle are calculated by interpolation from the grid of the hydrodynamic models.

Burial processes: function F

The tagged grains may be trapped in the bed to different depths and durations by a number of processes, listed here with their typical depths and timescales of disturbance:

- deposits from suspension (mm, hours)
- ripple migration (cm, minutes)
- sandwave migration (m, days to weeks)
- general bed movement (cm to m, storm to season)
- bioturbation (cm, hours)
- anthroturbation (cm to m, weeks)

(The term 'anthroturbation' is coined to denote disturbance of sediments by human activities, such as trawling, dredging, trenching and anchoring.) Ideally, each of the above processes would be represented by a separate distinctive function. However, within the current version of SandTrack they are all parameterised together by a single function F, in which burial and re-emergence of grains is simulated by a modified vertical random walk process. In this, the magnitude of change in burial depth depends on the bed mobility, given by function P (see below) applied to the *ambient* grains, i.e. those forming the natural sea-bed as opposed to the *tagged* grains which can optionally be defined separately. A random number (in range 0 to 1, generated for each grain at each time-step by the computer code) then decides whether the burial depth increases or decreases. The vertical change in bed-level (and hence burial depth of the tagged grain) is given by $\delta z = (+/-1).P.\delta b$, where δb is a scale depth (specified as an input to the model), and $(+/-1)$ is specified at each step according to whether the random number is $>$ or <0.5. If this process results in a negative burial depth (i.e. grain above the seabed level) then the burial depth is set to zero. Function F is computed as follows:

If burial depth >0, then $F=0$
If burial depth $=0$, then $F=1$.

It should be noted that the concept is that the grain becomes buried at some time when it lies on the bed surface and is then covered by accretion of ambient sediment. Subsequent accretion and erosion of the bed surface then vary the burial depth, while the grain itself stays still. This excludes bioturbation and anthroturbation processes, in which the grain itself is moved. In the SandTrack context, sheet-flow of sand is treated as a form of bedload, so that grains within the mobile sheet-flow layer have $F=1$, while grains below it have $F=0$.

Figure 1 shows an example of the variation in burial depth of a typical grain over a seven-day period simulated by a random walk algorithm (a simplified version of that described above). Tagged grains typically spend 15–20% of the time on or very near the bed surface (as has been observed in experiments), and are only very occasionally buried deeper than 0.5 m.

It is necessary to introduce a scale depth (δb), which can be chosen by calibration if data on burial depths is available. However, this choice is only important if the *vertical* distribution of tagged particles in the bed is a required output for a particular study. It does not affect the *horizontal* dispersion of tagged particles at all, because this is only governed by whether F is 0 or

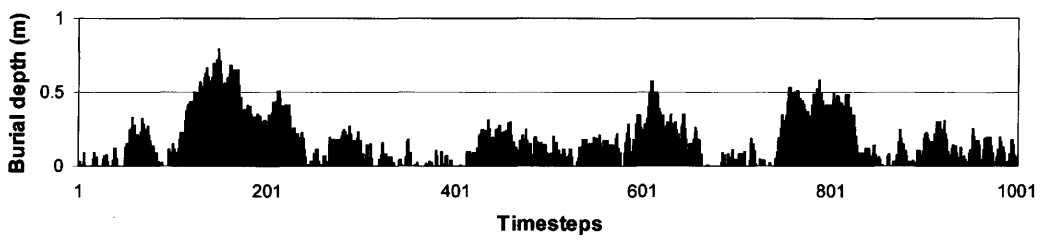

Fig. 1. Example of a random walk burial simulation, showing how the depth of sediment covering an individual grain is predicted to vary with time. If $\Delta t = 10$ minutes, then 1000 time-steps is about 7 days.

1 at each time step, which is independent of the depth-scale of burial. The vertical movement of the bed is only notional, so as to introduce the effects of burial, and is not intended to represent the actual morphodynamic behaviour of the bed. However, areas of sand and areas of rock can be defined in the model, so that burial only takes place in sandy areas.

Mobility formulation: function P

If a tagged grain is 'free' (i.e. $F=1$) it lies on the surface of the bed until it is moved by the waves and currents. The P function represents the probability (or equivalently, percent of time) that a given tagged grain (on the bed surface) is mobile. It is a function of the grain properties and the maximum bed shear-stress due to combined waves and current, τ_{max}. If the shear-stress is less than the threshold value τ_{cr} for movement of the tagged grains (taking into account that they might be a different size to the ambient grains on which they lie) then the probability of movement is taken to be zero. For larger shear-stresses there is an increasing probability that an individual grain will move during a time-step of the model. This is formulated as follows:

$P=0$, if $\tau_{max} < \tau_{cr}$
P increases with τ_{max} to 1, if $\tau_{max} > \tau_{cr}$

The functional dependence of the probability (Fig. 2) is written in terms of the maximum Shields parameter, $\theta_{max}=\tau_{max}/g(\rho_s-\rho)d$, due to combined waves and currents. The function is based on an expression given by Fredsøe & Deigaard (1992, eq 7.58), which in turn is based on the work of Engelund & Fredsøe (1976) as part of a bedload transport theory for sand grains in steady flows. Here we have adapted it to combined waves and currents by replacing their steady shear-stress with τ_{max}. The maximum bed shear-stress, τ_{max}, is calculated from the current speed and wave orbital velocity using the 'DATA2' method given by Soulsby (1997, p.92). The wave orbital velocity at the sea bed is calculated from the significant wave-height, peak-period and water depth by transforming all the frequencies in an assumed JONSWAP spectrum using linear wave theory by the method of Soulsby (1987).

The possible difference in size of the tagged particles and the ambient grains is accounted for by using a 'hiding and exposure' function when calculating the threshold bed shear-stress. A range of sizes of the tagged particles is dealt with by performing separate runs of SandTrack for a number of different sizes. The degree of grading of the ambient sediment is not accounted for, and nor is the possibility that the tagged particles might carpet the ambient sediment at the point of release. Thus it is assumed that the tagged grains form a very small proportion of the ambient grains and do not affect their movement, which will generally be true some time after the release. In some cases the tagged and ambient

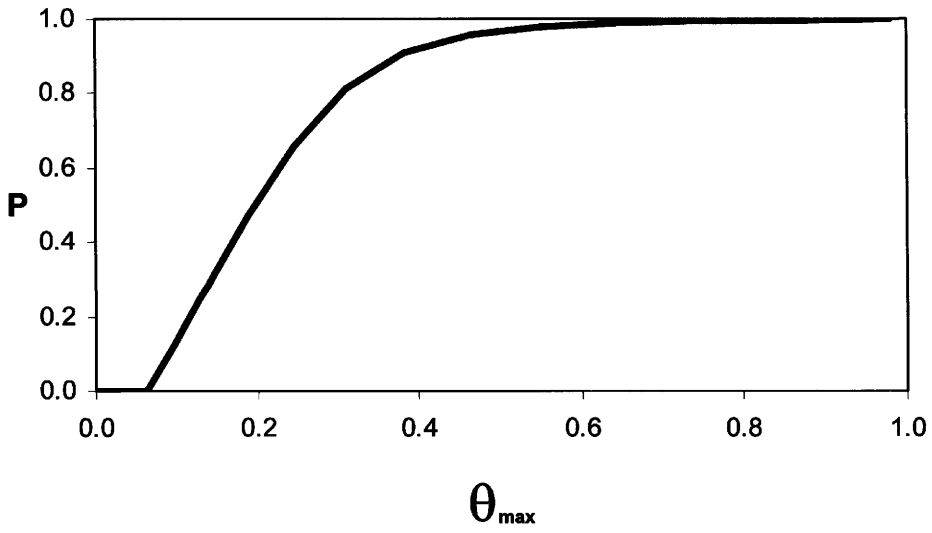

Fig. 2. Dependence of function P (probability that a grain is mobile) on the maximum Shields parameter θ_{max}. Threshold Shields parameter $\theta_{cr}=0.063$ in this example.

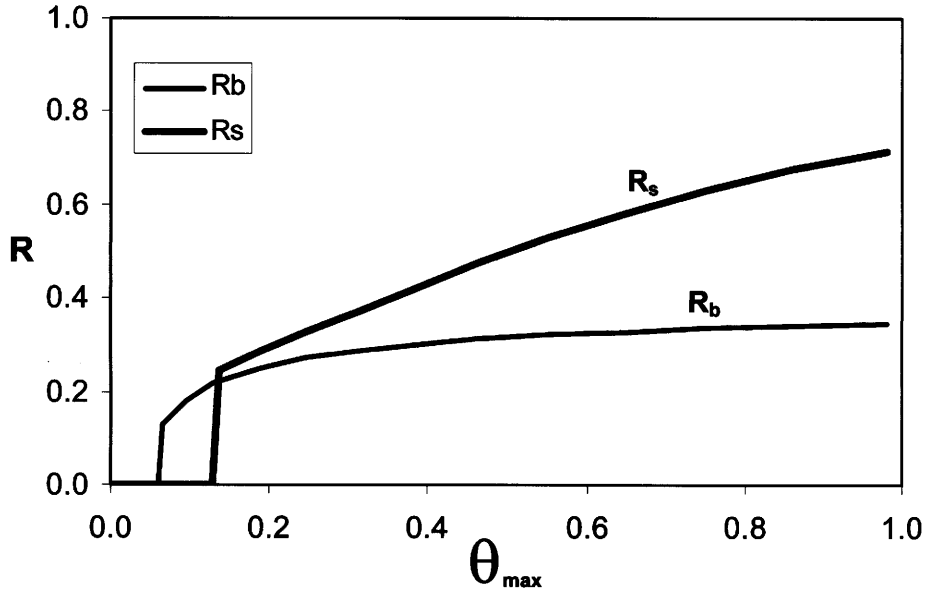

Fig. 3. Examples of functions R_b and R_s for the speed of a mobile grain (relative to the near-bed current speed) travelling as bedload and in suspension respectively, for the case $d=0.2$ mm, $h=5$ m, with no waves.

grains can be given the same size: for example, if it was desired to track the movement of the ambient sand.

Relative speed formulation: function R

Once a grain is mobile (i.e. $P>0$), it will move either as bedload or in suspension. Its speed of movement will be some fraction of the current speed near the bed (usually taken to be the lowest 1 m, although this can be varied). The function R represents the speed of a given mobile tagged grain relative to the near-bottom current speed. It is a function of the grain properties and maximum and mean bed shear-stress in combined waves and current, (τ_{max}, τ_{mean}). It is formulated as follows:

- for bedload, R increases with τ_{max} to about 0.3 – 0.5
- for suspended load, R increases with τ_{max} (and with decreasing settling velocity) to 1.

The expression for bedload speed R_b is based on the same work by Fredsøe & Deigaard (1992, eq 7.51, following Engelund & Fredsøe 1976) as the P function, and hence is compatible with it. It is adapted from steady flow to waves-plus-currents by assuming that the particle mobility depends on τ_{max}, while the speed is scaled by $u_{*m}=(\tau_{mean}/\rho)^{1/2}$. The expression for speed in suspension R_s is based on the concentration-weighted average speed in the bottom layer, assuming a power-law concentration profile (e.g. Soulsby 1997, eq 106). A power-law concentration profile corresponds to an eddy diffusivity that increases linearly with height above the bed. No account is taken of density stratification by suspended sediment. R_s is taken for R if a criterion for the threshold of suspension is exceeded, otherwise R_b is taken. The value of R only approaches 1 for cases with very fine grains, very fast currents, or large wave orbital velocities. Figure 3 shows a site-specific example of the behaviour of the R function. In this example, the threshold of motion is exceeded for $\theta_{max}=0.063$, and the threshold of suspension for $\theta_{max}=0.129$, above which the value R_s is taken. Figure 4 shows how the speed of the grain varies with the depth-averaged current speed for a particular site-specific example (depth $=5$ m, grain-diameter $=0.2$ mm, current only), ignoring the burial and diffusion processes. Thus it shows U_{gr} as the product of the P function, the R function and U_c. For current speeds less than about 0.4 m s^{-1} the grain is stationary, between 0.4 and 1.0 m s^{-1} the grain moves at a speed considerably slower than the current, while for very strong currents the grain moves at a large fraction of the current speed.

Formulation of turbulent diffusion

As well as responding to the deterministic forcing by the mean currents and waves, mobile grains

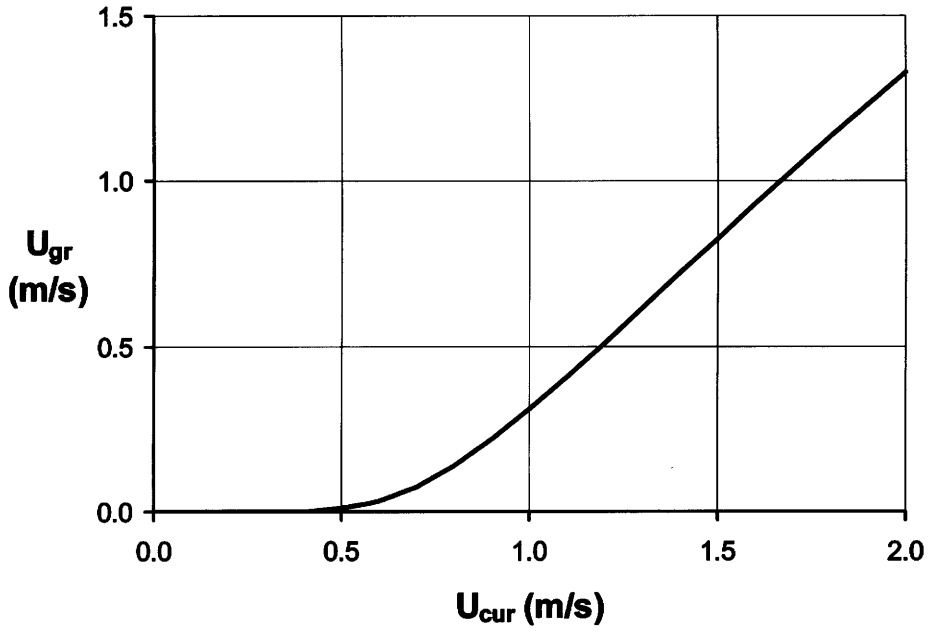

Fig. 4. Example of the speed of a mobile grain (U_{gr}) as a function of the depth-averaged current speed (U_{cur}), for the case $d=0.2$ mm, $h=5$ m, with no waves and no burial.

will be affected by the turbulent fluctuations in velocity near the bed. SEDPLUME-RW already contained a random walk function to cater for diffusion of dissolved pollutants or fine mud (i.e. diffusion of the water) by adding in a random (2D-vector) step of length/direction Δx_t.

This deals with horizontal diffusion, since vertical diffusion had already been dealt with in the formulation for suspension of sediment. The horizontal diffusion coefficient is given a constant value, typical of coastal flows, and is different from the value for vertical diffusion described earlier. No account is taken of shear-dispersion in the current version of SandTrack. The approach to horizontal diffusion of the water is described in detail by Mead & Rodger (1991). This is adapted in SandTrack by multiplying the step Δx_t by the product of the F, P and R functions, and adding this to the deterministic step-length Δx. In practice, it is found that diffusion by large-scale, slowly varying processes (e.g. waves, wind) is much greater than the small-scale turbulent diffusion. This is in line with known behaviour of turbulent diffusion. However, the randomness applied to individual tagged grains in SandTrack in both the F function and the diffusion term ensures that grains released simultaneously from the same point source end up following different and diverging paths, as they would in nature.

Implementation in model

The SandTrack algorithm has been incorporated into the SEDPLUME-RW model, utilizing some of the same code and plotting software. It is driven (off-line) by water-levels, currents and waves computed over the study area on a variable-sized triangular (finite element) grid by the TELEMAC suite of models (http://www.telemacsystem.com/gb/default.html). TELEMAC was developed originally by Laboratoire National d'Hydraulique of Electricité de France, and has been extensively calibrated and applied by HR Wallingford in coastal hydraulic studies throughout the world. The wave distribution over the study area can be calculated by a number of methods, depending on the application. For example, by hindcasting offshore wave-heights, periods and directions from a long time-series of wind, and propagating them inshore using a ray model. For simple bathymetries it is sometimes adequate to hold wave heights constant until the water is so shallow that they break, and inshore of the break-point make wave height proportional to water depth. In the applications of the model to date, wave-induced currents due to radiation stresses have not been included, but they could easily be included if required.

Once a set of hydrodynamic inputs has been computed, different grain-sizes, release points and scenarios (e.g. instantaneous or continuous source of particles, different times of release) can be run using SandTrack. The tagged grains travel around the study area according to the algorithm for their individual x and y step-lengths at each time-step as described above. The model can be driven by a simple repeating tide or a full time-series of synthesized currents and waves, depending on the nature of the problem and the budget available.

Time-steps from 3 to 20 minutes, numbers of grains from 800 to 12 000, and durations of simulation from 6 weeks to 30 years have been run for different applications. Sensitivity to the time-step chosen relates to the goodness of approximation of the tidal excursion in discrete steps. For example, a 20-minute time-step for a 12-hour sinusoidal tidal cycle introduces less than 0.6% error in the excursion of a sand grain in 6 hours, compared to an infinitesimal time-step. The time-step must also be sufficiently small that the corresponding spatial step does not carry the particle to a location where the currents and waves are greatly different from the starting point. This will depend on the geomorphology of the study area. The output analysis software produces plots of snap-shots and envelopes of all the particle positions in the study area at selected times, movement of the centroid and spread of particles, and the distribution of burial depths, among others.

Example application: Morecambe Bay

A validation exercise was undertaken to compare SandTrack with observations of dispersal of radioactive and fluorescent sand tracers from an experiment in 1968 in connection with a proposed barrage in Morecambe Bay (HRS 1969). The sediment was fine sand, which was suspended by strong tidal currents of up to 1.8 m s^{-1}, but with negligible waves. The distribution of the tracer was measured at intervals over six weeks following release. The experiment was simulated using SandTrack with synthesised currents, a time-step of 20 minutes, and 12 000 sand grains of 0.12 mm diameter all released at the same point but over several tidal cycles. As an example of the speed of the SandTrack model, the Morecambe Bay study took 2 hours of computer time to model particle tracks over 39 days of real time.

The simulated grains spread both longitudinally and laterally relative to the axis of the tidal current, and drifted slowly SW in response to the ebb-dominant tidal current. Figure 5 shows that the modelled movement of the centroid of the cloud of simulated grains over 50 tides was an accurate prediction of the observed movement, in that it moved in the correct direction at the about the correct speed, both initially and subsequently. The longitudinal and lateral spreads were also seen by eye to be similar to the measured contours of radioactivity.

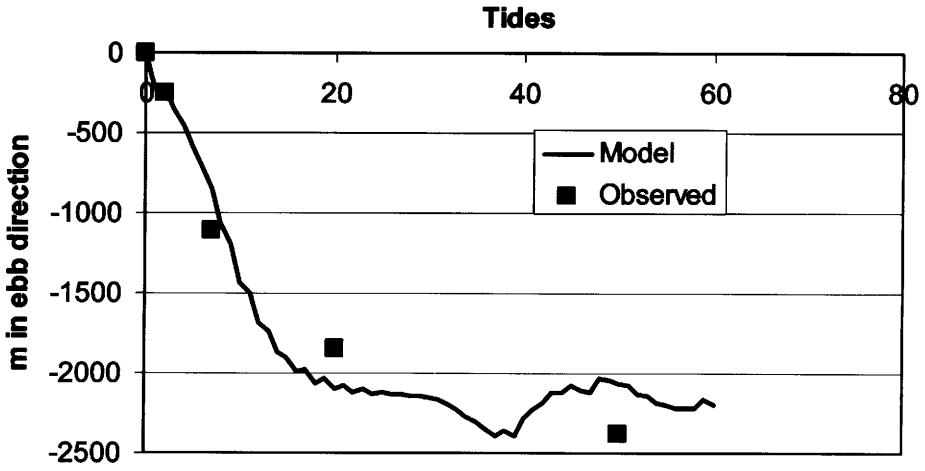

Fig. 5. Variation of the displacement of the centroid of the plume of tracer grains in the Morecambe Bay tracer surveys with time (measured in tides). Comparison between SandTrack simulation (curve) and observations (squares).

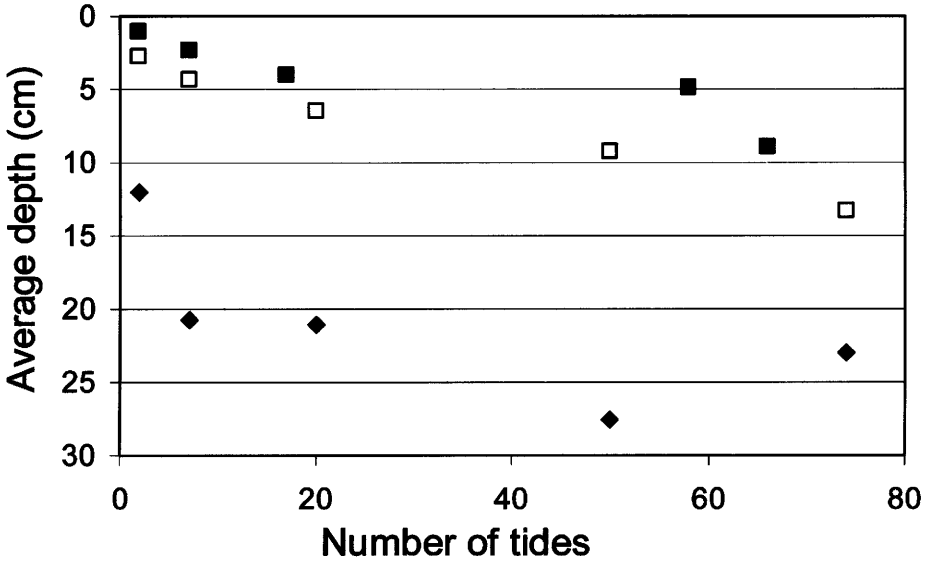

Fig. 6. Variation of the mean depth of burial of tracer grains in the Morecambe Bay tracer surveys with time (measured in tides). Comparison between SandTrack simulation (diamonds) and observations by two methods (open and filled squares).

Figure 6 shows that while the model predicted the general behaviour of the variation in the average burial depth of the tagged particles, the modelled depths were too large by a factor of about 3. This is because the scale depth δb used as an input to the burial algorithm was too large, although it could easily be calibrated to the observations if required.

Overall, the SandTrack model correctly simulated:

- the rapid initial spread and slower subsequent spread and redistribution of tracer
- the rate and direction of movement of the centroid of the tracer patch
- the amplitude of the initial spread
- the development of the longitudinal profile
- time history of burial – but 3 times too deep.

The burial formulation has been found to overestimate the burial depths and under-estimate the residence times of grains in the bed. This will be rectified in the next version of SandTrack, by adopting an improved burial/trapping algorithm. However, the overall movement of the grains is not affected by the actual depths of burial, but only by the percentage of time they lie on the surface, so simulations of the dispersal patterns are satisfactorily reproduced. Increasing the residence times will result in a larger proportion of grains remaining buried at deep depths over longer periods.

Summary

SandTrack fills a gap in the modelling capabilities: to predict the long-term paths of 'tagged' sand grains. It uses a novel approach based on a product of functions describing burial, mobility and speed of individual grains.

Tests against measurements in Morecambe Bay reproduced the main features and speeds of sediment dispersal. The SandTrack model has also been applied in simulations for a dredged spoil disposal study and a study of 30-year movement of released particles, and in both cases it gave valuable insights into the dispersal speeds and paths of the particles.

The development of the SandTrack model was carried out under contract to the United Kingdom Atomic Energy Authority (UKAEA).

References

ENGELUND, F. & FREDSØE, J. 1976. A sediment transport model for straight alluvial channels. *Nordic Hydrology*, 7, 293–306.

FREDSØE, J. & DEIGAARD, R. 1992. *Mechanics of Sediment Transport*. World Scientific Publishing, Singapore.

HRS 1969. *Sand movements in Morecambe Bay – a radioactive tracer study*. Report EX471, Hydraulics Research Station, Wallingford, UK.

MEAD, C. T. & RODGER, J. G. 1991. Random Walk Simulations of the Dispersal of Dredged Spoil. *In*: LEE, J. H. W. & CHEUNG, Y. K. (eds) *Environmental Hydraulics.* Balkema, Rotterdam, 783–788.

SOULSBY, R. L. 1987. Calculating bottom orbital velocity beneath waves. *Coastal Engineering*, **11**, 371–380.

SOULSBY, R. L. 1997. *Dynamics of Marine Sands.* Thomas Telford Publications, London, UK.

The use of particle tracking in sediment transport studies: a review

KEVIN S. BLACK[1], SAM ATHEY[1], PETER WILSON[1] & DARREN EVANS[2]

[1]*Partrac Ltd. 141 St James Road, Glasgow G4 OLT, UK (e-mail: kblack@partrac.com)*

[2]*Department of Geography, Loughborough University, Loughborough, UK.*

Abstract: New European environmental legislation such as the Shellfish and Habitats Directives, together with the more recent Water Framework Directive, are driving new and fresh approaches to sediment management. Regional authorities, environment protection agencies and consultants are increasingly being required to adopt a holistic, system-wide appreciation of sediment flux in aquatic systems. Increasingly, and necessarily, there is a need to describe sediment (and contaminant) transport pathways on dynamically variable and spatially distributed scales rather than at single point localities. 'Particle tracking', or as it is also known 'particle' or 'sediment tracing', providing certain assumptions are satisfied, offers a practical methodology for the assessment of transport pathways of a variety of sediments across wider temporal and spatial scales, and is available for silts, sands, granules, pebbles and cobbles. Although not a new technique, particle tracking has experienced a resurgence of interest and application by geologists, hydrologists and oceanographers principally as a result of the arrival of new, innovative manufacturing and measurement technologies. These have overcome previous limitations presented by the method, and have also provided a foundation for silt tracking that previously did not exist. The purpose of this paper is to provide an overview of the particle tracking methodology in the modern context, with a bias towards the practicalities of conducting a tracking experiment. We present a detailed summary of the factors and considerations involved in conducting tracking studies, including an assessment of tolerance limits on synthetic tracers and the importance of appropriate sampling strategies. In addition, we highlight the principal technical limitations of the method. We summarise the historical background regarding the use of the particle tracking method outlining the dominance of studies on sand transport and the paucity of silt tracking studies, and draw attention to some of the potential areas of application of this innovative approach.

The movement of sediment through natural processes (e.g. bed resuspension, longshore transport) or anthropogenic activities (such as sea bed dredging or piling construction) creates a unique series of contemporary sediment management problems. These problems include eutrophication of rivers; siltation in harbours; smothering of benthic fauna and flora in conservation and other areas; and, unwarranted transfer of contaminated sediments, amongst a great many others. In order that effective management strategies may be devised to combat these, and also so that appropriate monitoring schemes can be put in place, a firm scientific understanding of the nature of the transport including the source and sink areas, the volume (or mass) in transit, and the rate and direction of transport is necessary. This is by no means a trivial problem. Traditional techniques such as instrumented rigs (e.g. Williams *et al.* 1999) or gauging stations used in fluvial systems are inherently limited as they only measure fluid and sediment transport at a point, and yet sediment transfer on such scales is an inherently geospatial phenomenon. Remote sensing (e.g. CZCS, CASI, SeaWiFS, AVHR) possibly offers a more expansive view, but few systems are tailored specifically to address sediment transport problems, and those that are (e.g. the CASI technology, Lavender 2001) view only a fraction of the sediment in transit (the uppermost 1 m). This possibly leaves only mathematical or numerical modelling as an appropriate approach and yet, as always, the utility of models is proportional to their ability to accurately represent real-world processes (Dyke 1996).

Particle tracking, or as it is also known 'particle' or 'sediment tracing'[1], providing certain

[1] Particle tracking as described here is not to be confused with the type of tracing described in the book by Foster (2000). In fluvial and geomorphological studies a type of tracing known as 'sediment source ascription' or 'sediment fingerprinting' is routinely performed. This uses signatures associated with *natural* particles such as colour, magnetism, geochemical nature and lithology. Environmental samples are obtained usually from a basin or downstream location and sophisticated mathematical models are required to 'un-mix' the signatures arising from multiple source areas. Interestingly, the papers by Lee *et al.* (2000), and Sear *et al.* (2000), in this publication relate to tracing as we have defined it here, and are worth consulting if interested in cobble or shingle transport.

From: BALSON, P. S. & COLLINS, M. B. 2007. *Coastal and Shelf Sediment Transport*. Geological Society of London, Special Publications, **274**, 73–91. 0305-8719/07/$15.00

assumptions are satisfied, is a technique which offers a practical solution to the assessment of transport pathways of a variety of sediments ranging from fine silts to pebbles and cobbles. It is particularly well-suited to pathway (source-sink) determination, and can be used in mass-balance and transport rate estimation if applied correctly. Particle tracking in this context involves deliberate marking or 'tagging' of either natural or artificial sediments with an identifiable signature (e.g. fluorescence), and then use of the spatial and temporal distribution of these 'tagged' sediments to provide some insight into the transport pathways of the sediment. Tagged particles are usually referred to as tracers, although some people (notably biologists) use the term 'luminophore' to describe tracers (e.g. Mahaut & Graf 1987). Particle tracking, perhaps surprisingly, is not a new method or technique (at least for sand and shingle applications) and has a history extending back over 100 years (White 1998). It has, nonetheless, experienced resurgence in application by geologists, hydrologists and oceanographers, as a result of the arrival of new, innovative manufacturing and measurement technologies which have overcome previous limitations presented by the method. Further, the desire for data generally has also increased dramatically.

Crickmore (1976) provided a comprehensive early review of the tracking methodology, but since that time an up-to-date review of the use of particle tracking in relation to sediment transport has never been written. The purpose of this paper is to provide an overview of the particle tracking methodology in the modern context, with a bias towards the practicalities of conducting a tracking experiment. We present a detailed summary of the factors and considerations involved in conducting tracking studies, including an assessment of tolerance limits on synthetic tracers, and the importance of appropriate sampling. In addition, we highlight the principal technical limitations of the method. We summarize the historical background regarding the use of the particle tracking method outlining the dominance of studies on sand transport and the paucity of silt tracking studies, and draw attention to some of the potential areas of application of this innovative approach.

We recognize that particle tracking is also used quite widely in other sciences and refer the reader to Zhang *et al.* (2001), Milne *et al.* (1997) and Leighton *et al.* (1965) for useful overviews. We also acknowledge the pioneering publications of Ingle (1966) and Louisse *et al.* (1986), which established many of the scientific and logistic factors associated with sand and silt tracking (respectively), and these factors remain relevant to all contemporary studies. Also, we refer the reader to the excellent review of the status of measurement techniques at the turn of the last century by White (1998), which includes a review of predominantly sandy shoreface tracer methods (including relevant equations). Finally, we deal principally with the tracking of silt and sand sediments here, as Sear *et al.* (2000) have reviewed shingle tracking recently in considerable detail, and we do not deal with tracking studies using natural minerals (see Salomons & Mook 1987).

Historical overview

Possibly the first use of tracers in a scientific sense was the brickbat study of Richardson (1902) on longshore transport of shingle on Chesil Beach, UK. However, it was during the 1950s and early 1960s that serious development of the technique took place. Studies involved the use of radioactively tagged particles to determine transport, and although it was never shown to be of great utility for tracking silt (Sarma & Iya 1960; Caillot 1970), it was used with considerable success in many sand transport studies (e.g. Inose & Shiraishi 1956; Davidson 1958; Inman & Chamberlain 1959; Arlman *et al.* 1960; Crickmore & Lean 1962; Cummins & Ingram 1963; Hubel & Sayre 1964; Smith & Parsons 1967; Long *et al.* 1978; refer also to Ingle's 1966 bibliography). Caillot (1973) lists detailed instructions for preparing radioactive tracers, and the problems and advantages of their use may be found in Sauzay (1973). This method is now not permitted in most environments on the basis of health and safety considerations (although see Heathershaw & Carr 1987; Drapeau *et al.* 1991; Beck *et al.* 1991; Cheong *et al.* 1993). This is unfortunate, if only because it is comparatively easy to monitor the presence of radioactivity over reasonably large distances in aquatic environments.

Other historical attempts at tracking sediment have included the use of materials such as pulverised coal (Shinohara *et al.* 1958), broken bricks (West 1949; Kidson & Carr 1961), magnetic concrete and other ferromagnetically marked sediments (Pantin 1961; Grisseier & Hoeg 1964), painted shingle (Dobbs 1958; Kidson *et al.* 1962; Longuet-Higgins & Parkin 1962), and dyed non-fluorescent hues (King 1951; Luneberg 1960). By the 1960s research had begun to investigate the use of sand coated with fluorescent paint, dye or ink (e.g. Zenkovitch 1960, 1962; Abecasis *et al.* 1962), and this

technique gradually became the predominant and most successful of particle tagging methods. By the time of Ingle's (1966) now classic paper, there were over 100 reported studies in the literature employing this approach, albeit many in obscure Russian sources (refer to Ingle's bibliography for details) and almost exclusively concerning beachface sand transport (notably along the shores of the Black Sea). Historically, silt tracking has received virtually no scientific attention excepting Sarma & Iya (1960) and a handful of Dutch studies (van Leussen, undated; Draaijer *et al.* 1984; Louisse *et al.* 1986).

Finally, a variety of miscellaneous approaches to sediment tracking have appeared in literature sources. These include use of the naturally fluorescent mineral fluorite (Waters 1986), labelling of grains with rare earth elements (Zhang *et al.* 2001) and use of fluorescent glass beads (Ventura *et al.* 2001).

Assumptions of the particle tracking technique

Foster (2000) noted that it is essential that the assumptions that underpin tracer application and tracking methodology are fully identified and tested. Table 1 identifies those assumptions that are applicable to all tracer studies, regardless of the context. In the event that any of these assumptions becomes violated or invalid, concerns must be raised as to the utility of a tracing study. The fundamental assumptions are that the tracer must mimic the behaviour of target sediments adequately (for sand) else must integrate within and be transported via floc aggregates (silts), and this must remain so for the experimental duration. Finally, that the tracer can be monitored effectively.

Tracer particle types

Tracer types

Two principal types of tracer have been utilised in sediment tracking studies. These are:

(1) labelled (coated) natural particles
(2) labelled synthetic particles.

In both instances, the label given to particles is commonly referred to as a 'signature'. The majority of historical studies have used coated natural particles, principally as this was the technology of the day, but also because it retained use of the natural sediment particles. Using the natural mineral grains was, and still is, a preferred methodology since it is relatively easy to demonstrate equivalence of hydraulic behaviour between uncoated (native) and coated grains (Ingle 1966), and mineral density is not an issue. More recently, however, the emphasis has shifted to the use of manufactured, labelled synthetic particles (Harvey *et al.* 1989; Harvey & Harms 2002).

Coated natural tracers. A number of different signatures have been used historically to label natural sand particles, and these are radioactivity and fluorescent colour. Although now banned for health and environmental reasons, the radioactive technology proved eventually to have a limited application due to the cost implications for large-scale studies, and the necessity to process sediment samples immediately to avoid loss of the radioactive signal. Fluorescent tagging of particles is perhaps the most pervasive tracer tagging methodology employed. In the past this used to involve application of a fluorescent substance (both organic and non-organic; Teleki 1962) in a colloidal state to sand particles along with a binding material (e.g. agar or a resin). This process produced particles that were entirely benign, and therefore in contrast to radiated sand there was no need for special precautions during subsequent sampling and processing. Fluorescent dyes such as rhodamine (red) or anthracene (yellow-green) have also been coated to natural sand particles (Ingle 1966).

Ingle (1966) and references therein describe in detail a number of coating application methods. Various dye formulations and application methodologies may also be found in Teleki (1966*a*), Zenkovitch (1960), and Yasso (1966). Coating/dyeing sand particles for beachface dynamics

Table 1. *Assumptions surrounding the use of tracers in particle tracking studies*

1.	The tracer hydraulic and bio-organic properties mimic those of the sediment of interest, and therefore the tracer is transported in the same fashion as native sediment
2.	The tracer does not change properties* through time (at least over the timescales of interest) and can be monitored
3.	The tracer does not manifestly change the transporting system in any way

*Includes not only size and density but also fluorescence tincture

studies is not problematic, with many studies undertaking the coating process using a cement mixer actually at the field site. Coatings applied in this manner typically have a short life-time, particularly in the high-energy surf-zone. Ironically, this may prove an advantage in that coloured particles then do not persist in the nearshore environment for long periods of time. Ciavola *et al.* (1997*a*, *b*, 1998) provide accounts of the modern usage of labelled natural sand particles. Finally, exotic substances such as gold and silver and rare earth elements (REE e.g. Nd_2O_3) have been used as coatings in particle tracking studies (Olmez *et al.* 1994; Zhang *et al.* 2001).

Labelled synthetic tracers. The arrival of new, innovative manufacturing technologies has given rise to the use of labelled, entirely artificial particles in tracking studies. These particles comprise a carrier substance mixed together with a commercially available fluorescent dye, pigment (e.g. Harvey *et al.* 1989; Black *et al.* 2004*a*, *b*; McComb & Black 2005) or other signature. Ventura *et al.* (2001), for example, explored the utility of polystyrene plastic beads embedded with a magnetic powder. The carrier substance is frequently polymer-based (i.e. plastic e.g. Harvey *et al.* 1989; Tanaka *et al.* 1998), but concerns related to the use of polymer-based particles in the natural environment, particularly in ecologically sensitive regions (Thompson *et al.* 2004), have prompted the use of natural materials (e.g. Black *et al.* 2004*a*). Black *et al.* (2004) have taken synthetic tracers a step further and produced a 'dual signature' tracer, comprising both fluorescent colour and para-magnetic character. 'Paramagnetic' means that the particles are attracted by strong permanent or electro-magnets, thereby facilitating a simple and efficient separation from native sediment, but they are not themselves magnetic. The authors state that four spectrally distinctive tracer colours are available.

Density can be controlled during the manufacturing process to within 5–10% of most common natural mineral densities (e.g. quartz, feldspar, kaolinite), but there is limited control on particle shape. Synthetic particles may be manufactured with confidence across the size range 1–5000 μm, appropriate for the tracking of silt and sand-gravel. Specific size fractions are obtained through sieving. Far stricter quality assurance testing is usually required to demonstrate hydraulic equivalence of manufactured particles in comparison to naturally dyed/painted particles.

Miscellaneous methods

Van der Post *et al.* (1995) adopted a rather different approach whilst still making use of natural sediment (sand). Ordinary beach sand can be made magnetic by heating at 500–900 °C which converts small quantities of iron compounds on grain surfaces to magnetic oxides. This process, termed 'thermal magnetic enhancement', increases the magnetic signal of the material by over 300 times, and has been used previously in the terrestrial soil transport context (e.g. Arkell *et al.* 1983; Parsons *et al.* 1993). The quantity of tracer sand is then measured using a field-portable magnetic susceptibility sensor supported by laboratory methods. This technique has considerable potential as a tracer method as the analytical equipment is reasonably cheap, magnetizing the material is comparatively simple and, although not especially straightforward, the analysis is non-destructive, allowing scope for re-analysis.

A Generalized tracking methodology

A generalized 'tracking methodology' exists that applies uniformly to all particle or sediment tracking studies regardless of context (Munoz-Perez *et al.* 1999). Firstly, a number of sediment samples from the environment of interest and encompassing the temporal and spatial scales of interest are required to be collected and tested for their sedimentological properties. On the basis of this information tracer needs to be formed (through coating/manufacture); tracer properties must then be verified to establish their hydraulic similarity to the native sediments. Thereafter, logistic factors such as the method of tracer introduction and sampling are of concern, and these are of equal importance to ensuring that a contrived tracer experiment is representative of natural patterns of sedimentation.

Matching tracer with in situ sediment

The central tenet of all tracer experiments is that the tracer possesses the same (or nearly the same) physical, biological and electrochemical properties as the native sediment (Ambulatov & Patrikeiev 1963; Madsen 1987; Foster 2000). The principal sediment physical properties or relevance are particle size, ϕ (note that it is not always necessary to reproduce the entire size spectrum e.g. Duane & James 1980), particle density, ρ_s, and settling velocity, ω_s (White 1998). Other readily measured physical parameters that may also be used for hydraulic matching include the critical entrainment stress, τ_{cr}, the angle of repose and/or final repose, α, grain shape (Caldwell 1981), and bedload transport rate, q_s (Dyer 1986). Chief amongst the biological properties is organic coating (e.g. Black *et al.* 2002). The principal characterization test of silts and

clays in addition to particle size is the mass sedimentation character (i.e. deposition rate; Louisse *et al.* 1986).

Dyeing the surfaces of quartz sand does not seem to measurably change either grain size or density (Ingle 1966; Teleki 1966*a*; White & Inman 1989, quote a value of 0.1% of the total volume of a sand grain to be occupied by dye), whereas coating with pigment can cause modifications to the size (see Ciavola *et al.* 1998; Vila-Concejo *et al.* 2004). For manufacturing reasons, synthetic particles for geoscientific purposes cannot currently be manufactured to be precisely the same as native sediment. For coated and synthetic particles, therefore, some tolerances on permissible differences between the tracer and the natural sediment need to be established. In terms of particle size, White & Inman (1989) use the modal grain diameter of a population in sand tracking studies; following a number of field studies they note that 'mis-match of tracer sand and native sand on the order of 10% of the modal diameter will not greatly affect the quality of the experiment'. White (1998) further noted that skewness and kurtosis of tracer size spectra are adequate if they are the same sign as the native sediment. It is of interest that Vila-Concejo *et al.* (2004) accept much wider limits than this (85–125% relative to the mean grain size), and, while a sensitivity analysis was not undertaken, this tolerance has been accepted in the peer-reviewed literature.

The density (specific gravity), ρ_s, of sediment is a fundamental attribute governing sediment mobility (Dyer 1986), and, in order for tracer to match hydraulically the native sediment tracer, the density must be equal or nearly equal to the native mineral density. In order to assess appropriate tolerances on tracer density for manufactured particles, it is informative to examine the influence of changes in ρ_s on the generalized transport equation used in beach sand tracking studies:

$$i_b = (\rho_s - \rho) g n \bar{U} K. \quad (1)$$

where i_b is the immersed weight longshore transport rate, $(\rho_s - \rho)$ is the submerged density, g is the acceleration due to gravity, n is the sediment porosity (≈ 0.6 for sand), K_o is the depth of tracer mixing, and $\bar{U}$ is the mean horizontal sediment velocity determined from the centroid displacement. Analysis shows that a change in ρ_s of 6% gives a corresponding change in the excess density term $(\rho_s - \rho)$ of *c.* 10% (using a seawater density, ρ, of 1027 kg m^{-3}; Soulsby 1997), and a change in ρ_s of 10% gives a corresponding change in $(\rho_s - \rho)$ of ca. 16%. Since Equation 1 is linear, these changes propagate through and hence the transport rate, i_b, will experience a corresponding change. To keep errors in i_b to within 10%[2] tracer should be manufactured according to the following tolerance: 2491 kg m$^{-3} < \rho_s < 2809$ kg m^{-3}. Of course, this assumes that the sediment density is 2650 kg m^{-3}, which may be valid for quartz sands. Natural sediments, though, typically comprise a range of mineralogies (Dyer 1986), and it is of most profit (as well as good practice) to actually measure the density (e.g. using the volumetric method) where synthetic tracer will be used to track transport. We recommend adoption of the $\pm 6\%$ value on the mean density value in such instances.

Settling velocity is also a useful hydraulic measure with which to assess similitude of tracer and native sand. McComb & Black (2005), for instance, used tracer manufactured with an equivalent particle size distribution (assuming quartz spheres) based on the settling velocity of the native sediment from the study site. Where it can be independently confirmed that grain size and density are correct, settling velocity can also be used in a diagnostic fashion to highlight any departures in settling velocity between the tracer and native sand due to shape differences. This approach permits batches of synthetic tracer with erroneous shape to be rejected and is thus useful as a quality assurance measure. Caldwell (1981) discusses the impacts of variations on particle shape in respect of tracer behaviour.

Both particle density and size distribution can also be used in a similitude analysis for silt tracers. In addition, it is relatively simple to assess the gross sedimentation character of small sub-samples by measuring the decrease in turbidity through time of a unit mass of particles. It is important to ensure the mass concentration in tests is generally < 2–10 kg m^{-3} (the demarcation for hindered settling; Whitehouse *et al.* 2000). Louisse *et al.* (1986) conducted a settling test to compare natural silt with their neat tracer powder. For silt tracking it is also necessary to demonstrate that incorporation of tracer within natural floc aggregates following mixing does not measurably change the sedimentation character of the flocs. This is achieved simply by comparing the settling rate of native sediment with that for various silt-tracer admixtures (e.g. 1:90, 50:50:90:1). In addition, there is a line of reasoning that the bulk or engineering properties of the tracer-mud admixture, such as shear strength

[2] This error is fully tolerable if one considers that uncertainties associated with the predictive power of mathematical models of sediment transport are judged to be of the order of a factor of 10 (Eidsvik 2004), reducing to 5 or better for validated models (Soulsby 1997).

and surface layer moisture content, should closely mimic that of the native mud. Whilst in practise this is rather difficult to achieve, instruments now exist to measure (vane) shear strength *in situ* (Hauton & Paterson 2003), and field-portable direct-reading moisture content meters are available to undertake measurement in grabbed samples. Therefore, it is possible to verify equality (or otherwise) of the engineering properties of a tracer-mud admix. Furthermore, it is now possible to measure quickly and easily seabed erodibility/erosion potential in the field (Black & Paterson 1997, discuss recent technological advances in this area) using the Cohesive Strength Meter (CSM) of Tolhurst *et al.* (1999). This provides an additional, as well as key, parameter that can be used to assess the mobility of the tracer mixture in relation to the native sediment.

Tracer injection

Teleki (1966*a*) highlighted many of the problems associated with injection of tracers in the field (the tracer 'drop zone'). In so far as the majority of studies are 'sea bed transport' rather than 'suspended particle' studies (or at least begin so), it becomes necessary to place the tracer (or tracer–sediment admixture) on the sea bed without loss of particles to the water column. Whilst this is not generally a serious issue for beachface sand transport studies (where bags are split in the waves else tracer is raked into the surface sediment layers at low tide), it can be problematic for deeper subtidal and fluvial environments. A simple solution is to use water-soluble bags (comprising methyl cellulose or polyvinylalcohol) for packaging the tracer, and these have been around since the early 1960s. Bags of dissolution time 2–3 minutes at typical ocean temperature and salinity (15 °C, $S \approx 35$) are available commercially. An immediate problem appears here, however, which relates to the form of the tracer–sediment admixture on the sea or river bed. As the bags dissolve, they leave a mound of tracer on the seabed, although some avalanching may occur around the periphery. The authors have observed directly that when acted upon by a moving flow, this mound will erode preferentially in relation to the surrounding sediments giving a false conclusion as to the mobility of the sediments (counter to the use of tracers in the first place).

In order to obviate this it is necessary to form low-profile tracer blocks, e.g. 2–3 cm high at most, or to investigate alternative injection methods. These can include careful emplacement by divers (e.g. McComb & Black 2005), ice encapsulation methods (in which the tracer admixture is entombed in a weighted ice block), remotely operated bottles or chambers lowered from a ship (Ingle 1966; White 1987), or barge dumps for very large experiments (Louisse *et al.* 1986; White 1998). Sprinkling the tracer–sediment admixture represents perhaps the best method of tracer injection onto a seabed (e.g. Ferreira *et al.* 2002), although, in fact, this is rarely performed and consideration of the local tidal and wave conditions is necessary. Tudhope & Scoffin (1987) used a novel device resembling a seed disperser to sprinkle tracer onto the seabed in the deep ocean, and various other mechanical solutions to tracer injection in deep water, including a weighted knife blade that rips through a bag of tracer upon contact with the sea bottom (Vernon 1963) and an oil drum fitted with a hinged false-bottom (Ingle 1966, p.104). Initially intuitive attempts to feed tracer down a tube to the seabed (e.g. Jolliffe 1963) have met with limited success.

For more applied projects, other injection methods have been used. Louisse *et al.* (1986), for example, introduced tracer directly into the supply line of a dredger during active excavations. Six samples taken from the hopper indicated a well mixed tracer-mud mixture.

Continuous injection method (CIM)

The foregoing injection method(s) relate to emplacement of a tracer mass on the seafloor at a single moment in time in order to assess the sediment transport rate. Some tracer studies (e.g. Lean & Crickmore 1963; Russell *et al.* 1963) used a method known as the 'Russell–Abbott concentration' or 'continuous injection method' (CIM) to measure rates of sediment transport in both the laboratory and field. The basis of the CIM method was to inject tracer continuously through time at a known steady rate and then to measure the concentration at a point downdrift of the injection site. Although some success was reported, it is unlikely that such an approach would be valid in tidal systems, although it may be appropriate to point source pollution inputs to water bodies. In any case, by its nature the CIM involves large quantities of tracer, and thus may not be economically feasible in most instances, especially where post-release dispersion rates are high.

Injection mass

Use of an appropriate quantity of tracer is essential and fundamental to a successful tracer study. It is not possible to be prescriptive here as to tracer quantity since inevitably this is a study and

site specific issue. The dynamic nature of coastal marine environments means that dilution and dispersal to beyond the analytical limit can occur quite quickly, and therefore it is important to work well within this limit (White 1998). The factors which must be formed into an equation to guide determination of tracer mass include the (maximum) areal extent of the region of interest, the approximate volume of sediment in the active layer, the sediment porosity, and the analytical limit of detection (e.g. 1 ppm = 1 mg kg^{-1}). In addition, one ordinarily incorporates a safety factor into this as to work well within the limit of detection, and to minimise the influence of sampling errors at low tracer contents[3]. As examples of differing injection mass, Levoy *et al.* (1998) used around 30 kg of tracer for a beach longshore transport investigation, whereas Tanaka *et al.* (1998) used 3 tonnes in a down-canyon transport study.

Environmental sampling

Particle tracking is, fundamentally, Lagrangian in nature since it involves monitoring in both space and time a 'cloud' of tracer (Madsen 1987). Sampling, whether of the water column or of the sea bottom, and whether achieved using cores or grabs (or a combination), is at the heart of the particle tracking method. The particle tracking method is beset by a classic problem; since it is neither practicable nor cost-effective to sample an entire area of interest, studies are faced with mapping a continuous variable (tracer mass), whose distribution cannot be known *a priori* and which may be patchily distributed, across a spatial area with only limited resources. This is not a trivial problem. Poorly defined sampling schemes at best give rise to low information content datasets, from which it is impossible or dangerous even, to interpolate or draw contour maps of tracer mass (Haining 1990; Cromey *et al.* 2002). Further, these schemes can be prone to erroneous conclusions; the most prominent of these is to conclude that there is no deposition of tracer, when in fact there is – it is simply that it has not been sampled. This type of conclusion rises in importance where ecological or political sensitivities surround particular studies.

[3] 'Content' indicates a mass per unit mass (e.g. g tracer per kg dry sediment), whereas 'concentration' refers to a mass per unit volume (e.g. g tracer per litre wet sediment). These terms should not be confused (Flemming & Delafontaine 2000, provide a discussion of this). Tracer abundance may also be expressed as mass per unit area (e.g. g tracer per m^2 as done by Louisse *et al.* 1986), although this necessitates use of a fixed volume sampler.

The principal factors of concern in tracer recovery are the area of the region to be sampled (which governs, ultimately, maximum tracer dilution), organization of the sampling grid, sample number (including replication), and minimum sample mass.

Sample size is of fundamental importance to sediment tracking, simply on the basis that turbulent diffusion and advection in most marine and fluvial environments disperses tracer content to levels approaching (for practical purposes) $10^{-2} - 10^{-6}$ % of the original injection mass, and processing of a greater mass gives rise to a proportionate rise in the probability of discovering tracer. For beach face sand transport studies a comparatively large fraction of released tracer can be recovered with 100g samples (>60–70%; e.g. Ciavola *et al.* 1997*a*, *b*; Vila-Concejo *et al.* 2004) and minimum sample size is not an issue (White 1998). However, in most offshore and deeper water studies only a small fraction ($<10\%$) of tracer may be recovered (e.g. Pantin 1961; Louisse *et al.* 1986; McComb & Black 2005) and therefore an earnest search for tracer which sifts through as much sediment as practicable given the available resources is necessary. Two-stage or sub-sampling, wherein smaller sub-samples are taken from a larger sample is permissible (e.g. McComb & Black 2005) provided relevant statistical checks are made to ensure homogeneity of the bulk sample (e.g. Elliot 1971, p. 136).

Definition of an appropriate number of samples for a tracking study is difficult, and quite often is governed by logistic factors such as budgetary restrictions and the time available, as well as sample processing time. From the ecological literature Elliot (1971) states a greater number of (smaller) samples has more degrees of freedom and the statistical error is reduced; further, collection of many samples with some level of replication can more effectively sample a contagious (heterogeneous) distribution region lending some statistical accuracy to studies. Whilst there is no need to follow closely the sampling strategies used in ecological studies (and indeed, often this is not possible), these points form useful guidance in tracking studies. Choice of the number of samples is inevitably site/project specific, and it is interesting to observe that sampling strategy designs for studies similar in design to tracking studies, such as spatial sediment quality assessment, show substantial differences in sample density (from 0.018 to 135 locations per km^2; see Haining 1990) in spite of similar goals, i.e. to the map a spatially distributed variable.

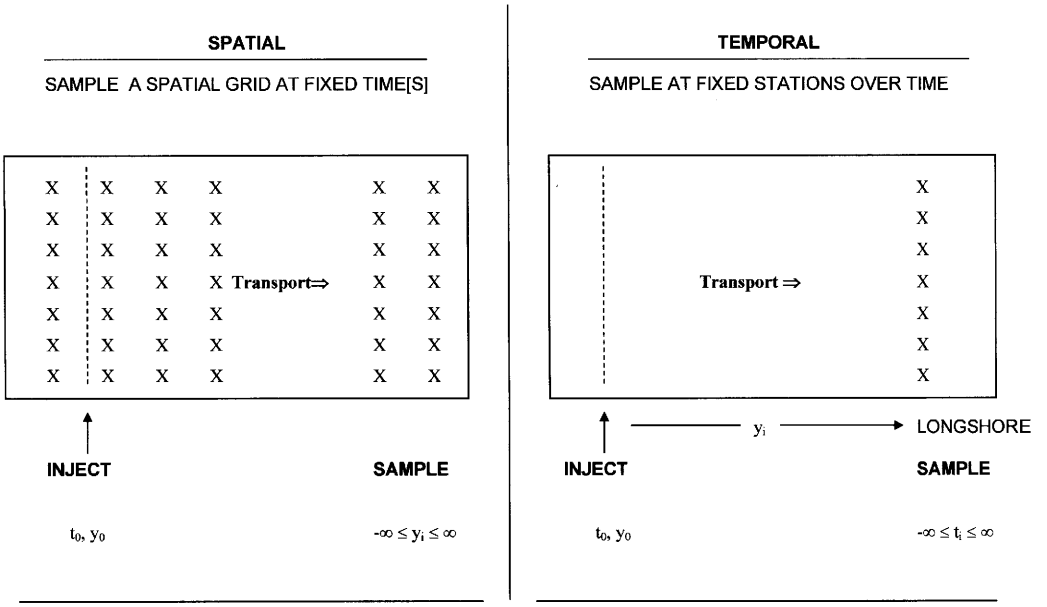

Fig. 1. Spatial and temporal grids for monitoring tracer motion (after Inman *et al.* 1980). Although the context of these is beachface studies, the principles apply to sediment tracking in general terms and to sampling of sediments transported as bedload (SIM) and in suspension (TIM).

The three main forms of spatial configuration of sampling points are simple random sampling, stratified sampling and systematic sampling (Caeiro *et al.* 2003). Tracking studies overwhelmingly have utilized a rudimentary, non-randomized systematic grid with sampling at grid nodes (Fig. 1). This configuration is appropriate where no prior information on transport direction exists and is usually arranged in two directions with respect to the tracer injection point. Where information is present on transport direction, systematic grids can introduce bias (Webster 1999), and more complex approaches such as systematic unaligned sampling (e.g. Clarke & Hosking 1986) may be more appropriate. Grids may frequently be irregular simply due to coastal features e.g. the presence of headlands and promontories or man-made features such as harbour walls (e.g. Sherman *et al.* 1990; Vila-Concejo *et al.* 2004), and may also be logarithmically spaced in the dominant transport direction. Boyd *et al.* (2002) discuss the relative merits of various grid-based sample strategies, including use of regular, irregular, random and radial tessellations, and nested and stratified sampling schemes. Additional information that may be used to guide sampling in sediment tracking studies is provided by Elliott (1971), Green (1979) and Fowler *et al.* (1998).

Sand tracking studies

The historical literature is dominated by sand tracking studies, with examples of use on sandy shorefaces (Komar & Inman 1970; Knoth & Nummeda 1977; Komar 1977; Kraus 1981, 1985; Kraus *et al.* 1982; Galvin 1987; Stepanian *et al.* 2001; Howa & Resseguier 1994; Howa *et al.* 1994; Michel 1997; Ciavola *et al.* 1997*a*, *b*; 1998; Levoy *et al.* 1997, 1998; Wong *et al.* 1998; Munoz-Perez *et al.* 1999), in tidal inlets (Balouin *et al.* 2003; Vila Concejo *et al.* 2004), in submarine canyon systems (see Ingle 1966; Dingler & Anima 1982; Tanaka *et al.* 1998), in the shallow sub-tidal (Foster *et al.* 1996; Johnson 2005) and wave-dominated coastal environment (Beck *et al.* 1991; McComb & Black 2005), and in harbours (e.g. Ferreira *et al.* 2002) and in rivers (e.g. Kennedy & Kouba 1970; Rathburn & Nording 1971). These studies have provided a wealth of information on qualitative transport pathways on beaches and in rivers, as well as provided quantitative estimates of sand transport in relation to hydrodynamic driving forces, and on the sand mixing depth. As noted by Knoth & Nummeda (1977), the primary advantage of use of a sand tracer is that regardless of the mechanism or mode of transport the amount of sand moved is measured directly without any reliance on predictive equations or calibration.

The method has also been applied to more complex systems such as swash platforms (Oertel 1972), submarine sand banks (Collins *et al.* 1995), and in sediment bypassing studies (e.g. Sherman *et al.* 1990; Uda *et al.* 1991). As noted by P. Ciavola's research group (Ciavola *et al.* 1998), who have brought fluorescent sand tracking back into the mainstream (e.g. Vila-Concejo *et al.* 2004), the usage of fluorescent sand is simple, and marking can be done easily and rapidly (Teleki 1966*a*). In addition, whilst a government permit is required (in the UK at least) to use particulate (and fluid) tracers in aquatic systems, the controlled use of tracers is environmentally safe, different colours can be used to tag grains of differing size fraction, solubility of binding media can be adjusted so that dye will adhere to grains for periods ranging days to years, and the sensitivity of the technique is at least 1 ppm. Perhaps the most onerous characteristic of the sand tracking method is that many hundreds of samples over a period of time are required to assess sediment transport. Badr & Lofty (1998), for example, collected 672 samples from 12 consecutive sampling campaigns.

The movement of sediment tracer can be described in terms of the translation of the centre of mass (centroid), and the advance of the area occupied by the tracer (Madsen 1987; White & Inman 1989; McComb 2001). The former indicates the flux of sediment transport in response to horizontal advective forces, while the latter reflects the spread of the tracer into the surrounding environment, which is due to horizontal diffusion and advection by currents (Miller & Komar 1979).

A Lagrangian sampling strategy based upon a 2D grid and referred to as the 'spatial integration method' (SIM) is used to compute sediment transport (White 1998; Vila-Concejo *et al.* 2004). This involves sampling the bed across the grid at a single instant, t'. Assuming samples have sampled tracer throughout the mobile layer (thickness K_o[4]) this produces a dataset of tracer content $C(x,y,t')$. The tracer content values are then used to obtain the average sand velocity ($U(t')$ between the time of tracer injection ($t=0$), and the time of sampling, t'. White (1998) provides the following equation for calculation of $U(t')$:

$$U(t') = \frac{\sum_{x,y} C(x,y,t') \frac{x}{t'}}{\sum_{x,y} C(x,y,t')} \quad (2)$$

If one considers the x-direction in Equation 2 corresponds to the longshore direction then Equation 2 provides an estimate of the longshore sand transport velocity. An underlying assumption of the method is that there are no significant cross-shore variations in $U(t')$, which may be indicated, for example, by morphological features on the beachface. White (1998) notes that in many historical investigations, this assumption was not frequently met, and provides a method to account for this. Calculation of the immersed weight longshore transport rate is via Equation 1 integrated across the width of the surf zone (or zone of interest).

A second assumption of the method is that all grid nodes (whose spacing will be a reflection of the contemporary wave conditions and longshore current strength and therefore variable between experiments) are sampled simultaneously. Since this can never be achieved in reality, time itself influences the data. Whilst most researchers choose to ignore this, Ingle (1966) normalized tracer concentration values to an arbitrary elapsed time after tracer release by multiplication with the ratio of the arbitrary time to the elapsed time at the moment of collection. A further concern, which has never been addressed in the literature, is the permanent removal of tracer mass during sampling and how to statistically account for this removal in the final results; this must be calculated to derive accurate mass balance.

Tracer analysis

Particle tracking experiments by their very nature involve the collection of many environmental (sediment/water) samples, and this consequently incurs considerable effort in both the field and laboratory (e.g. Badr & Lofty 1998). A simple, rapid and reliable analytical method for separation and enumeration of tracer is therefore necessary.

The issue of separation of tracer grains from a bulk sediment sample appears to have been resolved recently by Black *et al.* (2004*a*, *b*), who used magnetic tracer particles ranging from silts to gravel and consequently used powerful magnets to separate the tracer from the native sediment (an approach first used by Pantin 1961). Previously there were no published accounts of effective separation methods. Aside from the method of Pantin/Black, in which tracer (once

[4] Determination of K_o is central to computation of the tracer/sand transport layer thickness. Most simply, it is given by the depth of penetration of tracer observed in cores, however this is valid only when there is *no* increase in tracer content with depth. White (1998) provides a more detailed discussion of this aspect. Note that if tracer particles are known to be fully mixed (no vertical gradient) and K_o is known then transport rate may be deduced from surface tracer distribution only.

separated) is weighed thereby giving mass directly, as soon as tracer grains are recovered, two methods exist: counting grains or measuring fluorescence. Counting, which has been the dominant method for most historical studies, involves simply washing and drying of samples, spreading a thin layer and counting using the eye under ultraviolet light. Beach studies have often employed the simple method of scanning the sand surface with an ultraviolet light at night-time to assess general tracer presence (Russell 1960; Ingle 1966; Ciavola *et al.* 1997*b*). Counting is a lengthy and time-consuming process, particularly where particle abundances exceed 100, and counting is problematic where multiple colours are used owing to spectral overlap and the resolution of the human eye. It is also subject to human error. Teleki (1966*b*) recognized the limitations of visual assessment of sand tracer grains and devised an automated fluorescent particle counting instrument using high resolution photo-multipliers and sharply delineating transmission filters, and nowadays several sophisticated image-analysis methods have been developed to count particles (Pinto *et al.* 1994; Vila-Concejo *et al.* 2004 cf. their FENIX system; Forsyth 2000). Pinto *et al.*'s (1994) was used extensively during the recent Luminoferos na Areia (LUAR) experiments undertaken by the DISPELA research group (Taborda *et al.* 1994; Ciavola *et al.* 1997*a*).

Photodetection devices have been used to detect the amount of fluorescing light emitted from a sample (De Vries 1967; Nelson & Coakley 1974; Ignatov *et al.* 1979; Farinato & Kraus 1980; Howa *et al.* 1994), as well as the quantity of dye dissolved from the surfaces of coated tracer grains (Zenkovitch *in* Teleki 1963; Farinato & Kraus 1980). Gallagher *et al.* (1991) developed a video camera system to measure the tracer fluorescence. McComb & Black (2005) use synthetic (polymer) tracer and used a spectorophotometric method following grinding of particles and dissolution in acetone. This method proved effective at determining very low concentrations of tracer particles, but has inherent assumptions including a dependence on tracer volume, a uniform pigment concentration across all tracer particles and presumes there is no loss of fluorescence through time (photo-bleaching).

Computation of tracer budget

At given times (e.g. at each sampling interval), it is good practice to compute the tracer budget to assess the sediment transport that has taken place. Ingle (1966) uses this approach to plot 'depletion curves' – graphs of the percentage of released tracer sand to that found in the sampling grid. A thorough analysis of this method is also given by Vila-Concejo *et al.* (2004). One can assume that the tracer mass within a given core ($C(x,y)$) of area πr^2 represents the content in a rectangle ($\Delta x \Delta y$) surrounding the core locality of thickness K_o, the boundaries lying midway between sample points (an approach first used by Inman and Chamberlain 1957). The total mass (M_{TOT}) across the sampling grid is then given by the summation of mass in contiguous rectangles in the alongshore and across-shore directions:

$$M_{TOT} = \sum_x \sum_y \left[\sum_{K_o} C(x,y,K_o) \right] \frac{\Delta x \Delta y}{\pi r^2} \qquad (3)$$

where C is tracer mass. This procedure works successfully for beachface studies, where grid node-node spacing is not large. For large Lagrangian grids[5] (e.g. Louisse *et al.* 1986) errors arise as the spacing increases, since the assumption of uniform tracer content over such scales is increasingly tenuous; in addition it is clear that replication (e.g. > 1 core) is necessary in order to attach significance (in a statistical sense) to the value of $C(x,y)$, especially where the tracer distribution is contagious (patchy) or where tracer 'hotspots' may occur.

Tracer burial

Tracer burial during the course of a study through direct sedimentation (e.g. beneath plumes) or due to migrating bedforms is a potential confounding factor, since it can give rise to an apparent loss of tracer through a mechanism other than resuspension. Of course, enhanced levels of deposition leading to burial may be a characteristic of a particular environment. In the absence of *a priori* information on local sedimentation rates or rates of bedload transport, it is useful to obtain measurement of bed level at one locality (using altimetry, for instance) concomitantly with any tracking study, or to use short cores to sample the bed.

Silt tracking

The tracking of silt (< 63 μm) has always been a more formidable task. Whilst Sarma & Iya (1960) used a (now banned) radioactive method to tag

[5] Although is not possible here to prescribe what constitutes a 'large' sampling grid as this is a study specific length scale, the important issue is that single core samples based on a relatively disparate sampling scale represents a low-information content and should be avoided.

coarse silt particles, it remains extremely difficult to coat natural silt sediments with a fluorescent pigment without undue modification of particle size and density. However, technological improvements made during the 1980s gave rise to silt (and smaller) size powders with a fluorescent signature embedded throughout the particle (e.g. Harvey *et al.* 1989). Indeed, ultra-fine powders (0.1–1 μm) have been widely used in hydrogeological applications to track bacterial transport pathways (see Harvey & Harms 2002, and references therein).

The earliest evidence of attempts to track silt derive from the Dutch. Van Leussen (undated) investigated the utility of a fine (≈10 μm) commercial powder and it would seem these investigations were taken up and expanded by Draaijer *et al.* (1984), and were continued in the form of a field trial to track the dispersal of dredge spoil in the Ems–Dollard estuary by Louisse *et al.* (1986). The success of the method of Louisse *et al.* (1986) is attributable, in part, to arrival of a new measurement technology especially suited to fine particles – environmental flow cytometry (EFC). Environmental flow cytometry is a laser-induced fluorescence technique originally used to excite and enumerate phytoplankton cells (e.g. Detmer & Jochem 1992). Flow cytometry works on the principle of stimulating fluorescent pigments using laser radiation, and then measuring the frequency of backscattered light energy. Through the frequency it becomes possible to detect simultaneously the presence of differently coloured tracer particles. The principal disadvantage of EFC is that the maximum permissible particle size is ≈10 – 15 μm, otherwise clogging of the tubing of the flow-through chamber occurs and unwarranted particle obscuration influences the results.

Louisse *et al.* (1986) followed the generic methodology outlined previously. A series of verification tests (particle size, sedimentation rate) indicated the suitability of the powder as a tracer. Note, however, these authors aimed *not* to mimic individual floc aggregates with their tracer, rather to incorporate tracer particles within natural aggregates in order to tag them. This is a different style of tracking to sand tracking. The tracer was introduced directly into the supply line of a dredger during active excavations, following which it was dispersed throughout the estuary by tidal action. In the absence of any means to trap the tracer–silt aggregates in suspension, the authors conducted a series of grid-based benthic sampling campaigns during the ensuing weeks (akin to SIM-based sampling) to map the extent of deposition of tracer. The authors used specially designed coring devices to avoid disturbing the fine, mobile layer in which the tracer was present. Unlike many sand tracking studies, only a fraction (*c.* 10%) of tracer on a mass basis was retrieved, precluding use of the spatial integration mathematics to estimate transport. The utility of the study rested principally on demonstrating the spatial extent of dredge spoil contamination (a useful piece of information of itself).

More recently, Newman *et al.* (1990*a*, *b*) and Adams *et al.* (1998) also used flow cytometry to count tracer particles comprising fine (1–10 μm) commercially available paint pigment during sewage tracking studies in Boston Harbour. In these studies, the tracer was used in a similar fashion to sand tracer, i.e. the discrete paint particles possessed the same hydraulic properties as the sewage particles.

Whilst the above authors all used bottom sampling to describe transport pathways, fine sediment tracer studies lend themselves to 'temporal' or 'Eulerian' sampling (although this form of sampling has been used in sand studies e.g. Knoth & Nummeda 1977; McComb & Black 2005). Essentially, this approach tracks the centroid of motion from a single reference point over time. This is similar in principle to the determination of fluid discharge by tracing soluble dyes (Crickmore & Lean 1962), and is referred to as the 'time integration method' (TIM). TIM methodologies are discussed in greater depth by White & Inman (1989). Eulerian sampling is an appropriate approach where the rate of loss of a sediment or contaminant from a specific locality is more important than the eventual (geographic) fate, or where the rate of dilution through time and in space is excessive. Eulerian sampling requires a temporally dense sampling scheme in order that significant mass is not 'missed'.

Black *et al.* (2004*a*) describe a new sampling instrument appropriate to temporally based sampling of suspended sediments. Their instrument captures sediment moving horizontally within a flow on a continuous basis, and it has a mechanism to provide a time-stamp as to when sediments are captured. In addition, the instrument is equipped with a variety of sensors to measure flow and sediment properties. The device is ideally suited to fine sediment tracking studies using the TIM method since it permits capture and measurement of the mass of tracer in suspension through time. Moreover, the instrument can be deployed in a manner whereby tracer is captured before it becomes thoroughly dispersed by the flow turbulence i.e. in the 'near-field' (Black *et al.* 2004*a*). Were the technology available at the time of the Louisse *et al.* (1986) study, it would have formed a useful additional sampling tool in

the evaluation of the rate of sediment transport away from the dredge placement zone. As a point of interest, combination of the technology and approach used by Black *et al.* (2004*a*) with time-series vertical sedimentation traps (e.g. Eadie 1997) would substantially aid sampling for tracer, as well as provide an insight into the relative importance of advective versus vertical (settling) sediment transport .

Discussion

Particle tracking constitutes an attractive, practical method for use in sediment transport studies if used correctly, and if applied only within the context of the limitations of the method. Indeed, Drapeau *et al.* (1991) noted that tracers do fulfil the purpose for which they are used, and can supply valid scientific data if knowledge and care are exercised. The method clearly has found a far wider application for sand, but equally now that a method for silt tracking is becoming established the method is of greater generic utility. The merit of the particle tracking method is related to the fact that it is, fundamentally, a geospatial method, and can delineate sediment transport pathways or trends in a way no other method can. Further, it is a field method which, if done correctly, can provide a direct picture of sediment transport trends with no dependence on empiricism or calibration. Indeed, particle tracking offers the potential to provide transport data on a Lagrangian basis, and to provide information on sources, pathways and rates of sediment movement, and to reveal physical impact within benthic environments. Few, if any, other field-based technologies can offer such an integrated measurement capability. Numerical modeling is the only comparable method that can provide information on similar temporal and spatial scales, and yet the utility of models is proportional to their ability to accurately represent real-world processes (Dyke 1996). Numerical schemes continue to have difficulties, for example, mathematically representing real-world features such as the temporal variability of bottom roughness (Van Rijn *et al.* 2001), the stress-erosion rate function for cohesive muds (Black *et al.* 2002), and biological influences such microbial bio-cohesion (Paterson 1994) with sufficient accuracy. Of course, a poorly conducted tracking experiment must be viewed with caution, but at least particle tracking inherently integrates these real-world effects (Knoth & Nummeda 1977).

The flexibility of the method undoubtedly lies within the ease of use, the range of colours available, the range of grain sizes available (silt to cobbles), and the cost is not (relative to other methods, including modelling) overly expensive. White (1998) published a table comparing tracking as a singular method with other available methods and techniques for measuring sediment transport. This is reproduced in modified form in Table 2. It may be seen that the tracking method has perhaps the widest applicability of the various methods, warranting a more mainstream position for the tracking approach. Notwithstanding this, sediment tracking is a tool

Table 2. *Comparison of sediment transport measurement techniques (modified after White, 1998)*

	Large scale traps	Suspension pumps	Suspension samplers	Cloth traps	Tracers	Optical methods	Acoustic methods
Bedload	X				X		
Suspension	X	X	X	X	X	X	X
Near-bed suspension	X	X	?	?	X	X	X
Point measurement*	X	X	X	X	X	X	X
Global measurement†	X				X	‡	
Concentration		X	X		X	X	X
Velocity					X		X
Transport	X			X	X		
Accuracy	A	M	M	M	M	A	A
Relative cost	*M/E*	*I*	*I*	*I*	*M/E*	*M*	*M/E*

X indicates that the method has that characteristic
A is accurate (10–30% range)
M is moderately accurate (30–60% range)
E: expensive, M: moderate, I: inexpensive
*Point measurement implies very localized study e.g. longshore drift study
†Global measurement implies studies on a wider spatial scale (e.g. coastal/basin scale)
‡Not including aerial remote sensing

and compliments more traditional approaches to sediment monitoring and measurement (e.g. current and turbidity monitoring, erosion–deposition measurement). Ultimately, most benefit will be gained from the use of particle tracking in conjunction with these other methods.

In spite of the long history of the particle tracking technique, especially for sands and gravels, the method remains beset by several methodological problems and could be improved. These problems include a generally rudimentary approach to sampling design, a lack of replicate sampling (statistical rigour), the inability until recently to separate tracer from native sediment in a simple fashion, and a method recurrently based upon grain counts rather than tracer mass. These can be examined in turn.

Organization of sampling

Van Rijn (1993) notes that 'the quality of the total study can only be as good as the quality of the information gained from sampling', and nowhere is this more true than for particle tracking studies. If one adopts the view that there is usually a need to differentiate tracer content amongst and between sites, rather than simply identify trends or determine presence–absence, then there is much to learn from other sciences and disciplines that also have quantitative sampling at their heart. For instance, other sampling schemes used for benthic monitoring and contaminated land assessment such as probability based sampling schemes or generalised random tessellation (GRTS) sampling designs may find useful application in tracking studies. GTRS (a method devised by the US Environmental Protection Agency) combines elements of random and systematic sampling, whilst maintaining a uniform spread of sampling stations across a given area (Stevens 1997). For an inherently geospatial methodology, it is remarkable that geostatistical methods have not been used to underpin the sediment tracking studies. Geostatistical methods include sampling strategies, interpolation methods, semi-variogram modelling (spatial correlation analysis) and data visualization (Gouvaerts 1999). Geostatistics, in particular, has the capacity to predict values at unsampled locations (Webster & Oliver 1993), and can provide some quantitative measure of the uncertainty about unsampled values (Flatman *et al.* 1987; Gouvaerts 1999). Saito & Goovaerts (2001) published a study in which they account for source location and transport direction of lead-contaminated soils around Dallas, which may be of special relevance to tracking studies. A geostatistically based approach to sediment tracking would undoubtedly provide a firmer theoretical foundation for a range of tracking studies, as well as contribute to more refined and statistically defensible field sampling schemes. For these reasons alone, these related areas of study are worthy of our attention.

Replication

Sampling is time-consuming, often difficult and costly, and for these reasons replication at every sampling location (i.e. a second drop of the grab) is perhaps unrealistic. This issue can be addressed effectively through use of sampling equipment that collects multiple samples in one drop, such as a multiple corer or a sectioned box corer (e.g. Gooday & Gabriella Malzone 2004). Although such sampling in a strict sense constitutes pseodoreplication (Hurlbert 1984), for the purposes of sediment tracking the increase in statistical confidence are judged to outweigh this factor. Effective use of replicate sampling becomes important where localised tracer 'hotspots' may occur, since without some level of replication interpretation of the significance of a single (high) data value becomes difficult.

Tracer separation

The lack (historically) of an effective method to separate tracer from native sediment following sampling was the single, prominent impediment (in a practical sense) to tracking studies. Flow cytometry offers some scope in terms of an analytical method as a stream of tracer plus sediment is forced through the measurement volume. The drawback of the cytometric method, however, is that it is restricted to very fine silts (*c.* $< 10\ \mu m$) and comparatively very small sediment volumes of *c.* 1 ml only can be processed. For sands, either fluorescent grains have been handpicked (e.g. Ingle 1966) or else a small sample (e.g. 1 g; McComb & Black 2005) was photographed under ultra-violet light and image processing used to count grains. Neither method is ideal, especially where a large number of samples are collected or where the tracer sample is itself large. Pantin (1961) struck upon a simple and effective method of separation: use of a magnetic tracer. Although he was not able to tightly control grain density, an elegant consequence of direct tracer separation is that the data are in the form of mass, rather than counts, a unit that is of far greater use to oceanographers and geologists engaged in flux analysis in sediment transport problems (van Rijn 1993). Although there are inevitable problems associated with magnetic

tracers, such as contamination by magnetic accessory minerals (hematite, magnetite), it should not be overly difficult to surmount these. Magnetite, for instance, possess a specific gravity of *c.* 5100 kg m^{-3}; in order for a particle to be in hydraulic equilibrium with 200 μm quartz it would be around 30 μm in size (Soulsby 1997) and therefore simple sieving will separate the magnetite from the quartz. The magnetic tracer method first used by Pantin (1961) and subsequently refined and improved by Black *et al.* (2004*a*, *b*) constitutes a significant step-advance in tracer methodology. The potential now exists for the method to be used shipboard, which opens up the prospect of quasi-real-time, adaptive sampling.

The heated sand approach of Van der Post *et al.* (1995), a seemingly one-off study but in which it was not necessary to retrieve samples or separate out tracer, initially appears extremely attractive as an alternative method as it presents a non-intrusive, remote sensing option for tracer content determination (magnetic susceptibility). Ventura *et al.* (2001) also used magnetic susceptibility successfully to measure dispersion of a magnetic tracer on soils. The susceptibility technique is the closest there is to a fully field-based sensor for tracking studies. However, there are shortcomings of the method, not least the ability to discriminate the modified sand tracer from natural magnetic grains, but also information on the tracer mixing depth is required in order to quantitatively assess the mass content remotely from magnetic susceptibility readings. Cross-comparison of the susceptibility method with the Pantin/Black direct magnetic separation method may prove a fruitful avenue of research towards a generic field-sensor capability.

Limitations

A clear appreciation of the limitations of the particle tracking method is most certainly required, and particle tracking has a functional limit beyond which data gained may not be considered reliable. For suspended sediments the limiting factor is dilution, or, more specifically, excessive dilution (Ingle 1966; Louisse *et al.* 1986), whereas for bedload the limiting factor is burial. Burial can be addressed, to some extent, by taking and sectioning cores (e.g. Knoth & Nummeda 1977). For suspended sediment tracking studies there is a point along the transport pathway at which dilution is so great that either sampling and analytical errors rise to unacceptable levels, or that it is no longer possible to detect tracer in the environment. This is termed the operational limit. Although McComb & Black (2005) successfully conducted a bedload tracer study in a high wave energy coastal environment, and in spite of the fact that average grain transport velocities are in theory much slower than in shallower waters, generally these types of environments are challenging to the tracking methodology unless sampling is conducted within a few hours of tracer release (e.g. Bastin *et al.* 1983). Use of the sediment trap device described by Black *et al.* (2004*a*, *b*) is a particularly innovative method to capture suspended tracer in the 'nearfield', and so provide data on (suspended) tracer transport even in energetic environments. Clearly, tracking studies need to identify appropriate sampling strategies that will capture tracer well before the operational limit is reached. Of course, the operational limit is also a function of the analytical detection limit in the sense that an increased detection limit extends the operational limit, and vice versa. Simple use of a greater mass of tracer will obviously also extend the operational limit. It is important that the concept of operational limit is recognised by users of the particle tracking method.

Conclusions

Particle tracking within a geoscientific context has firm foundation as a field method for the investigation of sediment transport processes, with a research history reaching back to the 1900's. It offers a practical method for the assessment of transport pathways of sediments from silts to cobbles in almost all aquatic environments, and presents a measurement capability that few other contemporary technologies can provide. In recent years many specific elements of the method have been improved considerably. The issue of tracer separation has been resolved through the use of a modern magnetic tracer, and substantial advancements have arisen in synthetic particle manufacturing methods, sediment capture devices, and analytical methods (e.g. digital image analysis). The central feature of sediment tracking—sampling—can, in the authors' view, be improved, and there is benefit in using approaches adopted in other fields e.g. geostatistics. Used in conjunction with a range of more traditional methods, particle tracking is a useful tool which provides additional lines of evidence in sediment transport studies and thus contributes to forming a more detailed understanding of sediment transport pathways. The use of particle tracking in sediment transport studies will be of interest to a variety of professionals including sediment researchers, coastal managers, engineers and modellers, conservation agencies, regulatory authorities, and members of the dredging industry.

The authors appreciate the critical comments from P. Ciavola and reviews from two anonymous reviewers.

References

ABECASIS, F., MATIA, M. F., REIS DE CARVALHO, J. J. & VERA-CRUZ, D. 1962. *Methods of determinig sand and silt movement along the coast, in estuaries and in maritime rivers*. Laboratorio National d Engenharia Civi Technical Paper **186**. Lisbon Ministerio das Obras Publicas.

ADAMS, C. E., STOLZENBACH, K. D., LEE, J. J., CAROLI, J. & FUNK, D. 1998. Deposition of contaminated sediments in Boston Harbour studied using fluorescent dye and particle tracers. *Estuarine Coastal Shelf Science*, **46**, 371–382.

AMBULATOV, N. A. & PATRIKEIEV, V. V. 1963. On the influence of luminophoric and agaroid films on the hydrodynamic properties of tracer sand. *Okeanologia*, **3**, 921–924.

ARKELL, B., LEEKS, G., NEWSON, M. & OLDFIELD, F. 1983. Trapping and tracing: some recent observations of supply and transport of coarse sediment from upland Wales. *In*: COLLINSON, J. D. & LEWIN, J. (eds) *Modern and Ancient Fluvial Systems*. Special Publication of the International Association of Sedimentologists, **6**, 107–119.

ARLMAN, J. J., SVASEK, J. N. & VERKERK, B. 1960. The use of radioactive isotopes for the study of littoral drift. *Dock Harbour Authority*, **61**, 57–64.

BADR, A. A. & LOFTY, M. F. 1998. Tracing beach sand movement using fluorescent quartz along the Nile delta promontories, Egypt. *Journal of Coastal Research*, **15**, 261–265.

BALOUIN, Y., VAN BOXEL, J. H. *et al.* 2003. Tidal inlet function: field evidence and numerical simulation in the INDIA project. *Journal of Coastal Research*, **19**, 189–211.

BASTIN, A. L., CAILLOT, A. & MALHERBE, B. 1983. Zeebruge port extension: sediment transport measurements on and off the Belgian coast by means of tracers. *In*: *Proceedings 8th International Harbour Congress, Antwerp, 13–17 June, 1983*, 1–14.

BECK, C., CLABAUT, P., DEWEZ, S., VICAIRE, O., CHAMLEY, H., AUGRIS, C., HOSLIN, R. & CAILLOT, A. 1991. Sand bodies and sand transport paths at the English Channel–North Sea border: morphology, hydrodynamics and radioactive tracing. *Oceanologica Acta*, **11**, 111–121.

BLACK, K. S. & PATERSON, D. M. 1997. Measurement of the erosion potential of cohesive marine sediments: a review of current in situ technology. *Journal of Marine Environmental Engineering*, **4**, 43–83.

BLACK, K. S., TOLHURST, T. J., HAGERTHEY, S. E. & PATERSON, D. M. 2002. Working with natural cohesive sediments. *Journal of Hydraulic Engineering*, **128**, 1–7.

BLACK, K. S., WILSON, P., ATHEY, S., BLACK, I. & EVANS, D. 2004*a*. Direct assessment of dredging impact in sensitive environments using particle tracking technology. *In*: *Proceedings, World Organisation of Dredging Organisations, September 04, Hamburg*. Paper P.

BLACK, K. S., ATHEY, S., WILSON, P. & EVANS, D. 2004*b*. Particle Tracking: a new tool for coastal zone sediment management. *In*: *Proceedings of the 4th International Conference, Littoral'04, Aberdeen, September, 2004*, 525–530.

BOYD, S. E. (ed.) 2002. *Guidelines for the conduct of benthic studies at aggregate dredging sites*. Report produced by the Centre for Environment, Fisheries and Aquaculture Science on behalf of the Department for Transport, Local Government and the Regions.

CAEIRO, S., PAINHO, M., GOOVAERTS, P., COSTA, H. & SOUSA, S. 2003. Spatial sampling design for sediment quality assessment in estuaries. *Environmental Modelling and Software*, **18**, 853–859.

CAILLOT, A. 1970. Les methods de marquage des sediments par des indicateurs radioactifs. *La Houille Blanch*, **25**, 661–674.

CAILLOT, A. 1973. Sediment labelling with radioisotopes. *In*: *Tracer Techniques in Sediment Transport*. IAEA Technical Report. **145**, 169–176.

CALDWELL, N. E. 1981. Relationship between tracers and background beach material. *Journal of Sedimentary Petrology*, **51**, 1163–1168.

CHEONG, H. F., SHANKAR, J., RADHAKRISHNAN, R. & TOH, A. C. 1993. Esimation of sand transport by use of tracers along a reclaimed shoreline at Singapore airport. *Coastal Engineering*, **19**, 311–325.

CIAVOLA, P., TABORDA, R., FERREIRA, O. & DIAS, J. A. 1997*a*. Field observations of sand-mixing on beaches. Marine Geology, **141**, 147–156.

CIAVOLA, P., TABORDA, R., FERREIRA, O. & DIAS, J. A. 1997*b*. Field measurements of longshore sand transport and control processes on a steep meso-tidal ebach in Portugal. *Journal of Coastal Research*, **13**, 1119–11129.

CIAVOLA, P., DIAS, N., FERREIRA, O., TABORDA, R. & DIAS, J. M. A. 1998. Fluorescent sands for measurement of longshore transport rates: a case study from Praia de Faro in southern Portugal. *Geomarine Letters*, **18**, 49–57.

CLARK, W. A. V. & HOSKING, P. L. 1986. *Statistical Methods for Geographers*. John Wiley & Sons, New York.

COLLINS, M. B., SIMWELL, S. J., GAO, S. S., POWELL, H., HEWITSON, C. & TAYLOR, J. A. 1995. Water and sediment movement in the vicinity of linear sandbanks: the Norfolk Banks, southern North Sea. *Marine Geology*, **123**, 125–142.

CRICKMORE, M. J. 1967. Measurement of sand transport in rivers with special reference to tracer methods. *Sedimentology*, **8**, 175–228.

CRICKMORE, M. J. 1976. Tracer techniques for sediment studies; their use, interpretation and limitations. *In*: *Diamond Jubilee Symposium on Modelling Techniques in Hydraulic Eng.*, Vol. **1**. Central Power and Water Research Station, Paper A13.

CRICKMORE, M. J. & LEAN, G. H. J. 1962. The measurement of sand transport by the time-integration method with radioactive tracers. *Proceeding of the Royal Society London*, **A270**, 27–47.

CROMEY, C. J., NICKELL, T., BLACK, K., PROVOST, P. & GRIFFITHS, C. 2002. Validation of a fish farm waste resuspension model by use of a particulate

tracer discharged from a point source in a coastal environment. *Estuaries*, **25**, 916–929.

CUMMINS, R. S. & INGRAM, L. F. 1963. Tracing sediment movement with radioisotopes. *Military Engineering*, **55**, 161–164.

DAVIDSON, J. 1958. Investigations of sand movement using radioactive sand. Lund University, *Studies in Physical Geography*, **A12**, 69–126.

DE VRIES, M. 1967. Photometric counter for fluorescent tracers. *La Houlile Blanche*, **22**, 717–722.

DETMER, A. E. & JOCHEM, F. J. 1992. Phototrophic pico- and nanoplankton in the Central Baltic Sea – estimates by fluorescence microscopy and flow cytometry. *Signal & Noise*, **5**, 1–2.

DINGLER, J. R. & ANIMA, R. J. 1982. Sand movement into Carmel submarine canyon, California. *In*: *Proceeding of the 18th Coastal Engineering Conference, Capetown*. ASCE, 168–1287.

DOBBS, P. H. 1958. Effects of wave action on the shape of beach gravel. *Compass*, **35**, 269–275.

DRAAIJER, A., TADEMA WIELANDT, R. & HOUPT, P. M. 1984. *Investigation on the applicability of fluorescent synthetic particles for the tracing of silt*. Netherlands Organisation for Applied Scientific Research, Report R84/152 [in Dutch].

DRAPEAU, G., LONG, B. & KAMPHIUS, W. 1991. Evaluation of radioactive sand tracers to measure longshore sediment transport rates. *In*: Proceeding of the 22nd International Conference on Coastal Engineering ASCE, New York, 2710–2723.

DUANE, D. B. & JAMES, W. J. 1980. Littoral transport in the surf zone elucidated by an Eulerian tracer experiment. *Journal of Sedimentary Petrology*, **50**, 929–942.

DYER, K. R. 1986. *Coastal and Estuarine Sediment Dynamics*. John Wiley and Sons Ltd, Chichester.

DYKE, P. 1996. *Modelling Marine Processes*. Prentice Hall.

EADIE, B. J. 1997. Probing particle processes in Lake Michigan using sediment traps. *Water, Air, and Soil Pollution*, **99**, 133–139.

EIDSVIK, K. J. 2004. Some contributions to the uncertainty of sediment transport predictions. *Continental Shelf Research*, **24**, 739–754.

ELLIOT, J. M. 1971. *Some methods for the statistical analysis of samples of benthic invertebrates*. Freshwater Biological Association Publication No. 25.

FARINATO, R. S. & KRAUS, N. C. 1980. Spectrofluorometric determination of sand tracer concentrations. *Journal Sedimentary Petrology*, **51**, 663–665.

FERREIRA, O., FACHIN, S., BRAGA COLI, A., TABORDA, R., ALVEIRINHO DIAS, G. & LONTRA, G. 2002. Study of harbour infilling using sand tracer experiment. *Journal of Coastal Research*, **36**, 283–289.

FLATMAN, G. T., ENGLUND, E. J. & YFANTIS, A. A. 1987. Geostatistical approaches to the design of sampling regimes. *In*: KEITH, L.H. (ed.) *Principles of Environmental Sampling*. ACS Professional Reference Book. American Chemical Society, Washington, 73–92.

FLEMMING, B. W. & DELAFONTAINE, M. T. 2000. Mass physical properties of muddy intertidal sediments: applications, misapplications and non-applications. *Continental Shelf Research*, **20**, 1179–1198.

FORSYTH, S. H. 2000. *New developments in artificial fluorescent tracer counting techniques applied to sand transport studies*. MSc Thesis, University of Waikato, Hamilton, New Zealand.

FOSTER, G. A., HEALY, T. R. & DELANGE, W. P. 1996. Presaging beach renourishment from a nearshore dredge dump mound, Mt. Maunganui beach, New Zealand. *Journal of Coastal Research*, **12(2)**, 395–405.

FOSTER, I. D. L. 2000. *Tracers in Geomorphology*. Wiley, Chichester.

FOWLER, J., COHEN, L. & JARVIS, P. 1998. *Practical statistics for field biology*. John Wiley and Sons, Chichester.

GALLAGHER, E. L., SEYMOUR, R. J. & KING, D. B. JR 1991. Bedload transport by imaging of tracers. *In*: *Coastal Sediment* '91. ASCE, New York, 717–725.

GALVIN C. J. 1987. Vertical profile of littoral sand tracers from a distribution of waiting time. *In*: Proceedings, Coastal Sediments 1987. ASCE, New York, 436–451.

GOODAY, A. J. & GABRIELLA MALZONE, M. 2004. Yperammina micaceus sp. nov.: a new foraminiferan species (Protista) from the Porcupine Abyssal Plain, northeast Atlantic. *Journal of Micropalaeontology*, **23**, 171–179.

GOUVAERTS, P. 1999. Geostatistics in soil science: state of the art and perspectives. *Geoderma*, **89**, 1–45.

GREEN, R. H. 1979. *Sampling design and statistical methods for environmental biologists*. John Wiley and Sons. Toronto, Canada.

GRISSEIER, H. & HOEG, S. 1964. Durch ferromagnetika markierte sedimente und moglichkeiten irher automastichen zahlung. *Acta Hydrophysica*, **9**, 35–53.

HAINING, R. 1990. *Spatial Data Analysis in the Social and Environmental Sciences*. Cambridge University Press, Cambridge.

HARVEY, R. W. & HARMS, H. 2002. Tracers in groundwater: use of microorganisms and microspheres. *In*: BITTON, G. (ed.) *Encyclopaedia of Environmental Microbiology*, John Wiley and Sons Inc., New York, **6**, 3194–3202.

HARVEY, R. W., GEORGE, L. H., SMITH, R. L. & LEBLANC, D. R. 1989. Transport of microspheres and indigenous bacteria through a sandy aquifer: Results of natural and forced-gradient tracer experiments. *Environmental Science and Technology*, **23**, 51–56.

HAUTON, C. & PATERSON, D. M. 2003. A novel vane shear instrument used to determine evolution of hydraulic dredge tracks in subtidal marine systems. *Estuarine and Coastal Shelf Science*, **56**, 1–8.

HEATHERSHAW, A. D. & CARR, A. P. 1987. Measurements of sediment transport rates using radioactive tracers. *In*: *Proceeding of the Coastal Sediments 1987* ASCE, New York, 399–412.

HOWA, H. & DE RESSEGUIER D. 1994. Application of a fluorescent grain detector/counter for sand transport evaluation in the littoral zone. *In*: *Proceedings of the International Conference on Ocean Osates 98*, **III**, 254–257.

HOWA, H., MICHEL, D. & DE RESSEGUIER, D. 1994. Quantifications des deplacements sableux en

domain littoral. Calculs theoriques et tracages fluorescents. *In: Colloque franco-bresilien Acquitaine-Ocean*, **3**, 79–91.

HUBEL, D. W. & SAYRE, W. W. 1964. Sand transport studies with radioactive tracers. *Journal of the Hydraulics Division, ASCE*, **90(Hy3)**, 39.

HURLBERT, S. H. 1984. Pseudoreplication and the design of ecological field experiments. *Ecological Monographs*, **54**, 187–211.

IGNATOV, Y. I., KATAGOSCHCHIN, O. D., PROKHODSKY, I. S., ROBSMAN, V. A. & SHLYUKOV., A. I. 1979. Determination of lithodynamic elements by the luminescent tagged sand method along the coast of the Sea of Japan. *Oceanology*, **19**, 112–114.

INGLE, J. C. 1966. *The movement of beach sand: an analysis using fluorescent grains.* Developments in Sedimentology, **5**. Elsevier, Amsterdam.

INMAN, D. L. & CHAMBERLAIN, T. K. 1959. Tracing beach sand movement with irradiated quartz. *Journal Geophysical Research*, **64**, 41–47.

INMAN, D. L., ZAMPOL, J. A., WHITE, T. E., HANES, D. M., WALDORF, B. W. & KASTENS, K. A. 1980. Field measurements of sand motion in the surf zone. *In: Proceedings 17th Coastal Engineering Conference, March 23–28, 1980, Sydney, Australia.* ASCE, 1215–1234.

INOSE, S. & SHIRAISHI, N. 1956. The measurement of littoral drift by radioisotopes. *Dock Harbour Authority*, **36**, 284–288.

JOHNSON, C. 2005. *Migration of dredged material mounds: predictions based on field measurements of waves, currents, and suspended sediments, Brunswick, GA.* PhD thesis, School of Civil and Environmental Engineering, Georgia Institute of Technology. Savannah.

JOLLIFFE, I. P. 1963. A study of sand movements on the Lowestoft sandbank using fluorescent tracers. *Geogrrphical Journal*, **129**, 480–493.

KENNEDY, V. C. & KOUBA, D. L. 1970. *Fluorescent sand as a tracer of fluvial sediment.* USGS, Professional Paper, **562E**.

KIDSON, C. & CARR, A. P. 1961. Beach drift experiments at Bridgewater Bay, Somerset. *Proceeding of the Bristol Nature Society*, **30**, 163–180.

KIDSON, C. STEERS, J. A. & FLEMMING, N. C. 1962. A trial of the potential value of diving to coastal physiography on British coats. *Geographical Journal*, **128**, 49–53.

KING, C. A. M. 1951. Depth of disturbance of sand on sea beaches by waves. *Journal of Sedimentary Petrology*, **21**, 131–140.

KNOTH, J. S. & NUMMEDA, D. 1977. Longshore sediment transport using fluorescent tracer. *In: Proceedings of Coastal Sediments*, ASCE, 383–398.

KOMAR, P. D. 1977. Selective longshore transport rates of different grain-size fractions within a beach. *Journal of Sedimentary Research*, **47**, 144–1453.

KOMAR, P. D. & INMAN, D. L. 1970. The longshore transport of sand on beaches. *Journal Geophysical Research*, **75**, 5914–5927.

KRAUS, N. 1981. Field experiments on longshore sand transport in the surf zone. *Coastal Engineering in Japan*, **24**, 171–194.

KRAUS, N. C. 1985. Field experiments on the vertical mixing of sand in the surf zone. *Journal of Sedimentary Petrology*, **55**, 3–14.

KRAUS, N. C. ISOBE, M. IGARASHI, H. SASAI, T. O. & HORIKAWA, K. 1982. Field experiments on longshore transport in the surf zone. *In: Proceeding of the 18th International Conference of Coastal Engineering*, 969–988.

LAVENDER, S. J. 2001. A review of remote sensing in the marine environment. *The Hydrographic Journal*, **99**, 9–13.

LEAN, G. H. & CRICKMORE, M. J. 1963. Methods for measuring sand transport using radioactive tracers. *In: Radioisotopes in Hydrology IAEA Symposium, Tokyo*, 111–131.

LEE, M. W. BRAY, M. J., WORKMAN, M., COLLINS, M. B. & POPE, D. 2000. Coastal shingle tracing: a case study using the electronic tracer system. *In*: FOSTER, I. D. L. (ed.) *Tracers in Geomorphology*. Wiley, Chichester, 413–436.

LEIGHTON, P. A., PERKINS, W. A., GRINEELL, S. W. & WEBSTER, F. X. 1965. The fluorescent particle atmospheric tracer. *Journal Applied Meteorology*, **11**, 221–226.

LEVOY, F., MONFORT, O. & LARSONNEUR, C. 1997. Transports Solides sur les Plages Macrotidales : Traçage Fluorescent et Application à la Côte Ouest du Cotentin. *Oceanologica Acta*, **20**, 811–822.

LEVOY, F., ANTHONY, E., BARUSSEAU, J., HOWA H. & TESSIER, B. 1998. Morphodynamique d'une Plage Macrotidale à Barres. *Comptes Rendus de l'Académie des Sciences (Paris)*, **327**, 811–818.

LONG, B. KULKARNI, N. & JOICE, G. 1978. Radioisotopes as sediment tracer: risks involved and proposed guidelines. Bedford Institute of Oceanography Report Series BI-R-78-3, 38pp.

LONGUET-HIGGINS, M. S. & PARKIN, D. W. 1962. Sea waves and beach cusps. *Geographical Journal*, **128**,194–201.

LOUISSE, C. J., AKKERMAN, R. J. & SUYLEN, J. M. 1986. A fluorescent tracer for cohesive sediment. *In: International Conference on Measuring Techniques of Hydraulics Phenomena in Offshore, Coastal and Inland Waters. London, England, 9–11 April, 1986*, 367–391.

LUNEBERG, H. 1960. Sediment transport, sedimentation and erosion on the outer sands of the Weser estuary. *In*: List International Geological Congress, Copenhagen, 1960, 247.

MADSEN, O. S. 1987. Use of tracers in sediment transport studies. *In: Coastal Sediments '87*, 424–435.

MADSEN, O. S. 1989. Transport determination by tracers A. tracer theory. *In*: SEYMOUR, R. J. (ed.) *Nearshore Sediment Transport*. Plenum Press, New York, 103–114.

MAHAUT, M. L. & GRAF, G. 1987. A luminophore tracer technique for bioturbation studies. *Oceanologica Acta*, **10**, 323–328.

MCCOMB, P. J. 2001. *Coastal and sediment dynamics in a high-energy, rocky environment.* PhD Thesis, University of Waikato, New Zealand.

MCCOMB, P. J. & BLACK, K. P. 2005. Detailed observations of littoral transport using artificial sediment tracer in a high-energy, rocky-reef and iron sand

environment. *Journal of Coastal Research*, **21**, 358–373.

Michel, M. D. 1997. *Evolution Morphodynamique d'un Littoral Sableux Situe a l'Aval d'une Embochadure Lagunaire*. PhD Thesis, Univ. Bordeaux I.

MILLER, M. C. & KOMAR, P. D. 1979. Measurements of sand spreading rates under near-bottom wave orbital motions. *Journal of Geology*, **87**, 593–608.

MILNE, R. G. MCSTAY, D. & POLLARD, P. 1997. Comparison of tracers for environmental applications. *In*: AUGOUSTI, A. & WHITE, N. (eds) *Environmental and Biomedical Sensors – Proceedings of Sensors and Their Applications VIII*. Bristol: IOP Publishing, p. 27–32.

MUNOZ-PEREZ, J. J., GUTIERREZ-MAS, J. M., PARRADO, J. M. & MORENO, L. 1999. Sediment transport velocity by tracer experiment at Regla Beach (Spain). *Journal of Waterway, Port, Coastal, and Ocean Engineering, ASCE*, 332–335.

NELSON, D. E. & CROAKLEY, J. P. 1974. *Techniques for tracing sediment movement*. Inland Waters Directorate Scientific Series No. 32, Ottawa, Canada.

NEWMAN, K. A., MOREL, F. M. M. & STOLZENBACH, K. D. 1990*a*. Settling and coagulation characteristics of fluorescent tracer particles determined by flow cytometry and fluorometry. *Environmental Science and Technology*, **24**, 506–512.

NEWMAN, K. A., FRANKEL, S. & STOLZENBACH, K. D. 1990*b*. Flow cytometric detection and sizing of fluorescent tracer particles deposited at a sewage outfall site. *Environmental Science and Technology*, **24**, 513–519.

OERTEL, G. F. 1972. Sediment transport of estuary entrance shoals and the formation of swash platforms. *Journal Sedimental Petrology*, **42**, 857–863

OLMEZ, I., PINK, F. X. & WHEATCROFT, R. A. 1994. New particle-labeling technique for use in biological and physical sediment transport methods. *Environmental Science and Technology*, **28**, 1487–1490.

PANTIN, H. 1961. Magnetic concrete as an artificial tracer material. *New Zealand Journal of Geology and Geophysics*, **4**, 424–433.

PARSONS, A. J., WAINWRIGHT, J. & ABRAHAMS, B. 1993. Tracing sediment movement in inter-rill overland flow on a semi-arid grassland hill slope using magnetic susceptibility. *Earth Surface Processes and Landforms*, **18**, 721–732.

PATERSON, D. M. 1994. The biological mediation of sediment erodibility. *In*: BURT, N., PARKER, W. R. & WATTS, J. (eds) *Cohesive Sediments*. John Wiley and Sons, 215–229.

PINTO, J. C. R., DIAS, J. M. A., FERNANDEZ, S. P., FERREIRA, O., SILVA, A. V. & TABORDA, R. 1994. Automated system for tagged sand detection. *Gaia*, **8**, 161–164.

RATHBURN, R. E. & NORDING, C. F. 1971. Tracer studies of sediment transport processes. *Journal of the Hydraulics Divisoin, ASCE*, **97**, 1305–16.

RICHARDSON, N. M. 1902. An experiment on the movements of a load of brickbats deposited on Chesil Beach. *Proceedings of the Dorset Natural History Field Club*, **23**, 123–133.

RUSSELL, R. C. H. 1960. Use of fluorescent tracers for the measurement of littoral drift. *In*: *Proceedings of the 77th Conference on Coastal Engineering Univ. California, Berkely*, 418–444.

RUSSELL, R. C. H., NEWMAN, D. E. & TOMLINSON, K. W. 1963. Sediment discharge measured by continous discharge of tracers from a point. *In*: *IAHR 10th Congress, London*, 69–76.

SAITO, H. & GOOVAERTS, P. 2001. Accounting for source location and transport direction into geostatistical prediction of contaminants. *Environmental Science & Technology*, **35**, 4823–4829.

SALOMONS, W. & MOOK, W. G. 1987. Natural tracers for sediment transport studies. *Continental Shelf Research*, **7**, 1333–1343.

SARMA, T. P. & IYA, K. K. 1960. Preparation of artificial silt for tracer studies near Bombay Harbour. Journal Scientic Indeed Research India, astrinli, **19**, 99–101.

SAUZAY, G. 1973. Tracer techniques in sediment transport: report of the panel. *In*: *Tracer Techniques in Sediment Transport*, IAEA Technical Report, **145**, 3–8.

SEAR, D., LEE, M. W., OAKEY, R. J., CARLING, P. A. & COLLINS, M. B. 2000. Coarse sediment tracing technology in littoral and fluvial environments: a review. *In*: FOSTER, I. D. L. (ed.) *Tracers in Geomorphology*, Wiley, Chichester, 21–56.

SHERMAN, D. J., BAUER, B. O., NORDSTROM, K. F. & ALLEN, J. R. 1990. A tracer study of sediment transport in the vicinity of a groin: New York, USA. *Journal of Coastal Research*, **6**, 427–438.

SHINOHARA, K., TSUBAKI, T., YOSHITAKA, M. & AGEMORI, C., 1958. Sand transport along a model sandy beach by waves. *Coastal, Engineering, Japan* **1**, 111–129.

SMITH, D. B. & PARSONS, T. V. 1967. The investigation of spoil movement in the Firth of Forth using radioactive tracers. *In*: *Proceedings of Symposium on Dredging, London*, 47–54.

SOULSBY, R. 1997. *Dynamics of Marine Sands*. Thomas Telford, London, 248.

STEPANIAN, A., VLASVINKEL, B., LEVOY, F. & LARSONNEUR, C. 2001. Fluorescent tracer experiment on a macrotidal ridge and runnel beach : a case study at Omaha beach, North France. *In*: HANSON, H. & LARSON, M. (eds) *Coastal Dynamic'01*. Lund, Sweden, 1017–1027.

STEVENS, D. L. JR. 1997. Variable density grid-based sampling designs for continuous spatial populations. *Environmetrics*, **8**, 167–95.

TABORDA, R., FERREIRA, O., DIAS, J. M. A. & MOITA, P. 1994. Field observations of longshore sand transport in high energy environments. *In*: CARVALHO, S. & GOMES, V. (eds.) *Proceedings of Littoral '94*. EUROCOAST, Lisbon, Portugal, 479–487.

TANAKA, S., YAMAMOTO, K., ITO, H., ARISAWA, T. & TAKAGI, T. 1998. Fieold investigation on sediment transport into the submarine canyon in the Fuji coast with new type tracers. *Coastal Engineering*, **20**, 3151–3164.

TELEKI, P. G. 1962. A summary of the production and scanning of fluorescent tracers. *In*: *Federal Interagency Sedimentation Conference Proceedings, Jackson, Miss, USA*, 11.

TELEKI, P. G. 1963. *A summary of the production and scanning of fluorescent tracers*. Florida Univ., Coastal Engineering, Lab, Mimeograph.

TELEKI, P. G. 1966*a*. Fluorescent sand tracers. *Journal of Sedimentary Petrology*, **36**, 468–485.

TELEKI, P. G. 1966*b*. Automatic tracer analysis of sands. *Journal of Sedimentary Petrology*, **37**, 749–759.

TOLHURST, T. J, BLACK, K. S., SHAYLER, S. A., MATHER, S., BLACK, I., BAKER, K. & PATERSON, D. M. 1999. Measuring the in situ erosion shear stress of intertidal sediments with the Cohesive Strength Meter (CSM). *Estuarine and Coastal Shelf Science*, **49**, 281–294.

THOMPSON, R. C., OLSEN, Y., MITCHELL, R. P., DAVIS, A., ROWLAND, S. J., JOHN, A. W. G., MCGONIGLE, D. & RUSSELL, A. E. 2004. Lost at sea: Where does all the plastic go? *Science*, **304**, 838.

TUDHOPE, A. W. & SCOFFIN, T. P. 1987. A device to deposit tracer sediment evenly on the deep sea bed. *Journal of Sedimentary Petrology*, **57**, 761–762.

UDA, T., NAITO, K. & KANDA, Y. 1991. Field experiment on sand bypass of the Iioka Coast. *Coastal Engineering in Japan*, **34**, 205–220.

VAN DER POST, K. D., OLDFIELD, F. & VOULGARIS, G. 1995. Magnetic tracing of beach sand: preliminary results. Coastal Dynamics '94, Proceedings of International Conference, 323–334.

VAN LEUSSEN, W. Undated. *Investigations with the fluorescent silt tracer Dayglo*. Delft Hydraulics Laboratory, Report WL-WGSL-84-17 [in Dutch].

VAN RIJN, L.1993. *Principles of sediment transport in rivers, estuaries and coastal seas*. Aqua Publications, Amsterdam.

VAN RIJN, L. C., Davies, A. G., VAN DE GRAAFF J. & RIBBERINK, J. S. (eds.) 2001. *SEDMOC : Sediment Transport Modelling in Marine Coastal Environments*. Aqua Publications, Amsterdam.

VENTURA, E. NEARING, M. & NORTON, L. D. 2001. Developing a magnetic tracer to study erosion. *Catena*, **43**, 277–291.

VERNON, J. 1963. *Fluorescent sand tracer tests, Zuniga Shoal, San Diego, California*. Deptartment Geology, Univ Sorithem California, unpublished.

VILA-CONCEJO, A., FERREIRA, O., CIAVOLA, P., TABORDA, R., DIAS, J. M. A. 2003. Quantitative and qualitative analyses of sediment transport paths: straight beaches, inlets and harbours. *In*: *Proceedings of the International Conference on Coastal Sediments 2003*. CD-ROM Published by World Scientific Publishing Corp.

VILA-CONCEJO, A., FERREIRA, O., CIAVOLA, P., MATIAS, A. & DIAS, J. M. A. 2004. Tracer studies on the updrift margin of a complex inlet system. *Marine Geology*, **208**, 43–72.

WATERS, C. B. 1986. *Thermoluminescent tracer: further evaluations. Dredge Spoil and Heavy Metals in Tidal Waters*. Hydraulics Research Wallingford, Publication SR91, Appendix B.

WEBSTER, R. 1999. Sampling, estimating and understanding soil pollution. *In*: GOMEZ-HERNÁNDEZ, J., SOARES, A., FROIDEVAUX, R. (eds.) *GeoEnv. II 98 — Geostatistics for Environmental Applications. Quantitative Geology and Geostatistics*. Kluwer Academic Publishers, Dordrecht, 25–37.

WEBSTER, R. & OLIVER, M. A. 1993. How large a sample is needed to estimate the regional variogram adequately? *In*: SOARES, A. (ed.) *Geostatistics Troia '92*, Kluwer Academic Publications, Dordrecht, 155–166.

WEST, P. J. 1949. *Transportation of cubical bricks in a cobble beach environment*. Department Geology University Society Califorlin Rept. unpublished.

WHITE, T. E. 1987. *Nearshore sand transport*. PhD dissertation, University of California, San Diego.

WHITE, T. E. 1998. Status of measurement techniques for coastal sediment transport. *Coastal Engineering*, **35**, 17–45.

WHITE, T. E. & INMAN, D. L. 1989. Application of tracer theory to NSTS experiments. *In*: SEYMOUR R.J. (ed.) *Nearshore Sediment Transport*, Plenum NY, 115–128.

WHITEHOUSE, R., SOULSBY, R., ROBERTS, W. & MITCHENER, H. 2000. *Dynamics of estuarine muds*. Telford Publishing Ltd., London.

WILLIAMS, J. J., ROSE, C. P. *et al.* 1999. Interactions between currents, waves and sediments in calm and storm conditions. Continental Shelf Research, **19**(4): 507–536.

WONG, P., KRAUS, N. & DAVIS, R. A. 1998. Total longshore sediment transport rates in the surf zone: field measurements and empirical predictions. *Journal of Coastal Research*, **14**, 269–282.

YASSO, W. E. 1966. Formulation and use of fluorescent tracer coatings in sediment transport studies. *Sedimentology*, **6**, 287–301.

ZENKOVITCH, V. P. 1960. Fluorescent substances as tracers for studying the movement of sand on the seabed; experiments conducted in the USSR. *Dock Harbour Authority*, **40**, 280–283.

ZENKOVITCH, V. P. 1962. Application of luminescent substances for sand drift investigations in the nearshore zone of the sea. *Ingeniuer (Utrecht)* **30**, 3.

ZHANG, X. C., FRIEDRICH, J. M., NEARING, M. A. & NORTON, L. D. 2001. Potential use of Rare Earth oxides as tracers for soil erosion. *Soil Science Society of America Journal*, **65**, 1508–1515.

Shoreface morphodynamics along the Holland Coast

C. L. HINTON[1] & R. J. NICHOLLS[2]

[1]*ABP Marine and Environmental Research Ltd, Pathfinder House, Maritime Way, Southampton, SO14 3AE, UK (email:chinton@abpmer.co.uk)*

[2]*School of Civil Engineering and the Environment and CCPEM, University of Southampton, Southampton SO17 1BJ, UK*

Abstract: The morphodynamic behaviour of the shoreface of the Holland coast has been investigated over the medium- and large-scales (years to decades). This is a wave-dominated, uniform coastline backed by dunes and uninterrupted by tidal inlets. The work takes a data-orientated approach using the 'long' profiles in a data set extending over 32 years and covering 81 km of coast. These profiles are spaced every 1 km alongshore and extend to a maximum offshore distance of 3 km (approximately 16 m water depth).

Previous work based upon cross-shore profiles suggests that there is a seaward limit to significant depth change, or activity, on the upper shoreface over the small- and medium-scales (termed 'depth of closure'). Examination of the data set shows that the middle and lower shoreface is also morphologically active in many instances, with the activity increasing with timescale. Many profiles exhibit closure on the upper shoreface, and then reopen on the middle/lower shoreface, exhibiting morphological activity. This deeper shoreface morphodynamics appears to be related to onshore supply of sand to the active zone. Hence, the analysis shows that the upper, middle and lower shoreface are coupled, as widely assumed, and has widespread significance for understanding long-term coastal evolution.

The coastal system is highly dynamic at a range of time and space scales, which can have potentially significant impacts upon both the ecological and human environments. As these dynamics are often poorly understood, especially at the longer timescales where detailed process knowledge is least developed, a systems perspective approach is often taken which considers integrated coastal behaviour, rather than focussing upon detailed processes.

In this approach, the coast is divided into several sub-systems, or compartments (e.g. Ruessink 1998), each of which has a distinct temporal and spatial scale (e.g. the shoreface, tidal inlets, beach, active zone). This is illustrated in the ASMITA (Aggregated Scale Morphological Interaction between a Tidal basin and the Adjacent coast) model of a tidal inlet and basin which consists of three interacting compartments; the tidal basin; ebb-tidal delta; and adjacent coast (Goor *et al.* 2003). Changes occur within these compartments at a wide range of scales, from individual grain motions through to development on the geological scale. Within each compartment, a morphodynamic system exists composed of the sub-systems of hydrodynamics, morphology and sediment transport. The coastal morphodynamic system involves feedback between these three main sub-systems. Indeed the temporal and spatial interaction of coastal compartments and the associated sub-systems has been investigated with the formalisation of the Coastal Tract Cascade concept, which discriminates between cause and effect on the basis of scale (Cowell *et al.* 2003*a*, *b*). It formalizes the concepts for separating coastal processes and behaviour into a hierarchy on the basis of scale distinguishing between those which are important for the modelling of coastal change and those which can be disregarded at that particular scale (i.e. representing 'noise').

The morphological unit between the beach and shelf represents the 'transition zone', or 'buffer zone' between the land and sea as here shoaling waves have a significant direct impact upon the sea floor. This unit is most commonly referred to as the shoreface (e.g. Vincent *et al.* 1983; Wright *et al.* 1985; Stive *et al.* 1990; van Rijn 1995; Walstra *et al.* 1998). Other terms are (i) the inner shelf (e.g. Wright 1995) and (ii) the offshore (e.g. Komar 1998). The shoreface makes an important long-term contribution to the coastal sediment budget as it will be acting as either a sink or source of sediment from/to the active zone. Hence, the shoreface can potentially act as an important control upon long-term shoreline movement. However, long-term shoreface behaviour remains poorly understood.

From: BALSON, P. S. & COLLINS, M. B. 2007. *Coastal and Shelf Sediment Transport*. Geological Society of London, Special Publications, **274**, 93–101. 0305-8719/07/$15.00

It is important that the response of the coastal region to different forcings can be anticipated over all relevant scales; 'in addition to being fundamental to understanding the morphodynamics of beaches, the spatial and temporal behaviour of the beach profile has direct application in coastal engineering projects involving beach nourishment and the siting of coastal structures' (Larson & Kraus 1994). For coastal management and engineering, relevant scales include sediment transport processes and individual storms, but they also include more aggregated long-term coastal behaviour over many decades or longer, due to the increasing pressures placed upon the coastal environment. An example of a long-term pressure is human-induced climate change that is expected to cause an acceleration in sea-level rise during the twenty first Century (Houghton *et al.* 2001). At present there is quite limited information available of coastal behaviour over the medium- and large-scale (1 km and years; 10 km and decades, respectively; Stive *et al.* 1990; see also Stive *et al.* 2002). This is primarily the result of:

(a) a lack of good–quality, long-term data sets which are required not only (i) to allow the observation of coastal behaviour, but also (ii) to validate and calibrate models which attempt to reproduce and predict this behaviour;
(b) limited understanding of the coastal system dynamics due to (i) the inherent non-linearity of the system dynamics; (ii) different interactions between forcings (i.e. hydrodynamics) through time and space; and (iii) the relative importance of these interactions through time and space.

It has proven hard to upscale process knowledge, as observed from short-term field experiments, to change on a longer timescale (cf. De Vriend 1993), resulting in a large knowledge gap. This problem has been investigated in some detail over the past 15 years: an example of a recent research project is the EU MAST-III PACE (Prediction of Aggregated-scale Coastal Evolution) project (De Vriend 1997, 1998).

This paper takes the 'long' profiles of an extensive data set along the Holland coast to investigate the spatial and temporal evolution of shoreface morphodynamic behaviour to approximately 16 m depth. The extensive temporal (>30 years) and spatial coverage (>80 km) of this data set means that it qualifies as the only dataset of its type in the world. Earlier analyses of more limited data from the Holland coast showed evidence of lower and middle shoreface dynamics (Stive *et al.* 1990; Stive & de Vriend 1995), which is causing concern about its future management (de Ruig 1998). This paper assesses these earlier observations and the general validity of present assumptions on shoreface behaviour. Hence, it extends many existing studies of upper shoreface behaviour (e.g. Larson & Kraus 1994; Nicholls *et al.* 1998*a*). There is also particular emphasis on generalizing the depth of closure concept to middle and lower shoreface activity and inactivity. It presents (i) details of the unique data set used; (ii) the methodology employed to determine the shoreface morphodynamic behaviour over the medium- and large-scales; and (iii) findings of this study. Conclusions are drawn regarding (i) the different timescales of shoreface behaviour; (ii) the validity of assumptions adopted in many medium- and long-term modelling tasks; and (iii) details of shoreface morphodynamic behaviour for application to generic shoreface studies.

Study area

The study area was the 'closed' Holland coast in the southern part of the North Sea, (Fig. 1). It is bound in the north by the Marsdiep tidal inlet, which has considerable influence on coastal behaviour due to the presence of a large ebb tidal shoal, from the inlet to, approximately, 12 km south (as observed from bathymetric profiles). In the south, the Rotterdam Waterway acts as a boundary between the 'closed' coast and Delta Region; the Waterway causes the deposition of sediment directly to the north in the dune, breaker and active zones due its interruption to longshore drift (De Ruig & Louisse 1991; Van Rijn 1995). The Holland coast is presently prograding in the centre and retreating in the north and south. The progradation is interpreted to be the result of onshore sediment exchange from the shelf and shoreface to the surf zone (Wiersma & van Alphen 1988; Stive & de Vriend 1987; Stive 1989; Stive *et al.* 1990). Retreat in the north is due to sediment loss through the Marsdiep Inlet to the Wadden Sea and in the south due to net northward longshore losses enhanced by the Rotterdam Waterway (Dijkman *et al.* 1990; Stive *et al.*1990; Van Rijn 1995).

To avoid the influence of tidal inlets, the precise boundaries of the study area were the shoreface between Callantsoog (km 16) and Schevingen (km 97), comprising 81 km of shoreline length (Fig. 1). This represents a wave-dominated, uniform coastline; backed by dunes and uninterrupted by tidal inlets. Major morphologic characteristics of the study area are: (i) continuous oblique multiple bars located in the

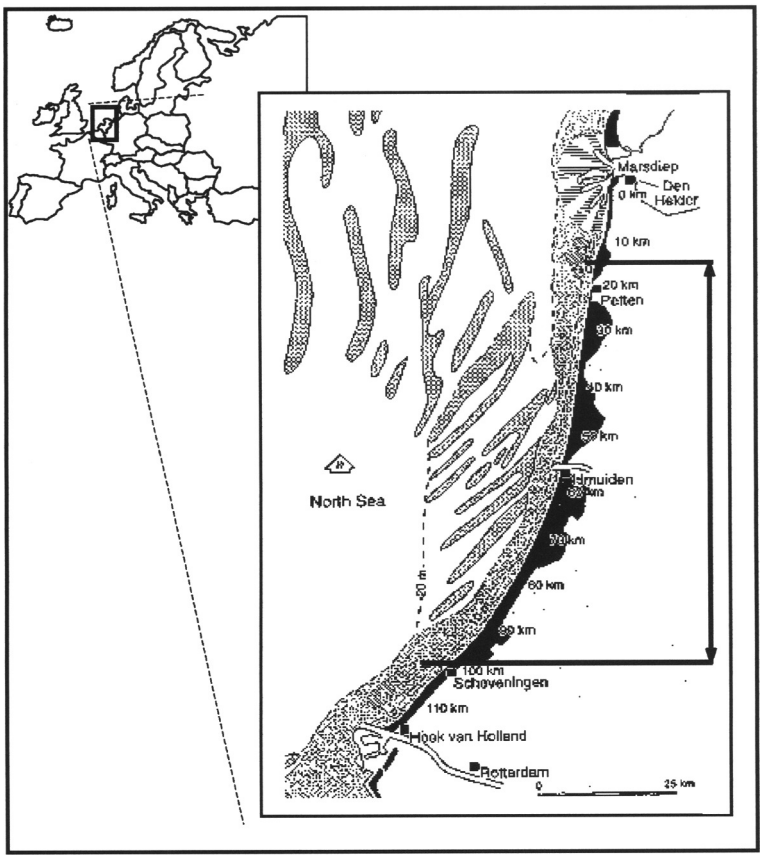

Fig. 1. The study area and the Holland shoreface (adapted from Wijnberg 1995).

active zone subject to frequent wave breaking, (ii) to seaward a shoreface with declining slope, and (iii) shoreface-connected ridges between km 35 and 65. Important anthropogenic features are the Hondsbossche and Pettermer seawall (km 20–26) and the IJmuiden harbour moles (km 55/56), in addition to relatively minor beach nourishments, although in the future this will be an increasingly important control on coastal evolution (de Ruig 1998).

Data set

One of the largest coastal morphological data sets in the world exists for the low-lying, densely populated Netherlands coast where data has been collected since 1963. This extensive data set is called JARKUS, an acronym for annual soundings (in Dutch 'JAaRlijkse KUStlodingen'; Ruessink 1998) and its extensive temporal and spatial coverage mean that it is the only dataset of its type in the world. The JARKUS data set comprises 'short' and 'long' profiles which extend to about 8 m (0.8 km offshore) and 16 m (3 km offshore) depths, respectively. Here the 'long' profiles collected from 1963 to 1995 are considered. Each 'long' cross-shore profile:

(a) is spaced 1 km in the longshore; the longshore spacing of the cross-shore profiles is marked by a permanent base of beach poles known as the RSP ('Rijks Strand Palen lijn') reference line. The poles are numbered relative to their distance from Den Helder (Fig. 1) and within this study each profile is labelled according to this distance. For example km 81 represents the profile located 81 km south of Den Helder at Noordwijk aan Zee;
(b) has a temporal resolution of 3 to 5 years;
(c) extends offshore to a distance of 3 km (approximately 16 m water depth);
(d) has a documented measurement accuracy of 0.25 m. This has been derived from both

analysis of the JARKUS data set (Hinton 2000) and the stochastic and systematic errors which arise from measurement techniques.

The cross-shore bathymetric profiles are typically surveyed (relative to NAP, Normal Amsterdams Peil which is approximately equal to Mean Sea Level) in the spring and summer months. As the morphodynamic behaviour investigated occurs over temporal periods greater than seasonal changes, seasonal bias is not considered to be important. In addition, preliminary investigations showed that where the profiles are active on the lower and middle shoreface, they generally undergo slow steady declines in elevation suggesting that there is limited seasonal variability.

Methodology

Two methods were selected to identify, shoreface behaviour and performed for all available profiles over a range of temporal periods: 5, 10, 15, 20, 25, 28 and 32 years between 1965 and 1997. Both methods were originally used to identify 'depth of closure'; which is 'the seaward limit of significant depth change but not the absolute limit to cross-shore sediment transport' (Nicholls *et al.* 1996). Significant depth change is a relative concept, which is dependant upon the criterion selected to identify the depth change. However these methods are easily adapted to identify shoreface morphodynamic in/activity. The use of two methods allowed the consistency of the results to be considered.

(1) *Standard deviation of elevation.* The standard deviation of elevation, or sde, method is a simple method particularly effective in dealing both with large data sets and removing bias from outlying values. The effectiveness of the method increases as the number of profiles increase, reducing the error influence. The sde method is implemented by calculating the 'variation in the standard deviation of elevation . . . as a function of the cross-shore distance for x number of profiles from the same alongshore location' (Kraus & Harikai 1983). Once the sde values were calculated, it then remained for the locations of 'activity' and 'inactivity' to be identified. This was performed by applying a 'fixed standard deviation value'. Inactivity is identified when the standard deviation falls below a fixed value; in the example given a value of 0.25 m is used, which represents a 66% confidence that a real change in the bathymetry has occurred. This takes the assumption that the data measurement errors are normally distributed with a standard deviation of 0.25 m. Two additional values have been used. 0.5 m and 0.75 m, which respectively represent a 95% and 99% confidence that a real bathymetric change has occurred. It is important that more than one criterion is used as it will ensure that a real bathymetric change is observed. It should be noted that the larger the criteria the more inactive the profile is as a larger degree of change is required in order to be active. However, the general pattern of results is mimicked with the different criteria. The 0.75 m cases were not investigated further after preliminary analysis showed that in the majority of cases, even the active nearshore bar system would be considered inactive using this value.

(2) *Fixed depth change.* The depth change between two profiles measured at the same location, but in different years, was calculated. When the change was more than, or equal to, the selected criterion then the shoreface was classified to be exhibiting morphodynamically active behaviour. The change criterion chosen matched those of the sde method, so representing a 66%, 95% and 99% confidence that a real bathymetric change has occurred.

The observed variation in standard deviation in the nearshore zone landward of 8 m depth typically relate to bar morphodynamics on the upper shoreface, whilst those changes observed further offshore equate to middle and lower shoreface morphodynamics.

Results and discussion

Previous work based upon cross-shore profiles (e.g. Nicholls *et al.* 1996, 1998*a*; Garcia *et al.* 1998) suggests that there is a seaward limit to significant depth change, or activity, on the upper shoreface over the small- and medium-scales (up to several years). This limit has been widely termed as the 'depth of closure' (D_c). Whilst the limit moved seaward as timescale increases, the effect was not dramatic. As most of the datasets considered only covered the upper shoreface, this precluded detailed observation of this process. Examination of the more extensive JARKUS data set clearly shows that in many instances the middle and lower shoreface also shows significant depth changes, especially over the medium- and long-term, and these changes progressively increase with timescale (Hinton

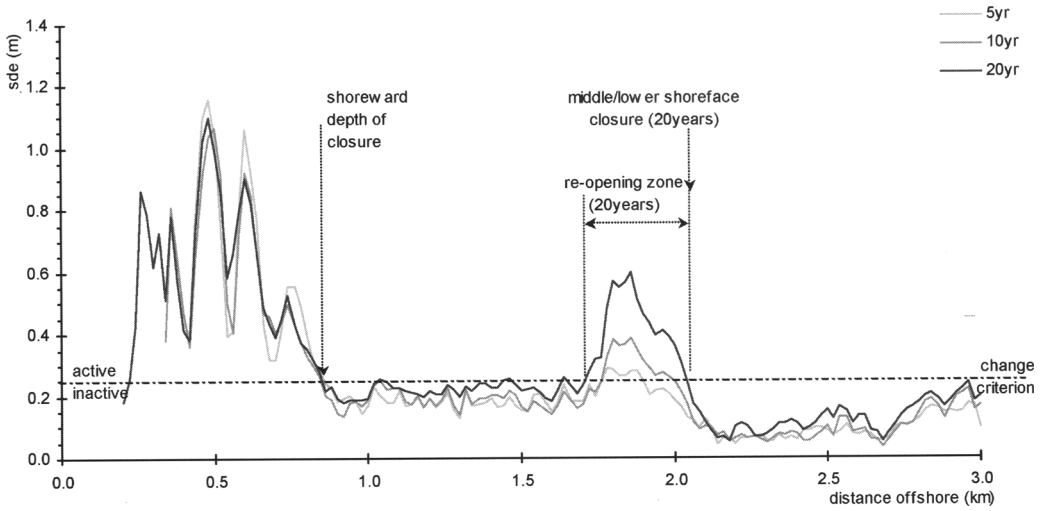

Fig. 2. Cross-shore phenomena identified in the analysis of bathymetric profiles along the Holland Coast. Shown using actual examples of profiles and the sde method.

et al. 1999; Hinton 2000). A common observation is that the profile becomes inactive at some distance x from the shore on the upper shoreface, but then becomes active again further seaward, and usually exhibiting a return to inactivity towards its seaward boundary (Fig. 2). These phenomena are hereafter termed as:

(a) the *shoreward closure* (D_{cs}). The limit to significant depth change, but not the absolute limit to cross-shore sediment transport, as located on the upper shoreface (in water depths of 8 m or less);
(b) the *re-opening point* (R_o) and associated *re-opening zone*; the shoreward point of significant depth changes which occur on the middle/lower shoreface is termed the 're-opening point'. The cross-shore zone in which significant depth changes are observed is termed the re-opening zone; and
(c) the *middle/lower shoreface closure* ($D_{cm/l}$). The seaward limit to the re-opening zone, observed within the 16 m depth data limits.

The identification of the 're-opening zone' allowed the further classification of four types of middle and lower shoreface behaviour that are observed (Fig. 3):

(a) an *inactive shoreface*. No morphodynamic activity is observed seaward of the upper shoreface and the profile only exhibits D_{cs};
(b) a *shoreward partially-active shoreface*. The shoreface is active until the middle/lower shoreface where it closes, exhibiting $D_{cm/l}$;
(c) a *seaward partially-active shoreface*. The shoreface exhibits re-opening i.e. the profile closes on the upper shoreface at D_{cs} and then reopens on the middle and lower shoreface and may exhibit a deeper closure towards the seaward limit of the profile;
(d) a *fully-active shoreface*. Morphodynamic activity occurs across the entire shoreface i.e. the profile does not exhibit any closure within the measured profile.

The shoreward closure appears to define two distinct zones in terms of process. Landward of D_{cs}, the profile fluctuates up and down due to bar migration, while seaward of D_{cs}, generally the profile slowly drops where it is active and there appears to be a net onshore flux of sand (see also Stive *et al.* 1990),

The Holland coast can be divided into two main longshore provinces as a function of shoreface characteristics and temporal evolution of D_{cs}, R_o and $D_{cm/l}$. There is an obvious behavioural division at, approximately, km 55/57 as indicated in Fig. 4. Here the division is illustrated using the D_{cs} behaviour over all temporal periods. It can be observed that D_{cs} is both (1) deeper between km 16 to 55/57 (Noord-Holland) and (2) more variable than in Zuid-Holland (km 55/57 to 97). For example the mean D_{cs} of Noord-Holland is 2.6 m deeper than that of Zuid-Holland, for a 20 year period (Table 1). Interestingly, the wave climate in the two provinces are quite similar, and this factor does not appear to be controlling this different

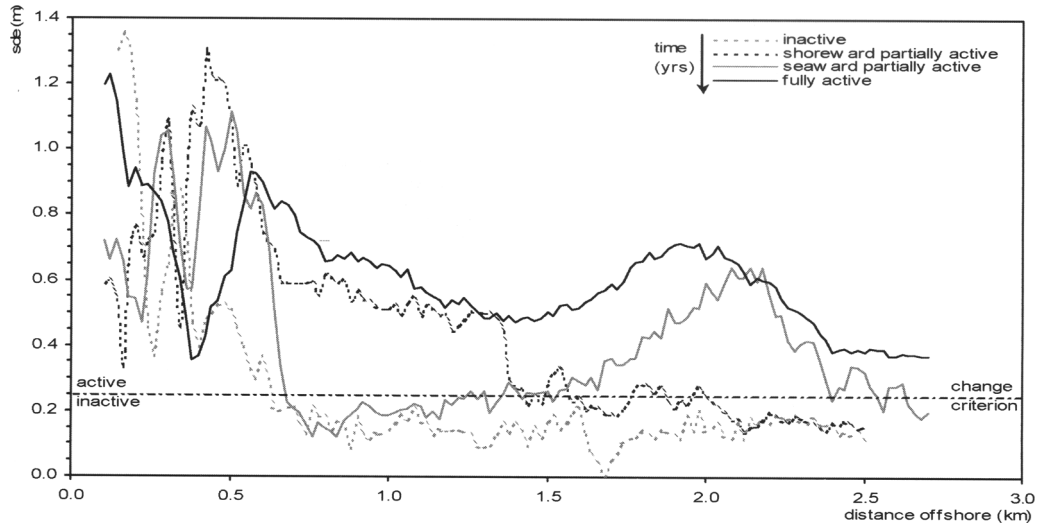

Fig. 3. Classifications of shoreface behaviour identified in the analysis of bathymetric profiles along the Holland Coast. Shown using actual examples of profiles and the sde method.

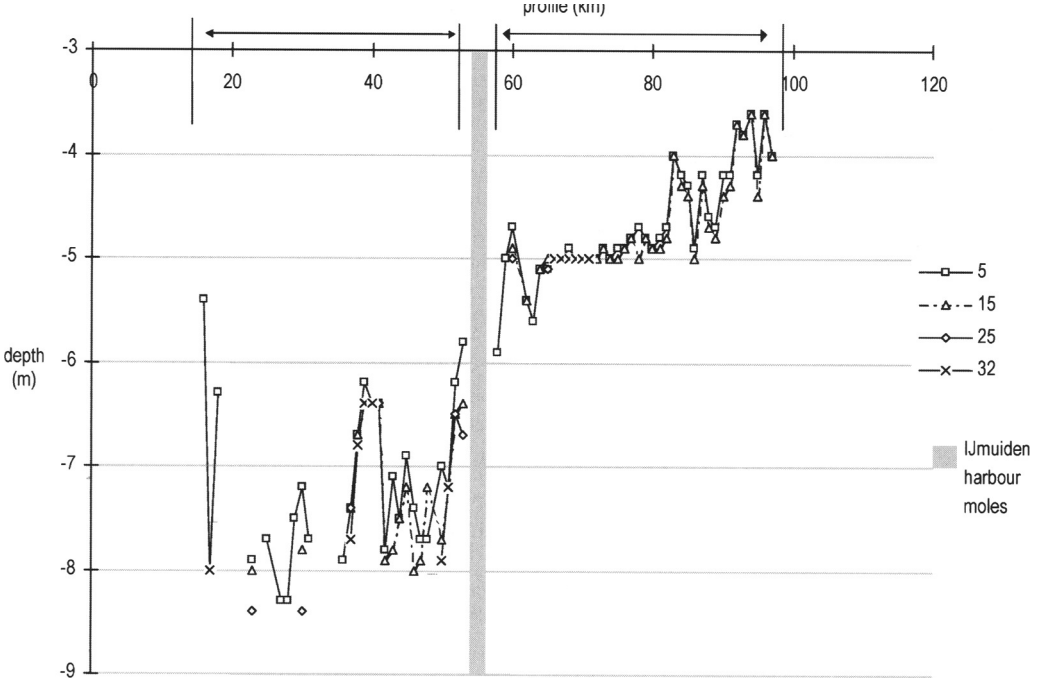

Fig. 4. Spatial variation of D_{cs} along the Holland coast over 5 to 32 year temporal periods.

behaviours. Rather, it is an abrupt change in bar dynamics, as observed by Wijnberg (1995).

It can also be observed that the frequency of occurrence of D_{cs} decreases as time interval increases (Table 2), due to the increasing occurrence of middle/lower shoreface activity. This suggests that ultimately, all the cross-shore profiles will become 'fully-active shorefaces' (see

Table 1. *Characteristics of D_{cs} over a 20 year temporal period within the two provinces*

Region name	Region extent	Mean depth (m)	Standard deviation (m)
Noord-Holland	km 16–54	7.3	0.8
Zuid-Holland	km 57–97	4.7	0.4

These values are observed using the sde method criterion of 0.25 m.

also Hinton 2000). This highlights the fact that the upper, middle and lower shoreface are coupled and should not be considered as independent units, especially over the medium- and long-term (decades and longer). This observation, unique due to its derivation from a high resolution, large-scale data set, reinforces conclusions reached by other authors (e.g. Wright *et al.* 1985; Stive & De Vriend 1995) that a fast response to forcing changes should be expected on the upper shoreface whilst a slower response should be expected on the lower shoreface. In the case of the Holland coast, this slower response comprises a source term for the shoreline.

These observations support the use of the *annual* shoreward closure as an important cross-shore boundary in short- and medium-term profile models (e.g. Stive & de Vriend 1995; Cowell *et al.* 2003*a*, *b*). It seems to separate a zone of cross-shore sand exchange (the zone where the classical equilibrium profile will apply), from a zone of onshore sand flux (where an equilibrium response is meaningless at the timescale considered in the JARKUS data). However, detailed prediction of the middle/lower shoreface evolution over the timescale of the observations is more problematic. This can be highlighted using the example of the Advection-Diffusion Model (ADM) (Niedoroda *et al.* 1995), which was used to simulate the evolution of D_c (as defined before this study revealed the presence of a re-opening zone) over time scales from 1 to 10 000 years for the Holland coast (Nicholls *et al.* 1998*b*). As the time period increases so D_c also increases, and after 10 000 years the cross-shore profile is active to the shelf. Indeed, after 100 years the ADM predicts closure to range between 12 and 20 m deep, the range being dependant upon the forcing conditions used. Whilst the model is consistent with the long-term trends implied in the data, it does not describe the observed shoreface evolution. Whilst D_{cs} along the Holland coast increases with time, the increase is quite slow and is best described with a logarithmic relationship with time (see also Nicholls *et al.* 1996). Rather it is the cross-shore growth of the reopening zone which produces fully-active profiles. So whilst the predicted geological- to long-term shoreface behaviour agrees with the observations made here, at smaller scales detailed behaviour differs. It appears that no existing shoreface model could reproduce the detailed empirical shoreface observations presented here.

This analysis of the JARKUS data set demonstrates the fact that the upper shoreface of Noord-Holland undergoes a greater degree of morphodynamic activity than Zuid-Holland, over the temporal periods investigated. Projection of this trend would suggest that the differing behaviour between the two provinces will continue until that point at which the morphodynamic activity within both reaches some point of maximum activity. However the continuation of this trend, as observed at present, is dependant upon numerous factors. For example variations in anthropogenic interference (i.e. coastal defence strategies) and natural processes (i.e. changing hydrodynamic conditions). Whilst this behaviour has wider implications than the Holland coast alone, application of these ideas to other coastlines with differing morphological and environmental characteristics needs to be undertaken with caution, and it should not be assumed to be universal.

The boundary at km 55/57 coincides with the location of the IJmuiden harbour moles which has been previously identified as the division between two nearshore bar systems with differing behaviour (Wijnberg 1995). As D_{cs} is largely controlled by bar migration processes a similar division based on this parameter is not surprising. However, this longshore division of

Table 2. *Percentage occurrence of D_{cs} between km 16 to 71 for each temporal period using all methods*

METHOD	0 yrs	5 yrs	10 yrs	15 yrs	20 yrs	25 yrs	28 yrs	32 yrs
sde 0.25 m	100	85	73	71	60	46	33	30
sde 0.5 m	100	96	98	98	96	98	93	93
fdc 0.25 m	100	100	76	52	96	72	16	12
fdc 0.5 m	100	100	96	96	100	96	68	35

the Holland coast is also supported by the morphodynamic behaviour of the middle and lower shoreface (Hinton *et al.* 1999). It is also worth noting that anthropogenic influences on shoreface behaviour are also apparent, especially due to the IJmuiden harbour moles (Hinton & Nicholls 2001).

The controls upon Dc_s are investigated further in Hinton (2000); controls analysed include sediment distribution and the shoreface-connected ridges found between km 35 and 65, however there does appear to be no correlation between these two phenomenon. These studies investigate the temporal and spatial variation in this upper shoreface phenomena drawing upon recently developed concepts, such as the Coastal Tract Cascade (Cowell *et al.* 2003*a*, *b*). Model studies of the different processes that might be controlling the observed shoreface changes are also required to link the behaviours to their underlying controls.

Conclusion

The analysis of the unique JARKUS data set, over varying temporal and spatial scales up to 32 years, has provided information relating to the evolution of shoreface morphodynamic behaviour for a wave-dominated, uninterrupted coastline characterised by a nearshore bar system. Over the medium- and large-scales, significant depth changes occur on the middle and lower shoreface, such that, in the more morphodynamically active regions of North Holland, over the longer temporal periods, the entire shoreface is active. Furthermore it has been shown that, as the temporal period increases, then the cross-shore profile evolves from exhibiting no / little activity to activity over its entirety (0 to 16 m water depth). This observation supports existing assumptions that the upper, middle and lower shoreface are coupled (e.g. Wright *et al.* 1985), that this effect increases with timescale and the more recent developments with regard to coastal modelling approaches based on scale (e.g. Cowell *et al.* 2003*a*).

The observations made here have significant implications for morphodynamic modelling efforts, including those which incorporate a fixed nearshore zone for sediment budgets. Present assumptions adopted in many medium- and long-term models may need to be re-addressed as important elements in the coastal sediment budget may have been ignored. Whatever their controls, the observed shoreface behaviour has important implications for the future evolution of the Holland coast, including its management (e.g. de Ruig 1998).

This research shows that the shoreface could be potentially be active anywhere, and this activity will increase with timescale. However, the rate at which this occurs will ultimately be dependant upon the morphological constitution of the shoreface in question, forces (both natural and anthropogenic) which act upon the different scales and their associated variation through time (i.e. changes in the rates of sea-level rise). This needs to be investigated systematically, including long-term measurements of the shoreface at other sites around the world.

This research was funded by the PACE (Prediction of Aggregated-scale Coastal Evolution) project which itself is part of the EU-sponsored MAST-III programme under contract number MAS3-CT95-002. The authors would like to thank all those that contributed ideas throughout the PACE project, in particular M. Stive (Delft University of Technology, previously of WL/Delft Hydraulics), H. Vriend (WL/Delft Hydraulics, previously of Twente University) and D. Dunsbergen (Dutch National Institute for Marine and Coastal Management/ Rijkswaterstaat).

References

COWELL, P. J., STIVE, M. J. F., NIEDORODA, A. W., DE VRIEND, H. J., SWIFT, D. J. P. KAMINSKY, G. M. & CAPOBIANCO, M. 2003*a*. The Coastal-Tract (Part 1): A conceptual approach to aggregated modelling of low-order coastal change. *Journal of Coastal Research*, **19**, 812–827.

COWELL, P., STIVE, M. J. F. *et al.* 2003*b*. The Coastal-Tract (Part 2): Applications of aggregated modeling to lower-order coastal change. *Journal of Coastal Research*, **19**, 828–848.

DE RUIG, J. H. M. 1998. Coastline management in the Netherlands: human use versus natural dynamics. *Journal of Coastal Conservation*, **4**, 127–134.

DE RUIG, J. H. M. & LOUISSE, C. J. 1991. Sand budget trends and changes along the Holland coast. *Journal of Coastal Research*, **7**, 1013–1026.

DE VRIEND, H. J. 1997*a*. Prediction of Aggregated-scale Coastal Evolution (PACE). *In: Proceedings of Coastal Dynamics*. ASCE New York, 644–653.

DE VRIEND, H. J. 1998*b*. *State of the art in process-orientated MTM-modelling*. EC/MAST Advanced Study Course, Renesse 1998.

DE VRIEND, H. J., CAPOBIANCO, M., CHESNER, T., DE SWART, H. E., LATTEUX, B. & STIVE, M. J. F. 1993. Approaches to long-term modelling of coastal morphology: a review. *Coastal Engineering*, **21**, 225–269.

DIJKMAN, M. J., BAKKER, W. T. & DE VROEG, J. H., 1990. Prediction of coastal evolution for the Holland coast. *In: Proceedings of 22nd Coastal Engineering Conference*. ASCE, New York, 1935–1947.

GOOR, M. A. VAN, ZITMAN, T. J., WANG, Z. B. & STIVE, M. J. F. 2003. Impact of sea level rise on the morphological equilibrium state of tidal inlets. *Marine Geology*, **202**, 211–227.

GRACIA, V., JIMENEZ, J. A., SANCHEZ-ARCILLA, A., GUILLEN, J. & PALANQUES, A. 1998. Short-term relatively deep sedimentation on the Ebro Delta coast. Opening the closure depth. *In: Proceeding of the 26th International Conference of Coastal Engineering, Copenhagen*. ASCE, New York, 2902–2912.

HINTON, C. L. 2000. *Decadal morphodynamic behaviour of the Holland shoreface*. PhD Thesis, Middlesex University.

HINTON, C. & NICHOLLS, R. J. 2001. Large-scale shoreface response to a prominent anthropogenic structure: A case study of the IJmuiden Harbour moles, *In: Holland. Proceedings of the Fourth Conference on Coastal Dynamics, June 11–15, Lund Sweden*. ASCE, New York, 798–807.

HINTON, C., NICHOLLS, R. J. & DUNSBERGEN, D. W. 1999. Profile re-opening on the shoreface of the Holland coast. *In: Proceedings of Coastal Sediments 1999*. ASCE, New York, 535–550.

HOUGHTON, J. T., DING, Y., GRIGGS, D. J., NOGUER, M., VAN DER LINDEN, P. J. & XIAOSU, D. (edn) 2001. *Climate Change 2001. The Scientific Basis*. Cambridge University Press, Cambridge.

KOMAR, P. D. 1998. *Beach processes and sedimentation* (2nd editor). Prentice-Hall, Englewood Cliffs, New Jersey.

KRAUS, N. C. & HARIKAI, S. 1983. Numerical model of shoreline change at Orai beach. *Coastal Engineering*, **7**, 1–28.

LARSON, M. & KRAUS, N. C. 1994. Temporal and spatial scales of beach profile change, Duck, N.Carolina. *Marine Geology*, 117, 75–94.

NICHOLLS, R. J., BIRKEMEIER, W. A. & HALLERMEIER, R. J. 1996. Application of the depth of closure concept. *In: Proceedings of the 25th International Conference of Coastal Engineering, Orlando (USA)*. ASCE, New York, 3874–3887.

NICHOLLS, R. J., BIRKEMEIER, W. A. & LEE, G. 1998*a*. Evaluation of depth of closure using data from Duck, NC, USA. *Marine Geology*, **148**, 179–201.

NICHOLLS, R. J., MARSH, S. & HINTON, C. 1998*b*. Analysis of depth of closure and morphological behaviour on natural and forced coasts. *In*: PACE 2-yearly scientific report, Abstract 1.3#5.

NIEDORODA, A. W., REED, C. W., SWIFT, D. J. P., ARATO, H. & HOYANAGI, K. 1995. Modelling shore-normal large-scale coastal evolution. *Marine Geology*, **126**, 181–199.

RUESSINK, B. G. 1998. *Infragravity waves in a dissipative multiple bar system*. PhD Thesis, Utrecht University.

STIVE, M. J. F. 1989. *Voorspelling ontwikkeling kustlijn 1990–2090*. Kustverdediging na 1990, Technisch Rapport 5, Rijkswaterstaat, Den Haag.

STIVE, M. J. F. & De Vriend, H. J. 1995. Modelling shoreface profile evolution. *Marine Geology*, **126**, 235–248.

STIVE, M. J. F. & DE VRIEND, H. J. 1987. Quasi-3D current modelling: wave-induced secondary current. *In: ASCE Speciality Conference 'Coastal Hydrodynamics'*, New York, 356–370.

STIVE, M. J. F. AARNINKOFF, S. J. C., HAMM, L., HANSON, H, LARSON, M., WIJNBERG, K., NICHOLLS, R. J. & CAPOBIANCO, M. 2002. Variability of shore and shoreline evolution. *Coastal Engineering*, **47**, 211–235.

STIVE, M. J. F., ROELVINK, J. A. & DE VRIEND, H. J. 1990. Large-scale coastal evolution concept. *In: Proceedings of the 22nd Coastal Engineering Conference*. ASCE, New York, 1962–1974.

VAN RIJN, L. C. 1995. *Sand budget and coastline changes of the central Dutch coast between Den Helder and Hoek van Holland*. Report H2129, Delft Hydraulics, The Netherlands.

VINCENT, C. E., YOUNG, R. A. & SWIFT, D. J. P. 1983. Sediment transport on the Long Island shoreface, North American Atlantic Shelf : role of waves and currents in shoreface maintenance. *Continental Shelf Research*, **2**, 163–181.

WALSTRA, D. J. R., VAN RIJN, L. C. & AARNINKHOF, S. G. J. 1998. *Sand transport at the middle and lower shoreface of the Dutch coast*. Report no. Z2378. Delft Hydraulics, The Netherlands.

WIERSMA, J. & VAN ALPHEN, J. S. L. J. 1988. The morphology of the Dutch shoreface between Hook of Holland and Den Helder (The Netherlands). *In*: DE BOER, P. L., *et al.* (eds) *Tide-influenced sedimentary environments and facies*. D. Reider Publishing, the Netherland, 101–111.

WIJNBERG, K. M. 1995. *Morphologic behaviour of a barred coast over a period of decades*. PhD Thesis, Utrecht University, The Netherlands.

WRIGHT, L. D. 1995. *Morphodynamics of inner continental shelves*. CRC Press Inc.

WRIGHT, L. D. MAY, S. K., SHORT, A. D. & GREEN, M. O. 1985. Beach and surf zone equilibria and response times. *In: Proceedings of the 19th International Conference of Coastal Engineering*. ASCE, New York. 2150–2164.

Mesoscale changes in present-day nearshore surface sediments and bedforms off the north coast of Ireland

J. LYN MCDOWELL[1], JASPER KNIGHT[2] & RORY QUINN[1]

[1]*Coastal Research Group, School of Environmental Sciences, University of Ulster, Coleraine, Co. Londonderry, Northern Ireland BT52 1SA, UK*

[2]*Department of Geography, University of Exeter, Tremough Campus, Penryn, Cornwall TR10 9EZ, UK (j.knight@exeter.ac.uk)*

Abstract: The distribution and spatial patterns of surficial nearshore sediments off the north coast of Ireland were mapped in detail using three repeated (over one year total duration) dual-frequency (100–500 kHz) side-scan sonar surveys which were ground-truthed using a bucket-grab sediment sampler. In the study area (40 km^2, <30 m water depth), three acoustic facies were identified (interpreted as sand, gravel, and bedrock). Planar sand with small sand waves dominates most of the study area; bedforms developed on sand and gravel substrates are located around the margins of a bedrock-floored bathymetric trench. Unusual sea-going gravel 'ribbons', which morphologically resemble rip current chutes, feed into the trench. Temporal changes in substrate and bedform patterns, mapped from the side-scan sonar data, suggest bedform development and facies boundary migration (by >100 m distance) over the winter season followed by sediment migration back again during the summer. Generally, substrate and bedform mobility is likely to be related to changes in the relative strengths of waves and tides along this exposed, mesotidal coast. More specifically, tidal asymmetry and the formation of a headland leeside eddy can account for scouring of the trench, trench-flank bedform patterns developed in sand, and the formation of the gravel ribbons.

The evolution and sediment dynamics of paraglacial shelves and coasts are dependent on a range of geological factors on different scales (FitzGerald & Rosen 1987; Carter 1990), most importantly the erosional and depositional effects of glaciation from adjacent landmasses, which generated large amounts of unconsolidated surficial sediment (Bridgland 2002; Taylor *et al.* 2002), and the role of postglacial changes in relative sea-level (RSL) in sediment redistribution (Shaw *et al.* 1993; Bridgland 2002).

A longstanding assumption in investigations of surface sediments on the NW European shelf is that they are relatively inactive geomorphically at the present time compared to the recent geological past, and that present-day sediment movement is forced by shelf-wide oceanographic events (e.g. Collins & Banner 1980; Anthony 2002). As a result, a veneer (<30 m thick) of mobile surface sediment covers relict signatures of much larger land-sea changes of the late Pleistocene and early Holocene (Bartek & Wellner 1995).

This paper aims to evaluate this assumption by describing preliminary side-scan sonar investigations of submarine sediments and bedforms from part of the inner shelf of the north coast of Ireland, and to discuss patterns of and controls on present-day sediment dynamics. This study forms part of a wider project looking at late Pleistocene to present-day shelf evolution in the region, linking climate, RSL changes and sediment supply (McDowell *et al.* 2005).

Location and geological setting of the study area

The continental shelf located between the north of Ireland and SW Scotland is known as the Malin Sea, an arm of the North Atlantic Ocean (Fig. 1). During the late Devensian glaciation (*c.* 22–13 ka BP) the Malin Sea region was influenced by ice sourced from both western Scotland and north-central Ireland which deposited a range of glaciomarine to marine diamictons and muds (Jura Formation) (Binns *et al.* 1974; Fyfe *et al.* 1993). These sediments are overlain by a variable thickness of late Holocene marine sands and gravels. Bedrock pinnacles through the sediment cover are common. Inshore water depths are up to 80 m; isolated and enclosed bathymetric lows of up to 200 m water depth are also present such as north of Rathlin Island (Fig. 1). At Portrush, 5 km east of the study area, tides are semidiurnal (M_2) and mesotidal in range

From: BALSON, P. S. & COLLINS, M. B. 2007. *Coastal and Shelf Sediment Transport*. Geological Society of London, Special Publications, **274**, 103–116. 0305-8719/07/$15.00

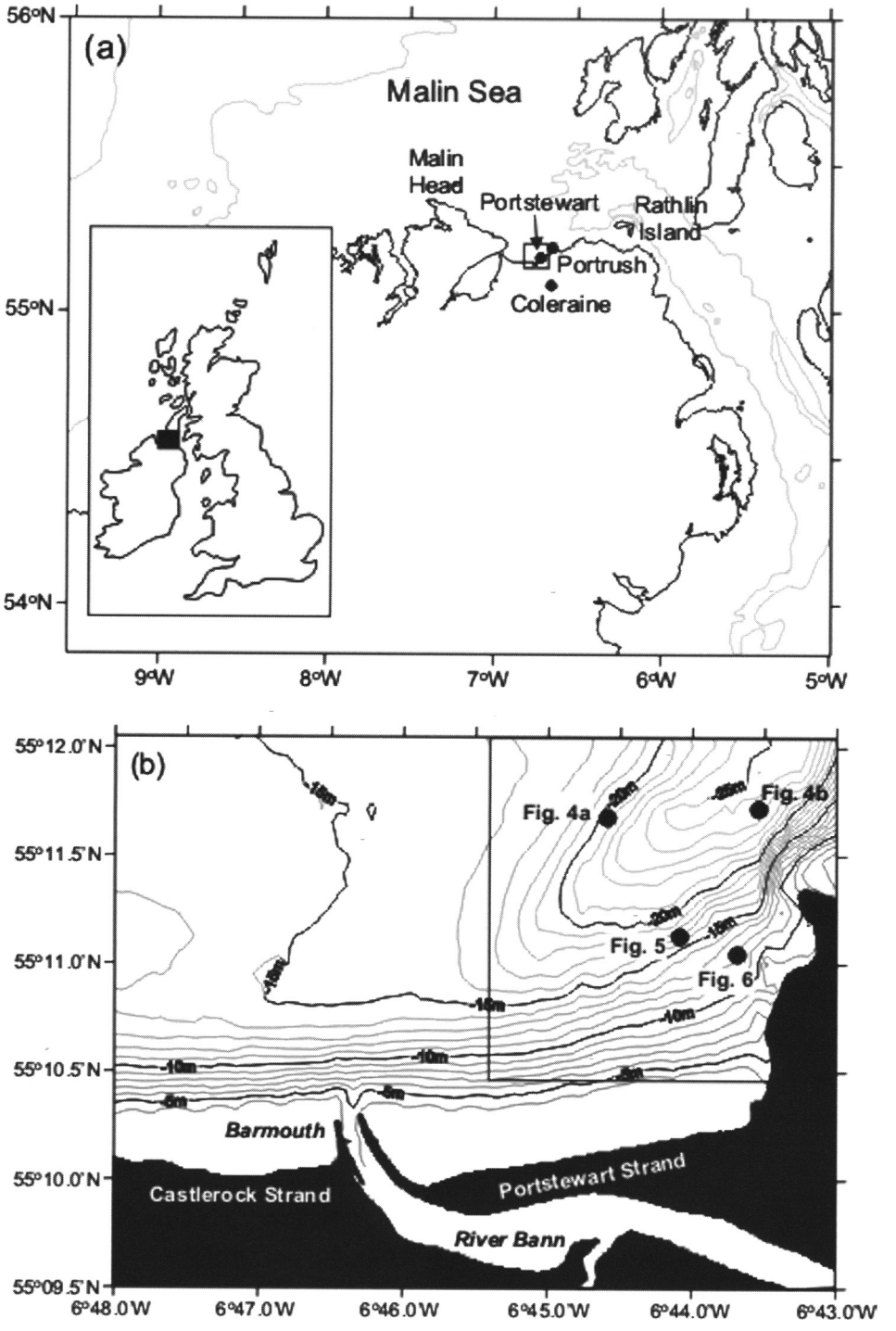

Fig. 1. Map of the British Isles (inset) with the Malin Sea region boxed. (**a**) Map of the Malin Sea region showing the location of the study area (boxed), regional bathymetry, and places named in the text. (**b**) Detailed surveyed bathymetry of the study area showing the location of surficial sediment maps (boxed) (Fig. 4) and side-scan sonar extracts (Figs. 5–7) located around the trench.

(3.10 m). Ebb tides are oriented towards 270–280°, and flood tides towards 90–100° with a near-bed spring-tide water velocity of 0.55 ms^{-1} and a small flood-tide residual (Lawlor 2000). During both flood and ebb tides, eddies on the scale of a few kilometres width are formed on the lee sides of coastal headlands along the north of Ireland (Hydrographic Office 1992). Atlantic swell waves have a strong geomorphic influence along this coastline and have a mean significant wave height of 2.5 m (Carter & Kitcher 1979).

Marine substrate types and regional-scale bedform patterns of the NW European shelf were mapped by Kenyon & Stride (1970) who, in the Malin Sea, identified sand ribbons aligned parallel to the strongest tidal flows. Net seabed sediment transport in this region is generally east-going from a bedload parting located off Malin Head. More locally, the Malin Sea region is dominated by areas of gravelly sand and sandy gravel with isolated areas of sand and gravel (Fyfe *et al.* 1993). Surface sediment types and bedforms were mapped in detail by Pendlebury & Dobson (1976), Carter & Kitcher (1979) and Lawlor (2000). Bedforms present include sand ribbons, sand waves and ripples, and gravel waves and ripples (Kenyon & Stride 1970; Pendlebury & Dobson 1976). These surveys were undertaken using different geophysical equipment at differing resolutions, and in non-overlapping spatial areas, making it difficult to compare results from these surveys.

Methods

Surface morphology and surficial sediments and bedforms in the study area (area of *c.* 40 km^2, water depth of <30 m) were investigated using repeated high-resolution geophysical surveys conducted during August 2000, April 2001 and August 2001 (Fig. 2). Bathymetric data were collected using an AutoHelm SeaTalk single-beam echo sounder operated at 50 kHz frequency. Seafloor data were collected along overlapping tracklines in a grid pattern using an EdgeTech 272-TD dual frequency side-scan sonar system operated at 100/500 kHz. Results from side-scan surveys were ground-truthed using sediments obtained from a trawled bucket-sampler. Positional data were obtained in all marine surveys using a Litton Marine LMX-400 series global positioning system (GPS) with real-time differential correction. Positional error in the marine environment using this equipment is estimated to be in the order of ± 5 m.

Bathymetric data were gridded and contoured using Surfer in order to produce a digital terrain model of the study area. Side-scan data, including boundaries between acoustic facies types, were digitised for each survey; bedform crests were identified on the basis of reflected acoustic signature, and were plotted manually. Absolute positional error of digitized facies boundaries and bedform crests is estimated to be on the order of ± 8–10 m and was consistent between all surveys.

Results

Substrate types

Seabed sediment samples ($n=69$) were obtained using a bucket dredge. These data were collected using both stratified and random sampling methods during August 2001 (the time of survey 3). The location of the samples, obtained by the shipboard GPS, is shown in Fig. 2a. No samples were retrieved from 12 stations (17%). The substrate at these locations is therefore interpreted to be rocky and generally devoid of sediment. Loss of sample from the bucket dredge during retrieval is not considered to be an important factor, since a wide range of sediment sizes (very fine sand to boulders) were recovered successfully. At all stations where sediments were recovered ($n=57$), fine sand (range of 46.8–92.0 wt%) and very fine sand (range 1.3–45.6 wt%) dominate, making up over 90% of the total sample in nearly all cases. These sand size classes are therefore ubiquitous across the study area and at all water depths. Medium and coarse sand is important only locally, mainly in deeper water and within the river barmouth. No samples containing gravel were retrieved. This is likely due to its low percentage cover in the study area and the 'hardness' of the gravel surface.

Sediments also vary over short distances. To the NW of Portstewart, stations 12, 17 and 54 show very different substrate characteristics (Fig. 2b). No sediments were recovered from station 54, suggesting it is hard-bottomed. Station 17 is dominated by fine sand whereas station 12 has an important medium sand component. Sediments retrieved from the study area provide ground-truth evidence for interpretations of substrate type made from side-scan sonar data.

Acoustic evidence for substrate type and mobility

Three acoustic facies were identified on the basis of the strength and lateral continuity of backscatter (Fig. 3). There is also a clear relationship

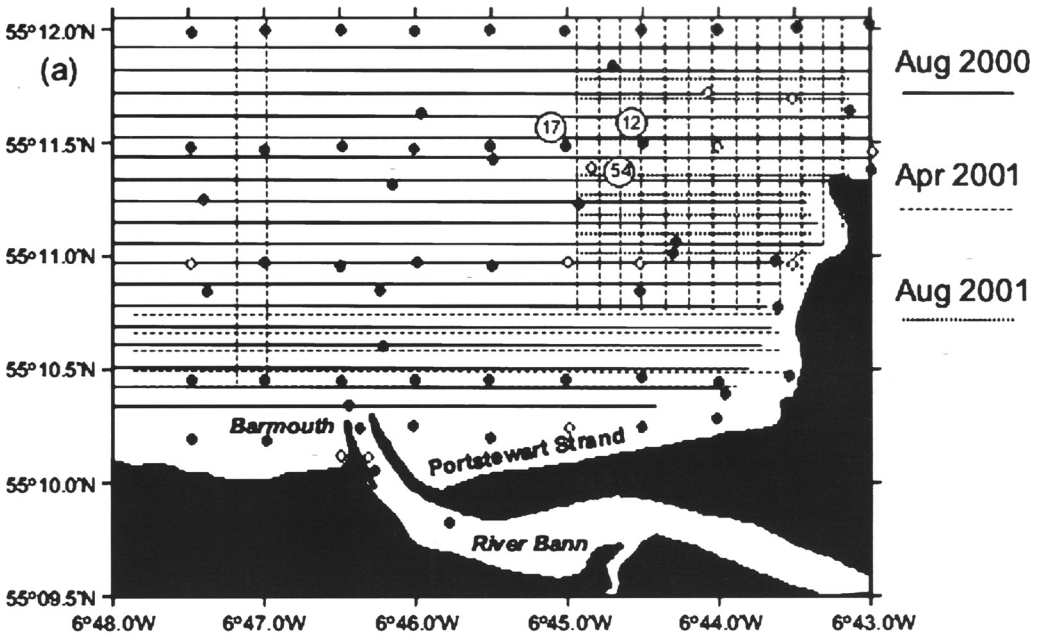

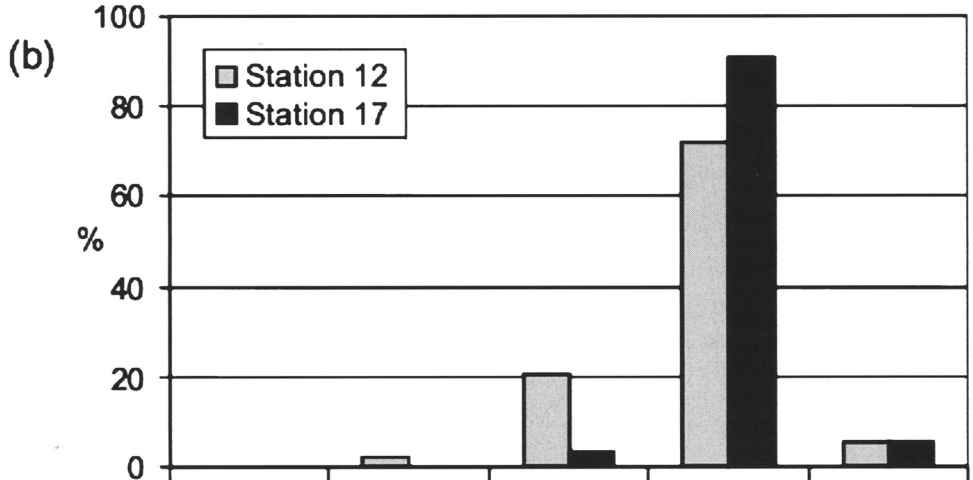

	% VCS	% CS	% MS	% FS	% VFS
Station 12	0	2.2	20.3	72	5.5
Station 17	0.2	0	3.3	91.1	5.4

Fig. 2. (**a**) Location of side-scan sonar survey lines (shown schematically) for the three surveys in the study area, and the position of stations at which seabed sediment samples were recovered (black circles) and were not recovered (white circles). The position of stations 12, 17 and 54, discussed in the text, is shown. (**b**) Histogram of grain size classes of sediments recovered from stations 12 and 17.

Facies	Description	Example	Interpretation
I	Moderate backscatter, uniform tonal returns, rippled bedforms, 3-25 m water depth	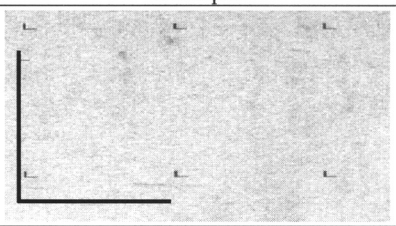	Medium to fine sand
II	Moderate/high backscatter, moderate tonal variations, locally developed bedforms, 12-22 m water depth	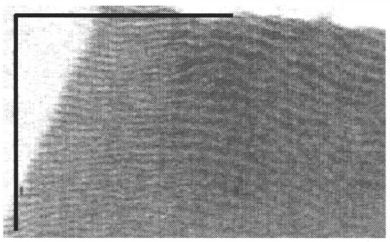	Gravel
III	High backscatter, rough surface texture, high individual targets, 15-25 m water depth	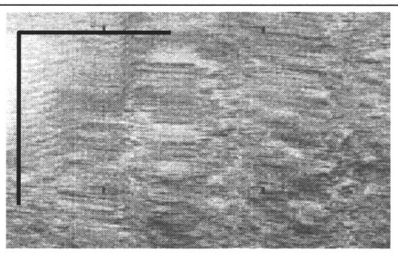	Bedrock or winnowed glacial diamicton (till) surface

Fig. 3. Description and interpretation of acoustic facies. The scale bar is 25 m long.

between acoustic signature and substrate sediment type (e.g. Collier & Brown 2005), which allows for interpretation of these acoustic facies. Facies I is characterized by moderate backscatter with a uniform tonal return, interpreted as medium to fine sand. Bedforms are sometimes developed in this substrate. Facies II is characterized by moderate to high backscatter with a variable tonal return, and is interpreted as gravel. Bedforms are common on gravel substrates. Facies III is characterized by high backscatter with highly variable tonal returns, and with highly-reflective individual targets up to 2 m in plan form dimensions. These acoustic characteristics suggest a rough substrate (either scoured bedrock, or a winnowed glacial diamicton (till) surface; Fyfe *et al.* 1993) with the individual targets interpreted as isolated surficial boulders. The presence of surficial boulders is consistent with both interpretations, and acoustic techniques alone cannot differentiate between these substrate types. Both substrate types have also been imaged on the surface off the north of Ireland coast using Chirp sub-bottom profiling (McDowell *et al.* 2005) and a remotely-operated vehicle (Lawlor 2000).

The mapping procedure shows that most of the study area comprises facies I. Facies II and III are found mainly in and around the partly-enclosed bathymetric low (termed the trench) located NW of Portstewart (Fig. 1). The surveys of August 2000 and August 2001 are almost identical, with facies II and III having a similar spatial extent and positioning (Fig. 4). In these surveys, the boundary between facies I and III is highly complex and shows sand (facies I) interfingering with bedrock (facies III). In contrast the survey of April 2001 (Fig. 4b) shows a very sharp boundary between facies I and III. Additionally, a new area of bedrock was exposed west of Portstewart (Fig. 4b). Facies II (gravel) occupies a similar location in all surveys on the southern flank of the trench.

Comparison between facies boundaries identified on succeeding surveys can indicate the net direction and time-averaged rate of sediment transport (Anthony & Leth 2002), which has implications for the strength and direction of

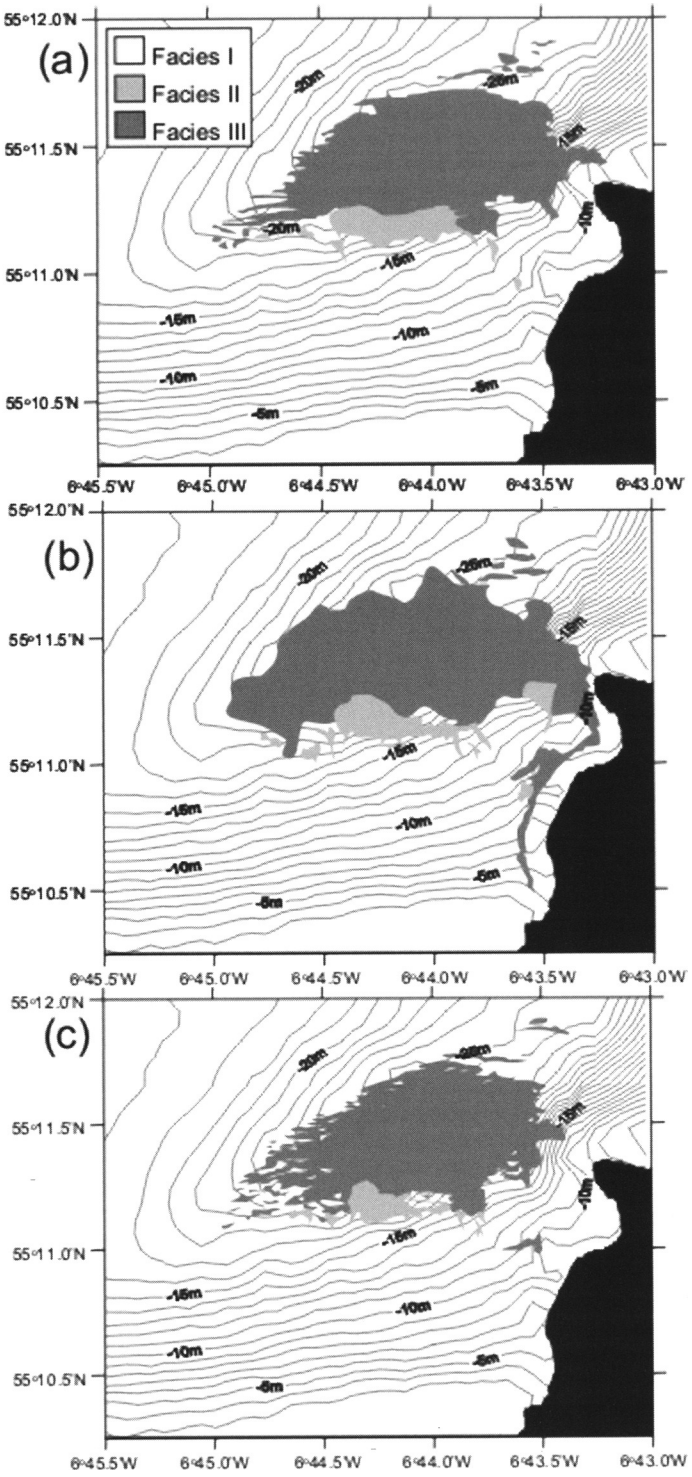

Fig. 4. Detailed maps showing the distribution of surficial sediments in the trench region from the surveys of (**a**) August 2000, (**b**) April 2001 and (**c**) August 2001. Acoustic facies I-III are described and interpreted in the text.

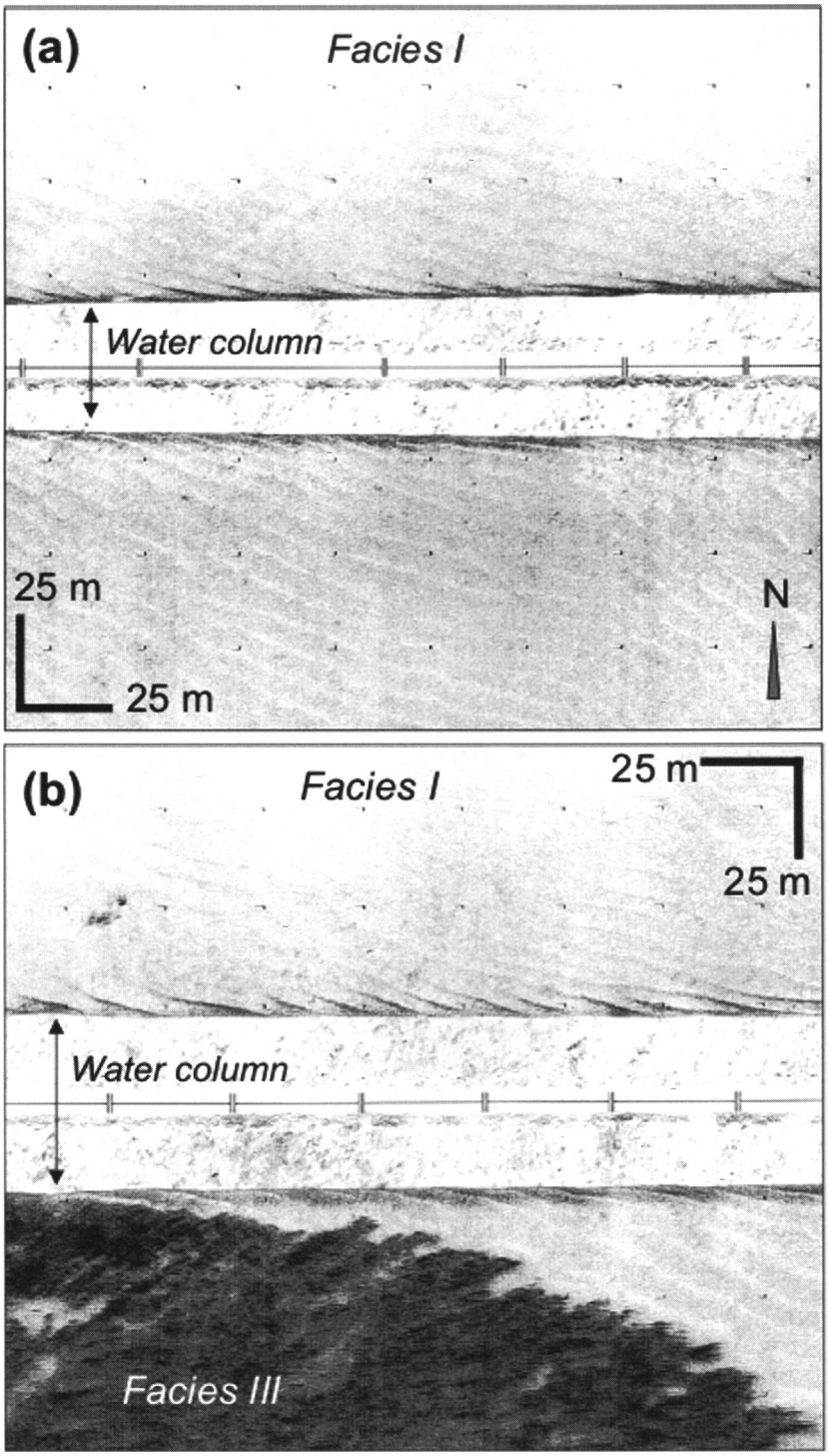

Fig. 5. (**a**) Side-scan sonar extract showing the morphology and relationship of bedforms developed in acoustic facies I (sand). (**b**) Example of bedforms developed in acoustic facies I and their 'feathered' bounding relationship with acoustic facies III (bedrock). Note that bedform crests are oriented parallel to the bedrock margin.

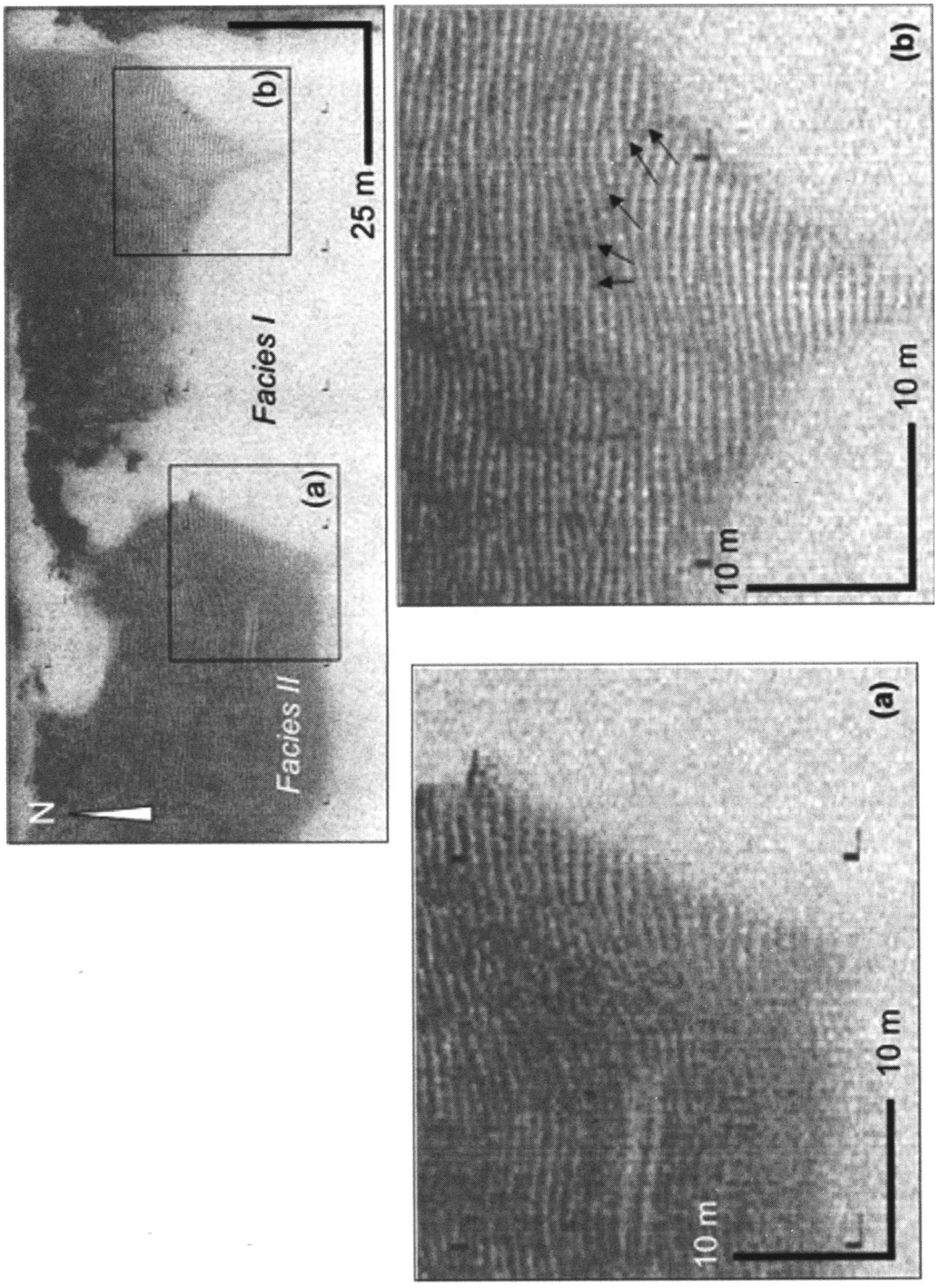
N
Facies II
Facies I
(a)
(b)
25 m
10 m
10 m
(a)
10 m
10 m
(b)

tidal currents and wave disturbance which force bottom-sediment transport (Zeiler *et al.* 2000; Anthony & Orford 2002; Bastos *et al.* 2002). Preliminary comparison between the August 2000 and April 2001 surveys shows that facies boundaries around the trench generally migrated upslope (e.g. towards the SW). The boundary between facies I and III (sand and bedrock) migrated westwards by an average of 114 m (0.48 m/day), whereas the boundary between facies I and II (sand and gravel) migrated towards the SSW by an average of 37 m (0.16 m/day). The survey of August 2001 shows these facies boundaries have migrated back to the positions of August 2000, suggesting that sediment dynamics displays a strongly seasonal behaviour.

Bedform types and directions of sediment transport

Bedforms were identified in both sand (facies I) and gravel (facies II) substrates and are described using the size-classes of Ashley (1990). Bedforms developed in sand are located in two areas: (1) in the nearshore up to water depths of about 8 m (broad, subtidal dunes with crests aligned oblique to the coastline), and (2) near the bedrock-floored trench (smaller current-perpendicular dunes). Only bedforms located in deeper water near the trench are discussed here.

Bedforms developed in sand around the trench are found in water depths of 15–25 m and are laterally continuous over several hundred metres distance. Medium dune bedforms have undulating to straight crests which occasionally bifurcate (Fig. 5a). The dune crests are generally aligned between NW–SE and NE–SW (approximately slope-parallel around the sides of the trench), and have wavelengths on the order of 5.4–6.4 m and amplitude of 1.0–1.4 m. Smaller ripples may be superimposed upon these dunes. On the eastern (deeper) margin of the trench the sand–bedrock boundary is sometimes complex, showing areas of sand penetration into troughs or low points on the bedrock surface, giving rise to a 'feathered' acoustic appearance (Fig. 5b).

Bedforms are also developed over most areas covered by the gravel facies. The gravel areas are arranged in two morphological types. (1) Large circular patches of gravel (< few hundred metres across) comprise straight-crested, east–west aligned small dunes with wavelengths of 0.7–1.4 m and amplitudes of 0.2–0.5 m (Fig. 6). The gravel patches have sharp northerly and southerly margins, often demarcated by a single bounding gravel ridge, and have 'feathered' easterly and westerly margins formed as a result of sand infilling dune troughs (Figs. 5 and 6). (2) 'Ribbon'-shaped gravel patches (here termed gravel ribbons) are elongate, north–south aligned features which are 8–10 m wide and up to 150 m long (Fig. 7). They are located particularly on the southern side of the trench ($n=6$) where they occupy slight bathymetric lows (1–2 m depth) which face downslope, and are therefore morphologically similar to rip current or debris flow chutes (Smith & Largier 1995). The head of the gravel ribbons start consistently at -13 m and -16 m below ordnance datum (OD) (Fig. 4). The ribbons are onlapped laterally by areas of planar sand. These lateral margins are generally sharp whereas the northern (downslope) and southern (upslope) margins are more diffuse and tapering in shape. Straight-crested small gravel dunes are developed within the gravel ribbons (Fig. 7). Dune crests (aligned east-west, wavelength of <1 m) are aligned at right angles to the direction in which the gravel ribbon is elongated. The gravel ribbons are observed on all three surveys but are most common on the second survey (April 2001). Some individual ribbons are present on all three surveys.

By tracing the lateral continuity of gravel bedform crests, and by noting patterns of superposition, it is possible to identify up to four different groups of bedforms, termed bedform sets, within the gravel ribbons. Bedform sets are identified on the basis of patterns of bedform crests. Within a single bedform set, individual bedform crests are parallel to one another and laterally continuous across a distance of 5–12 m. Boundaries between bedform sets are marked by concave breaks of slope where bedform crests change direction and/or continuity sharply (Figs. 6b, 7b). It is uncertain as to whether the surface bedforms form part of a larger migrating gravel lobe (<1 m high), or whether the bedforms

Fig. 6. Side-scan sonar extract showing the relationships between acoustic facies I (sand) and II (gravel). Note that the gravel forms both large circular patches and elongate ribbons. **(a)** Detailed side-scan extract showing the lateral margin of the gravel patch and the termination of gravel bedforms. **(b)** Detailed side-scan extract showing a gravel ribbon feeding into a larger gravel patch. Bedform terminations, suggestive of changes in substrate slope or direction of gravel migration, are arrowed. These mark the boundaries of individual bedform sets.

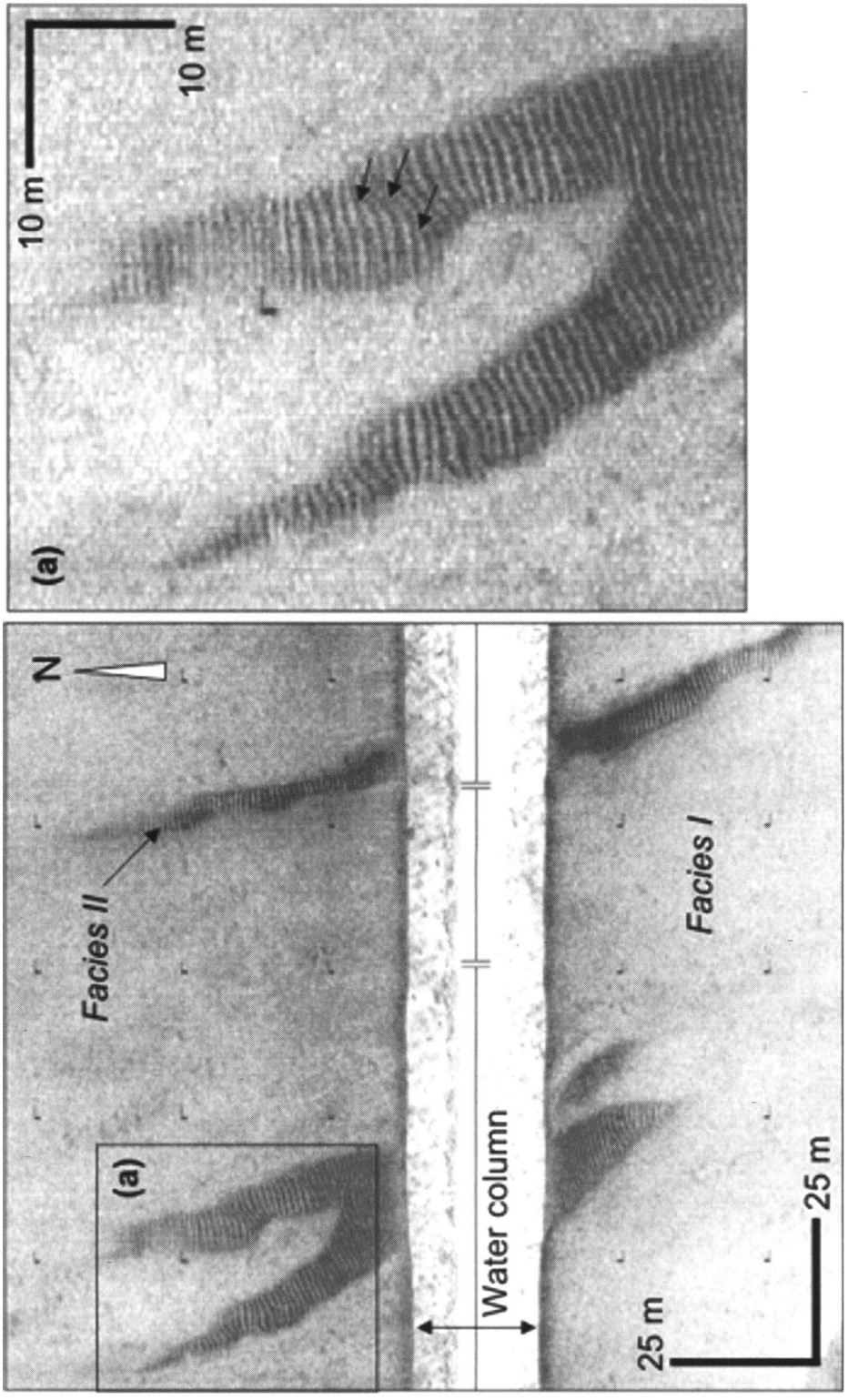
(a)
10 m
10 m
N
Facies II
(a)
Water column
Facies I
25 m
25 m

are developing across a pre-existing and partly buried gravel surface. Based on the direction of bedform set superposition, bedform migration is from south to north, downslope towards the trench.

Discussion

Formation and positioning of sand bedforms

Nearshore bedforms on the NW European shelf reflect a combination of, mainly, tidal and wave influences (Kenyon & Stride 1970; Banner & Culver 1979; Pingree & Griffiths 1979; Anthony & Leth 2002; Anthony & Orford 2002). Despite the preliminary nature of the data presented here, the positioning and orientation of sand and gravel bedforms off the north coast of Ireland suggest that these regional-scale controls are modified by local-scale factors including coastline shape and fluid interaction with seabed morphology (Zimmerman 1981). Generally, sand bedforms in this area lie oblique to both flood- and ebb-tide components, and lie approximately perpendicular to the direction of incoming long-period Atlantic swell waves from the NW (Pendlebury & Dobson 1976). As a result, the formation, maintenance and modification of these nearshore bedforms are the likely effects of tides and waves in combination, which may change in relative dominance seasonally or episodically as during large storms (cf. Anthony & Orford 2002). The observed migration of the boundaries between the sand and adjacent facies (facies I/II and facies I/III boundaries) throughout the surveyed period may reflect seasonal changes in tide/wave dominance.

Despite both strong flood and ebb tides in the study area, the small eastward (flood-oriented) tidal residual (Hydrographic Office 1992) suggests net easterly sediment transport, consistent with regional-scale bedform patterns (Kenyon & Stride 1970). Marine sand waves, reflecting this net easterly transport direction, are recorded east of Portstewart (Lawlor 2000). The presence of bedforms around the trench west of Portstewart, however, do not fit with evidence for this slight tidal asymmetry. A possible explanation is that the bathymetric irregularity of the trench acts to set up internal water vortices that scour the trench floor and recirculate sediment locally. Sand bedforms that follow the bedrock margin around the trench (Fig. 5) likely reflect this bottom current recirculation (cf. contourites), which may take place during both flood- and ebb-tides (e.g. Geyer 1993).

Tidal asymmetry, in combination with a coastline comprised of alternating headlands and bays, is known to lead to the formation of headland leeside eddies (Signell & Geyer 1991; Davis *et al.* 1995) which can impact on sediment transport and deposition patterns (Pingree & Griffiths 1979; Ferentinos & Collins 1980; Zimmerman 1981). The location of the sand bedforms around the trench and immediately adjacent to the headland near Portstewart suggests there may be a relationship between bedform development and the formation of attached leeside eddies, which are recorded in this area (Hydrographic Office 1992). Sandy bedforms are found in similar headland settings along the north coast of Ireland (Lawlor 2000), and may be associated with areas of tidal flow expansion adjacent to headlands and between islands (Carter & Kitcher 1979).

Model for water circulation and formation of the gravel ribbons

Based on the described field data, and regional geological and oceanographic data (Hydrographic Office 1992; Lawlor 2000), a model can be proposed to explain the temporal changes in substrate facies patterns and the development and migration of sand and gravel bedforms (Fig. 8). The alignment and positioning of sand bedforms suggest they were shaped, possibly tidally, when sediment was more mobile under enhanced winter waves. This is also consistent with their location north of the trench and facing a descending bathymetric slope. Similar shallow-water wave-influenced sandy bedforms have been observed off the coast of Denmark (Anthony & Leth 2002). The orientation of the gravel ribbons south of the trench suggests that the east-going flood tide flowing shore-parallel (at around the −13 m isobath) is turned northwards by the presence of the headland and directed down a steeper bathymetric slope towards the trench (Fig. 8). This can explain the pattern of superposed bedform sets within the gravel ribbons, and the flow-perpendicular orientation of gravel bedform crests.

Fig. 7. Side-scan sonar extract showing the morphology and bedform patterns of gravel ribbons. Note that there is a slight depression (substrate low) at the base of the water column, confirming that gravel ribbons are buried (onlapped) by facies I (sand). (a) Detailed side-scan extract showing ripple patterns within the gravel ribbon. Ripple terminations, suggestive of changes in substrate slope or direction of gravel migration, are arrowed. These mark the boundaries of individual bedform sets.

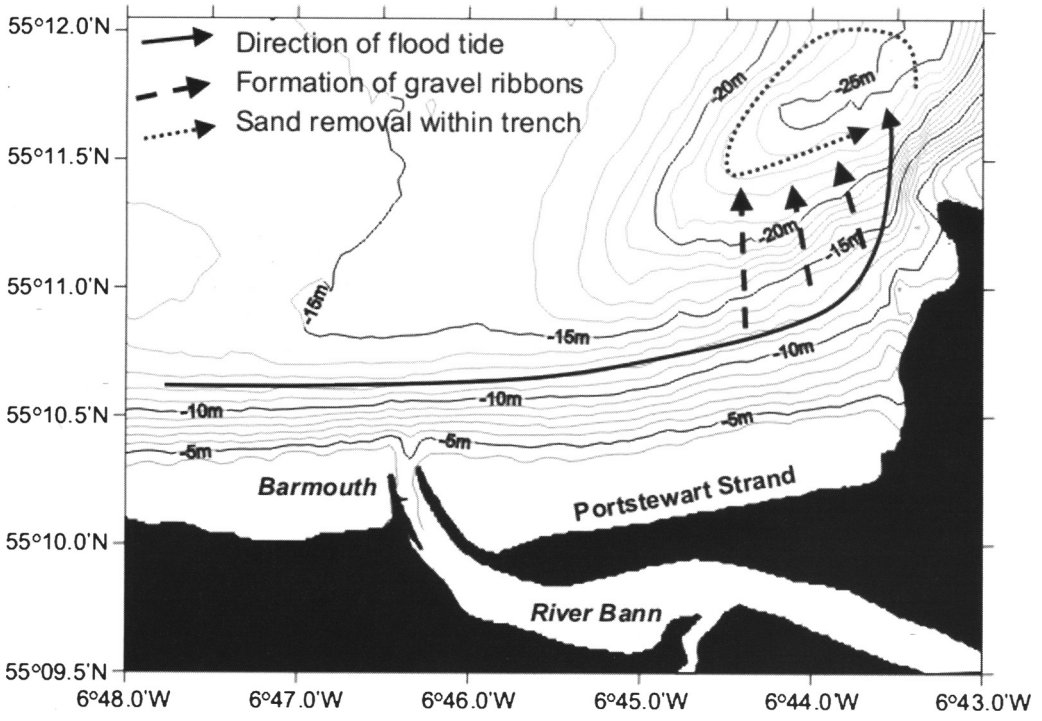

Fig. 8. Schematic model for nearshore bottom-water circulation off the north coast of Ireland.

The discrete morphology and scale of the gravel ribbons is of interest since they closely resemble rip current chutes (e.g. Antia 1994; Smith & Largier 1995; Aagaard *et al.* 1997). Although developed in too-deep water to be rip currents *sensu stricto* (Antia 1994), they may reflect areas of similar bottom current flow convergence. The location (in the April 2001 survey) of some of the gravel ribbons adjacent to an area of freshly sediment-stripped bedrock (Fig. 4b) may suggest that return-flow water in this area (of wave or flood-tide origin) contains a high sediment load, leading to dense, gravity-driven flows downslope. This matches seasonal changes in morphology seen on the adjacent beach (Wilcock 1976). This is also similar to a precondition required for rip current formation (Smith & Largier 1995).

There is no nearshore gravel source at the present time. However, high-resolution Chirp data from −12–14 m water depth in the area where the gravel ribbons are located show chaotic high-impedance reflectors at shallow depth (2–3 m) in the sediment profile, forming a discontinuous horizon that is located between acoustically-transparent units and which dips seaward. This horizon is interpreted as a thin and discontinuous gravel layer sandwiched between sand. The gravel layer may be the distal correlative to a gravel barrier upon which the Portstewart Strand sand dunes are anchored (Wilson & McKenna 1996). Alternatively, the gravel layer may represent a relict lag surface formed when meandering rivers extended onto the shelf during an early Holocene sea-level stillstand of about −15 m OD (McDowell *et al.* 2005). Given the absence of a present-day nearshore sediment source for the gravel ribbons, it is therefore likely that the subsurface gravel layer was exposed temporarily in the floor of the ribbons as overlying sand was removed by strong sea-going currents. Gravel was then organised and moved along the floor of the ribbons as they developed. This interpretation is similar to the winnowed gravel lags formed by deep-water contour currents (e.g. Howe *et al.* 2001).

The absence of sand in the trench suggests that, even if this sand is carried into it through the gravel ribbons (estimate of *c.* 200 m^3 volume based on ribbon geometry), it is quickly transported westwards out of the deepest part of the trench (Fig. 8). This anticlockwise, coriolis-driven sediment circulation into and out of the trench is consistent with overall bedform patterns and may indicate that, during winter, sand accumulates on the flat shelf west of the

trench from where it is reworked onshore and towards the trench under fairweather summer conditions. This model is consistent with other studies of sediment transport patterns around headlands (e.g. Ferentinos & Collins 1980; Zimmerman 1981; Bastos *et al.* 2002). It also indicates that regional-scale patterns of sediment transport (e.g. Kenyon & Stride 1970) considerably underestimate transport complexity particularly in the nearshore zone.

Conclusions

Paraglacial coasts are often considered to be essentially relict sediment systems with subdued present-day sediment dynamics (e.g. FitzGerald & Rosen 1987; Shaw *et al.* 1993; Belknap *et al.* 2002). Repeated side-scan sonar surveys off the north coast of Ireland, however, show marked mesoscale changes in the distribution and character of nearshore surficial sediments, including temporal changes in spatial patterns of sand and gravel bedforms. Despite having a overall balanced nearshore sediment budget with limited onshore sediment transport at the present time (Wilcock 1976), sediments are very mobile, driven by seasonal changes in the relative strengths of waves and tidal currents. Water interaction with substrate topography and coastline shape results in the formation of attached headland eddies which appear to be important in basal scouring and seasonal sediment redistribution. Although these results are preliminary they indicate far more complex local patterns of nearshore sediment transport than have been recognized hitherto at this location.

We thank Chris Evans, Peter Harris and Neil Kenyon for their comments.

References

AAGAARD, T., GREENWOOD, B. & NIELSEN, J. 1997. Mean currents and sediment transport in a rip channel. *Marine Geology*, **140**, 25–45.

ANTIA, E. E. 1994. Long-term and post-storm dynamic patterns of the subtidal rhythmic morphology along the East Frisian island coast, Germany. *Geologie en Mijnbouw*, **73**, 1–12.

ANTHONY, D. & LETH, J. O. 2002. Large-scale bedforms, sediment distribution and sand mobility in the eastern North Sea off the Danish west coast. *Marine Geology*, **182**, 247–263.

ANTHONY, E. J. 2002. Long-term marine bedload segregation, and sandy versus gravelly Holocene shorelines in the eastern English Channel. *Marine Geology*, **187**, 221–234.

ANTHONY, E. J. & ORFORD, J. D. 2002. Between wave- and tide-dominated coasts: the middle ground revisited. *Journal of Coastal Research (ICS 2002 Proceedings)*, **SI 36**, 8–15.

ASHLEY, G. M. 1990. Classification of large-scale subaqueous bedforms – a new look at an old problem. *Journal of Sedimentary Petrology*, **60**, 160–172.

BANNER, F. T. & CULVER, S. J. 1979. Sediments of the north-west European shelf. *In*: BANNER, F. T., COLLINS, M. B. & MASSIE, K. S. (eds) *The North-West European Shelf Seas: The Sea Bed and the Sea in Motion. I. Geology and sedimentology*. Elsevier Oceanography Series, **24B**, Elsevier, Amsterdam. 271–300.

BARTEK, L. R. & WELLNER, R. W. 1995. Do equilibrium conditions exist during sediment transport studies on continental margins? An example from the East China Sea. *Geo-Marine Letters*, **15**, 23–29.

BASTOS, A. C., KENYON, N. H. & COLLINS, M. 2002. Sedimentary processes, bedforms and facies, associated with a coastal headland: Portland Bill, Southern UK. *Marine Geology*, **187**, 235–258.

BELKNAP, D. F., KELLEY, J. T. & GONTZ, A. M. 2002. Evolution of the glaciated shelf and coastline of the northern Gulf of Maine, USA. *Journal of Coastal Research (ICS 2002 Proceedings)*, **SI 36**, 37–55.

BINNS, P. E., HARLAND, R. & HUGHES, M. J. 1974. Glacial and postglacial sedimentation in the Sea of the Hebrides. *Nature*, **248**, 751–754.

BRIDGLAND, D. R. 2002. Fluvial deposition on periodically emergent shelves in the Quaternary: example records from the shelf around Britain. *Quaternary International*, **92**, 25–34.

CARTER, R. W. G. 1990. Coastal processes in relation to geographic setting, with special reference to Europe. *Senckenbergiana Maritima*, **21**, 1–23.

CARTER, R. W. G. & KITCHER, K. J. 1979. The geomorphology of offshore sand bars on the north coast of Ireland. *Proceedings of the Royal Irish Academy*, **79B**, 43–61.

COLLIER, J. S. & BROWN, C. J. 2005. Correlation of sidescan backscatter with grain size distribution of surficial seabed sediments. *Marine Geology*, **214**, 431–449.

COLLINS, M. B. & BANNER, F. T. 1980. Sediment transport by waves and tides: problems exemplified by a study of Swansea Bay, Bristol Channel. *In*: BANNER, F. T., COLLINS, M. B. & MASSIE, K. S. (eds) *The North-West European Shelf Seas: The Sea Bed and the Sea in Motion. II. Physical and chemical oceanography, and physical resources*. Elsevier Oceanography Series, **24B**, Elsevier, Amsterdam. 369–389.

DAVIS, P. A., DAKIN, J. M. & FALCONER, R. A. 1995. Eddy formation behind a coastal headland. *Journal of Coastal Research*, **11**, 154–167.

FERENTINOS, G. & COLLINS, M. 1980. Effects of shoreline irregularities on rectilinear tidal current and their significance in sedimentation processes. *Journal of Sedimentary Petrology*, **50**, 1081–1094.

FITZGERALD, D. M. & ROSEN, P. S. (eds) 1987. *Glaciated Coasts*. Academic Press, San Diego.

FYFE, J. A., LONG, D. & EVANS, D. 1993. *United Kingdom offshore regional report: the geology of the Hebrides-Malin sea area*. HMSO, London, for the British Geological Survey.

GEYER, W. R. 1993. Three-dimensional tidal flow around headlands. *Journal of Geophysical Research*, **98**, 955–966.

HOWE, J. A., STOKER, M. S. & WOOLFE, K. J. 2001. Deep-marine seabed erosion and gravel lags in the northwest Rockall Trough, North Atlantic Ocean. *Journal of the Geological Society*, **158**, 427–438.

HYDROGRAPHIC OFFICE. 1992. *Tidal Stream Atlas. Firth of Clyde and Approaches*. NP 222. Hydrographic Office, Taunton.

KENYON, N. H. & STRIDE, A. H. 1970. The tide-swept continental shelf sediments between the Shetland Isles and France. *Sedimentology*, **14**, 159–173.

LAWLOR, D. P. 2000. *Inner shelf sedimentology off the North Coast of Northern Ireland*. DPhil thesis, University of Ulster.

MCDOWELL, J. L., KNIGHT, J. & QUINN, R. 2005. High-resolution geophysical investigations of the Bann estuary, Northern Ireland coast. *In*: FITZGERALD, D. M. & KNIGHT, J. (eds) *High-Resolution Morphodynamics and Sedimentary Evolution of Estuaries*. Springer, New York, 11–13.

PENDLEBURY, D. C. & DOBSON, M. R. 1976. Sediment and macrofaunal distribution in the eastern Malin Sea, as determined by side-scan sonar and sampling. *Scottish Journal of Geology*, **11**, 315–332.

PINGREE, R. D. & GRIFFITHS, D. K. 1979. Sand transport paths around the British Isles resulting from M2 and M4 tidal interactions. *Journal of the Marine Biological Association of the United Kingdom*, **59**, 497–513.

SHAW, J., TAYLOR, R. B. & FORBES, D. L. 1993. Impact of the Holocene transgression on the Atlantic coastline of Nova Scotia. *Géographie physique et Quaternaire*, **47**, 221–238.

SIGNELL, R. P. & GEYER, W. R. 1991. Transient eddy formation around headlands. *Journal of Geophysical Research*, **96**, 2561–2575.

SMITH, J. A. & LARGIER, J. L. 1995. Observations of nearshore circulation: Rip currents. *Journal of Geophysical Research*, **100**, 10967–10975.

TAYLOR, J., DOWDESWELL, J. A. & SIEGERT, M. J. 2002. Late Weichselian depositional processes, fluxes, and sediment volumes on the margins of the Norwegian Sea (62–75°N). *Marine Geology*, **188**, 61–77.

WILCOCK, F. A. 1976. *Dune physiography and the impact of recreation on the north coast of Ireland*. Unpublished D. Phil. thesis, New University of Ulster.

WILSON, P. & MCKENNA, J. 1996. Holocene evolution of the River Bann estuary and adjacent coast, Northern Ireland. *Proceedings of the Geologists' Association*, **107**, 241–252.

ZEILER, M., SCHULZ-OHLBERG, J. & FIGGE, K. 2000. Mobile sand deposits and shoreface sediment dynamics in the inner German Bight (North Sea). *Marine Geology*, **170**, 363–380.

ZIMMERMAN, J. T. F. 1981. Dynamics, diffusion and geomorphological significance of tidal residual eddies. *Nature*, **290**, 549–555.

An application of sediment trend analysis to Carmarthen Bay, Bristol Channel

BILL COOPER[1] & PATRICK MCLAREN[2]

[1]*ABP Marine Environmental Research Ltd, Suite B, Waterside House, Town Quay, Southampton SO14 2AQ, UK (e-mail: bcooper@abpmer.co.uk)*

[2]*GeoSea Consulting (Canada) Ltd, 789 Saunders Lane, Brentwood Bay, BC, V8M 1C5, Canada*

Abstract: Carmarthen Bay is a large embayment on the northern coast of the Bristol Channel; a location that is exposed directly exposed to both Atlantic waves and a macro-tidal environment. Until recently this embayment was comparatively poorly described in terms of its sediment regime. In particular, limited data were available to identify sediment types and sediment exchanges with the offshore.

The Bristol Channel is an active interest area for marine aggregate extraction, with the majority of licenses falling in Welsh Territorial Waters. To enable the Government View procedure on marine aggregate extraction in this area to develop with a more complete understanding a research project (Bristol Channel Marine Aggregates: Resource and Constraints, also commonly referred to as BCMA) was commissioned. This research project identified Carmarthen Bay as a strategic unit of the overall sediment regime, and defined a programme of primary research in this area to improve understanding of sediment exchanges. A key part of this research has been an application of sediment trend analysis (STA). This paper describes components of the STA technique, the rationale for its application, the survey design, results and subsequent interpretation of the information in the context of determining probable patterns of net sediment transport across Carmarthen Bay.

Sediment trend analysis (STA) has been applied previously to various marine locations across the world, including other parts of the Bristol Channel, to identify and understand better sediment transport pathways. The first application of STA in the Bristol Channel was in 1989 as part of the Severn Tidal Barrage Project investigations (ETSU 1989), and the most recent to assist in developing a view related to aggregate extraction in Barnstaple Bay (McLaren & Kirby 1998). In each case, a programme of marine surveys has been required to obtain a representative sequence of seabed sediment samples across respective study areas. The STA technique relies on a detailed interpretation of these samples, expressed in terms of a highly resolved grading analysis.

Study rationale

The National Assembly for Wales (NAW) has a responsibility to provide the Government View on the suitability of marine aggregate dredging for sites in Welsh Territorial Waters. To help inform this process the NAW commissioned the Bristol Channel Marine Aggregate: Resource and Constraint (BCMA) research project. A key objective for this research project was to develop a strategic view for the sediment regime across the whole of the Bristol Channel.

In Phase 1 of the BCMA project all relevant data from previous studies and research was collated. This included information relating to various sediment transport indicators (such as bedform asymmetry, tracer experiments, etc), and mapped distributions of sediment types. A synthesis of this information was used to identify areas where data coverage and knowledge was most limited. These data gaps were assessed for strategic importance, leading to a programme of primary research targets which was carried out under Phase 2 of the study.

Carmarthen Bay

Carmarthen Bay is a large embayment on the northern coast of the Bristol Channel, bounded by headlands of Giltar Point and Worms Head (Fig. 1). The bay is directly exposed to both Atlantic seas and a macro-tidal environment. The bay was identified from Phase 1 as an area weakly provided with data, but also a strategically important part of the Bristol Channel for marine sands, with the potential for sediment pathways and linkage for sediment exchange

From: BALSON, P. S. & COLLINS, M. B. 2007. *Coastal and Shelf Sediment Transport*. Geological Society of London, Special Publications, **274**, 117–125. 0305-8719/07/$15.00

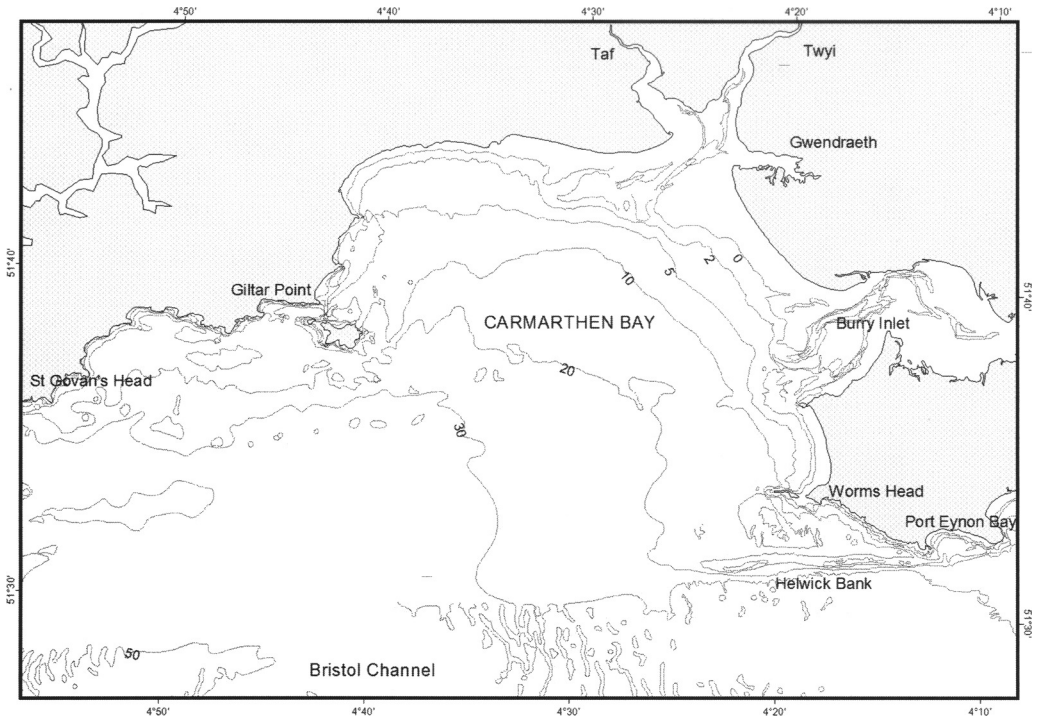

Fig. 1. Study area.

with the Celtic Sea. The site is presently a candidate Special Area of Conservation (cSAC) for primary habitat features, including:

- large shallow inlets and bays;
- sandbanks which are covered by sea water all the time;
- estuaries.

Study area

The available geophysical records (Al-Ghadban 1986) describe a sand cover of Quaternary deposits which thicken towards the inshore areas and eastern side of the bay. Within the bay there are also several in-filled palaeovalleys that appear to be extensions of the main Burry Inlet and the northern estuarine complex of the rivers Taf, Twyi and Gwendraeth. The texture of the sea bed appears to lack any major bedforms, with only patches of megaripples in deeper water which indicate an east–west orientation. Outside of the bay there is a distinct pattern of large sandwaves.

In the eastern part of the bay, and close to Worms Head, is a major linear sub-tidal sandbank, known as Helwick Bank. This feature is a large morphological bedform comprised of medium sand. The bank is around 14 km in length, 1.2 km width (taken at the 15 m CD isobath) and orientated to the axis of peak tidal flows. The bank is commonly described in three segments; West Helwick and East Helwick, which are separated by a slightly lower profile ad central part of the bank known as Helwick Swatch. It is Helwick Swatch that is presently an active dredging site for marine aggregates. East Helwick runs up to join the coast at the headland of Port Eynon Point, South Gower, and West Helwick extends into Carmarthen Bay, merging at its tip into the extensive set of large sandwaves.

Published maps of sediment distributions across Carmarthen Bay (IGS 1983) have been developed from a fairly sparse dataset, which comprise of around 50 sediment samples along with a limited number of geophysical survey lines.

Primary research

A structured programme of primary research was designed to improve data coverage across Carmarthen Bay and to help improve the understanding of sediment pathways, linkages to the sandbank and shoreline. The primary research

included sediment trends analysis (STA), based upon an extensive sea bed grab sampling campaign, sediment tracer experiments from specified sites and a series of macro-benthic analysis.

Sediment trend analysis

This paper focuses on the application of STA in Carmarthen Bay and studies that has been reported previously as part of the BCMA project (Haine & Cooper 2000; McLaren 1999). STA has also been applied previously at other sites within the Bristol Channel, including: Severn Estuary, Inner Bristol Channel, Nash Bank and Barnstaple Bay.

STA is a technique developed by GeoSea, whereby patterns of probable net sediment transport are determined from relative changes in the grain-size distributions of heterogeneous surficial seabed sediments. In addition, the method enables the dynamic behaviour of the sediments to be derived, i.e. net erosion, net accretion, dynamic equilibrium, etc. The original theory for determining sediment transport direction from changes in grain-size distributions was published initially by McLaren & Bowles (1985).

The sampled sediments are described in statistical terms (by the moment measures of mean, sorting and skewness) and the basic underlying assumption is that processes causing sediment transport will affect the statistics of the sediments in a predictable way. Following from this assumption, the size frequency distributions of the sediments provide the data with which to search for patterns of net sediment transport. In reality, perfect sequential changes along a transport path, as determined by the model, are rarely observed. This is because of a variety of uncertainties that may be introduced in sampling, the analytical technique to obtain grain-size distributions, the assumptions of the transport model, and the statistics used in describing the grain-size distributions. These uncertainties may be summarized, as follows.

The use of the log-normal distribution

Although sediments are typically described by a particle weight distribution based on the log of the grain-size (i.e., the phi scale) there is, in fact, no way to determine the 'best' descriptor for all sediments. The log-normal distribution has been found useful in practice since it appears to highlight important features of naturally occurring sediments. Bias can, however, be introduced in the choice of distribution. For example, the mean of the distribution in phi space is not equal to the mean of the distribution in linear space. Using the moment measures (mean, variance and skewness) may highlight important features and suppress those that are unimportant; however, information will also be lost. There is no way to determine if the lost information is significant.

Assumptions in the transport model

In providing a mathematical proof for the transport model used in STA (McLaren & Bowles 1985), a basic assumption is made that smaller grains are more easily transported than larger grains, although this assumption is not strictly true. Factors such as shielding whereby the presence of larger grains may impede the transport of smaller grains, or the decreasing ability of the eroding process to carry additional fines with increasing load, demonstrate that the transport process is a complicated function related to the sediment distribution and the strength of the erosion process.

Temporal fluctuations

Sediment samples may comprise the effects of several transport processes. It is assumed that what is sampled is the 'average' of all the transport processes affecting the sample site. The 'average' transport process may not conform to the transport model developed for a single transport process.

Sample spacing

Sample sites may be too far apart to detect relevant transport processes. With increasing distance between sample locations there is an increasing possibility of collecting sediments unrelated by transport (i.e., different facies). In practice, selection of a suitable sample spacing takes into account: (1) the number of sedimentological environments likely to be encountered; (2) the desired spatial scale of the sediment trends; and (3) the geographic shape of the study area (see below for further discussion of sample spacing).

Random environmental uncertainties

All samples will be affected by random errors. These may include unpredictable fluctuations in the depositional environment, the effects of sampling and sub-sampling a representative sediment population, and random measurement errors.

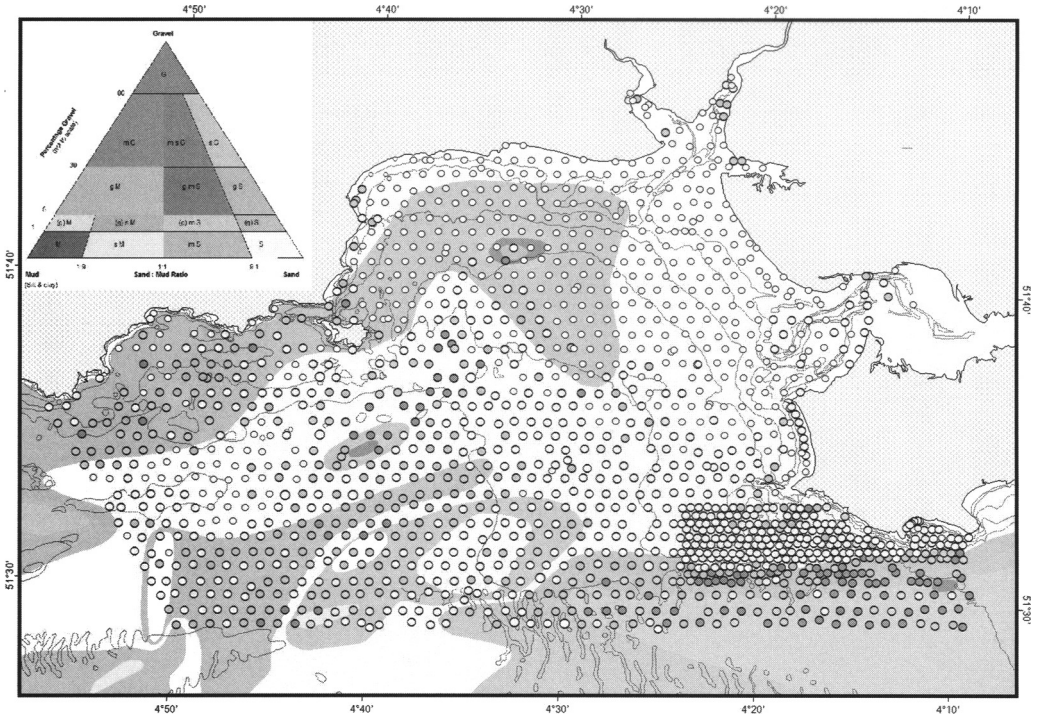

Fig. 2. Interpreted sediment samples across Carmarthen Bay.

Survey design

For the application of STA in Carmarthen Bay a hexagonal survey grid was designed with coverage extending from St Govan Head (in the west) to Oxwich Point (in the east) and into the head of the bay, along the beaches and into Burry Inlet (Fig. 2).

In total, 1574 grab samples of surficial sediments were attempted at regular intervals across the Carmarthen Bay with a general spacing of 1000 m. Across Helwick Bank and into Port Eynon Bay a finer spacing of 500 m was adopted due to the scale of these features and the special interest in this area.

Survey results

Grab Samples

The grab samples were analysed to determine a complete grain size distribution. The analysis methods utilized a combination of a Malvern 2600 l laser diffraction particle sizer (for material < 1500 mm) and dry sieves (for coarser sediments), to resolve the distribution of grain sizes in increments of 0.5 phi.

Along with the provision of data for use in the STA, the grab sampling analysis has enabled improved mapping and classification of sediment distributions across Carmarthen Bay. Details of the resolved sediment types, expressed according to the Folk classification (Folk 1965), are listed in Table 1, and presented in Figure 2 overlain onto the original IGS classification of surficial sediments (IGS 1983).

Sands are the dominant sediment type and account for almost 65% of all samples. In the inner part of the bay (within the 20 m contour) the main sediment type is a population of fine sands, with medium sands identified towards the deeper water and across Helwick Bank. To the south of Helwick Bank the sediment type grades into sandy gravel and gravel. Rhossili and Port Eynon beach appear to contain both fine sands in the lee of Worms Head and Port Eynon Point, respectively, and medium sands in the sub-tidal areas. Occasional mud patches are found in deeper water, these are believed to be exposed areas of underlying Pleistocene till. The general pattern of sediment types corresponds to a well-worked tidally sorted distribution.

Table 1. *Classification of sediment samples in Carmarthen Bay*

Sediment Classification (after Folk 1965)	N. samples	Percentage (%)
Sand Very fine	3	0.2
Fine	469	29.8
Medium	540	34.3
Coarse	10	0.6
Sub-total	*1022*	*64.9*
Muddy sand	70	4.4
Sandy mud	29	1.8
Mud	23	1.5
Muddy gravel	3	0.2
Muddy sandy gravel	48	3.0
Slightly gravely sandy mud	2	0.1
Slightly gravely sand	46	2.9
Slightly gravely muddy sand	13	0.8
Gravel	14	0.9
Gravelly muddy sand	39	2.5
Gravelly sand	74	4.7
Gravelly mud	7	0.4
Sandy gravel	65	4.1
Hard ground	123	7.8
Total	*1574*	*100*

Trend lines

STA provides a means of analysis to derive sediment pathways, based upon an inter-comparison between sets of sediment grading data, to identify coherent trends between various samples which are interpreted as trend lines. These trend lines represent the probable net transport pathways for mobile surface heterogeneous sediments. In the context of sediment gradings data collected across Carmarthen Bay, 216 trend lines were resolved for sand dominant sediments. The remaining mud dominant samples were considered too few and too widely scattered to resolve meaningful trend lines.

Along the trend lines the sediment transport process may be interpreted as follows.

Dynamic equilibrium. The bed is neither accreting nor eroding, with the probability of finding a particular grain in the deposit equal to the probability of its transport and re-deposition. There is a fine balance between erosion and accretion.

Net accretion. More fine grains are deposited along the transport path than eroded, with the result that the bed, though mobile, is accreting. The mean particle size becomes finer, with improved sorting and negative skewness (Fig. 3a).

Net erosion. Sediment coarsens along the transport path, more grains are eroded than deposited, and the bed is undergoing erosion. The mean particle size becomes coarser, with improved sorting and positive skewness (Fig. 3b).

Mixed case. The transport pattern is approaching that of Dynamic equilibrium.

Total deposition. The bed is no longer mobile and is accreting under a 'rain' of sediment deposition that fines with distance from source. Such deposits are normally associated with a muddy environment.

In addition, since the trend lines are resolved from statistical based techniques it is possible to attribute each trend line with a measure of correlation (R^2) between adjacent sequences of grain size distributions. Hence, for a poorly resolved trend line the value of R^2 is likely to be low, e.g. <0.49, whereas a perfectly resolved trend line would have $R^2=1$.

The breakdown of interpreted trend lines within in each category, and the associated average R^2 value, is listed in Table 2. The pattern of trend lines across Carmarthen Bay is illustrated in Figure 4.

Overall, the level of correlation for each trend line is considered to be high. The 'dynamic equilibrium' is the most common type of resolved trend line across the study area.

Further interpretation of these trend lines has considered the sub-division of Carmarthen Bay into discrete sediment transport environments. A total of nine transport environments are described (Fig. 5).

Helwick Bank

A set of transport lines suggest a linkage with material input from the Bristol Channel with westward transport south of Helwick Bank and extending to the western end of the sandbank, beyond which they trend northwards into Carmarthen Bay to form a clockwise gyre ending at the crest of the bank (net accretion). The sediments in this transport regime are evidently are derived from ebb dominated tidal transport out of the Bristol Channel. However, the south side of Helwick Bank is made up of a considerable mixture of sediment types (e.g. sands and gravels; Fig. 2). It is suggested that this mixture of sediments reflect the erosion of earlier, glacially derived deposits, which may have contributed a source of sediments to Carmarthen Bay and the crest of West Helwick. The general pattern of net transport agrees with both the asymmetry of local bedforms and the typical clockwise sand transport patterns around sandbanks.

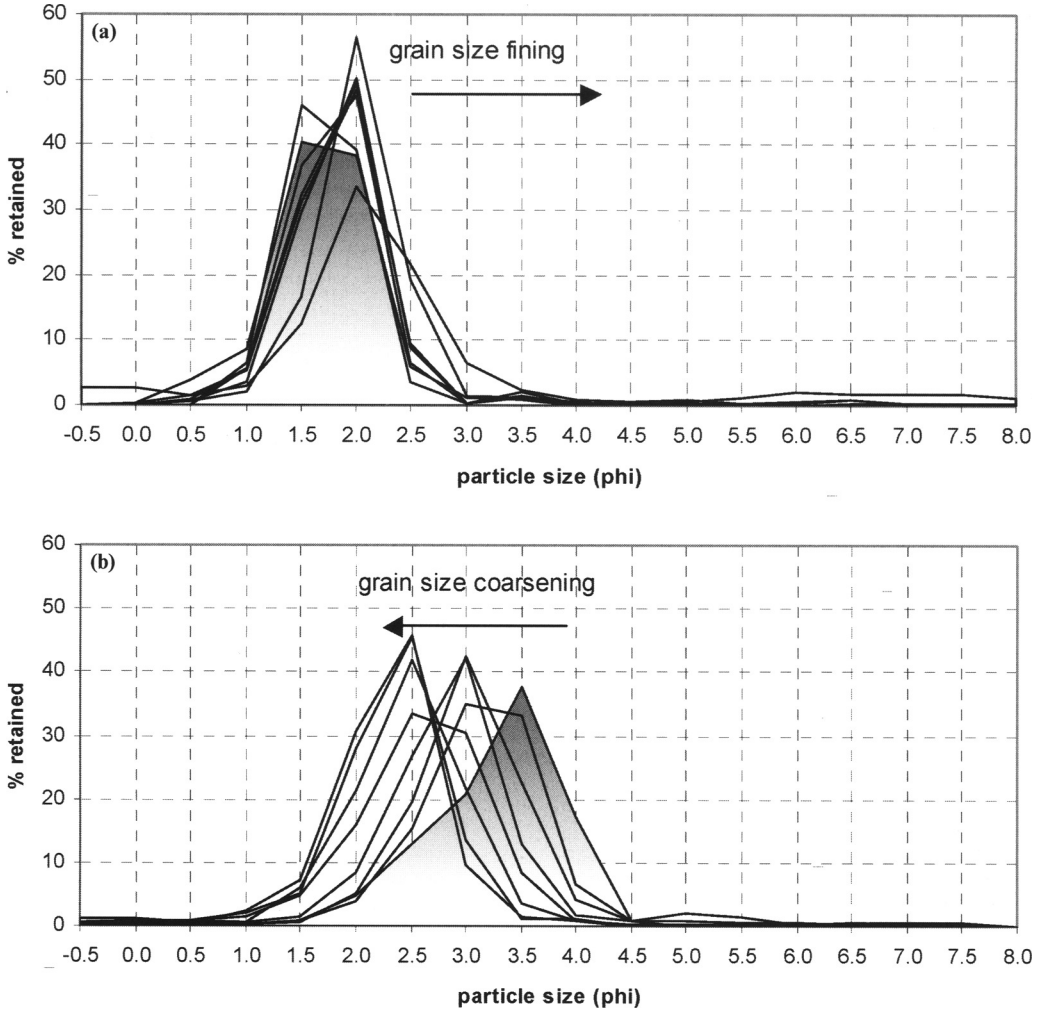

Fig. 3. Example of sediment trends along **(a)** a net accretion pathway and **(b)** a net erosion pathway.

Table 2. *Sediment trend lines*

Interpreted trend line	No. of lines	R^2 (all lines)
Dynamic equilibrium	84	0.93
Net accretion	47	0.89
Net Erosion	21	0.80
Mixed case	64	0.87
Total deposition	none	–

Port Eynon Bay Gyre

This small group of lines originates on the foreshore at the west end of Port Eynon Bay. They trend to the east along the beach in a direction compatible with the zeta, or 'fish hook' form of the bay, after which they curve seawards in a clockwise gyre. Here the trends are terminated by the strong ebb-directed transport regime described in the Helwick Bank transport environment. Of the four lines making up this transport regime, three of them show either mixed case or dynamic equilibrium, and one shows net erosion. It appears, therefore, that the coast of Port Eynon Bay may easily be subject to erosion as a result of a lowering foreshore.

Rhossili Bay Gyre

The sediment environment contains a set of trend lines which originate on the foreshore of Rhossili

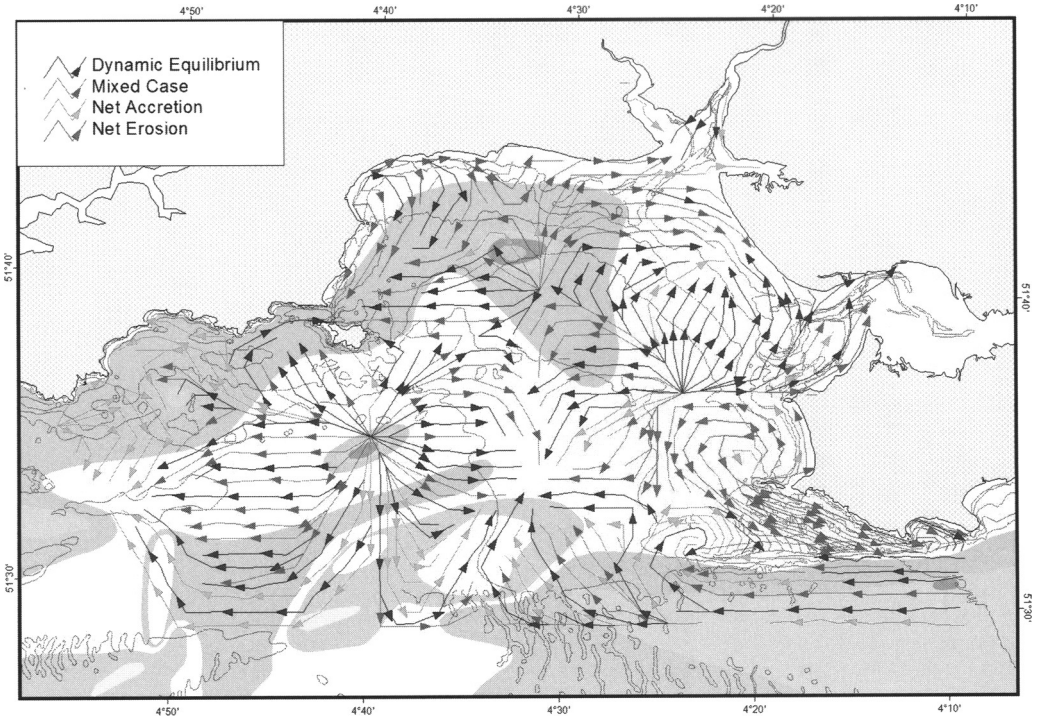

Fig. 4. Interpreted sediment trends across Carmarthen Bay.

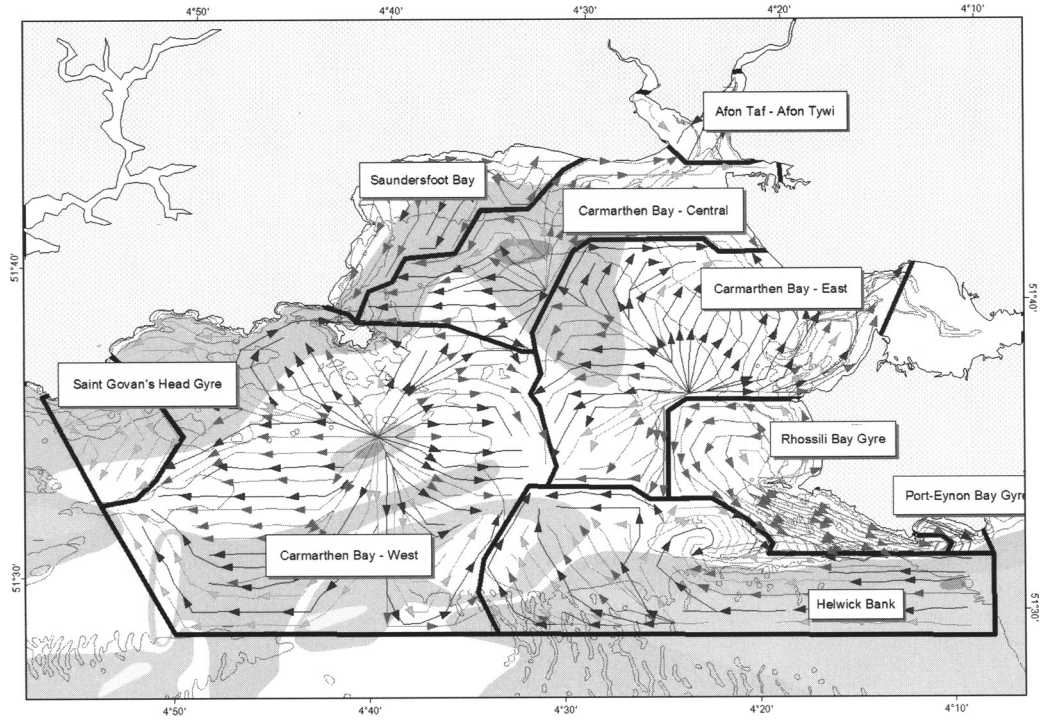

Fig. 5. Sediment transport environments.

Bay. Transport on the beach follows the zeta-form of the bay with trends to the north (assessed to be in response to a strong prevailing wave induced littoral transport), and extending clockwise to the offshore. From the offshore the lines eventually strike to the SE past Worms Head and into Helwick Channel. They terminate on the crest of Helwick Bank. The fact that over 90% of these lines show mixed case or net erosion suggests that the amount of sediment available for deposition is relatively small.

Carmarthen Bay East

This sediment transport environment contains a group of trend lines radiating to the north and into Burry Inlet, and comprise a combination of dynamic equilibrium and net accretion. Burry Inlet itself is regarded as a sink environment for sands.

Carmarthen Bay Central

Trend lines radiate to the west, north and NE where they link to pathways in the vicinity of the Afon Taf and Afon Tywi, where Net Accretion is resolved. The westward trending pathways are resolved as dynamic equilibrium and terminate north of Caldey Island.

Afon Taf–Afon Tywi

The sparsity of samples at this location may limit the interpretation. The few trend lines indicate that net sediment transport is in a seaward direction from both the Taf and Twyi rivers.

Saundersfoot Bay

The trend paths across Saundersfoot Bay are comparable to those described for Port Eynon Bay and Rhossili Bay. The transport paths originate on the foreshore and trend seawards to form a gyre. It is noteworthy that none of the lines shows net accretion; rather dynamic equilibrium, mixed case and net erosion dominate the dynamic behaviour of the sediments. It is to be expected that the shoreline of Saundersfoot Bay is susceptible to erosion.

Carmarthen Bay West

Trend lines radiate from the centre of this sediment transport environment in mainly east and west directions. Indirect evidence of a 'parting zone' at this point stems from the underlying pattern of sediment types which suggests a coarsening grading away from this location. Although lines of net accretion are scattered throughout this transport environment, they are relatively rare compared with those showing dynamic equilibrium and mixed case transport (78%).

Saint Govan's Head Gyre

This small group of lines forms a clockwise gyre in the vicinity of Saint Govan's Head. They are based on relatively few samples, and they are the only set of lines showing only net accretion. Against this finding is the irregular form of the sea bed with frequent areas of bedrock.

Limitations of STA

Whilst sediment trend analysis is a powerful technique in determining a probable net transport pathway for heterogeneous surface sediments, it is important to note a number of key limitations with the technique:

- STA does not identify the transport mechanism(s) along any trend line;
- STA does not identify the transport event(s) (i.e. a relict or contemporary event);
- it does not quantify the rate of transport;
- STA records the signature(s) of sediment transport which may be 'rewritten' after an atypical stronger transport event (i.e. a storm condition).

Hence, a set of STA results may contain a variety of mechanisms, events and rates across the set of trend lines. To support the further interpretation of the STA results across Carmarthen Bay the trend lines are considered against a range of other independent indicators of sediment distribution and transport. Further confidence in STA can be gained when all lines of evidence consistently support one general hypothesis. Consideration of individual sediment transport environments assists this interpretation where different process mechanisms may be responsible for the net transport, e.g. beach areas where littoral processes prevail.

Summary

Primary research for the BCMA project was targeted on Carmarthen Bay to understand better the relationship between the bay and the wider Bristol Channel sediment regime. A major part of the primary research related to the application of STA and the acquisition of over 1500 sediment samples. Results from the grab sampling provide an improved description of sediment coverage with a distribution that can be explained in relation to a tidally sorted system.

Fine sands are found in the inner part of the bay away from strong tidal flows characteristics of the main axis of the Bristol Channel, which is an area characterized by coarser sediment grades.

The grab samples provide the basis of the STA and reveal a complicated arrangement of net transport lines across Carmarthen Bay which suggest a semi-closed embayment with limited pathways exchanging sediments with the Bristol Channel. The main exception is around Helwick Bank, a large linear sandbank feature on the eastern side of the bay, and a site where aggregate extraction is presently licensed.

The authors wish to provide thanks to National Assembly for Wales, Hanson, Llanelli Sand Dredging and UKHO for providing data to the project.

References

AL-GHADBAN, A. N. 1986. *Sediment transport in Carmarthen Bay.* PhD Thesis. University of Wales.

ETSU 1989. *Tidal hydrodynamics, sediments, water quality, land drainage and sea defences. Detailed Report – Volume 1. Severn Tidal Barrage Project.* The Severn Tidal Power Group, ETSU TID 4060-P1.

FOLK, R. L. 1965. *Petrology of Sedimentary Rocks.* Hemphill Publishing Company, Austin, Texas.

HAINE, C. & COOPER, W. S. 2000. *Bristol Channel Marine Aggregates: Resources and Constraints.* Posford Duvivier Environment and ABP Research & Consultancy Ltd.

IGS 1983. *Lundy. Sheet 51°N–06°W. 1:25,000 Series. Sea bed sediments.* Institute of Geological Sciences, London.

MCLAREN, P. 1999. *Sediment Transport Analysis (STA) of Carmarthen Bay in support of the Bristol Channel Marine Aggregates Resources and Constraints Research Project.* Report to the National Assembly for Wales.

MCLAREN, P. & BOWLES, D. 1985. The effects of sediment transport on grain-size distributions. *Journal of Sedimentary Petrology*, **55**, 457–470.

MCLAREN, P. & KIRBY, R. 1998. *The sediment transport regime of Barnstaple Bay and its environs. Implications to shoreline management.* Report to Sedgemoor District Council.

Seabed sediment transport pathway investigations: review of scientific approach and methodologies

A. F. VELEGRAKIS[1], M. B. COLLINS[2,3], A. C. BASTOS[2], D. PAPHITIS [2] & A. BRAMPTON[4]

[1]*Department of Marine Sciences, University of the Aegean, University Hill, Mytilene 81100, Greece*

[2]*School of Ocean and Earth Science, University of Southampton, Southampton Oceanography Centre, European Way, Southampton SO14 3ZH, UK (email: mbc@noc.soton.ac.uk)*

[3]*Marine Research Division, AZTI Tecnalia, Herrera Kaia, Portu aldea z/g, Pasaia 20110, Gipuzkoa, Spain*

[4]*HR Wallingford, Howbery Park, Wallingford OX10 8BA, UK*

Abstract: An understanding of the geomorphological evolution of the coastal and inner continental shelf environments, in response to natural and/or anthropogenic forcings, depends upon a comprehensive knowledge of the prevailing sediment dynamics. In this contribution, selected methods/tools that can be used to study seabed mobility/transport patterns, are described and these all reviewed in relation to their inherent limitations.

The geological, morphological, hydrodynamic and sedimentary information (the environmental framework) necessary to develop a general understanding of the areas investigated are identified. This preliminary information prescribes the investigative tools to be utilized subsequently, i.e. the collection/analysis of data; these can define geomorphological and sedimentological indicators of sediment transport, hydrodynamic/sediment transport field observations and numerical simulations.

The results derived from the various methods can be used then independently or, preferably in combination, to establish conceptual models of seabed sediment dynamics over the investigated area. The coherence between the outputs of the different methods/tools controls the confidence level (high, medium or low) of the models. This approach is illustrated in relation to case studies from the southern UK inner continental shelf.

Coastal zones are presently under intensive development, represent some of the most popular tourist and recreational destinations, and constitute some of the most valuable real estate (GEO-3 2002). At the same time, the diverse usages of the coastal zones and nearshore areas (i.e. residential, commercial and industrial development, port development, pipeline placement, shipping, oil, gas and marine aggregate extraction, recreation, etc.) not only create conflicts of interest between different stakeholders, but also have significant environmental effects; these amplified further by various natural hazards, such as flooding, coastal erosion and other morphological changes (Flather *et al.* 1998; Eurosion 2003). Thus, there is an increasing demand for effective management, which should be based (amongst other considerations) on improved diagnoses and predictions of the coastal and shallow marine seabed morphodynamics. Such processes are controlled by the spatial and temporal variability in alongshore and/or onshore–offshore sediment transport (Wright 1995), sedimentary interactions between the coast and the inner continental shelf (<60 m) exert significant controls (e.g. Poulos *et al.* 2000) on the short-, medium- and long-term morphological evolution of these environments (e.g. De Vriend 1990; Cowel & Thom 1994). Therefore, the quantification/prediction of inner continental shelf seabed mobility, together with sediment transport pathways, are of considerable importance to coastal engineers/scientists and the public institutions responsible for the management of the coasts and the adjacent shallow-marine environments.

Sediment dynamics, i.e. the erosion, transport and deposition of sediments of the inner

From: BALSON, P. S. & COLLINS, M. B. 2007. *Coastal and Shelf Sediment Transport*. Geological Society of London, Special Publications, **274**, 127–146. 0305-8719/07/$15.00

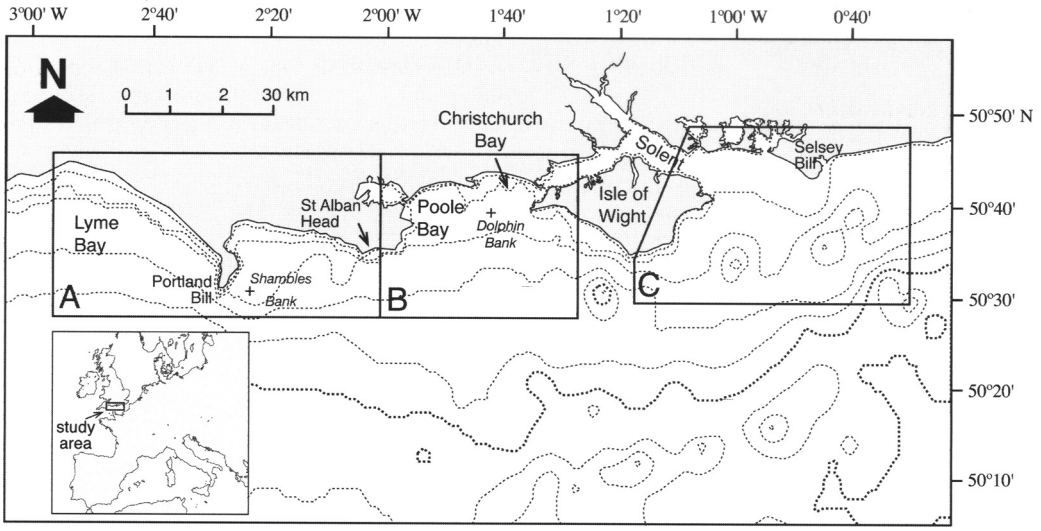

Fig. 1. Location of the regional sediment transport studies along the UK South Coast.

continental shelves, result from flow-seabed sediment interactions, i.e. form responses to momentum exchanges between the water flows and the sediments (Leeder 2000). However, as such momentum transfer functions are neither exact nor coherent (e.g. Sleath 1984; Soulsby 1997), the estimation of sediment mobility and transport rates is a complex undertaking; as such, it is subject to considerable error margins. Therefore, it would be beneficial, in terms of levels of accuracy and confidence in the determination of shelf sediment mobility and transport pathways, to use and compare different scientific methodologies and approaches. The final output of such investigations, i.e. a (conceptual) model of seabed sediment dynamics, should be based upon, and supported by, the weighted integration of the outputs of the different methods. Such methods could include: (a) seabed mapping, i.e. the mapping of the morphological elements of the seabed and the distribution of sediments and bedforms; (b) sediment transport studies, based upon hydrodynamic measurements (currents and waves) and the use of appropriate empirical formulae, to translate flow into sediment movement, taking into account sediment threshold; and (c) the construction/application of coupled hydrodynamic-sediment transport numerical models, to simulate seabed mobility and sediment transport pathways under different hydrodynamic regimes and time-scales.

The objective of the present contribution is to describe and review appropriate scientific methodologies, which can be used to provide seabed mobility estimations, through their application in three areas of the English Channel. These methods/tools are assessed here in terms of their accuracy and inherent limitations. A synthetic approach to sediment dynamics investigations is suggested, which consists of: (a) the study of the environmental framework, i.e. the background information necessary to provide an understanding of the basic processes of the investigated system; and (b) the application of various scientific tools/methodologies to investigate seabed sediment mobility and transport. Due to these inherent limitations involved in the tools/methods involved, it is important also to establish the levels of confidence that can be attached to the final products of such studies.

Case studies

Recently, a series of seabed mobility studies have been carried out over the southern UK inner continental shelf (Fig. 1), including: (a) the area between Lyme Bay and St Alban's Head (Bastos & Collins 2002); (b) Poole and Christchurch Bays, to the west of the Isle of Wight (IOW) (Brampton *et al.* 1998); and (c) the area between the eastern coast of the IOW and Selsey Bill (HR Wallingford 1993). Different methods have been used in each of these studies, including geomorphological and sedimentological investigations, hydrodynamic measurements and numerical simulations. Representative results are presented, in this contribution, together with conceptual models for two particular areas

of this region, namely the Shambles (Area A) and Dolphin (Area B) Banks.

Environmental framework

Characterization of the environmental setting forms the basis of sediment dynamic investigations and, as such, should be based upon the collation/acquisition of background environmental information concerning the geological/geomorphological setting; the seabed bathymetry; the prevailing hydrodynamic regime and its distribution; and the thickness and bedforms associated with the seabed sediments.

Solid geology and coastal geomorphology

The characterization of the geological and geomorphological setting of the area studied should be based upon a review of the seafloor solid geology and the adjacent coastal geomorphology. The influence of solid geology on the patterns of sediment transport and deposition, is evidently greater in the absence of any significant sedimentary cover; this, in turn is related to the differential erosion potential of the seabed, due to the presence/exposure of different rock types and structures and the development of solid geomorphological features (bedrock ridges) on the seafloor (Donovan & Stride 1961; Curry 1989; Evans 1992; Bastos *et al.* 2002). An assessment of the coastal geomorphology is relevant also at this stage of the investigation, as it provides information on the various offshore–onshore interactions as well as on the coastal sediment reservoirs, circulation cells and transport patterns.

Modern and antecedent seabed morphology

The study of seabed morphology constitutes a fundamental part of any investigation into sediment dynamics, as it can provide useful information on the location and extent of sedimentary deposits and potential areas of seabed erosion and deposition; in addition, accurate bathymetric data are fundamental inputs to sediment transport numerical simulations. The value of such information is exemplified by the bathymetric chart shown as Figure 2, which reveals the physiographic elements of the seabed in Area A. The chart indicates the presence of substantial concentrations of sediments (banks), on both sides of the headland; this in turn, suggests particular patterns of sediment transport and deposition. Finally, deposit dynamics can be resolved, through the comparison of sequential historical bathymetric charts and/or 'Fair Sheets' (see below).

The antecedent topography can also provide information on regional long-term sediment dynamics, as it controls the configuration of the seabed and the coastline by: (a) providing the regional slope and the large scale geomorphological elements; (b) establishing the original orientation with respect to prevailing hydrodynamic regime; and (c) the presence of Pleistocene ridges, valleys and interfluves, on which the Holocene coastal lithosomes have migrated and deposited (Belknap & Kraft 1981; Allen & Posamentier 1993).

Hydrodynamic regime

The regional hydrodynamic regime is assessed on the basis of existing time-series of current measurements (single-point and/or from bottom or hull-mounted acoustic doppler current profilers (ADCP)), wave rose diagrams, water level recordings and numerical model outputs (Fig. 3). Existing field data are essential also for the calibration/validation of numerical simulations; likewise, when designing subsequent field programmes of hydrodynamic observations.

Sediments

Characterization of the nature, distribution and thickness of the seabed sediments is necessary for the definition of the sedimentary facies distribution (Fig. 4); this, combined with a morphological chart, may provide crucial information on sediment transport pathways. In addition, the distributions of the sediment grain size parameters can be used in grain size trend analysis (GSTA) (see below), to form an essential input parameter for sediment dynamics numerical simulations.

Tools

The application of different research tools, independently or in combination (Table 1), in seabed mobility and sediment transport investigations has, as a main objective, the improvement of the levels of accuracy and confidence in the results. Each of the tools can provide 'independent' indicators of seabed sediment mobility and transport pathways, the coherence of which defines the levels of confidence in the results.

Geomorphological indicators

The integration of sediment erosion, transport and deposition processes shapes the seabed

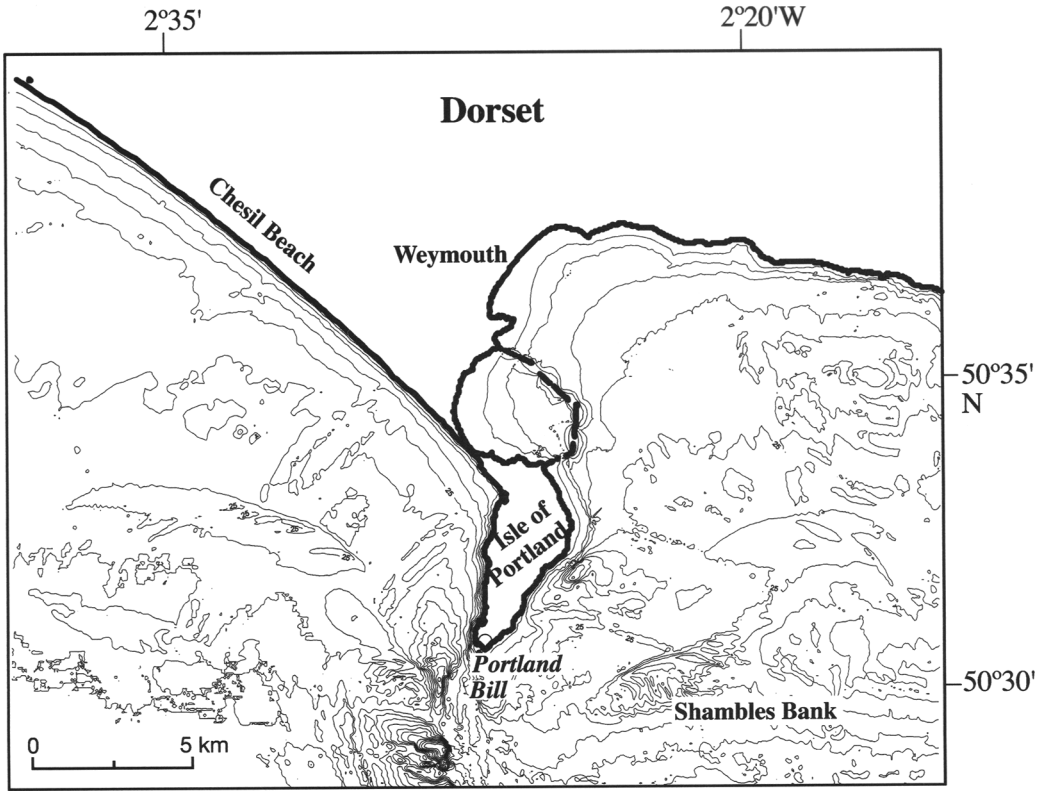

Fig. 2. Bathymetric map from the inner continental shelf around the Isle of Portland (Dorset). Contours are in metres below Chart Datum (after Bastos *et al.* 2002).

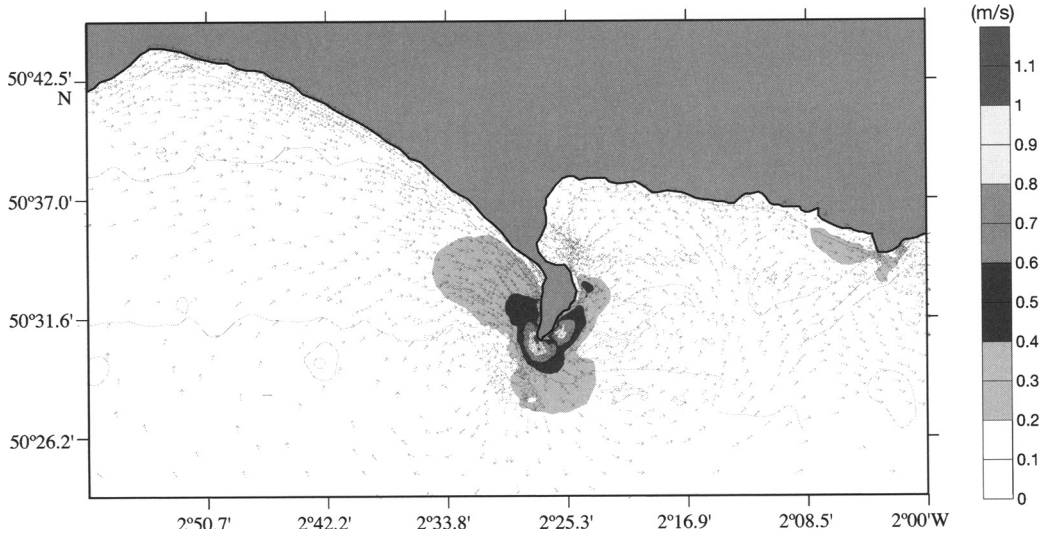

Fig. 3. Depth-averaged residual currents abstracted from the hydrodynamic model TELEMAC-2D, for the inner continental shelf around the Isle of Portland (after Bastos *et al.* 2003). It must be noted that hydrodynamic simulations require calibration/validation with field observations.

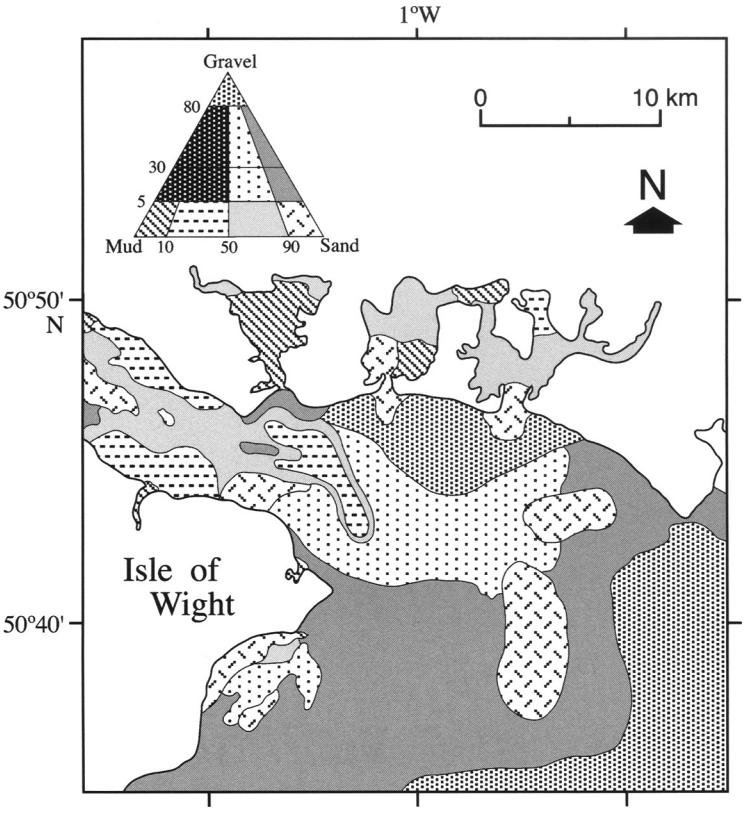

Fig. 4. Simplified surficial sediment distribution in the Eastern Approaches to the Solent (after Velegrakis, 2000).

Table 1. *Investigative tools used in each of the (case) study areas (for location, see Fig. 1)*

Investigative tools	Area a	Area b	Area c
Geomorphological indicators	√	√	√
Sedimentological indicators		√	√
Field observation	√	√	√
Potential seabed mobility	√		√
Sand transport rates	√	√	

morphology, whereas the temporal variability of these processes controls the seabed morphodynamics. Assuming that the seabed is in equilibrium with the prevailing hydrodynamic conditions, i.e. its sediments are being reworked by current and wave activity, it can be suggested that the seabed morphology and its changes reflect sediment transport patterns at different time-scales. Within this context, mobile surficial sedimentary structures (bedforms) can be considered also as significant geomorphological indicators (proxies) of seabed mobility and sediment transport pathways.

Seabed morphological evolution. The morphological evolution of the seabed can be investigated through the comparison of historical bathymetric charts and/or of time-series of recent bathymetric surveys. This comparison can provide information on deposit dynamics, at medium- and short-time scales, respectively. The technique of 'chart-differencing', to assess sequential bathymetric changes, has been used widely (Bowyer 1992; Brampton *et al.* 1998; Chamillon *et al.* 2002; Kapsimalis *et al.* 2005). This technique is based upon the comparison of sequences of historical bathymetric charts or, if available, of "Fair Sheets" which record the original depth measurements. The younger chart (or 'Fair sheet') is superimposed onto the older chart, and the depth difference at each point is recorded. However, in most cases the two data sets are transformed into regular grids of water

depths, the nodes of which have common geographical coordinates. The depths at each node are then compared with positive and negative residuals showing areas of net accretion and erosion, respectively. The resulting accretion–erosion patterns can be used subsequently as indicators of sediment transport patterns.

Nonetheless there are limitations of this technique concerning (Velegrakis 1994): (a) the actual accuracy of each individual data set, particularly those obtained in the distant past; (b) the utilization of different navigation/sounding systems within the various surveys, which results in comparisons between data sets with different errors; and (c) the different resolution of the charts–fair sheets, i.e. different spacings between the individual depth measurements. In addition, consideration should be given to errors arising from the usual practice of comparing interpolated depths at the constructed grid nodes, not actual depth measurements. The magnitude of these errors depends up on the density of the original measurements (Davis 1986), as well as the gridding method used (Bowyer 1992; Mat Zin *et al.* 1994). Finally, care should be taken when studying steeply sloping seabeds (e.g. bank flanks), where small navigational errors can result in the indication of large rates of accretion/deposition.

Bedforms. Over the inner continental shelf, two main types of structures develop on a sediment bed under the influence of water flows: flow parallel (e.g. sand ribbons) and flow transverse (e.g. sandwaves) bedforms (Belderson *et al.* 1982). Sand ribbons are longitudinal bedforms developing parallel to the flow (McLean 1981; Dalrymple *et al.* 1992), consisting of straight or slightly sinuous, elongate patches of sand; these rest upon a substrate of coarser sediments, or bedrock. Flow transverse bedforms are repetitive, dune-like shaped structures, which have their crests aligned perpendicular to the prevailing flow; they are characterized generally by a gently sloping upstream (stoss) flank and a steeply sloping downstream (lee) flank (Allen 1980; Amos & King 1984). The presence and morphological characteristics of bedforms can be used as proxies of seabed mobility and sediment transport pathways, respectively. Time-series of bathymetric/side scan sonar surveys can provide useful indications on short- to medium-term morphological changes, particularly in terms of bedform migration.

The asymmetry of flow-transverse (e.g. sandwaves) and the orientation of flow-parallel bedforms have been used extensively in the determination of sediment transport patterns on tidally-dominated continental shelves (e.g. Kenyon & Stride 1970; Johnson *et al.* 1982; Lanckneus & De Moor 1995). The use of flow-transverse bedforms, as indicators of sediment transport directions is based upon their cross-sectional asymmetry; the steeper side indicates the direction of transport and bedform migration. Nonetheless, some caution should be applied to the interpretation of such data sets.

As the cross-sectional asymmetry of the flow-transverse bedforms is hydrodynamically-controlled and shallow–marine environments are subjected to unsteady flows (i.e. tidal currents, wind and wave induced currents, waves), it can be temporally variable (e.g. Allen 1980; Berné *et al.* 1988, 1993; Harris 1991). Tidal flows, in particular, are characterized by significant temporal variability, in terms of their speed and direction, e.g. ebb–flood, spring–neap and longer period cycles. Thus, the cross-sectional asymmetry of tidally-controlled bedforms may be a function of the tidal stage during which the observations are obtained (Hawkins & Sebbage 1972; Harris & Collins 1984; Terwindt & Brouwer 1986; Bastos *et al.* 2004). This is especially true in the case of the smaller bedforms (e.g. the small and medium subaqueous dunes, see Ashley *et al.* 1990), which require smaller quantities of sediment to be transported across their crest by the reversing tidal flow in order to reverse their asymmetry. As such, their asymmetry should be used with particular care as an indicator of residual (net) tidal sediment transport.

The geometry of the large and very large dunes (with heights >1 m and wavelengths >10 m, Ashley *et al.* 1990) is more resilient than that of the smaller bedforms, as their cross-sectional asymmetry is less sensitive to ebb-flood and spring-neap flow modulations. However, if strong wind- and wave-induced currents are superimposed upon the tidal flow, then the morphology of these bedforms can also change significantly (Langhorne 1982; Harris 1991). It must be noted that highly energetic events are likely to be associated with large sediment fluxes (Vincent *et al.* 1998), which may define the regional residual (net) sediment transport. Thus, the direction of the net transport depends not only on local tidal flow asymmetries, but also on the resultant vector of the combined flows.

Particular considerations to be taken into account when using the cross-sectional asymmetry of flow-transverse bedforms as proxies of sediment transport directions are (Lanckneus *et al.* 2001): (a) the bedforms should be active, i.e.

their asymmetry should be defined by the prevailing hydrodynamic conditions; (b) the bedform asymmetry should represent long-term equilibrium, i.e. it should not reverse during a tidal cycle; and (c) the lee flank of the bedform (i.e. the steep slope) should be a depositional surface. In general, only the cross-sectional asymmetry of active large and very large subaqueous dunes (sandwaves) should be considered as an indicator of net (at least, tidally-induced) sediment transport directions. Nevertheless, the presence of small and medium dunes, which are often found superimposed upon the larger bedforms, provides an indication of seabed mobility and reveals short-term sediment transport. This approach, incorporating the interpretation of flow-parallel and flow-transverse bedforms over Area B, is summarized below.

In Area B, various bedforms have been observed (Velegrakis 1994): flow-transverse gravel waves, sand megaripples and sand waves (i.e. small, medium and large subaqueous dunes, according to Ashley *et al.* 1990), together with flow-parallel sand ribbons (Fig. 5). Cross-over point observations (i.e. side-scan sonar observations of the seabed obtained over the same area, at different tidal stages) have shown significant temporal variations in the cross-sectional asymmetry of the flow-transverse bedforms in most cases, particularly over the Dolphin Bank (Brampton *et al.* 1998). Moreover, the changes in the cross-sectional asymmetry of the sand megaripples/small sandwaves of the Dolphin Bank have been shown to be complex, as the bedforms do not simply reverse their cross sectional profile through the creation of 'ebb caps' (Boersma & Terwindt 1981) and/or by adopting 'cat back' forms (Smith 1969). Instead, they appear to change the orientation of their crests mostly by rotation (see below). These results show that bedform cross-sectional asymmetry should not always be considered as a reliable indicator of sediment transport directions, particularly over dynamic areas of the seabed.

Sedimentological indicators—grain size trend analysis

Seabed mobility studies have used a variety of indicators to assess sediment mobility and transport pathways. In addition to natural (Gao & Collins 1995) and artificial (Collins *et al.* 1995; Komar 1998; Voulgaris *et al.* 1999) tracers, grain–size distributions of seabed sediments can themselves provide useful information on sediment transport processes (e.g. Flemming 1977; Nordstrom 1989).

The presence of particular spatial relationships (trends) between the mean size, sorting and skewness of seabed sediments can be used to infer sediment transport directions and patterns. McLaren & Bowles (1985) developed a one-dimensional statistical technique (grain–size trend analysis), to define net sediment transport

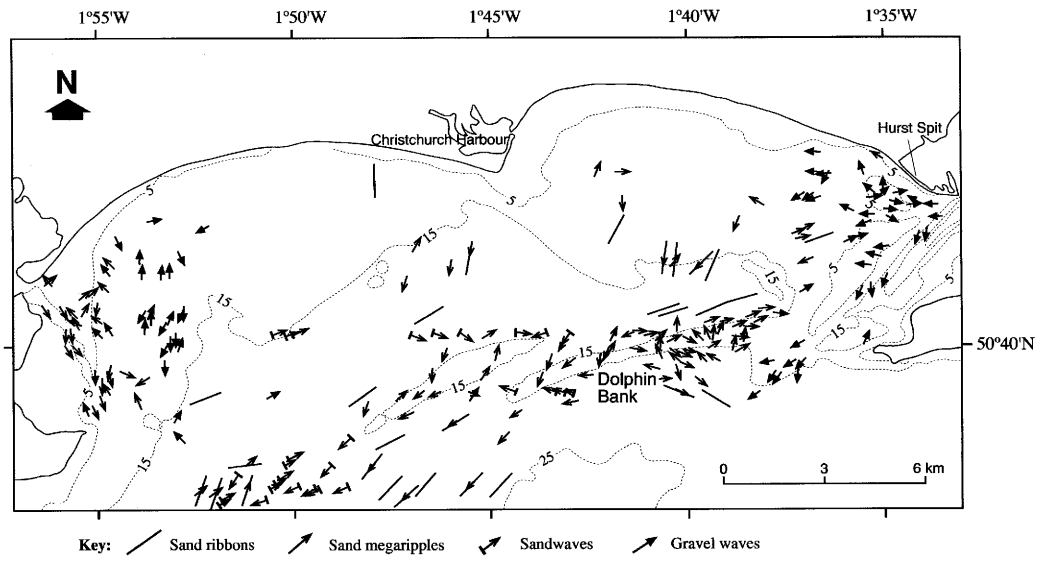

Fig. 5. Bedform distribution over Poole and Christchurch Bays (after Velegrakis, 1994).

along a particular sampling line. Gao & Collins (1992) refined and extended the technique to a two-dimensional procedure. The basic concept of the technique is that sediment size distributions are likely to show some ordered spatial patterns, in response to energy inputs and related sediment transport. The technique has been used in several coastal and inner shelf environments, with varying success (e.g. Masselink 1992; Gao *et al.* 1994; Pedreros *et al.* 1996; Van Wesenbeeck & Lanckneus 2000).

The limitations associated with the grain–size trend analysis are due mainly to: (i) the nature of the sampled sedimentary environments; and (ii) the nature of the data sets. The determination of sediment transport pathways, on the basis of grain size parameters (separately, or in combination) can be a complex exercise, as sediment transport can also be influenced by processes which may be independent of the transport mechanisms themselves. One basic requirement of the grain–size trend analysis is that its application should not extend beyond the boundaries of a particular sedimentary environment (Gao & Collins 1992). A sedimentary environment is characterized by (at least) one major process response mechanism, but in most cases there are several mechanisms acting either independently in different parts of the system or sequentially within the same area (Reineck & Singh 1973).

For example, abrasion along a transport pathway may affect both the mean size (Pettijohn *et al.* 1972) and the sorting of the sediments, depending on the mineralogy of the original deposit (Velegrakis 1994). Selective transport, caused by differences in particle density and shape, may also result in modification of the statistical parameters of the sediment grain–size distribution (Komar 1977), whereas mixing of sediments from different sources (Self 1977; McManus *et al.* 1980) may also change significantly the grain–size characteristics (Flemming 1988). Therefore, the grain–size trend analysis tends to produce the best results in areas with sediments consisting of unimodal and texturally 'mature' sediments (Folk 1980) of sufficient thickness, as polymodal distributions not only suggest different modes of transport and/or mixing of sediments, but impose serious limitations upon the accurate definition of the grain size parameters themselves. Sediments of low textural 'maturity' may show unpredictable changes in the grain–size parameters during the course of transport, in response to abrasion; they may introduce uncertainties concerning their hydraulic behaviour if mechanical sieving is used in their grain–size analysis (Flemming 1977). Finally, thin deposits may be subject to 'contamination', by sediments produced by the erosion of the underlying bedrock (Curry 1989).

An implicit requirement of the analytical procedure proposed by Gao & Collins (1992) is that the sampling sites should form a regular grid. In this case, the comparisons suggested in the technique do not introduce a bias in the residual trends, as the grain–size parameters of each sampling site are compared with the parameters of the same number of neighbouring sites; likewise, the resultant vectors of all the sites have the same statistical weight. In contrast, if the sampling sites do not form a regular grid, then a bias in terms of the length and direction of the resultant vectors might be introduced. In practice, very few data sets comply with this requirement as, in most cases, the sampling sites form irregular grids; this is either because they are so designed or due to sampling survey practicalities.

The Gao & Collins (1992) technique produces its best results when all the above limitations have been minimized. As a first step, sedimentary environments fulfilling the basic requirements of the method are identified and the spatial distribution of the sampling sites in these environments is considered. In order to avoid problems arising from comparing samples collected on the basis of an irregular grid, to increase the spatial resolution of the method, transformation of the data sets can be performed. The theoretical basis of this transformation lies in the principle that, in any sedimentary environment where the basic requirements of the trend analysis are fulfilled, the grain size parameters of the surficial sediments can be considered as regionalised (i.e. spatially continuous) variables (Davis 1986). In this case, it is possible to estimate the value of these variables, at any location of the sedimentary environment, by interpolation. Thus, the grain–size parameters derived from the analysis of the sediment samples can be transformed to form regular grids, within the area under investigation.

In summary, the trend analysis can provide its best results when it is applied to unimodal, texturally 'mature' deposits of sufficient thickness, which are subject to a singular principal mode of transport. If mechanical sieving is used in the grain size analysis, there are additional requirements concerning sediment origin (mineralogy) and mean grain size. Examples of the trend analysis application in two different areas, in terms of the technique's requirements (Areas B and C), are presented below.

In Area C (Fig. 6a), the grain–size trend analysis was applied over an area of the seabed characterized by a variety of seabed sediments (see Fig. 4), which can hardly be considered as a singular sedimentary environment. Although

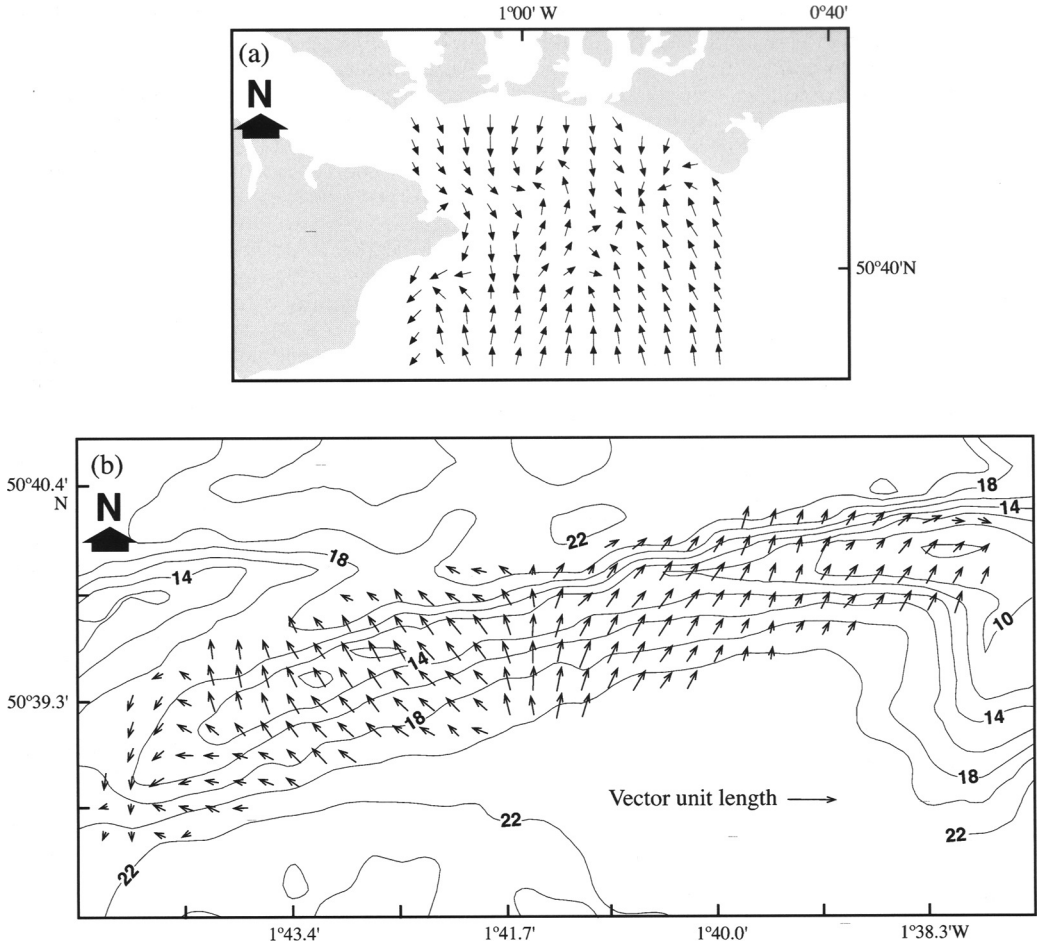

Fig. 6. Sediment transport pathways derived on the basis of grain size trend analysis, (a) over the East Solent (after Paphitis *et al.* 2000); and (b) over the Dolphin Bank, Christchurch Bay (after Velegrakis, 1994).

these results appear to be in broad agreement with those obtained from different methods/tools (Paphitis *et al.* 2000; Sharples 2000; Teles 2003) they should be, nevertheless, viewed with caution as this basic requirement of the technique is not fulfilled. In comparison, the application of the trend analysis over the Dolphin Bank area (Area B) fulfils all the requirements of the technique. The surficial sediments of the bank consist of medium to fine grained (mean size 1.4–2.45φ), moderately well to very well sorted (0.65–0.26φ) quartz sands, with both "opaque" minerals and biogenic material (shell debris) constituting less than 5% of the sediments (Velegrakis 1994). The results show intriguing patterns of trend vectors (Fig. 6b), suggesting divergence of sediment transport in the middle section of the bank.

Independently of whether or not the trend analysis is applied, any seabed mobility study should be based upon an accurate sediment distribution map. Thus, it is crucial to have a good sampling plan and consider the hydrodynamic conditions during and/or before the sampling, as these may influence the results.

Hydrodynamic and sediment transport field observations

Field hydrodynamic (Eulerian) observations, incorporating data from wave and near-bed flow sensors, can be used to characterize the hydrodynamic regime at specific locations of the investigated area. These observations can be coupled with concurrent observations of seabed mobility

and/or water column turbidity, to provide information on the ability of the water flow to mobilize and/or suspend the seabed sediments, i.e. on the momentum transfer function between the flow and the seabed sediments.

The observations can be either of low-frequency (i.e. less than 2 Hz, two measurements per second) or of high-frequency (higher than 3–4 Hz, 3–4 observations per sec). The benefit of using high-frequency sensors is that they allow analysis of particular flow characteristics (i.e. of the turbulent flow fluctuations). These can be then utilized to estimate bed shear stresses, using either the Reynolds stresses (e.g. Heathershaw 1988) and/or the inertia dissipation method (Huntley 1988). Limitations are related to the relatively short time-series they produce. In contrast, low-frequency flow measurements cannot resolve turbulence. Therefore, they provide less rigorous assessments of the bed shear stress using the logarithmic velocity profile method (if multiple height flow measurements are obtained) (Soulsby 1997) and/or the quadratic friction law (Sternberg 1972). However, they can be extensive in terms of time-series length.

Observations of seabed mobility/sediment resuspension can be carried out using various methods, such as sediment traps (Carling 1983), underwater cameras (Hammond *et al.* 1984), optical backscatter (Lecouturier *et al.* 2000; Paphitis & Collins 2005) and acoustic backscatter (Vincent *et al.* 1998) sensors, as well as the acoustic detection of sediment movement (Williams *et al.* 1989; Voulgaris *et al.* 1995). Such observations have been used extensively to assess seabed mobility and sediment resuspension, under various hydrodynamic forcings. In terms of establishing sediment transport rates and pathways, observation-derived bed shear stress time-series can be used, in conjunction with transport rate empirical formulae, to estimate sediment transport rates/directions at a particular location (Fig. 7). In tidal areas, averaging such transport rate time-series over an appropriate period (preferably over two complete neap/spring cycles, i.e. 29 days), can provide information on net (tidal) sediment transport directions. However, in wave-dominated or mixed-energy environments, superimposed wave effects should also be considered (Pattiarachi & Collins 1985; Vincent *et al.* 1998).

It must be noted that, although modern instrumentation is capable of measuring waves, currents and turbidity with an appropriate resolution/accuracy, the estimation of sediment transport rates is based upon theoretical models, algorithms and empirical formulae (Soulsby 1997). Consequently, the results may vary significantly depending on the particular method used (Heathershaw 1981; Dyer & Soulsby 1988; Van Rijn 1993). Moreover even though reasonable results can be obtained in terms of seabed mobility/sediment transport directions, estimated transport rates may vary within orders of magnitude. Indeed, it is an achievement to derive different predictions that lie within an order of magnitude.

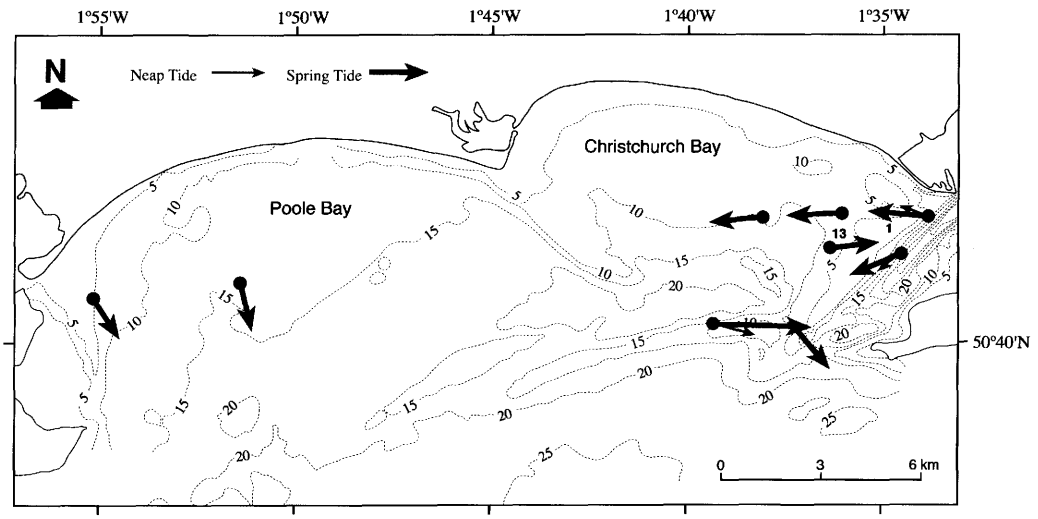

Fig. 7. Bedload transport vectors, predicted from near-bed current meter measurements, over Poole and Christchurch bays. Predictions are for currents alone during spring (thick arrows) and neap tides (thin arrows) (after Velegrakis, 1994).

Numerical simulations

Numerical sediment transport models are useful tools in sediment transport studies, particularly when a synoptic picture of potential seabed mobility and sediment transport patterns is required, over large areas of the inner continental shelf. Such models can be used to investigate patterns of sediment movement, under different sets of prevailing hydrodynamic conditions. It must be emphasized that in order to obtain successful predictions from such models, they must be calibrated/validated sufficiently by field data.

Seabed mobility and resuspension potentials. The assessment of the ability of the prevailing hydrodynamic conditions to mobilize and/or suspend the seabed sediments (i.e. seabed mobility and resuspension potentials), is of paramount importance in sediment dynamic investigations. These potentials can be assessed in terms of the percentage of time (at different temporal scales) during which the prevailing currents and waves are capable of mobilizing and suspending the seabed sediments within the investigated area. Thus, the bed shear stresses, estimated on the basis of a coupled hydrodynamic/sediment transport model can be compared with the stresses required to mobilize and/or suspend the seabed sediments (i.e. the threshold values for sediment movement and resuspension, respectively), at each cell of the model grid and at each time step; integration of the results provides the seabed mobility/resuspension potentials as percentages of time over a selected temporal scale (Fig. 8). Although these studies do not provide information on sediment transport patterns, they are extremely useful to investigate the combined effects of waves and currents (Velegrakis *et al.* 1999), as well as human interference effects on the seabed, such as sediment (aggregate) extraction (e.g. HR Wallingford 1993; Brampton *et al.* 1998).

Sediment transport rates and patterns. Sediment transport models can be used also to predict instantaneous and/or temporally integrated (net) transport rates and directions; they reveal patterns of sediment movement, at different time-scales and under various hydrodynamic conditions. Such models can provide assessments on the influence of superimposed wave activity on the background flow (Pattiaratchi & Collins 1987), indicating the presence of convergence and/or divergence of sediment movement (Fig. 9). Although numerical simulations of sediment transport rates and patterns have been used widely (e.g. Grochowski *et al.* 1993; Amos *et al.* 1995; Bastos *et al.* 2003), their application should always be carried out carefully; in particular, they require rigorous validation by field observations using, amongst other approaches, sediment traps, tracer dispersion and bedform migration studies.

The main problems in modelling sediment transport rates/patterns are related to: (a) the modelling of the bed shear stresses, in the case of combined flows (Soulsby 1997); (b) uncertainties involved in the translation of 'excess' bed shear stresses, i.e. the shear stresses above the critical values for sediment movement, into sediment transport rates (Williams *et al.* 1989; Huntley & Bowen 1990; Madsen 1993); (c) the effects of seabed morphology on both the threshold of motion (Evans & Hardisty 1989) and the sediment movement after the initiation of motion; and (d) uncertainties on seabed sediment characteristics and their associated roughness (Komar & Li 1986; Van Rijn 1993). Therefore, although numerical models can simulate flows quite efficiently, estimated transport rates may vary by orders of magnitude depending upon the algorithm used (Soulsby 1997).

'Levels of confidence' in conceptual seabed mobility models

In the previous Sections, the various tools/methods that can be used in the study of sediment transport patterns and pathways, in inner continental shelf environments, have been reviewed. Each of the methods described has shown to be associated with inherent limitations; and should be used with caution. Nevertheless, comparison and integration of the outputs from different methods can not only evaluate the precision of each of the methods, but also establish the levels of confidence in the final seabed mobility and sediment transport outputs (conceptual models). This approach is described here, using two examples: (a) the Shambles Bank (Area A); and (b) the Dolphin Bank (Area B).

The Shambles Bank

Sediment transport over the Shambles Bank (Fig. 1) has been investigated using different methods/tools including: (i) bedform asymmetry, obtained from bathymetric and side-scan sonar surveys; (ii) hydrodynamic (ADCP) field measurements; and (iii) a 2D coupled hydrodynamic sediment transport model. Although the model-derived sediment transport rates varied by $\pm 50\%$, depending up on the algorithm used, the results from the different methods have revealed

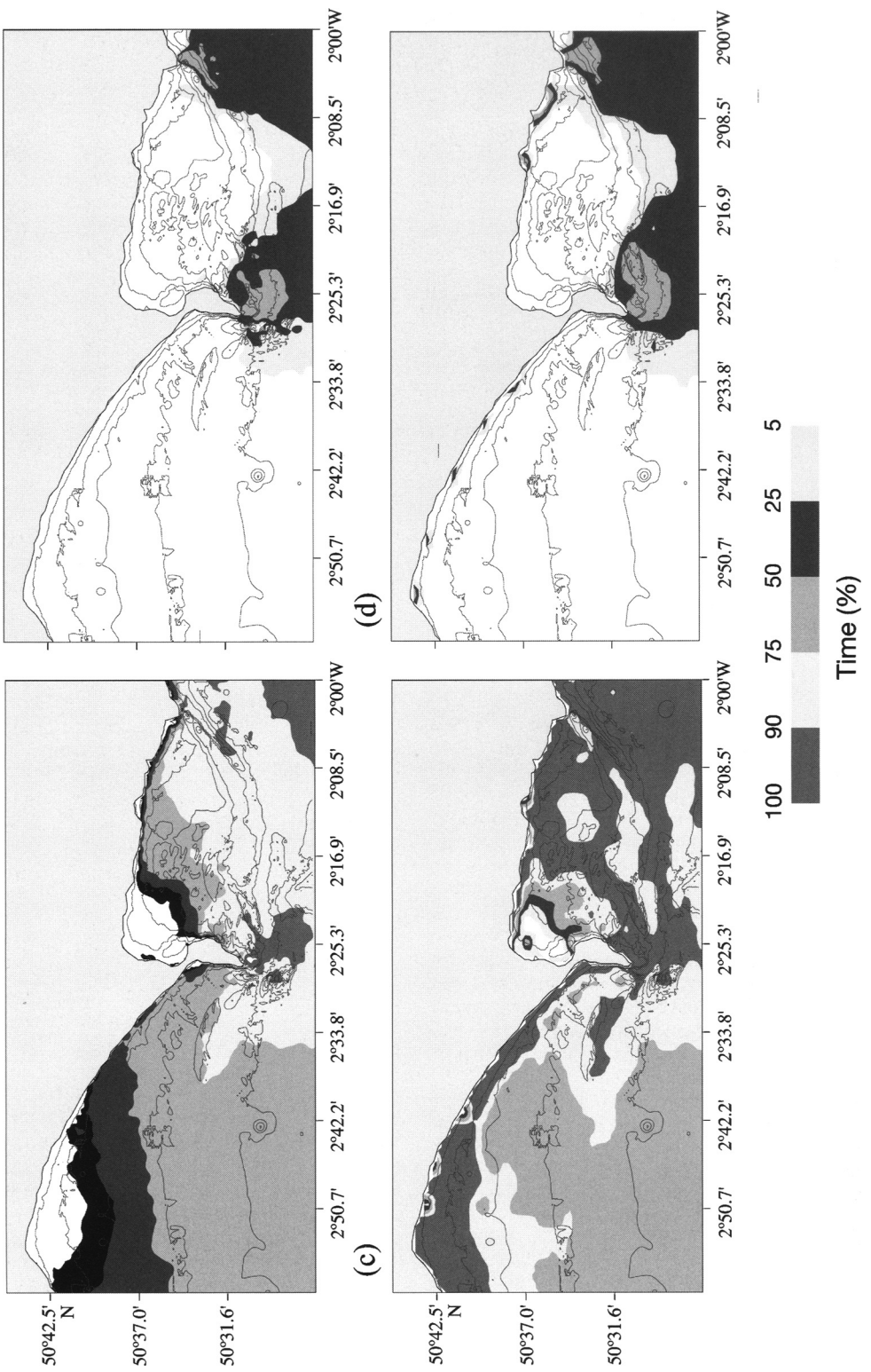
(a)
(b)
(c)
(d)
50°42.5' N
50°37.0'
50°31.6'
2°50.7'
2°42.2'
2°33.8'
2°25.3'
2°16.9'
2°08.5'
2°00'W
100
90
75
50
25
5
Time (%)

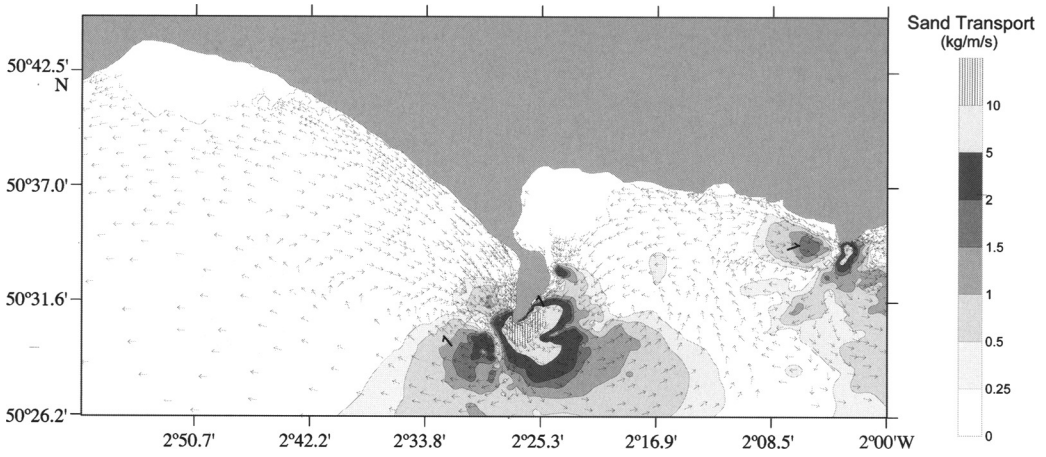

Fig. 9. Predicted net bedload transport rates (kg/m/s), under currents alone, over Area A (for location, see Fig. 1). This simulation was undertaken using hydrodynamic (the TELEMAC 2D) and sediment transport models (SEDTRANS).

similar sediment transport patterns over the bank, indicating sediment transport convergence towards its crest (Fig. 10a). Comparison of the bedload transport rates derived from the numerical model with hydrodynamic data has shown that this convergence zone is associated with a gradual (tidal) flow/sediment transport decrease towards the bank's crest; this suggests sediment deposition there. However, it must be noted that these results refer to the background (tidal) energy, i.e. do not consider wave-induced effects, which are likely to control the vertical growth of banks (Pattiarachi & Collins 1987; Houthuys *et al.* 1994; Dyer & Huntley 1999). The net sediment transport directions, inferred from the different methods, show relatively small discrepancies (differences of about 20°). This suggests, in turn, significant coherence between the outputs. In this comparison, only the asymmetries of the very large asymmetric subaqueous dunes (sandwaves) (with heights and wavelengths more than 5 and 100 m, respectively) have been considered, as indicators of net sediment transport directions. The smaller bedforms have been found to reverse their asymmetry, during the tidal cycle (Bastos *et al.* 2004). The integration of the results from the different methods show that a conceptual model (Fig. 10b) of sediment transport pathways around the Shambles Bank (Bastos & Collins 2002; Bastos *et al.* 2003) can be proposed with a *high* level of confidence, i.e. minimal contradiction between the outputs of the various approaches.

Fig. 8. Results of the simulation of potential seabed mobility and resuspension over Area A (for location, see Fig. 1): potential mobility (a) and resuspension (b), under currents alone; and (c) and (d) the same variables, under the combined action of currents and waves, respectively.

The Dolphin Bank

Transport patterns over the Dolphin Bank (Fig. 1) have been studied, using: (i) geological/sedimentological indicators, i.e. sediment distribution/thickness and grain–size trend analysis; (ii) bedform distribution and asymmetry; and (iii) sediment transport rates, derived on the basis of Eulerian current meter measurements and empirical sediment transport formulae. Seismic investigations undertaken over the area (Velegrakis 1994) have shown that the bank (Fig. 11a) forms one of the main sand stores in Poole and Christchurch Bays. The seabed to the north and south of the bank is covered by a mostly thin modern sedimentary cover (Brampton *et al.* 1998). To the ENE of the bank there is a large gravel/sandy gravel deposit (the Shingles Bank). The geophysical data have also shown that the Dolphin Bank sediments (max. thickness of 8 m) rest unconformably either on an undulating bedrock erosional surface or, in the case of the eastern extremity of the bank, on older coarser sediments. The sand deposit is non-uniform in thickness, forming two local 'depocentres', separated by a local thinning of the deposit situated within the middle section of the bank. In this area, the bedrock erosional surface is at a much higher elevation than that of the adjacent areas (Velegrakis 1994).

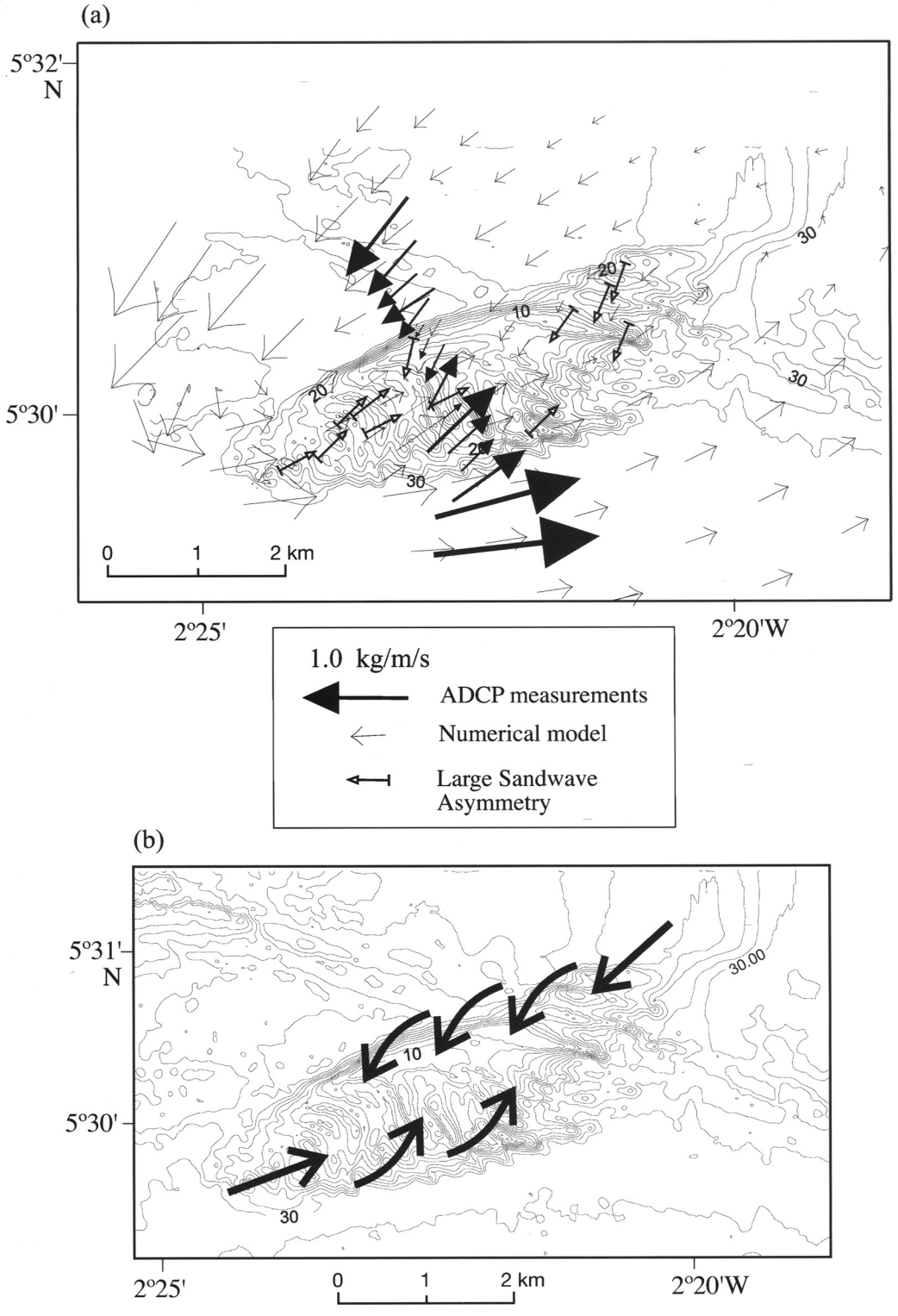
(a)
5°32' N
5°30'
10
20
30
0 1 2 km
2°25'
2°20'W
1.0 kg/m/s
ADCP measurements
Numerical model
Large Sandwave Asymmetry
(b)
5°31' N
5°30'
10
30.00
30
2°25'
0 1 2 km
2°20'W

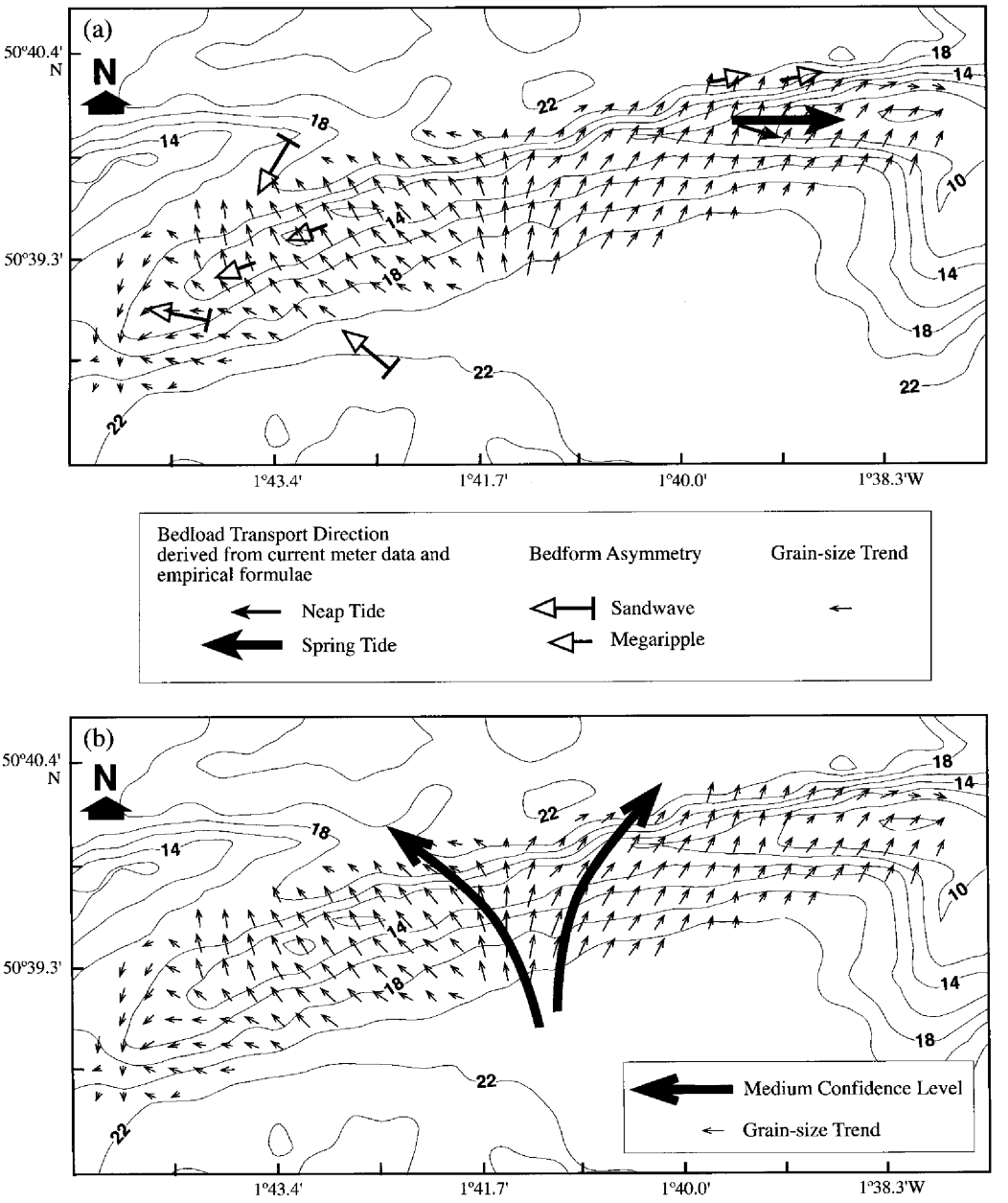

Fig. 11. (**a**) Integrated analysis of sediment transport pathways over the Dolphin Bank and (**b**) conceptual model of sediment transport pathways, showing the different levels of confidence. For location, see Fig. 6.

Fig. 10. (**a**) Integrated analysis of sediment transport pathways over the Shambles Bank; and (**b**) conceptual model of sediment transport pathways, showing a high confidence level based upon three different scientific methods.

The divergence of the grain size trend vectors, over the middle section of the sandbank (Figs 6 and 11a), suggests that material from this area moves towards both the east and the west. The general direction of the trend vectors suggests

that the bank is supplied mainly from the south and that there is no (net) sand transport from both flanks towards the crest; however, this does not mean that such sand movements do not occur; the averaging procedure used to obtain the resultant vectors may have filtered out all the minor trends. The architecture of the deposit appears to corroborate the output of the trend analysis, as thinning of the deposit over the middle section of the bank coincides with the area where the trend analysis shows divergence in the trend vectors. The evidence obtained from the bedform distribution and dynamics suggests high seabed mobility, but it is inconclusive in terms of sediment transport directions. Nevertheless, it must be noted, that, even if the bedform asymmetry were more consistent indicator, it is unlikely to be comparable directly to the trend analysis results (see also Van Wesenbeeck & Lanckneus 2000). This association is because bedform asymmetry is related mostly to tidal flow/sediment interactions, whereas grain size trends are likely to integrate also wave effects.

The near-bed (at 1 m above the bed) hydrodynamic data (Figs 7 and 11a) have shown there to be strong flood currents (of up to 110 cm s^{-1}, on springs) and weaker (of up to 90 cm s^{-1}, on neaps) temporally variable in terms of the direction of the ebb currents. This ebb current variability may explain the complex changes in the cross-sectional asymmetry of the bedforms over this area. Finally, sediment transport estimations established on the basis of the near-bed hydrodynamic data have shown that, at least over the area of the observations, there is a substantial sand transport towards the east.

Comparison between the results from all of the methods/tools used shows only partial agreement. Although the deposit architecture and the grain–size trend analysis suggest bedload divergence over the middle section of the Bank (Fig. 11a), the evidence provided by the bedform asymmetry is inconclusive. Moreover, hydrodynamic data have been collected at only one location. Thus, although these data suggest sediment transport towards the east, at this location (which is more or less compatible with the results of the trend analysis: a difference of about 45°), they cannot corroborate by themselves the results from the other methods, particularly as they do not represent wave conditions (Velegrakis *et al.* 2000). Therefore, the sediment transport conceptual model proposed for the Dolphin Bank (Fig. 11b) should be characterized as being of *low/medium* confidence, i.e. showing some disagreement between the various outputs.

Discussion

Following the review of the principles/limitations of the different methods/tools that can be used in sediment transport studies, together with the assignment of confidence levels on integrated/synthetic approaches, there are still two important issues to be discussed: (1) how and at what cost the confidence levels can be improved; and (2) at which temporal scales can results from the inevitably short-term observations/simulations be relied upon.

The answer to the first question posed is not straightforward, as it will be always dependent upon the research objectives, the funds available and the type of sedimentary environment being investigated. The experience gained from the southern UK inner continental shelf suggests that various sets of observations are essential to obtain a high level of confidence in the final models. However, marine research is subjected usually to time and financial restrictions; as such, it is only under ideal circumstances that a systematic and integrated approach can be completed in its entirety. Therefore, it must be decided beforehand which level of confidence within the final result is acceptable for each particular application. This decision will define the kind and spatial temporal resolution of the field observations, as well as the type of numerical simulations to be used.

Confidence levels improve on the basis of the spatial resolution of the field observations. Such spatial resolution should reflect the processes acting, not only at the scale of the sedimentary environment, but also at spatial scales representative of its different (hydrographical/sedimentological) elements. For example, the hydrodynamic/sediment transport observations carried out in Area B (Fig. 7) show large diversity in their concluding outputs; this reflects their different physiographic/sedimentary elements (ebb-tidal deltas, offshore banks etc). Observations of lower spatial resolution would have been inadequate for the purpose representing the processes acting and of the calibration/validation of any numerical simulations. At the same time, it should be kept in mind that very detailed information might reveal only minor trends of the system and obscure the larger picture.

The length and temporal resolution of the field data sets are very significant parameters in the characterization of sedimentary environment processes that act at different time-scales. For example, in order to identify changes in bedform morphology, sequential bathymetric surveys are required; the period of these is dependent upon

the bedform scale. Thus, repeated surveys undertaken during an ebb-flood tidal cycle will reveal only the dynamics of small bedforms (e.g. Bastos *et al.* 2004), whereas the study of the dynamics of large bedforms requires surveys of longer period (Lanckneus & De Moor 1995). Moreover, as sediment mobility and transport on the inner continental shelf is forced by various unsteady flows, the length/resolution of hydrodynamic/sediment transport field data should be sufficient to provide information on all the important forcings of the system (together with their variability). It should be kept in mind that, although the 'background' hydrodynamic energy of a sedimentary environment is very important, it is often the extreme events that produce large sediment energy fluxes (Vincent *et al.* 1998); these, in turn, can induce large morphological and sedimentological changes (Duke *et al.* 1991; Dalrymple *et al.* 1992).

Numerical simulations are powerful tools in sediment transport studies, as they can provide synoptic views at different time-scales. However, as the results are influenced by uncertainties, particularly in their sediment transport modules (see p. 16), their range increases with the time of simulation. Therefore, in the absence of data assimilation correction procedures, long-term predictions should be considered with caution. Moreover, the diagnostic/predictive ability of seabed mobility sediment transport models is highly dependent upon the quality of the data used for their set-up, calibration and validation. Thus, temptations to carry out simulations supported by the minimum amount of field data should be resisted.

Finally, it should be mentioned that the sedimentary processes of the inner continental shelf are controlled also by the sediment supply from the adjacent land drainage basins. Thus, natural precipitation/river discharge changes (Tsimplis *et al.* 2004) and/or anthropogenic changes in sediment supply (Poulos & Collins 2002) from the surrounding drainage basin areas might result in significant sedimentary and morphological changes on the inner continental shelf.

Conclusions

The planning and implementation of sediment dynamics investigations in shallow marine environments, present a substantial challenge. This contribution has reviewed the principles/limitations of different methods/tools that can be used to study sediment mobility and sediment transport; similarly, it has presented an approach based upon the integration of results from different methods/tools that can evaluate the individual results. Such integration can increase the level of confidence in the final conceptual model.

Different investigations (case studies) carried out in the southern UK inner continental shelf have been used to exemplify the proposed approach. Conceptual models of sediment dynamics have been presented for some of these areas, related to different levels of confidence. These confidence levels have been established on the basis of a comparison of the results from different methods. *High* confidence sediment transport patterns represent agreement between the results from all the methods used. When the results of (at least) two of the methods used are in agreement, the final model can be characterised as a *medium* confidence model. Finally, *low* confidence implies the absence of any coherence between the results.

The authors would like to thank the various organisations and institutions that supported in various ways the research on which this contribution is based. Appreciations are due (amongst others) to the Crown Estate Commissioners, SCOPAC, CIRIA, New Forest District and Dorset County Council. Kate Davis is thanked for her professional drawing of the figures. The two referees (J. Mc Manus and V. Van Lancker) are thanked for their valuable inputs, which improved the final manuscript.

References

ALLEN, G. P. & POSAMENTIER, H. W. 1993. Sequence stratigraphy and facies model of an incised valley fill, the Gironde Estuary, France. *Journal of Sedimentary Petrology*, **63**, 378–391.

ALLEN, J. R. L. 1980. Sand waves, a model of origin and internal structure. *Sedimentary Geology*, 26, 81–321.

AMOS, C. L. & KING, E. L. 1984. Sandwaves and sand ridges of Canadian Eastern Seaboard, a comparison to global occurrences. *Marine Geology*, **57**, 167–208.

AMOS, C. L., BARRIE, J. V. & JUDGE, J. T. 1995. Storm-enhanced sand transport in a macrotidal setting, Queen Charlotte Islands, British Columbia, Canada. *In*: FLEMMING, B. W. & BARTHOLOMA, A. (eds) *Tidal Signatures in Modern and Ancient Sediments*. Blackwell Science, 53–70.

ASHLEY, G. M., BOOTHROYD, J. C. *et al.* 1990. Classification of large-scale subaqueous bedforms, A new look at an old problem. *Journal of Sedimentary Petrology*, **60**, 160–172.

BASTOS, A. C. & COLLINS, M. B. 2002. *Seabed mobility and sand transport pathways along the inner continental shelf, Dorset, Southern UK*. SOES Technical Report to Standing Conference on Problems Associated with the Coastline (SCOPAC).

BASTOS, A. C., KENYON, N. H. & COLLINS, M. B. 2002. Sedimentary processes, bedforms and facies, associated with a coastal headland, Portland Bill, Southern UK. *Marine Geology*, **187**, 235–258.

BASTOS, A. C., COLLINS, M. & KENYON, N. 2003. Water and Sediment Movement around a coastal headland, Portland Bill, southern UK. *Ocean Dynamics*, **53**, 309–321.

BASTOS, A. C., PAPHITIS, D. & COLLINS, M. 2004. Short-term dynamics and maintenance processes of headland-associated sandbanks, Shambles Bank, English channel, UK. *Estuarine Coastal and Shelf Science*, **59**, 33–47.

BELDERSON, R. H., JOHNSON, M. A. & KENYON, N. H. 1982. Bedforms. *In*: STRIDE, A. H. (ed.) *Offshore Tidal Sands, Processes and Deposits*. Chapman and Hall, London, 27–57.

BELKNAP, D. F. & KRAFT, J. C. 1985. Influence of antecedent geology on stratigraphic preservation potential and evolution of Delaware's barrier systems. *Marine Geology*, **63**, 235–262.

BERNE, G., AUFFRET, J. P. & WALKER, P. 1988. Internal structure of subtidal sandwaves revealed by high resolution seismic reflection. *Sedimentology*, **35**, 5–20.

BERNE, S., CASTAING, P., LE DREZEN, E. & LERICOLAIS, G. 1993. Morphology, internal structure and reversal of asymmetry of large subtidal dunes in the entrance to Gironde Estuary (France). *Journal of Sedimentary Research*, **65**, 780–793.

BOERSMA, J. R. & TERWINDT, J. H. J. 1981. Neap spring tide sequences of intertidal shoal deposits in a mesotidal estuary. *Sedimentology*, **28**, 151–170.

BOWYER, J. K. 1992. Basin changes in Jervis Bay, New South Wales, 1894–1988. *Marine Geology*, **105**, 211–224.

BRAMPTON, A., EVANS, C. D. R. & VELEGRAKIS, A. F. 1998. *South Coast Mobility Study, West of the Isle of Wight*. Construction Industry Research and Information Association (CIRIA) Report **PR65**.

CARLING, P. A. 1983. Threshold of coarse sediment transport in broad and narrow natural streams. *Earth Surface Processes and Landforms*, **8**, 1–18.

CURRY, D. 1989. The rock floor of the English Channel and its significance for the interpretation of marine unconformities. *Proceedings of the Geologists' Association*, **100**, 339–352.

CHAMILLON, E., GILLET, H., WEBER, N. & TESSON, M. 2002. Evolution temporelle et architecture d'un banc sableux estuarien, la Longe de Boyard (Littoral Atlantique, France). *C.R. Geoscience*, **334**, 119–126.

COLLINS, M. B., SHIMWELL, S., GAO S., POWELL, H., HEWITSON, C. & TAYLOR J. A. 1995. Water and sediment movement in the vicinity of linear sandbanks: The Norfolk Banks, southern North Sea. *Marine Geology*, **123**, 125–142.

COWEL, P. J. & THOM, B. G. 1994. Morphodynamics of Coastal Evolution. *In*: CARTER, R. W. G. & WOODROFFE, C. D. (eds) *Coastal Evolution, Late Quaternary shoreline morphodynamics*, Cambridge University Press, 33–86.

DALRYMPLE, R. W., LEGRESLEY, E. M., FADER, G. B. J. & PETRIE, B. D. 1992. The western Grand Banks of Newfoundland, Transgressive Holocene sedimentation under the combined influence of waves and currents. *Marine Geology*, **105**, 95–118.

DAVIS, J. C. 1986. *Statistics and Data Analysis in Geology. (2nd Edition)*. John Wiley & Sons, New York.

DE VRIEND, H. J. 1990. Morphological Processes in Shallow Tidal Seas. *In*: CHENG, R. T. (ed.) *Residual Currents and Long Term Transport*. Springer Verlag, Berlin, 276–301.

DONOVAN, D. T. & STRIDE, A. H. 1961. Erosion of a rock floor by tidal sand streams. *Geological Magazine*, **48**, 393–398.

DUKE, W. L., ARNOTT, R. W. C. & CHEEL, R. J. 1991. Shelf sandstones and hummocky cross-stratification: New insights on a stormy debate. *Geology*, **19**, 625–628.

DYER, K. R. & SOULSBY, R. L. 1988. Sand transport on the continental shelf. *Annual Reviews in Fluid Mechanics*, **20**, 295–324.

DYER, K. R. & HUNTLEY, D. A. 1999. The origin, classification and modelling of sand banks and ridges. *Continental Shelf Research*, **19**, 1285–1330.

EUROSION 2003. *Ôrends in Coastal Erosion in Europe. Final Report of the Project 'Coastal erosion – Evaluation of the need for action'* Directorate General Environment, European Commission.

EVANS, A. W. & HARDISTY, J. 1989. An experimental investigation of the effect of bedslope and grain pivot angle on the threshold of marine gravel transport. *Marine Geology*, **89**, 163–167.

EVANS, G. 1992. Some aspects of continental shelf sedimentation, a discussion on ' The rock floor of the English Channel and its significance for the interpretation of marine unconformities' by Curry (1989) and 'Growth and burial of the English Channel unconformity' by Stride (1990). *Proceedings of the Geological Association*, **103**, 155–158.

FLATHER, R. A., SMITH, J. A., RICHARDS, J. D., BELL, C. & BLACKMAN, D. L. 1998. Direct estimates of extreme storm surge elevations from a 40-year numerical model simulation and from observations. *The Global Atmosphere and Ocean System*, **6**, 165–176.

FLEMMING, B. W. 1977. *Depositional Processes in Saldanha Bay and Langebaan Lagoon*. Report of Marine Geoscience Group, Bull. No 8, Department of Geology, University of Cape Town, 213 pp.

FLEMMING, B. W. 1988. Process and patterns of sediment mixing in a microtidal coastal lagoon along the west coast of South Africa. *In*: DEBOER, P. L., VAN GELDER, A. & NIO, S. D. (eds) *Tide Influenced Sedimentary Environments and Facies*. Reidel Publishing Company, Dordrecht, 275–288.

FOLK, R. L. 1980. *Petrology of the Sedimentary Rocks. (2nd Edition)*. Hemphill Publishing Company, Austin, Texas, U.S.A.

GAO, S. & COLLINS, M. B. 1992. Net sediment transport patterns from grain size trends, based upon definition of "transport vectors". *Sedimentary Geology*, **89**, 157–159.

GAO, S. & COLLINS, M. B. 1995. Net sand transport direction of sands in a tidal inlet, using foraminifera tests as natural tracers *Estuarine, Coastal and Shelf Science*, **40**, 681–697.

GAO, S., COLLINS, M. B., LANCKNEUS, J., DE MOOR, G. & VAN LANCKER, V. 1994. Grain size trends associated with net sediment transport patterns: an example from the Belgian Continental Shelf. *Marine Geology*, **121**, 171–185.

GEO-3 2002. *Global Environment Outlook 3, Past, Present and Future Perspectives*. United Nations Environment Programme. EarthScan Publications LTD, London.

GROCHOWSKI, N. T. L., COLLINS, M. B., BOXALL, S. R. & SALOMON, J. C. 1993. Sediment transport predictions for the English Channel, using numerical models. *Journal of the Geological Society of London*, **150**, 683–695.

HAMMOND, F. D. C., HEATHERSHAW, A. D. & LANGHORNE, D. N. 1984. A comparison between Shields' threshold criterion and the movement of loosely packed gravel in a tidal current. *Sedimentology*, **31**, 51–62.

HARRIS, P. T. 1991. Reversal of subtidal dune asymmetries caused by seasonally reversing wind-driven currents in Torres Strait northeastern Australia. *Continental Shelf Research*, **11**, 655–662.

HARRIS, P. T. & COLLINS, M. B. 1984. Side scan sonar investigations into temporal variation in sand wave morphology, Helwick Sand, Bristol Channel. *Geo Marine Letters*, **4**, 91–97.

HAWKINS, A. B. & SEBBAGE, M. J. 1972. The reversal of sand waves in the Bristol Channel. *Marine Geology*, **12**, M7–M9.

HEATHERSHAW, A. D. 1981. Comparisons of measured and predicted sediment transport rates in tidal currents. *Marine Geology*, **42**, 75–104.

HEATHERSHAW, A. D. 1988. Sediment Transport, Part I: Fundamental Principles. *Journal of Naval Science*, **14**, 154–170.

HOUTHUYS, R., TRENTESAUX, A. & DE WOLF, P. 1994. Storm influences on a tidal sandbank's surface (Middelkerke Bank, southern North Sea). *Marine Geology*, **121**, 23–41.

HR WALLINGFORD 1993. *South Coast Seabed Mobility Study*. Technical Report EX 2793, HR Wallingford, Wallingford.

HUNTLEY, D. A. 1988. A modified inertial dissipation method for estimating seabed stresses at low Reynolds numbers, with application to wave/current boundary layer measurements. *Journal of Physical Oceanography*, **18**, 339–346.

HUNTLEY, D. A. & BOWEN, A. J. 1990. Modelling sand transport on continental shelves. *In*: DAVIES, A. M. (ed.) *Modelling Marine Systems (Vol 1)*. CRC Press, Florida, 221–254.

JOHNSON, M. A., KENYON, N. H., BELDERSON, R. H. & STRIDE, A. H. 1982. Sand Transport. *In*: STRIDE, A. H. (ed.) *Offshore Tidal Sands, Processes and Deposits*. Chapman and Hall, London, 58–94.

KAPSIMALIS, V., MASSE, L., VELEGRAKIS, A. F., TASTET, J. P., PAIREAU, O. & LAGASQOUIE, M. H. 2004. Morphological development of an estuarine bank: St Georges Bank, Gironde Estuary, France. *Journal of Coastal Research*, **41**, 27–42.

KENYON, N. H. & STRIDE, A. H. 1970. The tide-swept continental shelf sediments between the Shetland Isles and France. *Sedimentology*, **14**, 159–173.

KOMAR, P. D. 1977. Selective longshore transport rates of different grain size fractions within a beach. *Journal of Sedimentary Petrology*, **56**, 258–266.

ÊOMAR, P. D. 1998. *Beach Processes and Sedimentation (2nd Edition)*. Prentice Hall, N.J. USA.

KOMAR, P. D. & LI, Z. 1986. Pivoting analyses of the selective entrainment of sediments by shape and size with application to gravel threshold. *Sedimentology*, **33**, 425–436

LANCKNEUS, J. & DE MOOR 1995. Bedforms on the Middelkerke Bank, southern North Sea. *In*: FLEMMING, B. W. & BARTHOLOMA, A. (eds) *Tidal Signatures in Modern and Ancient Sediments*. Blackwell Science, Oxford, 33–51.

LANCKNEUS, J., VAN LANCKER, V., MOERKERKE, G., VAN DEN EYNDE, D., FETTWEIS, M., DE BATIST, M. & JACOBS, P. 2001. *Investigation of the natural sand transport on the Belgian continental shelf*. BUDGET, Final Report. Federal Office for Scientific, Technical and Cultural Affairs (OSTC), Belgium.

LANGHORNE, D. N. 1982. A study of the dynamics of a marine sandwave. *Sedimentology*, **29**, 571–594.

LECOUTURIER, M., GROCHOWSKI, N. T., HEATHERSHAW, A., OIKONOMOU, E. & COLLINS, M. B. 2000. Turbulent and macro-turbulent structures developed in the benthic boundary layer, downstream of topographic features. *In*: *Estuarine, Coastal and Shelf Science*, **50**, 817–833.

LEEDER, M. R. 2000. *Sedimentology and Sedimentary Basins, from Turbulence to Tectonics*. Blackwell Science, Oxford.

MADSEN, O. S. 1993. *Sediment Transport on the Shelf*. Unpublished seminar notes.

MASSELINK, G. 1992. Longshore variation of grain size distributions along the coast of Rhone delta, Southern France: a test of the "McLaren model". *Journal of Coastal Research*, **8**, 286–291.

MCLEAN, S. R. 1981. The role of non uniform roughness in the formation of sand ribbons. *Marine Geology*, **42**, 49–74.

MCLAREN, P. & BOWLES, D. 1985. The effects of sediment transport on grain size distributions. *Journal of Sedimentary Petrology*, **55**, 457–470.

MCMANUS, J., BULLER, A. T. & GREEN, C. D. 1980. Sediments of the Tay Estuary, VI: Sediments of the lower and outer reaches. *Proceedings of the Royal Society Edinburgh*, **B78**, 133–154.

NORDSTROM, K. F. 1989. Downdrift coarsening of beach foreshore sediments at tidal inlets: an example from the coast of New Jersey. *Earth Surface Processes and Landforms*, **14**, 691–701.

PAPHITIS, D. & COLLINS, M. B. 2005. Sediment resuspension events within the microtidal coastal waters of Thermaikos Gulf, Northern Greece. *Continental Shelf Research*, **25**, 2350–2365.

PAPHITIS, D., VELEGRAKIS, A. F. & COLLINS, M. B. 2000. Residual circulation and associated sediment transport in the Eastern Approaches to the Solent. *In*: COLLINS, M. B. & ANSELL, K. (eds) *Solent Science-A Review*. Proceedings in Marine Science Series. Elsevier, Amsterdam, 107–110.

PATTIARATCHI, C. & COLLINS, M. B. 1985. Sand transport under the combined influence of waves and tidal currents, an assessment of available formulae. *Marine Geology*, **67**, 83–100.

PATTIARATCHI, C. & COLLINS, M. B. 1987. Mechanisms for linear sandbank formation and maintenance in relation to dynamical oceanographic observations. *Progress in Oceanography*, **19**, 117–176.

PEDREROS, R., HOWA, H. L. & MICHEL, D. 1996. Application of grain size trend analysis for the determination of sediment transport pathways in intertidal areas. *Marine Geology*, **135**, 35–49.

PETTIJOHN, F. G., POTTER, P. D. & SIEVER, R. 1972. *Sand and Sandstone*. Springer Verlag, New York.

REINECK, H. E. & SINGH, I. B. 1973. *Depositional Sedimentary Environments*. Springer Verlag, Berlin.

POULOS, S. E. & COLLINS, M. B. 2002. A quantitative evaluation of riverine/sediment fluxes to the Mediterranean Basin: Natural flows, coastal zone evolution and the role of dam construction. *In*: JONES, S. J. & FROSTICK, L. E. (eds) *Sediment Flux to Basins: Causes, Controls and Consequences*. Geological Society, London, Special Publications, **191**, 227–245.

POULOS, S. E., CHRONIS, G., COLLINS, M. B. & LYKOUSIS, V. 2000. Thermaikos Gulf Coastal System, NW Aegean Sea, an overview of water/sediment fluxes in relation to air-land-ocean interaction and human activities. *Journal of Marine Systems*, **25**, 47–76.

SELF, R. P. 1977. Longshore variation in beach sands, Nautla area, Veracruz, Mexico. *Journal of Sedimentary Petrology*, **47**, 1437–1443.

SHARPLES, J. 2000. Water circulation in Southampton Water and the Solent. *In*: COLLINS, M. B. & ANSELL, K. (eds) *Solent Science-A Review*. Proceedings in Marine Science. Elsevier, Amsterdam, 45–53.

SLEATH, J. F. A. 1984. *Seabed Mechanics*. John Wiley & Sons Inc. New York, USA.

SMITH, J. D. 1969. Geomorphology of a sand ridge. *Journal of Geology*, **17**, 39–55.

SOULSBY, R. L. 1997. *Dynamics of Marine Sands*. Thomas Telford, London.

STERNBERG, R. W. 1972. Predicting initial motion and bedload transport of sediment particles in the shallow marine environment. *In*: SWIFT, D. J. P., DUANE, D. B. & PILKEY, O. H. (eds) *Shelf Sediment Transport, Process and Pattern*. Dowden, Hutchison and Ross, Strasburg, 61–82.

TELES, A. P. 2003. *Hydrodynamics and Sediment Transport in the Solent, Southern England*. PhD Thesis, School of Ocean and Earth Sciences, Southampton Oceanography Centre, University of Southampton.

TSIMPLIS, M. N., JOSEY, S. A., RIXEN, M. & STANEV, E. V. 2004. On the forcing of the sea level in the Black Sea. *Journal of Geophysical Research*, **109(C8)**, c08015.

TERWINDT, J. H. J. & BROUWER, M. J. N. 1986. The behaviour of intertidal sandwaves during neap-spring tide cycles and the relevance for paleoflow reconstruction. *Sedimentology*, **33**, 1–31.

VAN RIJN, L. C. 1993. *Principles of Sediment Transport in Rivers, Estuaries and Coastal Seas*. Aqua Publications, Amsterdam.

VAN WESENBEECK, V. & LANCKNEUS, J. 2000. Residual sediment transport on a tidal sand bank: A comparison between the modified McLaren model and bedform analysis. *Journal of Sedimentary Research*, 70, 470–477.

VELEGRAKIS, A. F. 1994. *Aspects of the morphology and sedimentology of a transgressional embayment system, Poole and Christchurch Bays, Southern England*. PhD Thesis, Department of Oceanography, University of Southampton.

VELEGRAKIS, A. F. 2000. Geology, geomorphology and sediments of the Solent System. *In*: COLLINS, M. B. & ANSELL, K. (eds) *Solent Science-A Review*. Proceedings in Marine Science. Elsevier, 21–43.

VELEGRAKIS, A. F., MICHEL, D., COLLINS, M. B., LAFITE, R., OIKONOMOU, E., DUPONT, J. P., HUALT, M., LECOUTURIER, M., SALOMON, J. C. & BISHOP, C. 1999. Sources, sinks and resuspension of particulate matter in the eastern English Channel. *Continental Shelf Research*, **19**, 1933–1957.

VELEGRAKIS, A. F, BRAMPTON, A., EVANS, C. D. R. & COLLINS, M. B. 2000. Seabed mobility studies in the Solent region. *In*: COLLINS, M. B. & ANSELL, K. (eds) *Solent Science-A Review*, Proceedings in Marine Science. Elsevier, Amsterdam, 111–115.

VINCENT, C. E., STOLK A. & PORTER, C. F. C. 1998. Sand suspension and transport on the Middelkerke Bank (southern North Sea) by storms and tidal currents: *Marine Geology*, **150**, 113–129.

VOULGARIS, G., WILKIN, M. & COLLINS, M. B. 1995. The *in situ* acoustic measurements of shingle movement under waves and currents: instrument (TOSCA) development and preliminary results. *Continental Shelf Research*, **15**, 195–211.

VOULGARIS, G., WORKMAN, M. & COLLINS, M. B. 1999. Measurement techniques of shingle transport in the nearshore zone. *Journal of Coastal Research*, **15**, 1030–1039.

WILLIAMS, J. J., THORNE, P. D. & HEATHERSHAW, A. D. 1989. Comparisons between acoustic measurements and predictions of the bedload transport of marine gravels. *Sedimentology*, **36**, 973–979.

WRIGHT, L. D. 1995. *Morphodynamics of Inner Continental Shelves*. CRC Press,Boca Raton.

Modelling SPM on the NW European shelf seas

ALEJANDRO J. SOUZA, JASON T. HOLT & ROGER PROCTOR

Proudman Oceanographic Laboratory, 6Brownlow Street, Liverpool, L35 DA, UK
(e-mail: ajso@pol.ac.uk)

Abstract: The Proudman Oceanographic Laboratory Coastal Ocean Modelling System (POLCOMS) has been developed to tackle multidisciplinary studies in coastal/shelf environments. The central core is a sophisticated three-dimensional hydrodynamic model that provides realistic flow fields to interact with, and transport environmental parameters. The model uses realistic forcing with ocean currents and hydrography at the boundary, atmospheric forcing and tides.

Suspended particulate matter (SPM) is transported within the water, like any other scalar in the model; it is advected using a high-order scheme and mixed vertically using diffusion coefficients from a second moment turbulence closure. In addition, the SPM transport is influenced by a number of processes unique to this problem, such as: the transfer between the lowest level of the model and the bed layer in which the resuspension and deposition takes place is dependent on the erosion rate, the particle settling velocity and the critical stresses for erosion and deposition. The particular application described in this paper is an annual simulation for the NW European shelf for a single sediment class.

The simulation shows the expected seasonal variation in spatial patterns and a clear tidal signal in the SPM resuspension. Also evident is a fortnightly/monthly variability due to the spring–neaps and the M2–N2 cycles. There are also quarter-diurnal and semi-diurnal cycles in SPM, due to tidal resuspension and advection respectively. The above tidal suspension behaviour, as well as, the net transport direction are in agreement with historical observations of SPM.

The processes that redistribute suspended particulate matter (SPM) on continental shelves are important for several relevant economical, political, societal and climatic problems. These include: primary production, upper and benthic layer ecology, biogeochemical cycling, carbon fluxes, optical property variability, pollutant resuspension and transport, and water quality in general (e.g. Eisma 1990; Tett *et al.* 1993). As a result attention has been focused over the last decade on developing models of SPM dynamics that can be integrated with ecological models (Huthnance *et al.* 1993). This is presently the main application of the SPM model within the Proudman Oceanographic Laboratory Coastal Ocean Modelling System (POLCOMS).

The shelf seas are highly dynamic and complex, which results in variability on short as well as longer time and space scales. For example, water-column thermal structure and stratification are often controlled to first order by the competition of the stratifying influence of solar radiation and mixing caused by winds and tides (e.g. Simpson & Bowers 1981) which might drive jet-like currents. Near river outflows drive large-scale buoyancy-driven coastal currents that affect both the water column structure and transport. These structures are themselves influenced by the effect internal waves and tides and tidal straining. These same physical processes are important, to varying degrees, for sediment resuspension and/or transport (e.g. Agrawal & Traykovski 2001; Chang *et al.* 2001; Hill *et al.* 2001). As a coarse generalization, the vertical flux of SPM can be considered to be dependent upon bed shear stress, vertical mixing (turbulent diffusion), and particle settling under gravity (e.g. Jones *et al.* 1996). However, there can also be complex interactions among several other physical, geological, and biological processes via organisms and particles (especially cohesive particles), which can modify the particulates and their particle size distributions and setting velocities (e.g. Lick *et al.* 1993; McNeil *et al.* 1996; Hill *et al.* 2001).

Within the NW European shelf seas, the North Sea is the largest and probably the most studied, due to its political geography. For some time now it has been known that the sediment supply in this area is dominated by the inputs from the east coast of England, predominantly the Holderness coast of North Yorkshire (McCave 1987; McManus & Prandle 1997; Balson *et al.* 1998).The large-scale long-term transport path for this material follows the cyclonic meteorologically-driven flow in the

From: BALSON, P. S. & COLLINS, M. B. 2007. *Coastal and Shelf Sediment Transport*. Geological Society of London, Special Publications, **274**, 147–158. 0305-8719/07/$15.00

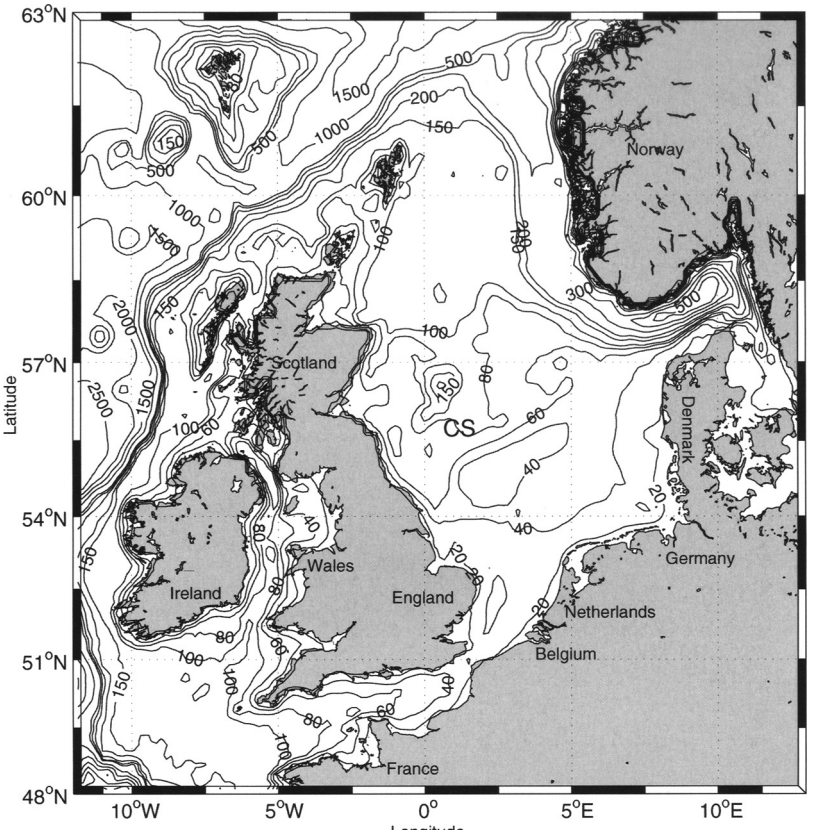

Fig. 1. Model domain and bathymetry, showing the position of station CS from which the time series are shown.

southern North Sea, such that the sediment is transported eastwards, across the Southern Bight then northeastwards through the German Bight, in what is been termed the 'English River', to finally deposit in the Skaggerak and the Norwegian Trench (Eisma & Kalf 1987).

On shorter scales, depending on the availability of bottom sediments, the resuspension distribution is controlled by tidal processes, hence the clear spring-neap, semi-diurnal and quarter-diurnal frequencies observed in the distribution of SPM (Jones *et al.* 1996).

The present work concerns with the implementation of POLCOMS (Holt & James 2001) to the NW European shelf seas at a horizontal resolution of 1/9° latitude by 1/6° longitude (approximately 12 km, see Fig. 1). The model has been proven to be successful in reproducing the tides, currents (Holt *et al.* 2001), density structure (Holt & James 2001) for the same area. We will concentrate on the distribution and structure of SPM and to discern the importance of the different physical processes affecting it.

The model

The three-dimensional, non-linear, incompressible, hydrostatic, Boussinesq shallow water equations of motion, together with the prognostic transport equations for temperature salinity and SPM are written in spherical polar coordinates in the horizontal and S coordinate (Song & Haidvogel 1994) in the vertical, which allows us to have terrain following depth coordinates while maintaining near surface and near bottom compressed resolution. The vertical eddy viscosity (N_z) and eddy diffusivity (K_z) are parameterized

Fig. 2. Comparison of modelled sea surface SPM concentration in g m^{-3} and ocean colour (courtesy of NASA and NERC-RSDAS).

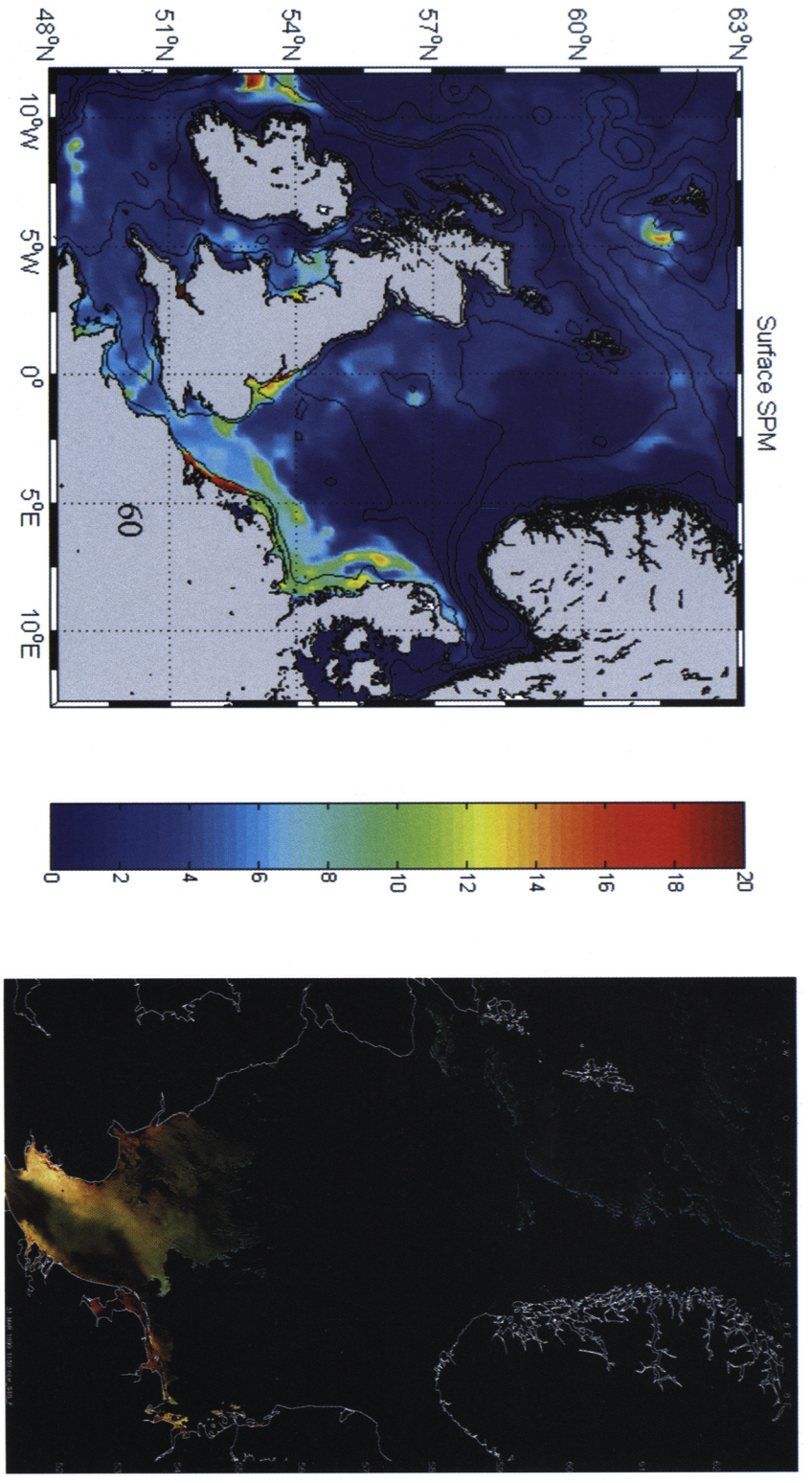
Surface SPM
63°N
60°N
57°N
54°N
51°N
48°N
10°W
5°W
0°
5°E
10°E
60
0
2
4
6
8
10
12
14
16
18
20

using a Mellor–Yamada 2.5 turbulence closure scheme (Mellor & Yamada 1974). The model uses a finite difference scheme on an Arakawa B grid (Arakawa 1972) and a Piecewise Parabolic Method (PPM) of advection (James 1996). The advantage of this grid combination and advection scheme is to maintain eddies and frontal structures, while avoiding numerical diffusion within the model. The model uses a forward-time, centred space, time splitting formulation, where the barotropic mode is solved at a time step limited by the Courant, Friedrichs, and Lewy (CFL) criteria, with the baroclinic time step between 10 and 100 times the barotropic time step. The advantage of this formulation is that it conserves mass, which is very important for SPM. The open boundary conditions are a relaxation to prescribed values for scalars and radiation (Flather & Heaps 1975) for the velocity and elevation. The computational grid has 150×134 points in the horizontal and 20 in the vertical. The typical depth over most of the domain is between 20 and 200 m, but the western part of the domain includes part of the shelf edge with depth of about 2000 m.

A full description of the model dynamics can be found in Holt & James (2001) and Holt & Proctor (2003).

The sediment transport formulation follows that of Holt & James (1999):

$$\frac{\partial C}{\partial t} = L(C) + \frac{1}{(H+\eta)^2}\frac{\partial}{\partial \sigma}\left(K_z \frac{\partial C}{\partial \sigma}\right) \quad (1)$$

$$L(C) = \frac{u}{R\cos(\varphi)}\frac{\partial C}{\partial \chi} + \frac{v}{R}\frac{\partial C}{\partial \varphi} + (w - w_s)\frac{\partial C}{\partial \sigma} \quad (2)$$

where C is the concentration of SPM in $\mathrm{g\,m^{-3}}$; u, v, w are the east (χ), north (φ) and vertical (positive upwards in the S-coordinate) components of velocity; R is the radius of the Earth; L, the advection term, is handled exactly the same as any other scalar in the model. The erosion, deposition and settling of SPM in the bottom boundary follows Puls & Sündermann (1990):

$$\frac{\partial C}{\partial t} = \frac{\varepsilon}{\Delta z}\left(\tau/\tau_{ero} - 1\right)\left(\frac{B}{\sum B}\right), \quad \tau > \tau_{ero}, \quad B > 0 \quad (3)$$

$$\frac{\partial C}{\partial t} = -\frac{w_s}{\Delta z}\left(1 - \tau_{dep}\right), \quad \tau < \tau_{dep}, \quad (4)$$

where $\Delta z = H\Delta\sigma$, w_s is the settling velocity; τ is the bottom stress, τ_{ero} and τ_{dep} are the critical stresses for erosion and deposition respectively and B is the sediment bed mass in $\mathrm{g\,m^{-2}}$. The conservation of sediment mass is given by:

$$\frac{\partial B}{\partial t} = -\frac{\partial C}{\partial t}\Delta z \quad (5)$$

allowing for deposition and erosion when $B > 0$ and deposition only when $B = 0$.

The coastal inputs of sediments are introduced by updating the concentration at each source point (C_j) around the boundary with the change in concentration. That is:

$$\frac{\partial C_j}{\partial t} = \frac{S_j}{N_j V} F_j(t), \quad (6)$$

where S_j is the total mass input, N_j is number of input points for source j and V is the volume of the fractional grid box surrounding the input point. $F_j(t)$ is the normalized time variation of the source.

Implementation to the NW European shelf.

In this paper we will describe an implementation for the NW European shelf, using fine particles, in particular silts, as those coupled with ecosystem models (e.g. Allen *et al.* 2001; Proctor *et al.* 2003).

For this simulation the settling velocity value used, is equivalent to that of fine silt (10^{-4} m s^{-1}), which is a characteristic value in the North Sea as observed by Jones *et al.* (1998) and Jago & Jones (1998). The critical erosion stress $\tau_{ero} = 0.41$ Pa and the critical deposition is $\tau_{dep} = 0.10$ Pa, while the erosion constant is $\varepsilon = 0.04\ \mathrm{g\,m^{-2}\,s}$. These values have been successfully used in the past by Puls & Sündemann (1990) and Holt & James (1999) to model the movement of SPM in the North Sea. The model was initialised with an homogeneous distribution of $1.5\ \mathrm{g\,m^{-3}}$ throughout the water column and $200\ \mathrm{g\,m^{-2}}$ constant bed sediment concentration throughout the entire domain, we used four coastal sources representing the Holderness area, which behaved as a step function with erosion only taking place between October and February based on values used by Holt & James (1999). The model was run for 3 years.

Fig. 3. Modelled SPM and bed material distribution for the month of February. (**a**) sea surface SPM; (**b**) near bottom SPM, both in $\mathrm{g\,m^{-3}}$ and (**c**) bed material in $\mathrm{g\,m^{-2}}$.

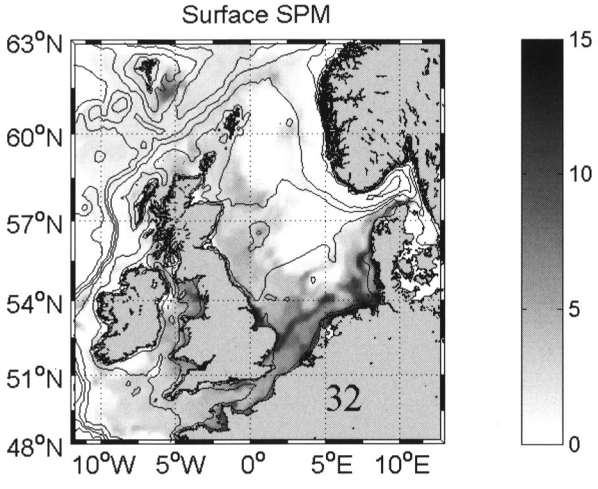
Surface SPM
63°N
60°N
57°N
54°N
51°N
48°N
10°W 5°W 0° 5°E 10°E
32
15
10
5
0

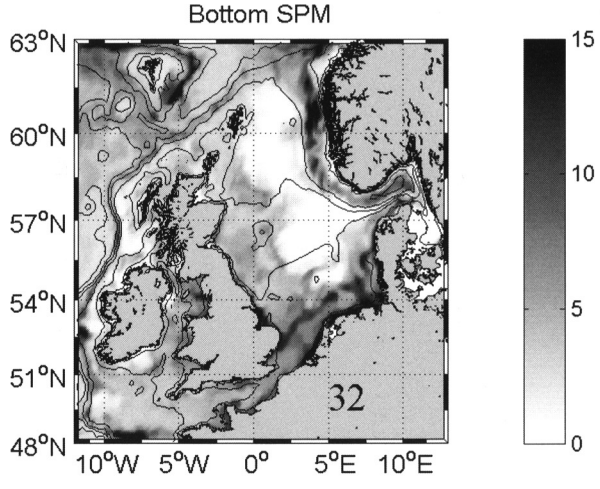
Bottom SPM
63°N
60°N
57°N
54°N
51°N
48°N
10°W 5°W 0° 5°E 10°E
32
15
10
5
0

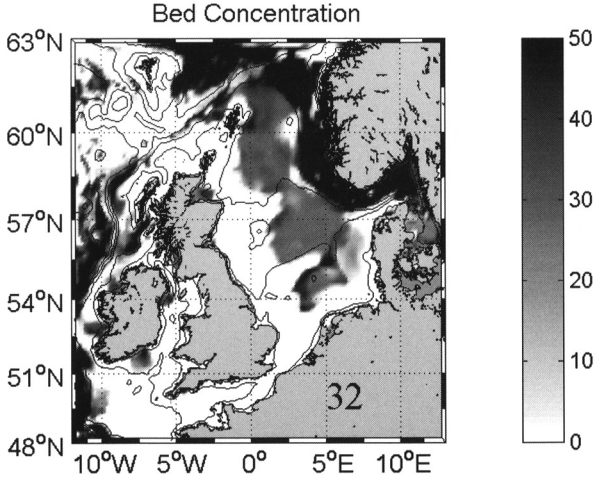
Bed Concentration
63°N
60°N
57°N
54°N
51°N
48°N
10°W 5°W 0° 5°E 10°E
32
50
40
30
20
10
0

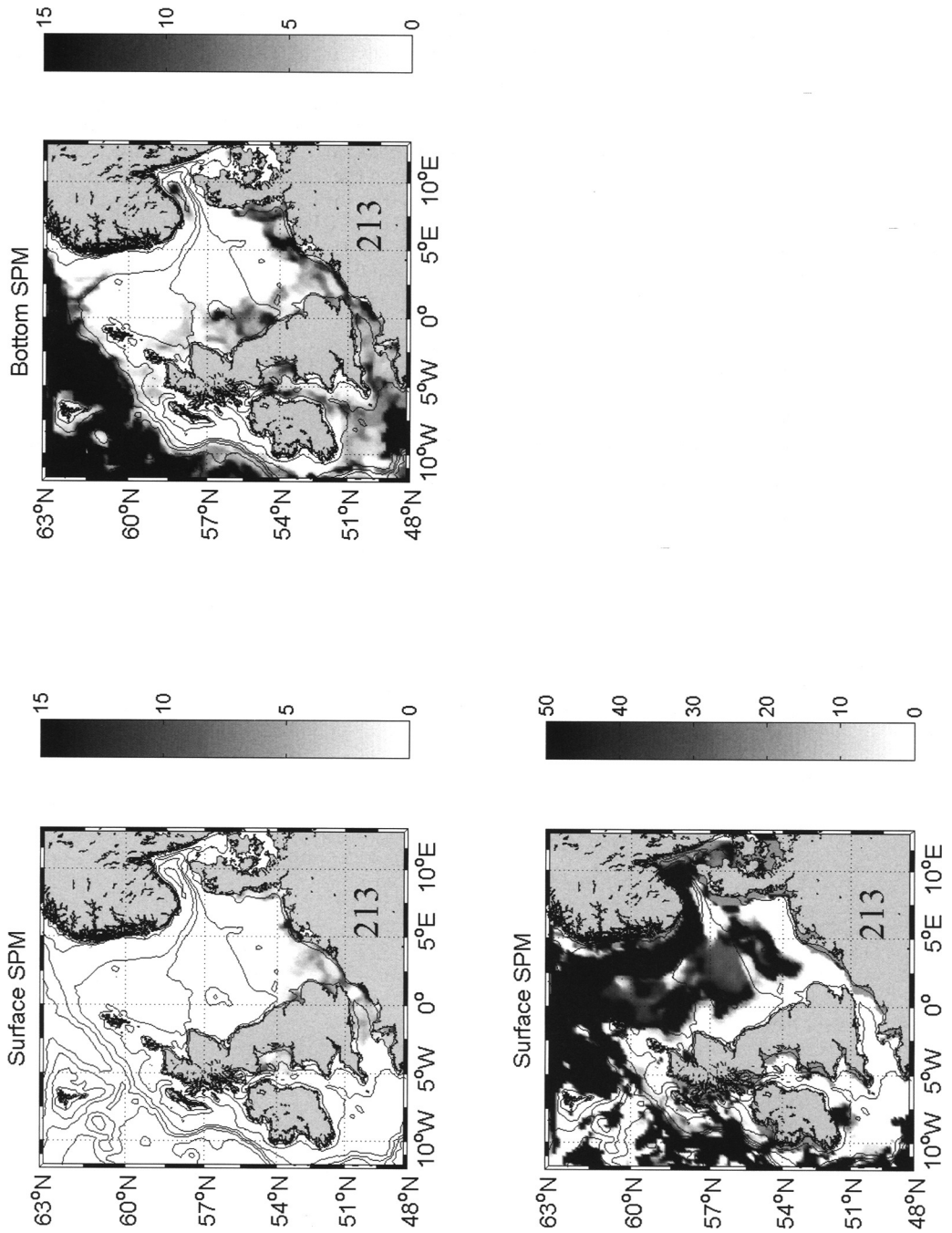
Bottom SPM
Surface SPM
Surface SPM
213
63°N
60°N
57°N
54°N
51°N
48°N
10°W
5°W
0°
5°E
10°E
15
10
5
0
50
40
30
20
10

Results

We are confident that the model accurately predicts the annual variation in density and current structure in the NW European shelf as discussed by Holt & James (2001) and Holt *et al.* (2001). So we will concentrate in explaining the SPM structure.

To assess the model's capability to reproduce the main characteristics of sea surface SPM we can make comparisons of the model results with sea-viewing wide field-of-view sensor (SeaWiFS) images of ocean colour (courtesy the NERC Remote Sensing Data Analysis Service). These images show, in a qualitative form, the main paths and structure that the surface SPM follows and the relative maximums observed. Figure 2 shows a model and SeaWiFS image for a typical winter-spring season demonstrating that the model reproduces the large-scale features of surface SPM in the North Sea. The typical SPM distribution of the winter–spring season is apparent with a plume with high SPM off eastern England, the result of the combined effect of the Holderness cliff erosion (coastal source) and the coastal plume of the River Humber. This material travels southwards, then it starts its path across the North Sea towards the German Bight in the so called 'English River'. It then follows the German / Danish coast before depositing in the Norwegian Trench as explained by Eisma & Kalf (1987). Another feature that can be observed is the plume of high SPM concentration from the Rhine/Meuse region of fresh water influence (ROFI) inputs. In the Irish Sea the model shows higher concentrations not only in the Bristol Channel where the tides are strong, but also around Liverpool Bay where there are also strong tides plus inputs from the rivers Dee, Mersey and Ribble, in agreement with historical observations.

Figure 3 shows, as expected, that there is vertical variability in the distribution of SPM. In this winter picture, showing the distribution of sediments at the beginning of February, we observe that bottom and surface SPM patterns are very similar, almost everywhere, but with a difference in the concentration values, with higher values near the bottom. We can also observe high concentration values along some parts of the shelf edge and the Norwegian Trench; this is probably due to current intensification. Typical patterns of deposition are observed in Figure 3c with erosion around the British Isles, and the Southern North Sea and deposition at the shelf edge and Norwegian Trench. This pattern of deposition is in agreement with Eisma (1990), which also shows that deposition of fine sediment in the North Sea occurs only in the Oyster Grounds and in the central North Sea.

Similar pictures for the month of August (Fig. 4) show changes to the surface SPM, generally a decrease in SPM, with a clear decrease of SPM in the 'English River'. This is because at this time of the year the coastal sources from the Holderness Cliffs are not present. There is also an obvious decrease in the riverine sources with the Meuse/Rhine sediment plume having disappeared. Near the sea bed the SPM is greater than the surface values (as in the winter) due to tidal resuspension which is more obvious in the shallow region. An increase of deposition in shallow areas appears to be to the result of the decreased summer wind stress. This seasonal cycle in resuspension has been observed from satellite imagery in the eastern Irish Sea, in particular in Cardigan Bay (Bowers *et al.* 1998).

The seasonal variability in SPM can probably be shown better from a time series in a single point (Fig. 5), we have chosen a position, in 65 m of water, equivalent to that of station CS of the NERC North Sea project (Charnock *et al.* 1993), so that we can observe the effect that seasonal thermal stratification has on the SPM distribution. From Figure 5 we can observe that during the first 100 days of the year (up to about mid-March), SPM is moderate with values of the order of 5 g m^{-3} and reaching the surface, then as the thermal stratification develops the SPM concentrates in the bottom 40 m of the water column, with high values of up to 15 g m^{-3}, but decreasing to zero at the surface. This can be explained if we observe the TKE distribution as represented by q^2 (the turbulence velocity square). From the distribution of q^2 (Fig. 5c) we can observe that when the water column is mixed, both the bottom and surface boundary layers merge, so that there is enough turbulence in the system to keep the SPM in suspension throughout the water, but when the water column stratifies, the reduction of eddy viscosity near the thermocline separates the two boundary layers. So that the TKE produced in the bottom boundary stays in the bottom boundary, some of this is TKE is then used for the resuspension of SPM which, because it cannot leave the bottom boundary due to the pycnocline, concentrates producing higher values of SPM near the bottom. This contrasts with the situation when the pycnocline does not exist (i.e. winter) and the SPM covers the entire water column.

Fig. 4. Same as Figure 3 but for the month of August.

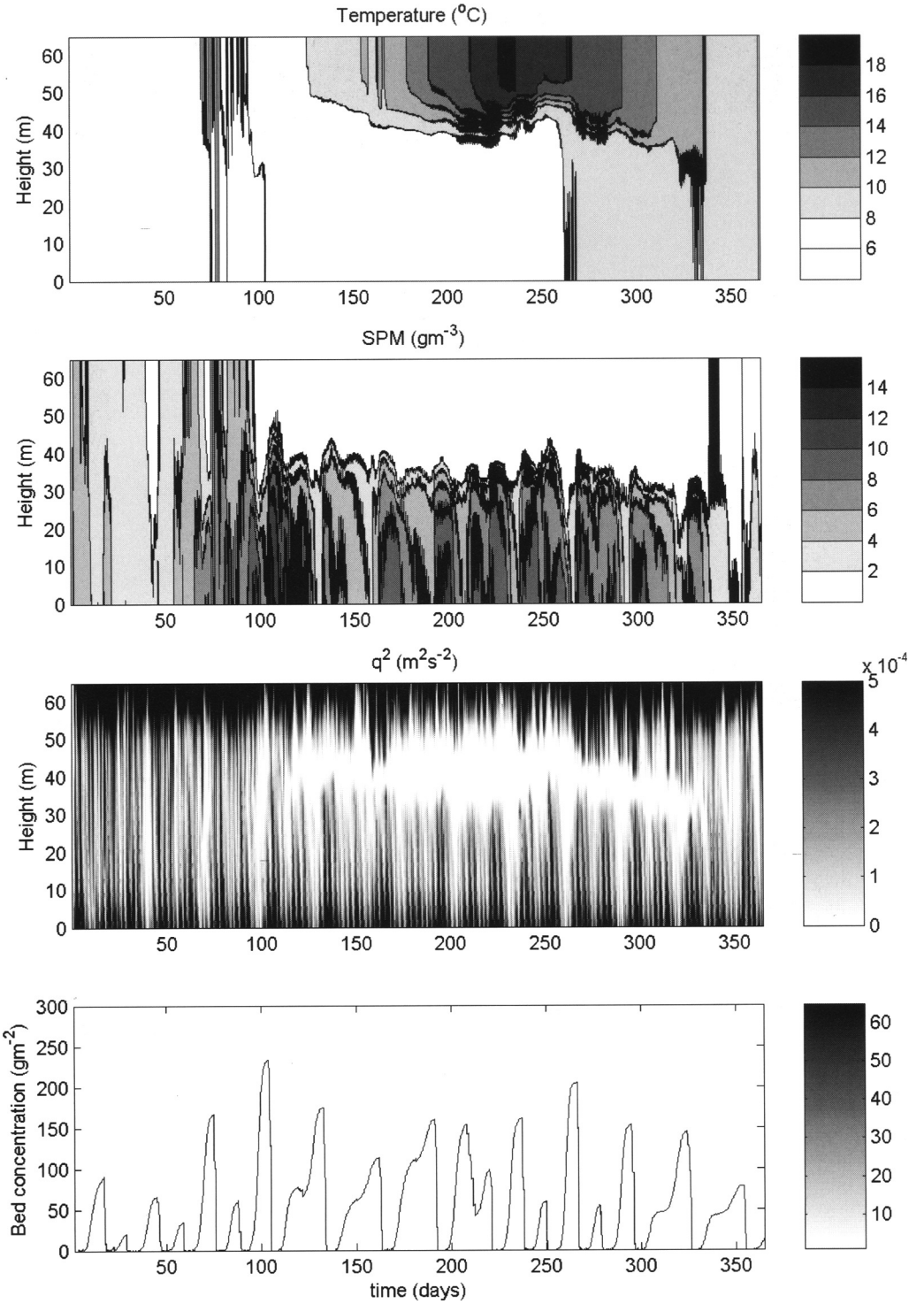

Fig. 5. Annual time series at station CS. (**a**) Temperature in °C; (**b**) SPM in gm^{-3}; (**c**) q^2 m^2 s^{-2} and (**d**) bed material in g m^{-2}.

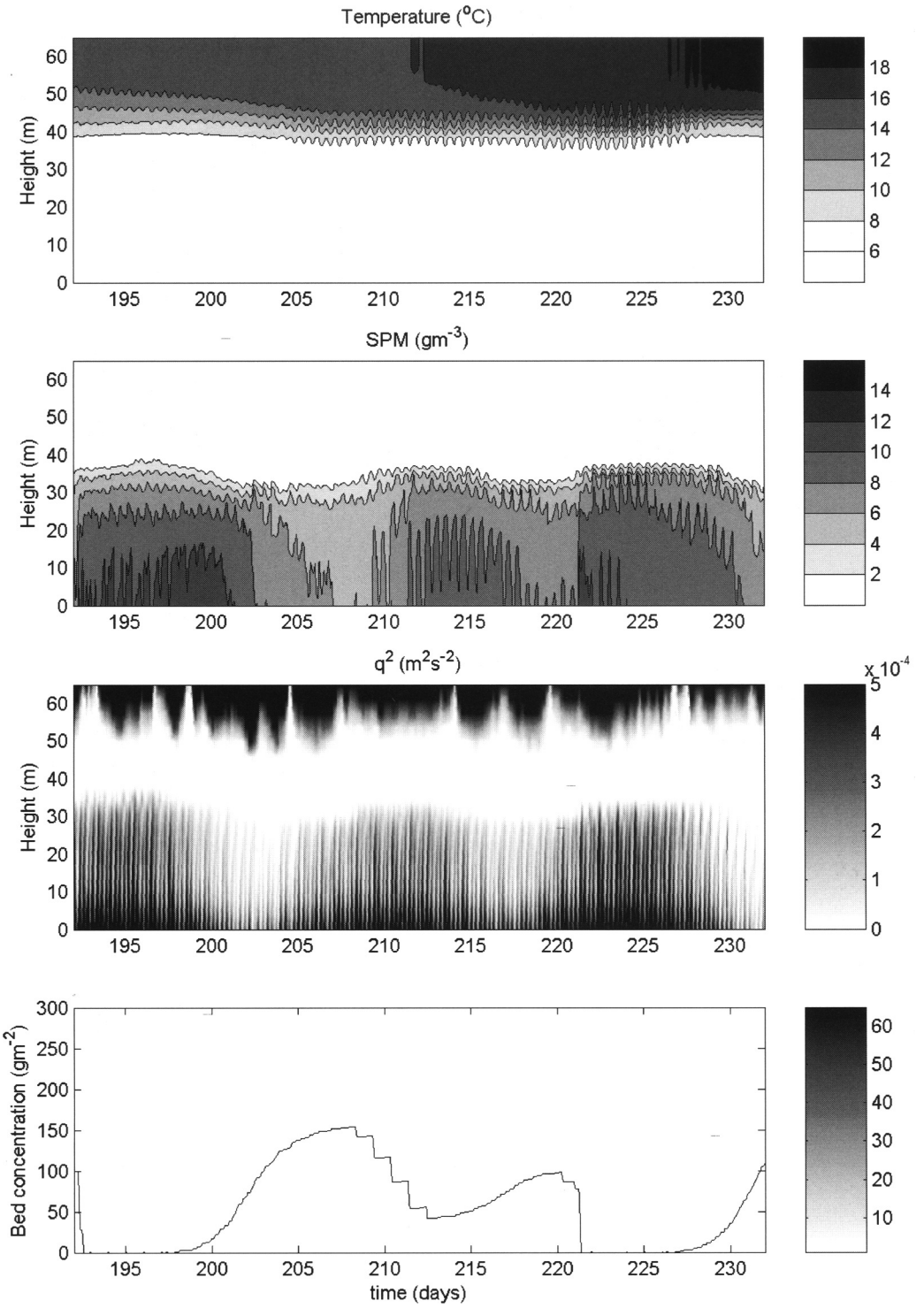

Fig. 6. Same as Figure 5 but concentrating on a 40 day period in summer to observe the spring–neap and monthly cycles.

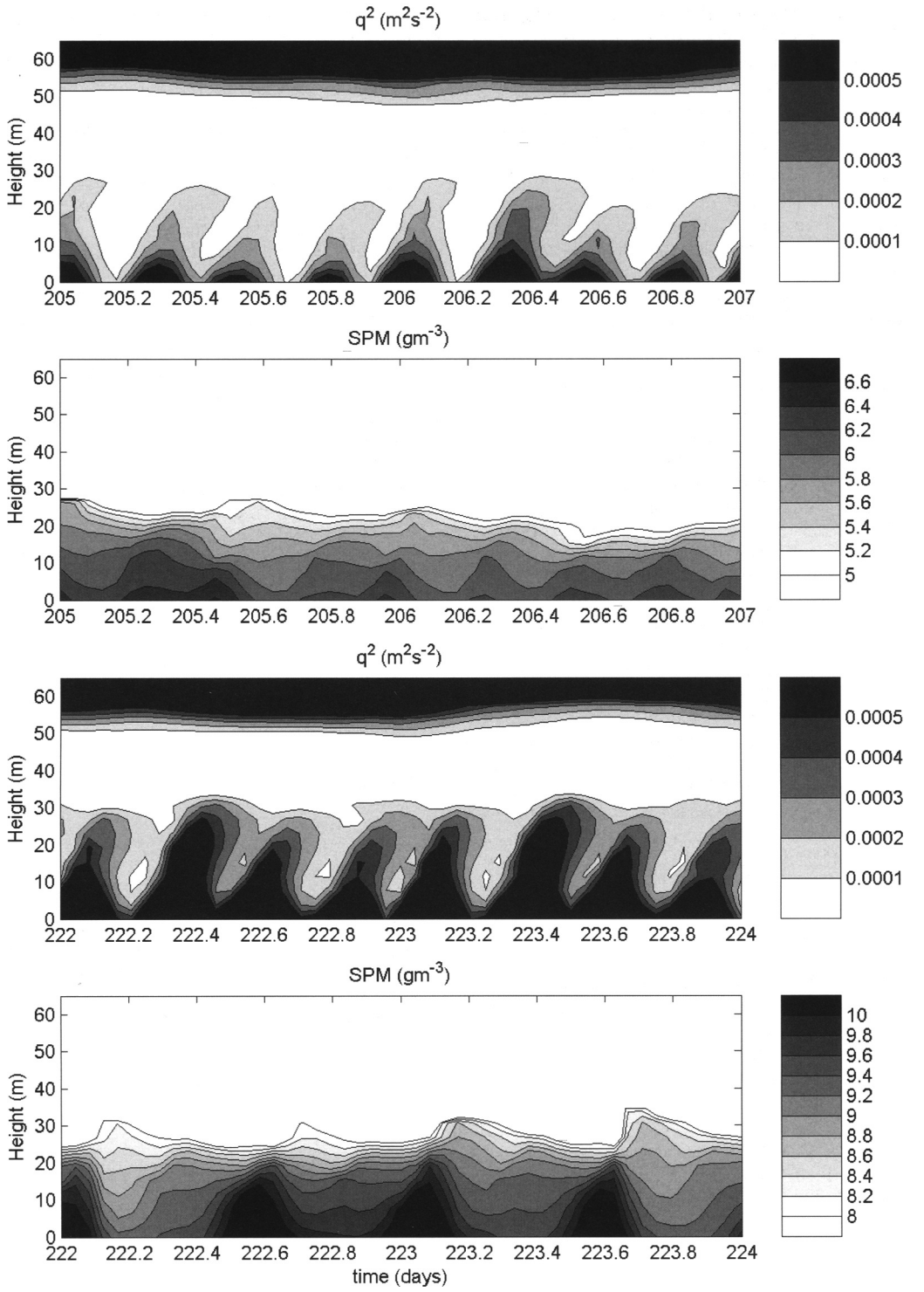

Fig. 7. SPM and q^2 showing semi-diurnal and quarter-diurnal variability. (**a**) and (**b**) neap tide and (**c**) and (**d**) spring tide.

A characteristic that can be observed in Figure 5 in SPM concentration, q^2 and bed material concentration is that there is a fortnightly pulse due to the spring-neap tidal cycle. If we concentrate on a couple of fortnightly cycles (Fig. 6), we can clearly observe the spring-neap variation in all properties, but we can also observe a monthly variability, especially clear in the deposition of material (Fig. 6d), but present also in SPM and q^2 and this is due to the interaction between the N_2 and M_2 tidal components.

Examining the variation in more detail, Fig. 7 shows two different periods during the simulation; one at neap tide when the bottom stresses and turbulence are relatively small and there is suspendable material on the seabed; and another period at spring tide when the bed stress-induced turbulence level is higher and the available bed material has been completely resuspended. During the neap tide period both the SPM and q^2 have a quarter-diurnal variability (Fig. 7a,b). The quarter-diurnal variability is due to the fact that q^2 is proportional to the speed of the current, i.e. it does not matter if it is positive or negative, so in the case of regions where M_2 is the dominant tidal current, like in the North Sea, q^2 will have an M_4 frequency. In the case of SPM the M_4 variability is the direct result of the tidal resuspension (Jago *et al.* 1993; Jones *et al.* 1996). At the same time we see a semi-diurnal inequality, due partly to asymmetry of the flood and the ebb, but also due to tidal advection. This semidiurnal frequency is more clearly observed in Figure 6d and although the q^2 has still got an M_4 frequency, SPM has M_2 variability. This is because the bed material has been depleted and the SPM has been advected passed this point (Jago *et al.* 1993).

Summary and conclusions

The model SPM distribution appears to follow the typical pattern depicted by satellite imagery, with the transport direction being eastwards from the Holderness region (east coast of England) towards the German Bight.

The model also shows a seasonal cycle of SPM concentration at the surface in the stratified area. When the thermocline starts to develop, there is a drop in SPM surface concentration and an increase on the bottom layer concentrations. The thermocline works as a 'lid' inhibiting the transport of turbulence or SPM to the surface layer. This is of ecological importance, as it will mean that nutrients do not reach the surface and will only reach the base of the thermocline maintaining a mid-water chlorophyll maxima.

The model shows a strong fortnightly/monthly variability in SPM and TKE, due to the spring–neaps cycle and the M2–N2 cycle respectively.

The model is also able to reproduce the observed quarter-diurnal variability in SPM and TKE. In the case when the bed material has been totally depleted only a semidiurnal variability is observed for SPM due to tidal advection.

Although the gross characteristics of SPM are reproduced, we must bear in mind that the low resolution of the model, 12 km, is not capable of properly resolving the river plumes and frontal systems and meso-scale eddies, and hence a lot of the observed patchiness is missing. Some of the caveats of the model are: it lacks wave–current interaction in its present form; it uses an over simplified formulation for the coastal sources and only one particle size class. Development of our SPM formulation has to be improved to include mixed particles as well as floculation/defloculation and more realistic distribution of bed material, as well as increasing the resolution to better describe physical processes. All the above aspects are under development.

We would like to thank NASA and the UK Natural Environmental Research Council (NERC) Remote Sensing Data Analysis Service (RSDAS) for supplying the SeaWiFS image. This work was partially funded by the UK NERC grant NER/M/S/2002/00076.

References

AGRAWAL, Y. C. & TRAYKOVSKI, P. 2001. Particles in the bottom boundary layer: Size dynamics through events. *Journal Geophysical Research*, **106**, 9533–9542.

ALLEN, J. I., BLACKFORD, J., HOLT, J. & PROCTOR, R., ASHWORTH, M. & SIDDORN, J. 2001. A highly spatially resolved ecosystem model for the North West European Continental Shelf. *Sarsia*, **86**, 423–440.

ARAKAWA, A. 1972. *Design of the UCLA general circulation model*, Technical Repart **7**, University of California, Los Angeles.

BALSON, P. S., Tragheim, D. & NEWSHAM, R. 1998. Determination and prediction of sediment yields from recession of the Holderness coast, eastern England, II. *Processdings of the 33rd MAFF conference of river and coastal engineers*, 4.5.1–4.511.

BOWERS, D. G., BOUDJELAS, S. & Harker, G. E. L. 1998. The distribution of fine suspended sediments in the surface waters of the Irish Sea and its relationship to tidal stirring. *International Journal of Remote Sensing*, **19**, 2789–2805

CHANG, G. C., DICKEY, T. D. & WILLIAMS, A. J. III. 2001. Sediment resuspension over a continental shelf during Hurricanes Edouard and Hortense. *Jounal of Geophysical Research*, **106**, 9517–9531.

CHARNOCK, H., DYER, K. F., HUTHNANCE, J. M., LISS, P. S., SIMPSON, J. H. & TETT, P. B. (eds) 1993. Understanding the North Sea system. *Philosophical Transactions of the Royal Society, Lond*, **A343**, 377–605.

EISMA, D. 1990. Transport and deposition of suspended matter in the North Sea and the relation to coastal siltation, pollution and bottom fauna distribution. *Reviews of Aquatic Science*, **3**, 181–216.

EISMA, D. & KALF, J. 1987. Dispersal, concentration and deposition of suspended matter in the North Sea. *Journal of the Geological Society, London*, **144**, 161–178.

FLATHER, R. A. & HEAPS, N. S. 1975. Tidal computations fro Morecambe Bay. *Geophysical Journal of the Royal Astronomical Society*, **42**, 489–517.

HILL, P. S., VOULGARIS, G. & TROWBRIDGE, J. H. 2001. Controls on floc size in a continental shelf bottom boundary layer. *Journal of Geophysical Research*, **106**, 9543–9549.

HOLT, J. T. & JAMES, I. D. 1999. A simulation of the southern North Sea in comparison with measurements from the North Sea Project Part 2 Suspended Particulate Matter. *Continental Shelf Research*, **19**, 1617–1642.

HOLT, J. T., JAMES I. D. & JONES, J. E. 2001. An s coordinate density evolving model of the northwest European continental shelf 2, Seasonal currents and Tides. *Journal of Geophysical Research*, **106**, **C7**, 14015–14034.

HOLT, J. T. & PROCTOR, R. 1993. The role of advection in determining the temperature structure of the Irish Sea. *Journal of Physical Oceanography*, **33**, 2288–2306.

HOLT, J. T. & JAMES, I. D. 2001. An s coordinate density evolving model of the northwest European continental shelf 1, Model description and density structure. *Journal of Geophysical Research*, **106**, **C7**, 14015–14034.

HUTHNANCE, J. M., ALLEN, J. I. *et al.* Towards water quality models. *Philosophical Transactions of the Royal Society, London*, **A343**, 569–584.

JAGO, C. F. & JONES, S. E. 1998. Observation and modelling of the dynamics of benthic fluf resuspended from a sandy bed in the southern North Sea. *Continental Shelf Research*, **18**, 1255–1282.

JAGO, C. F., BALE, A. J. *et al.* 1993. Resuspension processes and seston dynamics, southern North Sea. *Philosophical Transactions of the Royal Society, London*, **A343**, 475–491.

JAMES, I. D. 1996. Advection schemes for shelf sea models. *Journal Marine Systens*, **8**, 237–254.

JONES, S. E., JAGO, C. F. & SIMPSON, J. H. 1996. Modelling suspended sediment dynamics in tidally stirred and periodically stratified waters: Progress and pitfalls, *In*: PATTIARATCHI, C. (ed.) *Mixing in Estuaries and Coastal Seas*, AGU, Coastal and Estruarine Studies, **50**, 302–324.

JONES, S. E., JAGO, C. F., BALE, A. J., CHAPMAN, D., HOWLAND, R. J. M. & JACKSON, J. 1998. Aggregation and resuspension of suspended particulate matter at a seasonally stratified sitein southern North Sea. *Continental Shelf Research*, **18**, 1283–1310.

LICK, W., HUANG, H. & JEPSEN, R. 1993. Flocculation of fine-grained sediments due to differential settling. *Journal of Geophysical Research*, **98**, 10279–10288.

McCave, I. N. 1987. Fine sediment sources and sinks around the East Anglian Coast (UK). *Journal of the Geological Society, London*, **144**, 149–152.

MCMANUS, J. P. & PRANDLE, D. 1997. Development of a model to reproduce observed suspended sediment distributions in the southern North Sea using Principal Component Analysis and Multiple Linear Regressions. *Continental Shelf Research*, **17**, 761–778.

MCNEIL, J., TAYLOR, C. & LICK, W. 1996. Measurements of erosion of undisturbed bottom sediments with depth. *Journal of Hydraulic Engineering*, **122**, 316–324.

MELLOR, G. L. & YAMADA, T. 1974. A hierarchy of turbulence closure models for planetary boundary layers. *Journal Atmospheric Science*, **31**, 1791–1806.

PROCTOR, R., HOLT, J. T., ALLEN, J. I. & BLACKFORD, J. 2003. Nutrient fluxes and budgets for the North West European Shelf from a three-dimensional model. *Science of the Total Environment*, **314–316**, 769–785.

PULS, W. & SÜNDERMANN, J. 1990. Simulation of suspended sediment dispersion in the North Sea. *In*: CHENG, R. T. (ed.) *Residual Currents and Long Term Transport*. Springer, Berlin, 356–372.

SIMPSON, J. H. & BOWERS, D. 1981. Models of stratification and frontal movement in the shelf seas. *Deep-Sea Research*, **28**, 727–738.

SONG, Y & HAIDVOGEL, D. 1994. A semi-implicit ocean circulation moel using generalized topography-following coordinate system. *Journal of Computational Physics*, **115**, 228–244.

TETT, P. B., JOINT, I. R. *et al.* 1993. Biological consequences of tidal stirring gradients in the North Sea. *Philosophical Transactions of the Royal Society, London*, **A343**, 493–508.

Index

Page numbers in *italic* denote figures; page numbers in **bold** denote tables

Coastal and Shelf Sediment Transport

Edited by
P. S. Balson and M. B. Collins

For the geoscientist, interest in sediment dynamics relates to the understanding of modern processes, together with their extrapolation to the interpretation of ancient deposits within the stratigraphic record. Over the years, various measurement techniques and scientific approaches have been applied to the determination of sediment transport pathways and the derivation of erosion, transport and deposition rates. Recently, a number of new techniques and approaches have been developed, associated with different temporal and spatial scales, and it is appropriate and timely to review a representative selection, by reference to recently undertaken coastal and shelf investigations.

The various contributions in the volume cover, for example: optical and acoustic backscatter measurements; particle tracking; the use of multibeam imagery; grain-size trend analysis; and analytic, numerical and conceptual modelling. Although no single method provides a complete solution to the problem posed, this overview will assist sedimentologists and sediment dynamicists in their selection of the most appropriate approaches, towards the establishment of 'high confidence' in the interpretation of sediment transport rates and directions.

ISBN 978-1-86239-217-5

Cover illustration:

The Sediment Transport And Boundary Layer Equipment (STABLE) being deployed in the Irish Sea from the RV Prince Madog.

Photograph by Richard Cooke, Proudman Oceanographic Laboratory